J. Micropalaeontology, 44, 1–78, 2025
https://doi.org/10.5194/jm-44-1-2025

Journal of Micropalaeontology
Open Access

Upper Oligocene to Pleistocene planktonic foraminifera stratigraphy at North Atlantic DSDP Site 407, Reykjanes Ridge: diversity trends and biozonation using modern Neogene taxonomic concepts

Tirza Maria Weitkamp[1,2], **Mohammad Javad Razmjooei**[1,2], **Paul Nicholas Pearson**[3], **and Helen Katherine Coxall**[1,2]

[1]Department of Geological Sciences, Stockholm University, Svante Arrhenius väg 8, 114 18 Stockholm, Sweden
[2]Bolin Centre for Climate Research, Stockholm University, Stockholm, Sweden
[3]Department of Earth Sciences, University College London, Gower Street, London, WC1E 6BT, UK

Correspondence: Tirza Maria Weitkamp (tirza.weitkamp@geo.su.se)

Received: 2 August 2024 – Revised: 21 October 2024 – Accepted: 27 October 2024 – Published: 6 January 2025

Abstract. Deep Sea Drilling Project (DSDP) Site 407, located near the Reykjanes Ridge (southwest of Iceland) offers a rare and extensive record of Late Cenozoic planktonic foraminifera evolution spanning the Neogene and Quaternary periods. This ca. 300 m sequence provides a nearly continuous record of planktonic foraminifera with mostly good preservation quality, aiding the study of pelagic diversity changes over the past 25 million years as the modern North Atlantic Ocean system evolved. Initially investigated in 1979 by Poore, this study presents a taxonomic reassessment of upper Oligocene to Pleistocene planktonic foraminifera at Site 407, including species range documentation, assemblage analysis, biostratigraphic zonation, and age modelling based on planktonic foraminifera, calcareous nannofossils, and scanning electron microscopy. This study employs modern taxonomic perspectives that integrate morphological and stratophenetic frameworks for fossil species with genetic data for taxa having living representatives. Systematic species counts enable quantitative diversity analysis, with a particular focus on the genus *Neogloboquadrina*, which becomes increasingly prevalent at Site 407 from the late Neogene to Quaternary. The planktonic foraminifera assemblages at Site 407 exhibit a contraction in diversity and a shift in species dominance, notably around 160 m b.s.f. (metres below seafloor) (ca. 8.9–16.5 Ma) and 56 m b.s.f. (ca. 2–3.4 Ma). The upper Oligocene and lower Miocene include species belonging to the genera *Catapsydrax*, *Globoturborotalita*, *Dentoglobigerina*, and *Paragloborotalia*. An acme of "*Ciperoella*" *pseudociperoensis* (lower and middle Miocene), still of uncertain generic affiliation, may have biostratigraphic use. Well-preserved *Turborotalita quinqueloba* are relatively common throughout the sequence. In Oligocene and Miocene material, *T. quinqueloba* is accompanied by *Tenuitella* spp. From the upper Miocene onwards, neogloboquadrinids including *Neogloboquadrina praeatlantica*, *N. atlantica*, *N. incompta*, and *N. pachyderma* become increasingly common and dominate Pliocene assemblages, together with *Globigerina bulloides*. Assemblages with an increasingly high-latitude nature, i.e. where *N. pachyderma* dominates, take over in the lower Pleistocene. Multiple hiatuses are recorded, of which the largest is ca. 8 million years long, separating the middle and upper Miocene (8.9–16.5 Ma; 158.56–160.06 m b.s.f.). Continuous biozonation at Site 407 is challenged by limited species diversity and the absence of standard low-latitude biozone markers, rendering standard schemes ineffective. Recognizable biozones include the low-latitude O7 and M1 Zones in the late Oligocene and early Miocene, respectively; the high-latitude *Neogloboquadrina atlantica* sinistral Zone in the late Miocene and Pliocene; the *Globoconella inflata* Zone in the late Pliocene; and the *Neogloboquadrina pachyderma* Zone in the Pleistocene. The nannofossil biozonation faces similar challenges. A revised biostratigraphic age model integrates calibrated planktonic foraminifera and nannofossil events, incorporating abundant species like "*C.*"

pseudociperoensis, *N. atlantica* dextral and sinistral, *Globoconella puncticulata*, *G. inflata*, and *N. pachyderma*. These findings are expected to contribute to the Neogene–Quaternary Middle Atlas of planktonic foraminifera and potentially improve the use of neogloboquadrinids in palaeoceanography and biostratigraphy.

1 Introduction

The Neogene period (23.03 to 2.58 million years ago; Raffi et al., 2020) witnessed significant geological and climatic changes, transitioning from a warm early and middle Miocene climate and a cooler late Miocene period to the onset of Northern Hemisphere glaciation in the Pliocene and Pleistocene (e.g. Zachos et al., 2001; Raffi et al., 2020). The late Neogene climate change, combined with the closing of oceanic connections and the subsidence of tectonic ridges, resulted in steepening latitudinal temperature gradients and changes in ocean circulation and stratification globally (Valentine and Jablonski, 2015). These changes created new thermal and nutrient niche boundaries in the pelagic realm, causing the restructuring of global marine plankton communities (Boscolo-Galazzo et al., 2022; Valentine and Jablonski, 2015; Fenton et al., 2023; Woodhouse et al., 2023). This resulted in the latitudinal provincialisation of planktonic foraminifera and increasing separation into biogeographic provinces comprising specific assemblages referable to polar, subpolar, transitional, subtropical, and tropical categories (Kucera, 2007). Understanding the extent to which species will migrate, go extinct, and change their geographic range in the future in relation to warming poles is unclear. Therefore, understanding the development of marine biodiversity patterns over geological time and the factors that influence them are key to contextualizing current trends (Fenton et al., 2023; Woodhouse et al., 2023).

At the global scale, planktonic foraminifera in general experienced significant diversification during the late Neogene, with species diversity increasing through the early Miocene and reaching a peak in the Quaternary (e.g. Fraass et al., 2015). At the regional scale, however, patterns are varied. High latitudes experienced strong biodiversity contraction, and low latitudes remained stable, while temperate and subpolar latitudes, which experience overlapping communities, tended to retain high species richness (Woodhouse et al., 2023). Increasingly, large-scale syntheses of planktonic foraminifera data over long and shorter geological timescales are being used to explore these questions, utilizing plankton databases such as MARGO (Kucera et al., 2005; Strack et al., 2022), ForCenS (Siccha and Kucera, 2017), FORCIS (Chaabane et al., 2023), and, for longer-term Cenozoic timescales, Triton (Fenton et al., 2021, 2023; Woodhouse et al., 2023). While the Triton database puts effort into harmonizing taxonomy and biochronology across latitudes for the Late Cenozoic, a shortcoming is that the Neogene planktonic foraminifera taxonomy in general is rather out of date and strongly in need of revision, and key aspects are not well aligned with modern frameworks for the Paleogene (Olsson et al., 1999; Pearson et al., 2006; Wade et al., 2018) or modern species (underpinned by genetic studies) (Brummer and Kucera, 2022). Moreover, while renewed work on Neogene planktonic foraminifera from the low latitudes is underway, the high latitudes have received less attention (e.g. Wade et al., 2011; King et al., 2020; Lam and Leckie, 2020). Thus, a return to focused studies of targeted regions and specific localities where planktonic foraminifera distributions can be evaluated and their taxonomy analysed is needed.

Using stratigraphic species analysis and scanning electron microscopy (SEM) imaging, this study contributes to efforts towards refining Neogene planktonic foraminifera taxonomy through a detailed re-evaluation of Deep Sea Drilling Project (DSDP) Site 407. Site 407 represents one of the richest existing planktonic foraminifera sequences from the high-latitude North Atlantic and a more westerly positioned complement to the recently recovered cores from the International Ocean Discovery Program (IODP) Expedition 395 (Fig. 1) (Parnell-Turner et al., 2024). Originally studied by Poore (1979), Site 407 has long been known as one of the few existing carbonate-containing sites from the high-latitude North Atlantic that extends back as far as the Oligocene. While Poore (1979) produced an exemplary analysis of the sequence, with excellent-quality SEM images, aspects of the taxonomy are now out of date at both the species and higher taxonomic levels. Moreover, the biostratigraphic framework needs updating to help place microfossil evolutionary events in a consistent chronological model. Taxonomic re-evaluation is therefore needed to improve constraints on species stratigraphic ranges and align the taxonomy with treatments of Recent (Brummer and Kucera, 2022) and Oligocene species (Wade et al., 2018), which are now all underpinned by concepts of wall texture conservatism and, in the case of living taxa, genetics. Here we present the results of our quantitative species analysis, which includes a systematic taxonomy section using up-to-date principles. We produce planktonic foraminifera and nannofossil biostratigraphic zonation, utilizing previously published low-latitude and temperate North Atlantic zonation schemes and a proposed new zonal scheme with modifications. This work will contribute to identifying evidence of endemism at higher latitudes and testing and improving biostratigraphic schemes, including questions of diachroneity across latitudes. It represents part of wider ongoing efforts by the Neogene and Quaternary Planktonic Foraminifera Working Group to im-

prove and harmonize Late Cenozoic planktonic foraminifera taxonomy.

1.1 Geologic and oceanographic setting

DSDP Site 407 (63°56.32′ N, 30°34.56′ W; Fig. 1), with a modern water depth of 2472 m b.s.l. (metres below sea level; Shipboard Scientific Party, 1979), sits on late Eocene-age crust (magnetic anomaly chron C13; ca. 35 Ma; LaBrecque et al., 1977) on the western flank of the Reykjanes Ridge (Shipboard Scientific Party, 1979) (Fig. 1). This region is geologically complex, with an equally complex oceanographic history. At the time of the crust formation of Site 407, Icelandic hotspot volcanism was minimal, and the crust had transitional normal oceanic-/hotspot-type characteristics. The upper crust formed at shallow oceanic depths (ca. 1000 m) and subsided to its present depth as crustal spreading and cooling progressed (Luyendyk and Cann, 1979). Site 407 is situated southwest of Iceland today. Iceland itself did not emerge as an island until the early–middle Miocene (Talwani and Eldholm, 1977), when plume volcanism intensified, and nowadays the whole region is underlain by anomalously thick oceanic crust that reflects plume volcanism (Bott, 1983). The locus of seafloor spreading in the northeastern Atlantic has consistently been over the Reykjanes Ridge throughout the Late Cenozoic, with higher spreading rates compared to other ridges in the region (Le Breton et al., 2012).

Initially, Site 407 and the wider North Atlantic region were separated from the Norwegian Sea by the Greenland–Scotland Ridge (GSR), which extends from eastern Greenland to Iceland and the Faroe Islands across to Scotland. The GSR was formed during the Paleocene (anomaly 24; 56 Ma) by mantle-plume-generated hotspot volcanism (Luyendyk and Cann, 1979; Nilsen, 1983). Over time, subsidence and breaching of the GSR occurred during various phases of the Cenozoic (Miller and Tucholke, 1983), influencing the evolution of North Atlantic oceanography, including the development of the Atlantic Meridional Overturning Circulation (AMOC) (Berggren and Schnitker, 1983; Hutchinson et al., 2019; Stärz et al., 2017; Uenzelmann-Neben and Gruetzner, 2018; Wright and Miller, 1996).

Oceanographically, today Site 407 is located in the northern Irminger Sea (Fig. 1) at the confluence of the anticlockwise Atlantic subpolar gyre (Irminger Current; IC), which recirculates warmer Atlantic waters at the surface, with south-flowing polar surface currents exiting the Arctic (East Greenland Current – EGC), and the subarctic front situated to the southwest of Iceland (Fig. 1) (Hátún et al., 2016). Bottom-water flow at Site 407 is driven by deep-water overflows from the Iceland–Scotland and Denmark Strait sectors of the GSR, namely the Iceland–Scotland and Denmark Strait overflow waters (ISOW and DSOW, respectively). The DSOW represents the largest overflow and is joined by the ISOW on the western flank of Reykjanes Ridge to form the Deep Western Boundary Current (DWBC), which is exported southwards (Swift et al., 1980; Hansen and Osterhus, 2000). Modern planktonic foraminifera assemblages in the water column can be described as sub-polar, comprising *Neogloboquadrina pachyderma, N. incompta, Turborotalita quinqueloba, Globoconella inflata, Globigerinita glutinata, G. uvula*, and *Globigerina bulloides*, with occasional lower-latitude taxa (Sahoo et al., 2022).

1.2 The status of Neogene planktonic foraminifera taxonomy

In contrast to Paleogene and living species, Neogene planktonic foraminifera classification has not been systematically evaluated or refined since the 1980s and remains one of the current challenges in planktonic foraminifera stratigraphic and evolutionary research. A Neogene and Quaternary working group has been formed to work on Miocene to Recent taxa. The Neogene evolution and phylogeny of planktonic foraminifera have been addressed in several notable works, including Cifelli (1969), Kennett and Srinivasan (1983), Bolli and Saunders (1985), Jenkins (1985), Wei and Kennett (1986), Tappan and Loeblich (1988), Bolli et al. (1989), Aze et al. (2011), Ezard et al. (2011), Fraass et al. (2015), and Lowery et al. (2020). One of the major differences between these works is the usage of subgenera, in particular within the genus *Globorotalia*. This genus is diverse, with a large species diversity (36 recognized species) compared to other Neogene and Quaternary genera. *Globorotalia*, in its wider sense, consists of several distinct lineages characterized by the presence/absence of a keel, chamber, and test shape (e.g. conicotruncate vs. lenticular) and test size (Bandy, 1972). Many workers have treated these lineages as subgenera (e.g. Bandy 1972; Kennett and Srinivasan, 1983; Aze et al., 2011), whereas others have refrained from using subgenera (e.g. Triton database; Fenton et al., 2021; Woodhouse et al., 2023). Most recently, however, Brummer and Kucera (2022) note that the subdivision of *Globorotalia* is not necessary because it is a monophyletic genus and that the use of subgenera has little tradition among extant planktonic foraminifera. However, the usage of subgenera could be useful when tracing the phylogeny of the extant species (e.g. Aze et al., 2011). In this study, we acknowledge the various lineages within the genus *Globorotalia,* based on the phylogenetic trees in Aze et al. (2011), and use the subgenera *Globoconella* for classifying the Neogene precursors to *G. inflata* (Brummer and Kucera, 2022), following the taxonomy of *Globoconella* as listed in Lam and Leckie (2020b).

A limitation of existing Neogene works (including Kennett and Srinivasan, 1983) is that the taxonomic assessments and phylogenetic models are largely based on studies from low latitudes and the southwest Pacific, omitting higher latitudes and including the northern North Atlantic to Arctic sector. In the Atlantic Ocean, the low-latitude tropical region has remained the major centre for the dispersal of planktonic foraminifera throughout the Cenozoic (Bolli, 1957; Banner

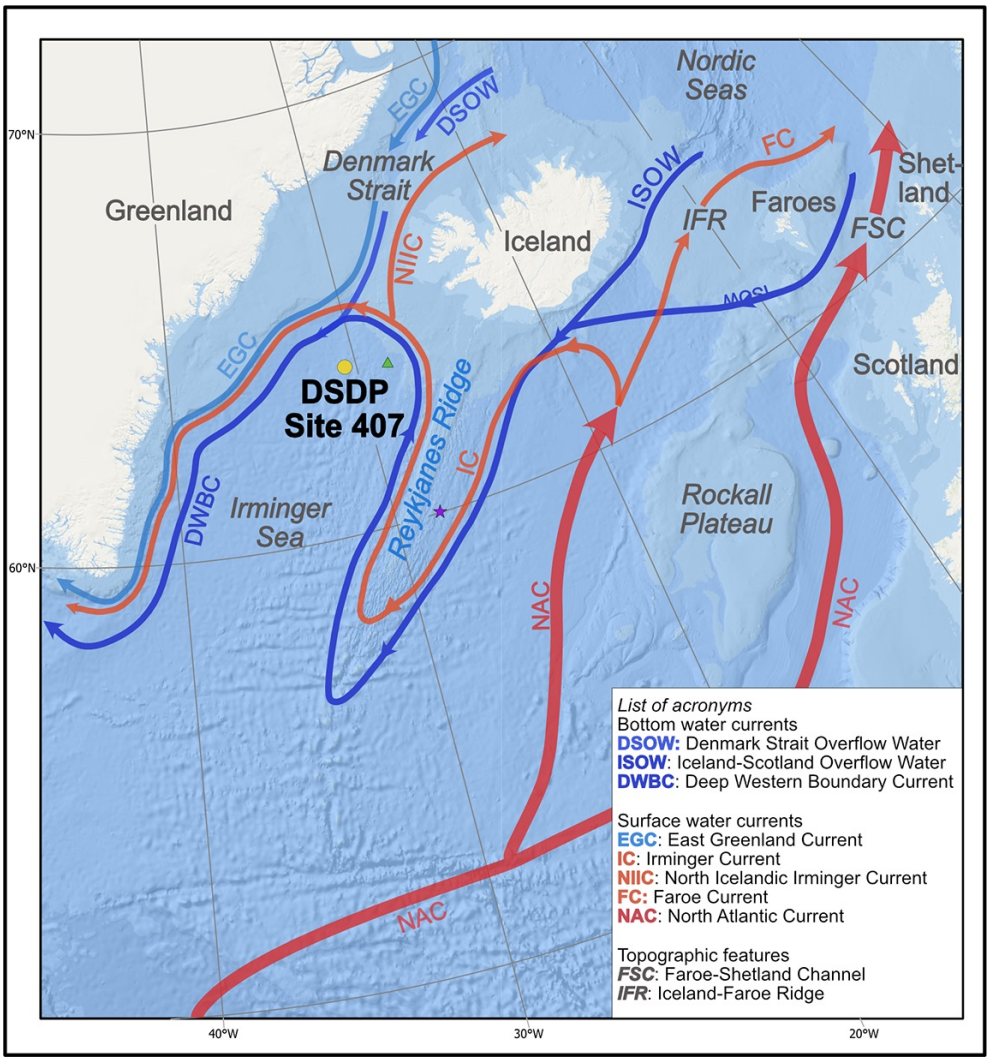

Figure 1. Schematic view of main circulation pathways in the Irminger Sea and Nordic Seas regions. DSDP Site 407 is indicated with the yellow circle. Sites mentioned in this study that are relevant to Site 407 are DSDP Site 408 (green triangle) and IODP Expedition 395 (purple star). Strength and temperature of the currents are represented by arrow width and colour (red is warmer; blue is colder). Ocean currents redrawn from Daniault et al. (2016).

and Blow, 1965; Bolli and Bermudez, 1965; Blow, 1969; Berggren, 1969, 1972; Lamb and Beard, 1972; Parker, 1973). Late Cenozoic planktonic foraminifera have received attention in the reports of individual DSDP, Ocean Drilling Program (ODP), and IODP expeditions (ODP Leg 105, Aksu and Kaminski, 1989; DSDP Leg 12, Berggren, 1972; DSDP Leg 48, Murray, 1979; DSDP Leg 49, Poore, 1979; DSDP Leg 81, Huddlestun, 1984; DSDP Leg 94, Weaver, 1987; ODP Leg 104, Spiegler and Jansen, 1989; ODP Leg 151, Spiegler, 1996; ODP Leg 152, Spezzaferri, 1998; ODP Leg 162, Flower, 1999; IODP Site 1313, Sierro et al., 2008), but these works have not been integrated. From some of these studies, temperate and high-latitude North Atlantic (Berggren, 1978; Poore and Berggren, 1975; Spiegler and Jansen, 1989; Weaver and Clement, 1986) and northeastern Atlantic (North Sea) (Anthonissen, 2009, 2012) biostratigraphic zonation schemes have been developed. Our reanalysis of Site 407 provides a good opportunity to assess the applicability of these zonations in the Irminger Sea.

2 Material and methods

2.1 Location and lithostratigraphy

A total of 183.31 m (40 % recovery) of Oligocene to Quaternary sediments was recovered at Site 407 by rotary coring (RCB) (Shipboard Scientific Party, 1979). For this study, upper Oligocene to Quaternary sediments were examined (0.57–329.5 m b.s.f.; metres below seafloor), comprising the entire sediment package above basement. The recovered sed-

iments, apparently pelagites, are characterized by the following lithologies (Shipboard Scientific Party, 1979): (1) Unit 1 (0–46.3 m), with calcareous sandy mud with intervals of calcareous and marly calcareous ooze with variable volcanic ash content (up to 20 %); (2) Unit 2 (46.3–160.7 m), with nannofossil ooze (46.3–124.0 m) and nannofossil chalk (124.0–160.7 m); (3) Unit 3 (160.7–272.0 m), with siliceous nannofossil chalk with an interbedded chalk–volcanic ash zone (215–224.5 m); and (4) Unit 4 (272.0–300.5 m), with nannofossil chalk (272.0–280.0 m) and nannofossil chalk basalt pebble gravel and (5) interlayered sediments between basalt, nannofossil chalk (320.3–321.3 m), and foraminiferal nannofossil chalk (329.4–331.2 m). Biostratigraphic studies conducted as part of the initial work on Site 407 identified at least two unconformities separating the middle Miocene from upper Miocene and the upper Pliocene from lower Pleistocene sediments (Shipboard Scientific Party, 1979; Poore, 1979). The initial Site 407 age framework was based on nannofossil and planktonic foraminifera biostratigraphy only, as the rotary cored sediments were unsuitable for palaeomagnetism measurements due to drilling disturbance (Shipboard Scientific Party, 1979). Core sample notation within the text, figures, and Appendix information sections follow the standard International Ocean Discovery Program (IODP) format, with sample names including site, core number, section number, and sample interval in centimetres within a section.

2.2 Planktonic foraminifera sample preparation, assemblage counting, and imaging

A total of 76 samples (20 cc volume) at ca. 1.5 m intervals were obtained from Cores 1R through 36R from sections 1, 2, and 3 in each core from the IODP Core Repository in Bremen. The initial Site 407 age model, indicating sedimentation rates between < 0.5 and > 4 cm kyr^{-1}, implies a sample resolution of a few 100 kyr to over 1 Myr (Shipboard Scientific Party, 1979). All samples were freeze-dried and weighed before disaggregation. Samples were soaked in demineralized water and agitated for 1–6 h in Erlenmeyer flasks. The flasks were immersed in an ultrasonic bath for up to 30 s as a final disaggregation step. Chalky samples from the deepest levels were first manually broken into fragments. The disaggregated material was wet-sieved over a 63 µm mesh sieve and dried overnight at 49 °C before reweighing to obtain the sand fraction dry mass.

For planktonic foraminifera relative abundance variations, the > 125 µm size fraction of each sample was split into aliquots of approximately 300 specimens (mean = 288; Table A1) using a microsplitter and sprinkled onto a black picking tray. Planktonic foraminifera were examined using a ZEISS Stemi 508 binocular light microscope and identified and counted to species level. The > 125 µm size fraction was found to be sufficient to capture the abundance of most species present in the assemblages, including small species such as *Globigerinita glutinata*, *G. uvula*, *Tenuitella* spp., and *Turborotalita quinqueloba*. However, very small species such as *Orcadia riedeli* and *Tenuitellita fleisheri* were only found in the > 63 µm size fraction. After each count, the full > 63 and > 125 µm size fraction residues were sprinkled evenly on a picking tray and inspected for these small and additionally rare species, some of which might have biostratigraphic value. In cases where additional species were identified, these are noted as "R" in the count tables (Appendix Tables A1 and A2). Certain intervals (47.48–158.56 m b.s.f.) were strongly affected by fragmentation. Here the high abundance of fragments meant that it was not always possible to do systematic 300 specimen counts, as the whole specimens were heavily diluted by the fragments. Sample 407-14R-1, 56–58 cm (120.56 m b.s.f.), had such a high degree of fragmentation that it would be too time-consuming to filter through all the fragments to find whole tests; thus, it was omitted. Since the Neogene taxonomy is undergoing a revision, a composite of reference classification frameworks was used for species identification. This included Kennett and Srinivasan (1983), the *Atlas of Oligocene Planktonic Foraminifera* (Wade et al., 2018), the review by Brummer and Kuèera (2022) of modern species, and the online database Mikrotax (Young et al., 2017), which includes current working species concepts and generic assignments (Young et al., 2017). Additionally, for some taxa, we refer back to the Poore (1979) species diagnosis. Preservation of whole foraminifers was classified as good, moderate, or bad and quantified by a fragmentation index (FI). Specimens missing > 50 % of their test were considered a fragment. Fragment percentages were determined in the same manner as relative abundance, i.e. counting all fragments in a sample (> 125 µm).

For biozonation, we apply the low-latitude planktonic foraminifera biozonation scheme of Wade et al. (2011), as far as possible in the Oligocene and Miocene, based on identification of bioevents including first (FOs) and last occurrences (LOs) of significant taxa (Table A1). For the Pliocene and Pleistocene, the North Atlantic zonation of Weaver and Clement (1986) and Nordic Seas zonation of Spiegler and Jansen (1989) were applied. Additionally, age-calibrated accessory events from Raffi et al. (2020) were used throughout the whole sequence. Coiling ratios were recorded for *Neogloboquadrina atlantica*, since the change from dominantly dextral to sinistral is an important age marker in the North Atlantic (e.g. Raffi et al., 2020; Weaver and Clement, 1986; Spiegler and Jansen, 1989). Our age–depth model was constructed by plotting FO and LO events using the "Age–depth plot" tool available through Mikrotax (https://www.mikrotax.org/system/age-depth-plot.php, last access: 20 June 2024). This tool also calculated sedimentation rates.

SEM imaging was conducted to document taxonomic concepts, including wall texture characteristics and the presence/absence of spine holes, focusing on well-preserved examples of each species (Plates 1–21). The instrument used was a JSM-7000F floor SEM, housed in the Depart-

ment of Materials and Environmental Chemistry at Stockholm University (accelerating voltage = 10 kV; working distance = 10 mm). The specimens were mounted on sticky carbon discs and gold-coated before analysis (2 × 60 s; applied current of 20 mA).

2.3 Planktonic foraminifera diversity measures

Species diversity, both simple diversity and diversity metrics that consider the relative abundance of species, were calculated throughout the upper Oligocene to Quaternary section using the following approaches:

- Species richness (number of species per sample).
- Shannon–Wiener Index (H'), i.e. $H' = -\sum(p_i) \cdot \ln(p_i)$, where p_i is the proportion of the entire community made up of species i. It assumes that individuals are randomly sampled from an independent large population and all the species are represented in the sample (Shannon and Weaver, 1949), where the higher the value, the more diverse the assemblage will be (Dirzo and Mendoza, 2008). It is a useful measure of biodiversity that considers the species richness and evenness of the species present in the assemblage.
- Evenness, where the concept of evenness refers to the extent to which each species is represented among the samples. Values vary between zero and one, representing one species being dominant and all other species being present in very low numbers (close to zero) or all species being represented by equal numbers (close to one) (Dirzo and Mendoza, 2018).
- Diversity and evenness were calculated using the PAST software, version 4.13 (Hammer et al., 2001).

Additionally, semiquantitative estimates of the abundance of lithic grains (mainly quartz) were determined based on of relative abundance in the > 125 µm fraction, using the following abundance categories: rare (1 %–3 %), few (4 %–15 %), and common (16 %–30 %). This was used as a proxy for the onset of Northern Hemisphere glaciation during the Pliocene and Pleistocene, assuming that the lithic grains represent ice-transported material (ice-rafted debris, IRD) that was carried to Site 407 by icebergs calved from marine-terminating ice sheets on Greenland, Iceland, and Svalbard.

2.4 Calcareous nannofossil samples and analysis

For calcareous nannofossil analysis, small amounts of unprocessed sediment from the same 76 samples used for the foraminifera studies were prepared using the Bown and Young (1998) smear slide technique. The smear slides were examined under a ZEISS Axio Scope.A1 polarizing light microscope at ×1000 magnification and imaged (Plates 22 and 23). Species identification followed the taxonomy of Perch Nielsen (1985) and Young (1998), as well as the most up-to-date descriptions and illustrations in the online database Nannotax3 (Young et al., 2022). The focus for this study was identifying nannofossil biostratigraphic markers, and the assemblages are only briefly summarized, in contrast to the planktonic foraminifera, which are the focus of this study and for which the assemblages and taxonomy are considered in detail. Nevertheless, qualitative calcareous nannofossil species relative abundances were recorded and presented as being dominant (D), present (P), reworked (RW), or rare (R) (Fig. S3). The calcareous nannofossil biozonation is based on identification of the first (FOs) and last occurrences (LOs) of significant taxa in the Site 407 samples (Table B1). The standard nannoplankton biozonation scheme of Martini (1971) was applied based on the selected bioevents.

3 Results

3.1 Planktonic foraminiferal assemblage and diversity changes

A total of 84 species was identified in the 76 new samples from Site 407, of which only 1 sample was barren of planktonic foraminifera (Sample 407-24R-2; 56–58 cm; 217.06 m b.s.f.). A summary of the species' downcore stratigraphic distributions is presented in Table 1 (full species ranges shown in Tables A1 and A2), where the most important species distributions are shown by depth against the epochs interpreted from the planktonic foraminifera and calcareous nannofossil biostratigraphy (see Sect. 3.3), whereas panel (B) in Table 1 shows the Neogene and Quaternary climate (benthic $\delta^{18}O$) and ice volume plotted against age and was used to make rough climatic interpretations based on the planktonic foraminifera assemblages. For 70 species from the > 125 µm size fraction, occurrences are reported as the relative abundances of the counted assemblage. On average, 268 specimens were counted per sample. A further 14 species, which were not found in the > 125 µm 300 specimen counts, but were observed when the whole sample fraction (> 63 µm size fraction) was examined, are recorded as semiquantitative estimates (Tables A1 and A2). For each species recognized, our taxonomic concept is described in the systematic taxonomy section, together with detailed taxonomic notes.

Fragmentation intensity (%) (Table 1), which could be useful as an indicator of preservation quality, especially regarding calcite dissolution, is variable downcore. In the lower part of the succession (161.56–329.5 m b.s.f.), the fragmentation intensity fluctuates between 11.7 % (169.56 m b.s.f.) and 67.7 % (196.56 m b.s.f.). At 161.56 m b.s.f., fragmentation increases from 12.4 %–49.5 % (160.06 m b.s.f.) and remains high (62.2 %) up to 47.48 m b.s.f. and up to 96.7 % at 120.56 m b.s.f. In the upper part of the sequence, fragmentation decreases from 77.6 % (47.48 m b.s.f.) to 20.4 %

(44.56 m b.s.f.) and remains low (average 3.7 %) up to 0.57 m b.s.f.

The majority of samples yielded abundant planktonic foraminifera, and only one sample (Sample 407-24R-2; 56–58 cm; 217.06 m b.s.f.) was barren. Also barren of calcareous nannofossils, the sample was instead dominated by biosilicous material, suggesting strong calcite dissolution. Starting from the base of the section, in intervals close to basement where sediments are intercalated with basalt (Cores 35R and 36R), planktonic foraminifera are common and moderately well preserved, although often infilled with glauconite. Preservation is poor in samples from Core 29R to 32R, but planktonic foraminifera remain common. Specimens in samples from Cores 28R to 19R are few but well preserved.

These samples are dominated by biosilicous grains (sponge spicules and radiolaria) and non-diagnostic, possibly juvenile, planktonic foraminifera based on their small size. In the remaining intervals (Cores 1R to 18R), foraminifera are well preserved and common, although the fragmentation intensity is high, especially in samples from Cores 6R to 18R (Table 1). Generally, the Site 407 planktonic foraminifera appear glassy (translucent and reflective) or more whitish (frosty) under the light microscope. SEM images show few signs of diagenetic alteration and dissolution, except around Sample 407-13R-1, 56–58 cm (111.06 m b.s.f.), assigned to the Pliocene, where specimens show signs of diagenetic alteration in the form of recrystallization (e.g. Plate 10; Figs. 11, 12).

We record the relative abundance of 76 planktonic foraminifera species from the > 125 µm size fraction (Table A2). Of these, 11 species record relative abundances > 25 % but with large variation through the sequence (Fig. 2). These common species include *"Ciperoella" pseudociperoensis* (still of an uncertain generic affiliation), *Dentoglobigerina venezuelana*, *Globigerina bulloides*, *Globigerinella obesa*, *Globorotalia praescitula*, *Neogloboquadrina atlantica* sinistral and dextral, *N. incompta*, *N. pachyderma*, *Turborotalita quinqueloba*, and *Globigerinita glutinata* (Fig. 2). This variability is reported below in more detail.

The lower part of the studied section (171.06–392.5 m b.s.f.) is dominated by *Globigerinella obesa* (average = 42.5 %) and the small microperforate species *Globigerinita glutinata* (average = 32.8 %). Accessory species are *Catapsydrax unicavus*, *Globoturborotalita woodi*, *Globorotaloides suteri*, and *Tenuitella munda*. The genus *Paragloborotalia* diversifies around 275.56–286.46 m b.s.f. (Table 1), contributing on average 7.1 % to assemblages, with *T. angustiumbilicata*, *T. clemenciae*, *Turborotalita quinqueloba*, *Globoturborotalita euapertura*, *G. connecta*, and *G. bulloides* making up much of the remainder. Rare species are *Globigerinoides neoparawoodi*, *Trilobatus quadrilobatus*, *Catapsydrax dissimilis*, *C.* cf. *indianus*, *Globigerinoides stainforthi*, *G. hexagonus*, and *Globigerinella praesiphonifera*. Diversity is highest during this interval, as shown by the species richness counts, which vary between 8 (215.56 m b.s.f.) and 20 (291.25 and 198.06 m b.s.f.), and the Shannon diversity (H' index), with values fluctuating between 1.25 and 2.49. Evenness fluctuates between 0.21 and 0.92 (Fig. 3). In this interval, 15 bioevents occur, involving the FO of *"Ciperoella" pseudociperoensis* (407-24R-3; 56–58 cm; 218.56 m b.s.f.), *Globoquadrina dehiscens* (407-29R-2; 20–22 cm; 264.2 m b.s.f.), *Trilobus quadrilobatus* (407-29R-2; 20–22 cm; 264.2 m b.s.f.), *Globorotalia zealandica* (407-19R-3; 56–58 cm; 171.06 m b.s.f.), *Globorotalia praescitula* (407-20R-1; 100–102 cm; 178 m b.s.f.), *Globoturborotalita connecta* (407-31R-4; 46–48 cm; 286.46 m b.s.f.), *Paragloborotalia continuosa* (407-35R-1; 86–88 cm; 320.36 m b.s.f.), *P. acrostoma* and *P. kugleri* (407-30R-2; 56–58 cm; 274.06 m b.s.f.), *P. mayeri* (407-32R-1; 25–27 cm; 291.25 m b.s.f.), *P. birnageae* and *P. semivera* (407-30R-3; 56–58 cm; 275.56 m b.s.f.), *Dentoglobigerina tripartita* (407-31R-4; 46–48 cm; 268.46 m b.s.f.), *D. venezuelana* (407-32R-1; 25–27 cm; 291.25 m b.s.f.), and *D. altispira* (407-35R-1; 86–88 cm; 320.36 m b.s.f.). LOs include *Tenuitella munda* (407-24R-3; 56–58 cm; 218.56 m b.s.f.), *Catapsydrax dissimilis* (407-23R-1; 56–58 cm; 206.06 m b.s.f.), *Globoturborotalita connecta*, *Catapsydrax unicavus* (407-22R-3; 50–52 cm; 199.39 m b.s.f.), *Ciperoella ciperoensis* (407-29R-2; 20–22 cm; 264.2 m b.s.f.), *Globorotaloides suteri* and *P. birnageae* (407-19R-3; 56–58 cm; 171.06 m b.s.f.), *P. kugleri* (407-28R-3; 56–58 cm; 256.56 m b.s.f.), *P. pseudokugleri* (407-29R-3; 20–22 cm; 264.5 m b.s.f.), and *D. altispira* (407-29R-2; 20–22 cm; 264.2 m b.s.f.) (Table A1).

The short interval between 160.06 and 171.06 m b.s.f. is characterized by the highest species richness (about 17; Fig. 2) and is dominated by *"Ciperoella" pseudociperoensis*, *Globorotalia praescitula*, and *Paragloborotalia* sp., accounting for roughly 69 % of the assemblage (Table 1). Accessory species are *Dentoglobigerina venezuelana*, *Globoturborotalita woodi*, and *Globigerinita glutinata*, accounting for 13 % of the assemblage. Minor amounts of *G. uvula*, *Trilobatus trilobus*, *T. immaturus*, *P. acrostoma*, *P. mayeri*, *P. continuosa*, *Neogloboquadrina* cf. *praeatlantica*, *D. altispira*, *D. baroemoenensis*, *Globigerina falconensis*, *G. umbilicata*, *Globorotaloides archeomenardii*, *G. praemenardii*, *G. zealandica*, *G. challengeri*, and *Tenuitella angustiumbilicata* account for the remaining part.

The interval between 47.48 and 158.56 m b.s.f. is dominated by the morphologically plastic species *Neogloboquadrina atlantica* (sinistral) (ca. 35 %; Fig. 2) (Plate 15; Figs. 1–7). A distinct coiling change from dominantly sinistral (average 35 %) to dextral (average 42 %) *N. atlantica* occurs at 150.56 m b.s.f. (Table 1 and Fig. 2). Other important taxa in this interval are *Globigerina bulloides*, *N. praeatlantica* (in the lower part; 139.56–158.56 m b.s.f.), *N. incompta*, *N. pachyderma*, *T. quinqueloba*, and *G. glutinata*, of which the latter is well represented in the > 125 µm size

Table 1. Stratigraphic occurrence of selected planktonic foraminifera abundances at Site 407, shown as a colour gradient (darker blue is for higher abundance). Additional data include lithology, preservation, lithic fragments, and biosilica. Stratigraphic ages are based on planktonic and calcareous nannofossil events from Table 2. Hiatuses are marked by black (major) and grey (potential) wavy lines. R is for rare, G is for good, and M is for medium. There are lithic fragments and biosilica, where D is for dominant, A is for abundant, F is for few, P is for present, and H is for high. **(B)** Neogene climatic indicators modified from Steinthorsdottir et al. (2021), with $\delta^{18}O$ from De Vleeschouwer et al. (2017) tracking ocean–climate patterns and Northern Hemisphere ice conditions. MCO is the Miocene Climatic Optimum.

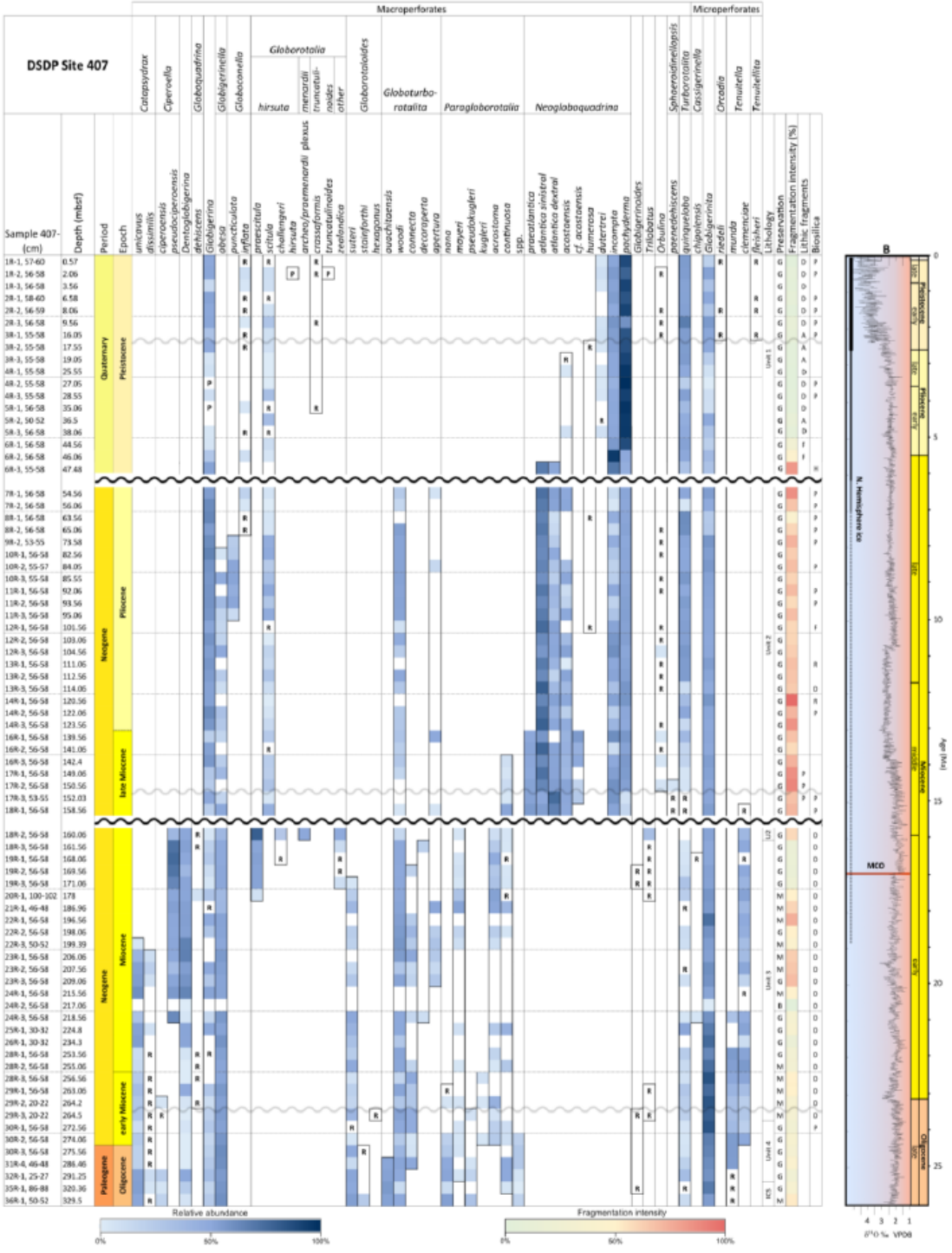

fraction. Five species of *Neogloboquadrina* (*N. acostaensis, N. atlantica, N. incompta, N. pachyderma*, and *N. praeatlantica*) appear abruptly in Sample 407-18R-1, 56–58 cm (158.56 m b.s.f.), except for *N. humerosa*, which appears in 407-12R-1, 56–58 cm (101.56 m b.s.f.). These species account for roughly 45 % of the assemblage. *Neogloboquadrina praeatlantica* is only present in the lower part of this interval, making up about 7 % of the assemblage (139.56–158.56 m b.s.f.). Accessory species are *G. woodi*, *G. apertura*, *G. decoraperta*, *Globoconella puncticulata*, *G. obesa*, *G. uvula*, and *P. continuosa* and account for the remaining part of the assemblage. *Sphaeroidinellopsis paenedehiscens* has a short range between 150.56 and 158.56 m b.s.f. This interval has two FO events, namely *G. inflata* (65.06 m b.s.f.) and *G. puncticulata* (95.06 m b.s.f.), and six LO events, namely *G. woodi* (54.56 m b.s.f.), *G. puncticulata* (9R-2; 53–55 cm; 73.58 m b.s.f.), *G. apertura* (7R-1; 56–58 cm; 54.56 m b.s.f.), *N. atlantica* (sinistral and dextral) (6R-3; 55–58 cm; 47.48 m b.s.f.), and *T. clemenciae* (18R-1; 56–58 cm; 158.56 m b.s.f.). Between Samples 407-18R-1, 56–58 cm (158.56 m b.s.f.), and 407-18R-2, 56–58 cm (160.06 m b.s.f.), 14 species abruptly disappear (*"C." pseudociperoensis, D. venezuelana, D. baroemoenensis, D. globosa, G. dehiscens, G. praescitula, G. archeomenardii, G. praemenardii, G. zealandica, G. challengeri, P. mayeri, P. acrostoma, T. immaturus,* and *T. trilobus*), and there is the sudden appearance of diverse and common species of the genus *Neogloboquadrina*, including *N. pachyderma*. Species richness is about 12, H', and the evenness values fluctuate between 1.36–2.22 and 0.36–0.80, respectively.

There is a progressive decrease in the overall number of species, yet evenness remains relatively stable throughout the zone. Shannon H′ increases steep between Samples 6R-2, 56–58 cm (46.06 m b.s.f.), and 6R-3, 55–58 cm (47.48 m b.s.f.) (Fig. 2; species diversity).

The upper part of the sequence (0.57–46.06 m b.s.f.) is dominated by *Neogloboquadrina pachyderma* (about 75 % of the total assemblage; Fig. 2). Within this interval, we recognize five morphotypes of *N. pachyderma* (Plate 16), which appear to be equivalent to the *N. pachyderma* morphotypes originally recognized in Quaternary sediments of the central Arctic Ocean and distinguished using a numbering system, Nps-1 through Nps-5 (El Bani Altuna et al., 2018; Eynaud et al., 2009; Eynaud, 2011). The most common of the *N. pachyderma* morphotypes are Nps-1, Nps-2, and Nps-3 (Plate 16; Figs. 3–8). Accessory species over this interval are *Globigerina bulloides*, *N. incompta*, *Turborotalita quinqueloba*, and *Globigerinita glutinata*. These accessory species together account for about 23 % of the assemblage. Minor amounts of *Globorotalia scitula*, *G. crassaformis*, *Globigerinita uvula*, *Globoconella inflata*, *N. acostaensis*, and *N. dutertrei* are recognized. Rare *Tenuitella fleisheri* and *Orcadia riedeli* occur in the > 63 µm size fraction. Other rare species include *Globorotalia truncatulinoides*, *G. hirsuta*, *G.* cf. *cariacoensis*, *G. umbilicata*, *N. humerosa*, *Orbulina universa*, *O. suturalis*, and *Globigerinella* cf. *siphonifera*. Two noteworthy LO events are present, namely *N. acostaensis* and *N. humerosa* at 19.05 and 17.55 m b.s.f., respectively. Species richness is low in the upper part of the sequence, with about 7 on average (Fig. 2).

3.2 Calcareous nannofossil assemblage

Calcareous nannofossils are moderately well preserved to well preserved, and the average species richness is highest in the middle Miocene (160.06–171.06 m b.s.f.) and lowest in the Quaternary (0.57–25.55 m b.s.f.) (Table B1). *Coccolithus pelagicus* dominates the interval between Samples 407-6R-1, 56–58 cm, and 407-36R-1, 50-52 cm (44.56–329.5 m b.s.f.); *Reticulofenestra* spp. dominates in the interval between 407-18R-1, 56–58 cm, and 407-36R-1, 50–52 cm and (158.56–329.5 m b.s.f.); *Gephyrocapsa* spp. dominates in the interval between 407-4R-1, 55–58 cm, and 407-10R-1, 56–58 cm (25.55–82.56 m b.s.f.); and *Gephyrocapsa huxleyi* dominates in 407-1R-1, 57–60 cm, to 407-2R-3, 56–58 cm (0.57–9.56 m b.s.f.). Accessory taxa, such as *Discoaster* spp. and *Helicosphaera* spp., are quite abundant during the Oligocene and Miocene but become few to rare after 158.56 m b.s.f. Sample 407-24R-2, 56–58 cm (217.06 m b.s.f.), is barren of calcareous microfossils, including calcareous nannofossils. Biosiliceous material, including radiolaria fragments and diatoms, is common in most smear slides. The most intense Paleogene reworking was recorded in Samples 407-18R-3, 56–58 cm, to 407-30R-3, 56–58 cm (161.56–275.56 m b.s.f.), as identified by the occurrence of *Zygrhablithus bijugatus* (Paleocene–Oligocene), *Chiasmolithus altus* (Eocene–Oligocene), and large *Reticulofenestra* spp. (Eocene–Oligocene?). In samples from 407-1R-1, 57–60 cm, to 407-5R-1, 56–58 cm (0.57–35.06 m b.s.f.), reworking of upper Cretaceous taxa, such as *Eiffellithus eximius*, *Prediscosphaera cretacea, Watznaueria* spp., *Microrhabdulus undosus, Micula staurophora, Arkhangelskiella* spp., and *Tranolithus orionatus* is common. Reworked Paleogene species are also present in this interval but less noticeable (mostly *Reticulofenestra* spp.).

3.3 Age–depth model and integrated planktonic foraminifera and calcareous nannofossil biostratigraphy

The lack of a palaeomagnetic record at Site 407 results in an age–depth model solely consisting of calibrated planktonic foraminifera and calcareous nannofossil bioevents for age control for the past approximately 25 million years. The stratigraphic range data of identified planktonic foraminifera species underpinning the biozonation are presented in Tables 4, A1, and A2, and the stratigraphic range data of calcareous nannofossils are presented in Table B1. Planktonic foraminifera and nannofossil evolutionary events that are important for the biozonation (Table 2) and establish-

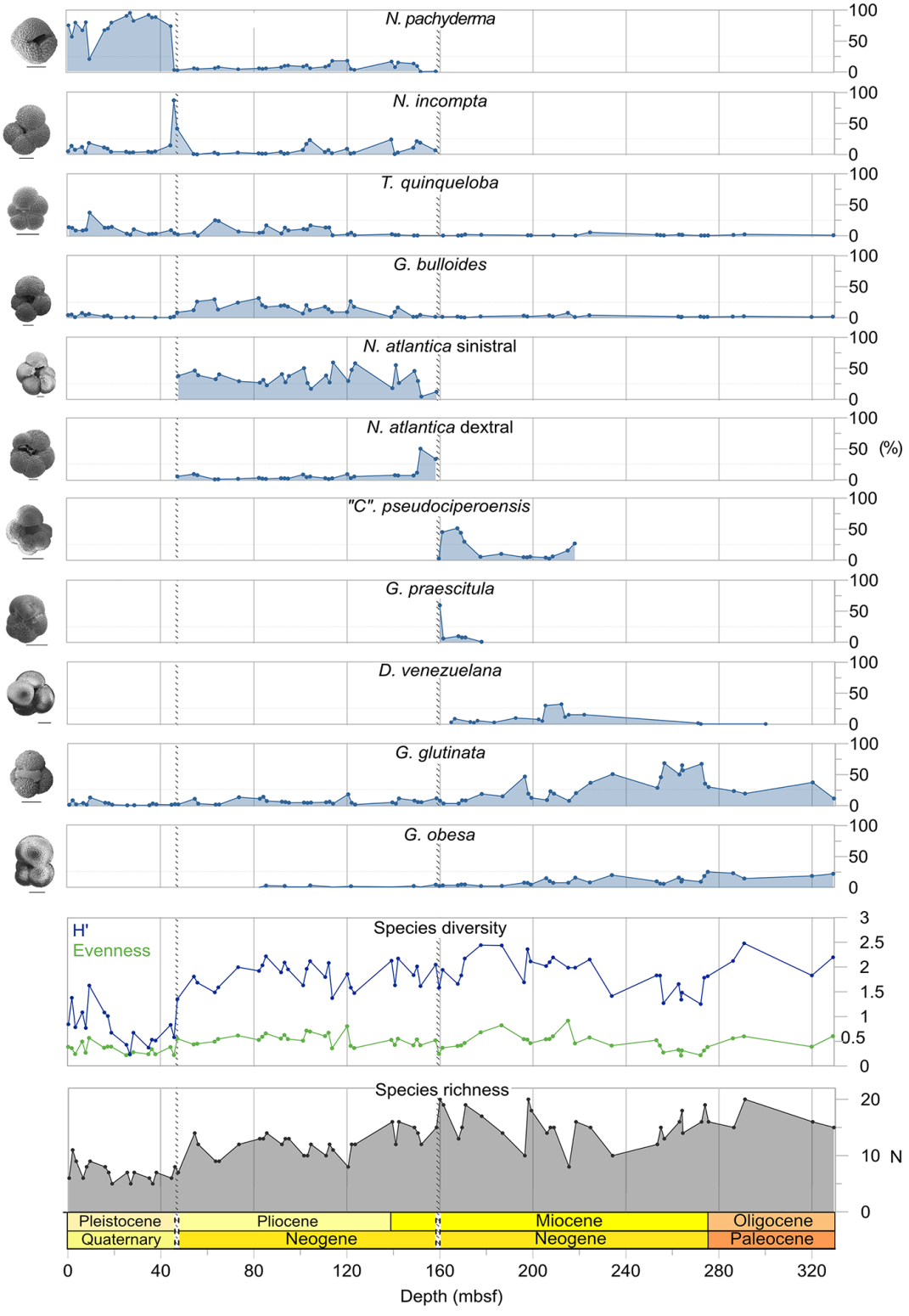

Figure 2. Summary of planktonic foraminifera metrics, including the relative abundance of 11 key species (i.e. with > 25 % relative abundance), and measures of foraminiferal preservation and assemblage diversity.

ing the age–depth control points were identified and compiled (Table 3; Appendix Tables C1 and C2). The planktonic foraminifera biostratigraphic zonation (Table 2) mainly follows the events described in Wade et al. (2011) and Raffi et al. (2020). As planktonic foraminifera diversity decreases in the upper part of the studied section, increasingly fewer low-latitude bioevents are recognized. Therefore, we also apply the local high-latitude North Atlantic biostratigraphic frameworks of Weaver and Clement (1987) and Spiegler and Jansen (1989). The studied planktonic foraminifera assemblages include 8 age diagnostic marker taxa and 19 recognized (calibrated) taxa from the late Oligocene to the Quaternary (Table C1). Marker taxa are highlighted in bold; all ages are included in GTS2020, except the ages given by Weaver and Clement (1986). The calcareous nannofossil biostratigraphic zonation follows the events described by Martini (1971) and Raffi et al. (2006, 2020). The studied calcareous nannofossil assemblages include 3 age diagnostic marker taxa and 14 recognized (calibrated) taxa from the early Miocene to the Quaternary (Table C2).

The distribution of calibrated bioevents reveals that sedimentation at Site 407 has been interrupted by numerous hiatuses (Fig. 3; Table 3), with the largest hiatus lasting from about 8.9–16.5 Ma between Samples 18R-2, 56–58 cm (160.06 m b.s.f.), and 18R-1, 56–58 cm (158.56 m b.s.f.), separating the late early Miocene from the late Miocene. Other likely hiatuses occur in the Pleistocene (0.36–1.49 Ma), Pleistocene–Pliocene boundary (1.98–3.39 Ma), late Miocene (5.56–8.16 Ma), and early Miocene (21.43–22.71 Ma). Sediment accumulation rates are around 20 m Myr^{-1}. in the early Miocene (H–I interval) and late Oligocene (J–K interval) (Fig. 3). A lower sedimentation rate of ca. 11 m Myr^{-1} is recorded in the late Miocene (F–G interval). Rates increase to ca. 44 m Myr^{-1} in the late Miocene-Pliocene (D–E interval), reaching the highest sedimentation rate at Site 407 in the Pleistocene (ca. 78 m Myr^{-1}.; B–C interval).

4 Discussion

4.1 Planktonic foraminifera assemblages and diversity at Site 407 during the Neogene to Quaternary

The assemblage analysis presented here, which is a development after the study by Poore (1979), allows a more quantitative analysis of Neogene plankton diversity patterns in the Site 407 for the northern North Atlantic record. Planktonic diversity and species richness were calculated to constrain diversity increases and decreases in response to late Oligocene to Quaternary climate events. Planktonic foraminifera are present in all samples (except Sample 407-24R-2; 56–58 cm) and show highly variable temporal changes in assemblage composition and relative abundance throughout the past 25 million years (Tables 1 and A1). A distinct faunal change occurred after the middle Miocene, involving increasing species losses and a general diversity decrease, suggestive of strong environmental forcing. These patterns are further detailed at the taxon level below.

Oligocene and early Miocene assemblages are diverse (average $H' = 1.9$) and relatively even (average evenness of 0.49), with higher abundances of *G. glutinata* and *G. obesa* (Fig. 2; Table B1). In the middle Miocene (160.06–171.06 m b.s.f.), notable changes in species composition and fluctuations in diversity occur, including the temporary appearance of low-latitude species (*T. trilobus*, *T. immaturus, T. bisphericus, G. ruber, G. praemenardii*, and *G. archeomenardii*), albeit in low numbers (Tables 2 and A1) between 16–17 Ma (Fig. 3). This is most likely related to the Miocene Climatic Optimum (MCO), as indicated in the $\delta^{18}O$ record shown in Table 1. The shift in evenness reflects the increasing dominance of a few species through this interval, including "*Ciperoella*" *pseudociperoensis*, still of uncertain generic affiliation, which jumps to contributing up to 51 % of the assemblages between 160.06 and 171.06 m b.s.f. (Fig. 2). *Globorotalia praescitula* also appears during this interval. At 160.06 m b.s.f., evenness is 0.2 and caused by a high abundance of *G. praescitula* making up 60 % of the assemblage.

From the late Miocene onwards, the pattern of Shannon H' diversity (Fig. 2), which records decreased species richness and evenness from 158.56 m b.s.f., suggests that planktonic foraminifera were possibly experiencing stress related to global cooling (Table 1). Neogloboquadrinids increasingly dominate assemblages from this point, with up to 63 % of Pliocene assemblages represented by *N. atlantica* (sinistral and dextral) and up to 96 % of assemblages represented by *N. pachyderma* in the Pleistocene. The first IRD, in the form of rare quartz grains, is tentatively placed at 152.03 m b.s.f. and assigned to the late Miocene (Table 1), suggesting an initial but temporary export of clast-carrying icebergs from early Greenlandic glaciers during the middle to late Miocene (St. John and Krissek, 2002). IRD becomes abundant throughout the Pleistocene around 1.77 Ma (from 46.06 m b.s.f. upwards), likely coincident with the persistent ice sheet cover on Greenland from the early Pleistocene.

Currently, and throughout the Quaternary period, both northern and southern Atlantic high-latitude regions exhibit comparable planktonic foraminifera communities, including *Neogloboquadrina pachyderma*, *Globigerina bulloides*, and *Turborotalita quinqueloba* (e.g. Bé, 1960a; Kennett, 1968; Vilks, 1970; Tolderlund and Bé, 1971; Hemleben et al., 1989; Eynaud, 2011). However, during the late Neogene, these high-latitude regions displayed different assemblages, particularly concerning the neogloboquadrinids. The Neogene North Atlantic region predominantly featured various neogloboquadrinids, with assemblages being dominated by the relatively large and morphologically variable morphospecies *N. atlantica*, whereas only *N. acostaensis* and *N. pachyderma* are documented in the Atlantic sector ((sub)Antarctic) of the Southern Ocean (55–90° S; e.g. DSDP Leg 28, Kaneps, 1975; DSDP Leg 35, Rögl, 1976;

Table 2. Planktonic foraminifera (PF) and calcareous nannofossil (NN) bioevents and zonation schemes at Site 407. Zonation schemes used for PF (grey) are Wade et al. (2011), Weaver and Clement (1986), Spiegler and Jansen (1989), and Poore (1979). Zonation schemes used for NN (grey) are Martini (1979) and Steinmertz (1979). The dark green zonation is a proposed PF zonation based on the zones from Spiegler and Jansen (1989), Wade et al. (2011), and Weaver and Clement (1986). New zones are the *G. inflata* partial range zone (PRZ) between the FO of *G. inflata* and the FO of "modern" *N. pachyderma*, the *G. puncticulata* Zone based on the FO of *G. puncticulata* and *G. inflata*, the *N. praeatlantica* Zone spanning the FO and LO of *N. praeatlantica*, and the "*C.*" *pseudociperoensis* Zone based on the FO and LO of this species. The stratigraphic age (epochs and periods) is based on the PF and NN events from Fig. 3.

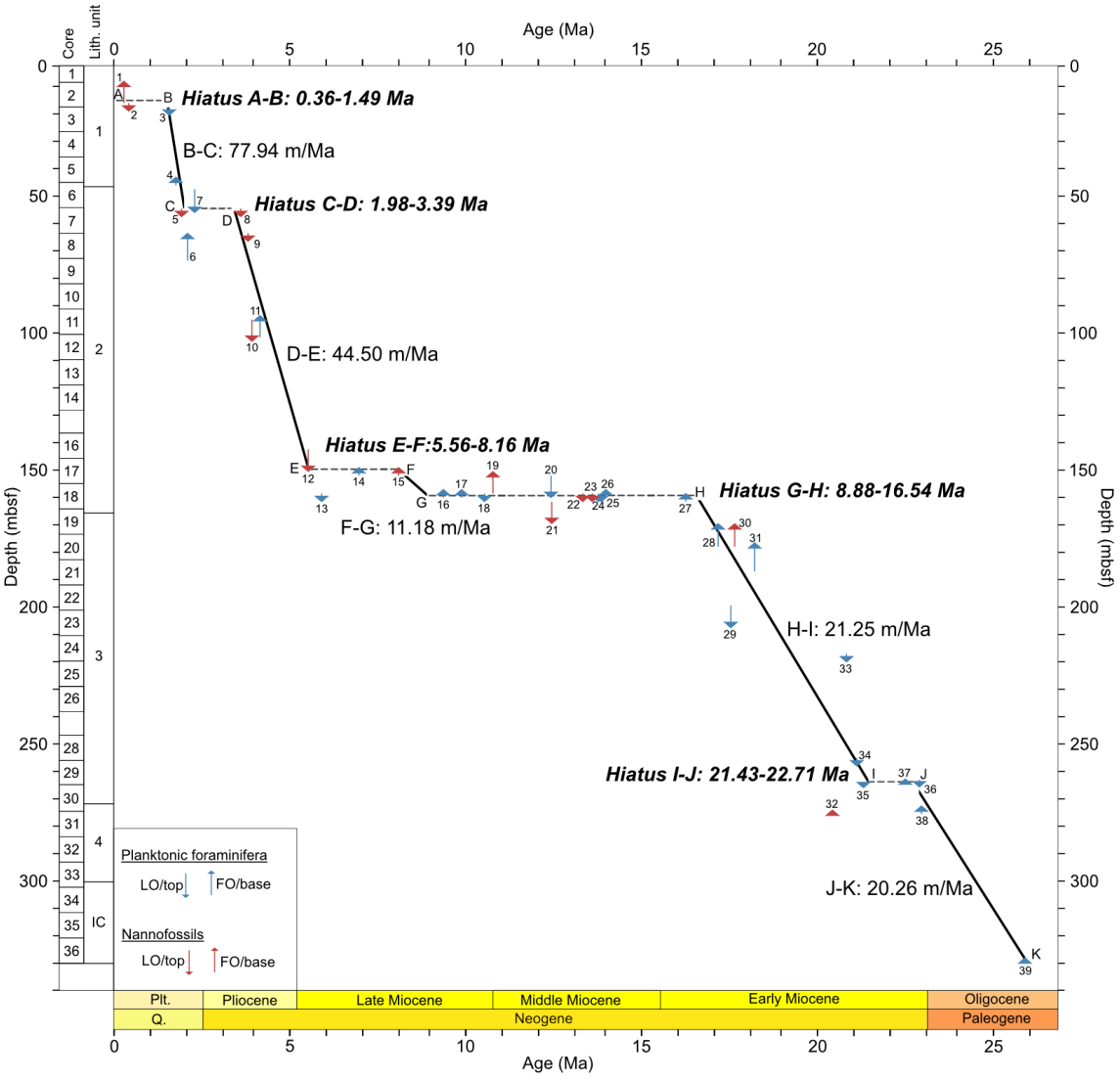

Figure 3. Age–depth plot based on our revised Site 407 planktonic foraminifera and nannofossil biostratigraphy, with core numbers and lithologic units (left column). Depth is given in metres below seafloor (m b.s.f.). Plt is for Pleistocene, and Q is for Quaternary. Age–depth control points used to calculate sedimentation rates are listed in Table 3. All ages are on GTS2020. Planktonic foraminifera and calcareous nannofossil events are indicated by the numbers 1–39 (Appendix Tables C1 and C2).

DSDP Leg 71, Krasheninnikov and Basov, 1983; ODP Leg 114, Pujol and Bourrouilh, 1991; ODP Site 1123, Crundwell and Nelson, 2007). To our knowledge, *N. atlantica* has not been recorded in the southern Indian Ocean or South Pacific (Berggren, 1992; Martin Crundwell, personal communication, 2023), although it has been recorded in the Pacific on the Californian margin (Dowsett and Poore, 2000). Further work is required to establish the distribution of *Neogloboquadrina praeatlantica* and *Neogloboquadrina atlantica* and the extent of possible endemism in the North Atlantic and Mediterranean region (e.g. Hilgen et al., 2000; Lirer et al., 2019).

4.2 Integrated planktonic foraminifera and calcareous nannofossil biostratigraphy and chronology

The planktonic foraminifera zonation schemes applied here are based on age diagnostic events described in Wade et al. (2011), Raffi et al. (2020), Weaver and Clement (1987), and Spiegler and Jansen (1989) (Tables 4 and C1). Application of a zone was only permitted when primary zonal markers defining the base and top of a zone were recorded. The nannofossil events are based on Martini (1971) (Tables 2 and C2). This section will describe the integrated biostratigraphy per epoch.

Table 3. DSDP Site 407 age–depth control points, sedimentation rates, and hiatus lengths. Calcareous nannofossil events are denoted by "N" and planktonic foraminifera events by "F".

	Event	Type of event	Metres below seafloor	Age (Ma)	Interval	Sedimentation rate (m Myr^{-1})	Hiatus length (Ma)
A	LO of *P. lacunosa*	N	17.55	0.43	A–B		1.13
B	LO of *N. acostaensis*	F	19.05	1.58	B-C	77.94	
C	LO of *D. brouweri*	N	56.06	1.93	C–D		1.41
D	LO of *Sphenolithus* spp.	N	56.06	3.61	D–E	44.50	
E	LO of *D. quinqueramus*	N	149.06	5.53	E–F		2.6
F	FO of *D. quinqueramus*	N	150.56	8.1	F–G	11.18	
G	FO of *N. pachyderma*	F	158.56	9.89	G–H		7.66
H	FO of *G. archeomenardii*	F	160.06	13.86	H–I	21.25	
I	LO of *P. kugleri*	F	256.56	21.12	I–J		1.28
J	LO of *C. ciperoensis*	F	264.2	22.9	J–K	20.26	
K	FO of *P. pseudokugleri*	F	329.5	25.9			

4.2.1 Late Oligocene and early Miocene

The base of the Site 407 sequence (329.5 m b.s.f.) recorded one planktonic foraminifera age marker, namely the presence of *Paragloborotalia pseudokugleri*. Other late Oligocene markers such as *P. opima* and *Chiloguembelina cubensis* (both Zone O5) are absent, placing the base in Zone O7 (Wade et al., 2011). The Oligocene/Miocene boundary is placed at the FO of *Paragloborotalia kugleri* (Sample 407-30R-2; 56–58 cm; 274.06 m b.s.f.), marking the base of Zone M1. The earliest Miocene Zone M1 extends to 28R-3, 56–58 cm (256.56 m b.s.f.), based on the LO of *P. kugleri*. The FO of *Globoquadrina dehiscens* at 264.2 m b.s.f. marks the boundary between zones M1a and M1b. The LO of *Ciperoella ciperoensis* is a M1a subzone marker (Wade et al., 2011), but at Site 407, the LO of *C. ciperoensis* (264.2 m b.s.f.) is recorded in the same depth as the FO of *G. dehiscens* (264.2 m b.s.f.). Zone M2 is commonly based on the LO of *P. kugleri* and the FO of *Globigerinatella* sp. (Wade et al., 2011); however, *Globigerinatella* sp. is absent at Site 407. Therefore, the boundary between zones M2 and M3 cannot be determined. Accessory datums in this interval are the LO of *Tenuitella munda* (407-24R-3; 56–58 cm; 218.6 m b.s.f.), the FO of *Globorotalia zealandica* at 171.06 m b.s.f. (19R-3; 56–58 cm), and the LO of *Catapsydrax dissimilis* at 206.1 m b.s.f. (407-23R-1; 56–58 cm). This interval is possibly interrupted by a minor hiatus (I–J; Fig. 3) of just over 1 Myr (21.43–22.71 Ma), as indicated by the LO of *C. ciperoensis* and FO of *G. dehiscens* recorded at the same depth. Common age diagnostic species such as *Fohsella* spp. and *Praeorbulina* spp., as well as the base of *Orbulina suturalis*, are missing at Site 407, making it difficult to assign any of the early Miocene zones of Wade et al. (2011).

The Oligocene/Miocene boundary cannot be precisely identified in the nannofossil record due to the reworking of Paleogene specimens into Miocene sediments. Specifically, *Zygrhablithus bijugatus* (from the Paleocene–Oligocene) and *Chiasmolithus altus* (from the Eocene–Oligocene) have been found in Miocene layers up to 161.56 m b.s.f. This reworking obscures the true LO of *Helicosphaera recta*, which marks the base of NN1 (early Miocene). Additionally, *Sphenolithus ciperoensis*, another early Miocene marker, is absent in all samples. The FO of the *Helicosphaera ampliaperta* group at 275.56 m b.s.f. (Sample 407-30R-3; 56–58 cm) indicates the earliest Miocene (Raffi et al., 2020). However, it is important to note that in the northwestern Atlantic the FO of *H. ampliaperta* is not considered a reliable datum (Fabbrini et al., 2019), corresponding with it being an outlier in our Site 407 age–depth model (Fig. 3). The late Oligocene and early Miocene sediments lack clear nannofossil age markers but contain a few accessory markers. The FO of *Discoaster druggii* (referred to as *Discoaster* cf. *druggii* in this study) at 263.06 m b.s.f. (Sample 407-29R-1; 56–58 cm) marks the base of zone NN2. *Triquetrorhabdulus carinatus*, which indicates the top of NN2, is extremely scarce and occurs sporadically throughout the sequence. The boundaries between NN2 and NN3 and NN3 and NN4 cannot be determined due to the absence of key age diagnostic events, such as the FO of *Sphenolithus belemnos*. However, *Sphenolithus heteromorphus*, an additional marker for NN3, is present but rare and scattered.

4.2.2 Middle Miocene (160.06–171.06 m b.s.f.)

No primary age diagnostic planktonic foraminifera are recorded in the middle Miocene. However, multiple accessory events are present. *Globorotalia archeomenardii/praemenardii*, *G. praescitula*, *Paragloborotalia acrostoma*, and *P. mayeri* are recorded at 160.06 m b.s.f. *Globorotalia archeomenardii/praemenardii* has its FO in the middle Miocene Zone M5b/M6, and *G. praescitula* has its LO in

Zone M7 (Raffi et al., 2020). The range of *Paragloborotalia acrostoma* extends into Zone M5 and *P. mayeri* into Zone M10 (Leckie et al., 2018). Thus, this interval is tentatively placed in the middle Miocene.

Likewise, the nannofossil data did not record any age diagnostic species in the middle Miocene. The presence of *Sphenolithus heteromorphus* and *Helicosphaera magnifica* at 171.06 m b.s.f., which are known globally to range from the middle part of zone NN2 to the lower part of NN4 (Boesiger et al., 2017), provides some stratigraphic control. The last recorded occurrences of *Sphenolithus puniceus, Cyclocargolitus floridanus, Helicosphaera ampliaperta*, and *S. heteromorphus* all occur at 160.06 m b.s.f., the same horizon at which a clustering of planktonic foraminifera disappearances occurs, which implies a large hiatus between (Table 3), which our age model suggests spans approximately 8 million years (8.88–16.54 Ma). The large hiatus indicates either sediment removal or a period of non-deposition at Site 407.

4.2.3 Pliocene and late Miocene (47.48–158.56 m b.s.f.)

The Pliocene and late Miocene sediments contain few age diagnostic species, with planktonic foraminifera assemblages being dominated by neogloboquadrinids. The temperate/subpolar and Nordic Seas events by Weaver and Clement (1986) and Spiegler and Jansen (1989) are somewhat applicable to this interval (Fig. 5). The Weaver and Clement (1987) Pliocene zonation is divided into five zones, of which only one is applicable on the material from Site 407, namely the *Globorotalia inflata* partial range zone (PRZ). This is the zone between the FOs of *Globoconella inflata* (1.90–2.18 Ma) and sinistrally coiled encrusted *Neogloboquadrina pachyderma* (1.66–1.77 Ma) (in our study referred to as "modern" *N. pachyderma*). At Site 407, *G. inflata* has its FO at 65.06 m b.s.f. (407-8R-2; 56–58 cm) and *N. pachyderma* at 44.56 m b.s.f. (407-6R-1; 56–58 cm). Therefore, the interval between 44.56 and 65.06 m b.s.f. is placed in the *G. inflata* PRZ (Fig. 2), corresponding to the late Pliocene Zone PL6 by Raffi et al. (2020).

The coiling change from dominantly dextral to sinistral of *N. atlantica* at 152.03 m b.s.f. (407-17R-3; 53–55 cm), which is an age-calibrated (6.8 Ma) accessory marker retained in the latest planktonic foraminifera biozonation (Wade et al., 2011; originally calibrated in the North Atlantic, Berggren et al., 1995) occurs in Zone M13b (Wade et al., 2011; Raffi et al., 2020). In the Spiegler and Jansen (1989) Nordic Seas (ODP Leg 104) zonation scheme, this change in coiling forms the boundary between the *N. atlantica* (dextral, hereafter dex.) and *N. atlantica* (sinistral, hereafter sin.) Zones and is assumed to be between 6 and 6.2 Ma. The top of their *N. atlantica* (sin.) Zone falls within PL6 (Raffi et al., 2020). In the North Atlantic *N. atlantica*'s LO is at 2.05–2.36 Ma (Weaver and Clement, 1987). This event was not used by Wade et al. (2011) on the grounds that it is likely a local event and in need of further evaluation. At Site 407, *N. atlantica* persists up to 47.48 m b.s.f., just above the Plio-Pleistocene boundary and above the C–D hiatus recognized in our data, which would imply a similar yet slightly younger age for this LO of ca. 1.8 Ma. This could be within error in the previous findings, given the uncertainty in both our sedimentation model and the position of this C–D hiatus around this horizon (1.98 to 3.39 Ma; Fig. 3 and Table 3). The *N. atlantica* (sin.) Zone thus spans 47.48–152 m b.s.f., and the Miocene/-Pliocene boundary falls within the lower part of this zone (Fig. 2). Spiegler and Jansen (1989) recorded a second *N. atlantica* coiling change involving a shift to dominantly dextral forms around 2.3 Ma. This *N. atlantica* (dex.) Zone, which overlays the *N. atlantica* (sin.) Zone at ODP Hole 644A, however, is relatively short and spans roughly 10 m of sediment. The top of this zone is placed at 1.84 Ma. A change from dominantly sinistral to dextral-coiling *N. atlantica* in the early Pleistocene is not observed in our Site 407 samples, since both sinistral and dextral *N. atlantica* go extinct when the coiling is still dominantly sinistral (Table 1). The latest Pliocene *N. atlantica* (dex.) Zone has thus far only been recorded at Hole 664A; however, the age falls within the recorded LO of *N. atlantica* in the work by Weaver and Clement (1986) (2.05–2.36 Ma), and when combined with the short duration of the Zone, it could be overlooked or not sampled at other North Atlantic sites. The presence of a hiatus at this horizon is further supported by a sharp lithological change, marking the contact between lithological Units 1 (calcareous sandy mud) and 2 (nannofossil ooze) between 46.06 and 47.48 m b.s.f. (Sample 407-6R-3; 55–58 cm). The hiatus may have removed the interval of abundant dextral-coiling *N. atlantica*, with the result producing an apparent simultaneous disappearance of both *N. atlantica* (sin. and dex.) in our Site 407 records. The presence of a latest Pliocene *N. atlantica* (dex.) Zone needs further investigation as it has the possibility of being a useful marker elsewhere in the high-latitude North Atlantic.

Another notable older neogloboquadrinid event at Site 407 is the abrupt and simultaneous appearance at 158.56 m b.s.f. of various *Neogloboquadrina* species, including *N. acostaensis*, *N. atlantica* (dex.), *N. atlantica* (sin.), *N. incompta*, and *N. praeatlantica*, together with the well-known modern polar specialist *N. pachyderma*, indicating a late Miocene age. *Neogloboquadrina acostaensis* (Wade et al., 2011) and *N. pachyderma* have their evolutionary first occurrences in Zone M13a (Raffi et al., 2020) and *N. humerosa* in Zone M13b (Raffi et al., 2020). *Neogloboquadrina humerosa* is rare and first recorded at 101.56 m b.s.f. (407-12R-1; 56–58 cm). Because of the clustering of calibrated nannofossil and planktonic foraminifera bioevents between 160.06–158.56 m b.s.f. close to these neogloboquadrinid FOs in our age–depth model (Table 3, Fig. 5), we infer that this pattern does not represent true first appearances but the presence of a major hiatus. It should be noted that the FO of the *N. pachyderma* sinistral age marker utilized in our age model is 9.37 Ma, which was calibrated in the southern Indian Ocean

(Kerguelen Plateau) (Berggren et al., 1995). This date might not be accurate in the high-latitude North Atlantic due to diachroneity between latitudes (see Lam and Leckie, 2020a). It is not possible to investigate the possibility of cross-latitude diachroneity of the *N. pachyderma* FO datum at Site 407, as the true FO of this species is lost due to the hiatus. Age calibration of the FO of *N. pachyderma* in stratigraphically complete North Atlantic Neogene sequences is thus still needed. IODP Expedition (Exp.) 395 records (Parnell-Turner et al., 2024) promise new opportunities to do this. Weaver and Clement (1986) and Spiegler and Jansen (1989) made other late Miocene observations. In the temperate North Atlantic (ODP Leg 94), Weaver and Clement (1986) recorded a change from dominantly sinistral to dextral *N. pachyderma* at 5 Ma, with their "*N. pachyderma*" remaining dominantly dextral until the latest Pliocene. With current knowledge, we can assume that the Weaver and Clement (1986) *N. pachyderma* dextral is *N. incompta*, based on modern DNA perspectives of both species (Darling et al., 2006). Nevertheless, at Site 407, *N. incompta* is also more abundant than *N. pachyderma* in the interval between 139.56-158.56 m b.s.f., after which *N. pachyderma* reaches higher abundances. Spiegler and Jansen (1989) recorded a *N. acostaensis* Zone between the FOs of *N. acostaensis* and *N. atlantica*. At Site 407, both species appear simultaneously.

In the Pliocene and late Miocene of Site 407, multiple-accessory-calibrated planktonic foraminifera bioevents exist. This includes the latest Pliocene LO of *Globoturborotalita woodi* (Wade et al., 2011; Raffi et al., 2020), which in Site 407 occurs at 54.56 m b.s.f. (7R-1; 56–58 cm), and the FO of *Globoconella puncticulata* at 95.06 m b.s.f. (11R-3; 56–58 cm). *Globoconella puncticulata* is a common marker in sediments recovered during DSDP Leg 94 around 4.06–4.30 Ma (Weaver and Clement, 1987), corresponding with PL1-2 (Raffi et al., 2020), and is used as the base of the Weaver and Clement (1987) *Globorotalia puncticulata* PRZ. The top of this PRZ is marked by the LO of *Globorotalia* cf. *crassula* (sensu Weaver), which was not recorded at Site 407. The LO of *Paragloborotalia continuosa* occurs at 142.4 m b.s.f. (Sample 407-16R-3; 56–58 cm). Although not formally calibrated, this event is reported to occur in late Miocene Zone M13, based on global data sets, including those from the North Atlantic (Leckie et al., 2018). *N. praeatlantica* (Plate 17) and *N.* cf. *acostaensis* (Plate 14; Figs. 4–6) disappear at 139.56 m b.s.f. (407-16R-1; 56–58 cm). The range of *N. praeatlantica* in the North Atlantic is still unknown. In the Mediterranean, the FO is recorded in Zone M10 (Hilgen et al., 2000a; 2005) and extends into the Tortonian (Foresi et al., 2002). The sudden disappearance of *N. praeatlantica* and *N.* cf. *acostaensis* could suggest a second hiatus. However, no sediment was recovered in Core 15 (Shipboard Scientific Party, 1979), and no noteworthy events are recorded in the nannofossil record, fragmentation intensity, or lithology supporting this.

The Pliocene–late Miocene nannofossils are similarly limited in terms of their biostratigraphic utility. Only one biozone, NN11, was recorded based on the presence of primary zonal markers. Zone NN11 is a fairly long total range zone comprising the interval between the FO and LO of *Discoaster quinqueramus* (150.56 and 149.06 m b.s.f., respectively), with an age calibration of about 8.10–5.53 Ma (Raffi et al., 2020). This corresponds broadly with the shift from dominantly dextral to sinistral coiling in *N. atlantica* calibrated to 6.8 Ma at 150.56 m b.s.f. Multiple calibrated accessory calcareous nannofossil events are recorded (Table B1), which contribute to the age model. *Discoaster hamatus*, the marker for the base and top of NN9; *Catinaster coalitus*, the marker for the base of NN8; and *Discoaster kugleri*, the marker for the base of NN7 all have a short-term range in the late Miocene that were not found in this study because the base of the late Miocene sequence is most likely younger than the ranges of these species. *Discoaster asymmetricus* and *Ceratolithus rugosus*, the marker species for the top of NN13 and NN12, respectively, were not recorded in any samples, most likely because they are low-latitude taxa.

4.2.4 Pleistocene (0.57–46.06 m b.s.f.)

The Pleistocene interval lacks any age diagnostic planktonic foraminifera species that delineate established low-latitude biozones. One event that is considered to be a useful marker in high northern latitudes is the first common occurrence (FCO) of "modern" *N. pachyderma* (Plate 16; Figs. 3–12), which are larger and more encrusted than early morphotypes (Plate 16; Figs. 1, 2). In Site 407, this occurs at 44.56 m b.s.f. (407-6R-1; 56–58 cm), after which the species dominates assemblages to the top of the sequence. In the high-latitude North Atlantic, the FCO of *N. pachyderma* is around 1.7 Ma (subchron Olduvai at DSDP Site 611; Weaver and Clement, 1987). The low- to mid-latitude marker for the base of Zone PT1a (also the Pliocene/Pleistocene boundary), *Globigerinoides fistulosus*, is not present at Site 407; thus, this zone cannot be recognized (Wade et al., 2011). We can, however, approximate the start of the Pleistocene by the first occurrence of abundant lithic clasts at 46.06 m b.s.f. (Sample 407-6R-2; 56–58 cm), implying the arrival of ice rafted debris (IRD) that is indicative of extensive Northern Hemisphere glaciation. This is represented by a downcore lithological transition from calcareous sandy mud to nannofossil ooze at 46.3 m b.s.f. (Shipboard Scientific Party, 1979). The IRD persists to the top of the sequence. A secondary event in the Pleistocene is the LO of *N. acostaensis* at 19.05 m b.s.f. (407-3R-3, 55–58 cm) that occurs in PT1a based on age-calibrated data from Raffi et al. (2020). However, the boundary between Zone PT1a and PT1b cannot be determined because the marker *Globorotalia tosaensis* is missing. The Arctic Zone 1 (AZ1) corresponds to the *N. pachyderma* (sin.). Zones of Weaver and Clement (1986) and Spiegler and Jansen (1989) span the entire Quaternary.

The calcareous nannofossil record divides the AZ1 into the early and late Pleistocene based on two datums, namely the LO of *Pseudoemiliania lacunosa* at 17.55 m b.s.f. and the FO of *Gephyrocapsa huxleyi* at 9.56 m b.s.f. (Table B1). A possible erosional unconformity (A–B; Fig. 3) in the late Pleistocene caused a hiatus of about 1 Ma (0.36–1.49 Ma), based on the LOs of *P. lacunosa* and *N. acostaensis*. A similar erosional unconformity is found at ODP Site 918, causing a hiatus of about 320 kyr (1.39–1.71 Ma) (St. John and Krissek, 2002). The presence of *G. huxleyi* in the interval from 9.56 m b.s.f. (407-2R-3; 56–58 cm) to the top of the core (407-1R-1; 57–60 cm) represents Zone NN20/21 (Martini, 1971), where *G. huxleyi* and *Gephyrocapsa* spp. can be found in high numbers (Fig. S3). The early Pleistocene is based on Zone NN19/20 (Martini, 1971), based on the interval between the LO of *Discoaster brouweri* at 56.06 m b.s.f. (407-7R-2; 56–58 cm) and the LO of *P. lacunosa* at 17.55 m b.s.f. (407-3R-2; 55–58 cm). An accessory event in AZ1 is the LO of *Helicosphaera sellii* at 44.56 m b.s.f. (407-6R-1; 56–58 cm) calibrated to 1.24 Ma (Raffi et al., 2020).

4.2.5 Sedimentation rates and identified hiatuses

Sedimentation rates at Site 407 varied considerably over time; in the late Oligocene and early Miocene, rates were around 20 m Myr^{-1}, decreasing to 11 m Myr^{-1} in the late Miocene, then increasing to 44 m Myr^{-1} in the late Miocene–Pliocene, and peaking at 78 m Myr^{-1} in the Pleistocene (Fig. 3). Initial rates calculated by Shor and Poore (1979) show 15 m Myr^{-1} in the upper Oligocene to lower Miocene and 45 m Myr^{-1} in the upper Miocene/Pliocene at Site 407, which are comparable to the rates from this study. At the nearby Site 408 (see Fig. 1), the rates were 17 and 35 m Myr^{-1}, respectively. On the eastern flank of the Reykjanes Ridge, the average sediment accumulation rates in the Pleistocene were higher compared to the western flank up to 120 m Myr^{-1} (DSDP Site 114; Laughton and the Exp. 12 Scientific Party, 1972). This difference is attributed to sediment drift formation (e.g. Björn Drift) occurring along rises on the western sides of the basins related to bottom-water circulation and the Coriolis force (see Wold, 1999, for more details), whereas the sediment drift on the western flank of Reykjanes Ridge (Snorri Drift) has an indistinct morphology possibly related to low sediment supply (Wold, 1999). West of Site 407, on the Greenland continental rise (ODP Site 918), sedimentation rates were 22 m Myr^{-1} in the Miocene, reaching 199 m Myr^{-1} in the Pliocene and then decreasing to approximately 80 m Myr^{-1} from the mid-Pliocene to present (Larsen et al., 1994a). Sedimentation on the Greenland continental rise is influenced by regional factors (Rasmussen et al., 2003). Overall, increased sediment supply after the mid-Pliocene resulted from the uplifted GSR and turbidity currents from Iceland, with terrigenous input from Iceland increasing during the Pleistocene (Wold, 1999).

The hiatuses identified at Site 407 likely reflect periods when bottom waters were vigorously eroding sediments, as reflected by the sudden increase in fragmentation in the middle Miocene, which may represent winnowed transported material (49.5 %; 160.06 m b.s.f.) (Fig. 3). The large middle Miocene hiatus is widespread in the region of Site 407 (DSDP Sites 406, 408, and 112; Shor and Poore, 1979) and in the Iceland–Faroe Ridge (IFR) (DSDP Sites 336 and 352; Talwani and Udintsev, 1976), reflecting the initiation of overflow water through the IFR as a proto-ISOW as the GSR became deeper and wider (Uenzelmann and Neben, 2018) (Fig. 1).

In the late Miocene, deposition restarted at Site 407, as well as at other sites along the path of the overflow waters (Sites 403–406, 408, 114), so the renewal of the deposition might be related to the increasing depth of the Reykjanes Ridge crest (Shor and Poore, 1979). Strong bottom waters occurred throughout the late Miocene up to the late Pliocene, as reflected in the high fragmentation throughout this period (about 62 %). Planktonic foraminifera tests are well preserved in this interval and do not show signs of corrosion. The Pliocene–Pleistocene hiatus only occurred on the western flank of the Reykjanes Ridge (Sites 407 and 408) and may be correlated with the uplift of the ridge crest (Shor and Poore, 1979) and an increase in ISOW and DSOW. That only minor test fragmentation recorded in the Pleistocene could be interpreted to suggest that the bottom waters were not as erosive then as during the Miocene and Pliocene. On the other hand, the dominance of *N. pachyderma* in the Pleistocene, which has a very robust dissolution resilience test, could explain the reduced fragmentation.

Changes in GSR sill depth have influenced the bottom-water exchange between the North Atlantic and the Nordic Seas throughout the Late Cenozoic, with different segments of the GSR deepening at different times (Wright and Millers, 1996; Uenzelmann-Neben and Gruetzner, 2018). An important step in this process was subsidence of the Iceland–Faroe Ridge below sea level sometime in the Oligocene; this allowed the initiation of strong bottom waters via a proto-ISOW during the Neogene (Fig. 1) that entrained large quantities of sediment, eroding and depositing it as hiatuses/sediment drifts in the North Atlantic (Nilsen, 1983; Uenzelmann-Neben and Gruetzner, 2018). This continued periodically during the late Oligocene and Miocene (Uenzelmann-Neben and Gruetzner, 2018).

4.2.6 Suggestions for a revised planktonic foraminifera zonation for the northeastern Atlantic

Since the majority of biostratigraphic frameworks are based on low-latitude taxa, their applicability at Site 407 does not work beyond Zone M1, after which all the zonal markers from Wade et al. (2011) are absent. This section will discuss a revised planktonic foraminifera zonation for the northeastern Atlantic based on the zonation schemes by Wade et

al. (2011), Weaver and Clement (1986), and Spiegler and Jansen (1989). A summary of these schemes is shown in Fig. 3.

The Neogene planktonic foraminiferal zonation has stayed relatively stable over the past decades, as several key markers initially introduced by Bolli (1957) and Banner and Blow (1965) remain in current zonal schemes such as the low-latitude scheme by Wade et al. (2011). The standard set of low-latitude zones has changed from Paleogene ("P") and the Neogene ("N") zones, applied by Poore (Blow, 1969; Kennett and Srinivasan, 1983), to the "O", "M", "Pl", and "PT" zones for the Oligocene, Miocene, Pliocene, and Pleistocene, respectively (Berggren et al., 1995; Wade et al., 2011). Since the Poore (1979) Site 407 study, biostratigraphic frameworks have developed considerably. Moreover, the stratigraphic range of various species have been extended, and new age-calibrated marker species have been identified, based on new observations (Olsson et al., 1999; Pearson et al., 2006; Wade et al., 2018).

The application of the Weaver and Clement (1987) zonation based on the DSDP Leg 94 results (North Atlantic; ca. 38–52° N), has improved age control for the late Miocene and Pliocene by applying several additional palaeomagnetically calibrated events, e.g. the change in coiling direction (dextral to sinistral) in *N. atlantica*, the LO of *G. puncticulata*, the FO of *G. inflata*, and the FCO of *N. pachyderma*. Nonetheless, only two of the Weaver and Clement (1986) zones work at Site 407 (Fig. 2); these include the *N. pachyderma* Zone and the *G. inflata* PRZ, as the zonal marker *Globorotalia* cf. *crassula* that delineates other zonal boundaries is absent at Site 407. The Spiegler and Jansen (1989) alternative zonation scheme, which was based on records from the Nordic Seas (Vøring Plateau; ODP Leg 104), relies more heavily on neogloboquadrinids, and from this, we can apply the *N. atlantica* (dex.), *N. atlantica* (sin.), and *N. pachyderma* Zones, spanning the late Miocene to Quaternary, to Site 407 sediments. A downside of the Spiegler and Jansen zonation is the age resolution; the lower diversity and longer evolutionary ranges of species at higher latitudes, including *N. atlantica* (sin.), results in zones of long time duration.

A proposed zonation for Site 407 involves a combination of the zones by Spiegler and Jansen (1986), Wade et al. (2011), and Weaver and Clement (1986), with three additional local events, i.e. *Globoconella puncticulata* Zone, *Neogloboquadrina praeatlantica* Zone, and the "*Ciperoella*" *pseudociperoensis* Zone (Table 2). These zones are defined as the biostratigraphic interval characterized by the FO and LO of the nominate taxa, based on their distinct stratigraphic range. In particular, the *G. puncticulata* and *N. praeatlantica* Zones increase the resolution of the *N. atlantica* sinistral "superzone". Additionally, a fourth zone could be added between the LO of *Tenuitella munda* and the FO of "*C.*" *pseudociperoensis*, covering the whole sequence. However, the large middle/late Miocene hiatus and the missing sediments from Core 15R impact the extent of the zones; i.e. the true LO of "*C.*" *pseudociperoensis* and true FO of *N. praeatlantica* fall within the large hiatus, and the true LO of *N. praeatlantica* is most likely in Core 15R. Furthermore, both species need more investigation as their geographic and stratigraphic extent are not known yet (see the "Taxonomic notes" for "*C.*" *pseudociperoensis* and Sect. 4.2 for *N. praeatlantica*).

Other aspects of Poore's biostratigraphy, however, remain the same after our work, including the inability to differentiate planktonic foraminifera Zones N5 and N6 (here updated to Zones M2 and M3, respectively; Raffi et al., 2020) due to the absence of *Globigerinatella* sp. at Site 407. The explanation for the decreasing biostratigraphic resolution is a general decrease in faunal diversity (Figs. 4 and 5) and increasing endemism particularly related to *N. pachyderma* dominance forced by Neogene climate change. This likely explains the absence or extreme scarcity of key low-latitude marker species such as the *Fohsella* lineage (middle Miocene Zones M7–M10), *Globigerinatella* sp. (base M3), *Praeorbulina* (Zone M5; Wade et al., 2011), and *Orbulina*. All the Pliocene and Pleistocene markers are missing, namely FO *Globorotalia tumida*, LO *Globorotalia margaritae*, LO *Sphaeroidinellopsis seminulina*, LO *Dentoglobigerina altispira*, LO *Globorotalia miocenica*, LO *Globigerinoidesella fistulosa*, and LO *Globorotalia tosaensis* (Wade et al., 2011). Other species that might have been present could be missing in the large hiatuses, e.g. the FO of *Globoturborotalita nepenthes* (base of M11; Wade et al., 2011). This species has been recorded at other sites in the North Atlantic. At DSDP Site 408 and Holes 410 and 410A, their abundance is sparse to few (Poore, 1979). It is more common on the Rockall Plateau at ODP Hole 982B (Flower, 1999), DSDP Sites 404 and 406 (Murray, 1979), and DSDP Leg 81 (Huddlestun, 1984). It seems more likely that *G. nepenthes* is absent at higher North Atlantic latitudes because it is a warm-water species (Huddlestun, 1984), confirmed by its absence in the East Greenland Margin (ODP Leg 152; Spezzaferri, 1998), where the middle Miocene record is continuous (compared to Site 407). We largely agree with the Poore (1979) species level assignment based on his SEM images; however, many changes have occurred on the genus level as will be discussed in the next section.

4.3 Taxonomic and biostratigraphic developments since Poore's 1979 study

Several aspects of planktonic foraminifera taxonomy and systematics, and their use in biostratigraphy, have changed in the 50 years since the Poore (1979) study (Schiebel et al., 2018). First, following developments presented in the Paleocene, Eocene, and Oligocene taxonomic atlases (Olsson et al., 1999; Pearson et al., 2006; Wade et al., 2018), taxonomic frameworks are now underpinned by the principle of quasi-conservativism in wall textures (Pearson, 2018), i.e. that spinose and non-spinose groups have independent origins that can be traced forward from the early Paleocene

(Morard et al., 2022) and that microperforates may include multiple separate origins from benthic ancestors (Leckie 2009; Pearson 2018). Species that have remained within the same genus for the past 50 years are *Neogloboquadrina* spp., *Turborotalita quinqueloba*, *Globigerinita glutinata*, *G. uvula*, *Globorotalia scitula*, *G. praescitula*, *G. archeomenardii/praemenardii*, *G. hirsuta*, *G. truncatulinoides*, *G. crassaformis*, and *G. zealandica* (Kennett and Srinivasan, 1983; Brummer and Kucera, 2022).

In the original Site 407 study, many species were classified in either *Globigerina* or *Globorotalia*. The biggest change concerns the genus *Globigerina* (Table 4). In the original study, many species were classified as *Globigerina*; e.g. *G. apertura*, *G. ciperoensis*, *G. connecta*, *G. decoraperta*, *G. euapertura*, *G. galavisi*, *G. obesa*, *G. ouachitaensis*, *G. pseudociperoensis*, *G. tripartita*, and *G. woodi* were initially classed as *Globigerina*. Nowadays, these species are placed in *Ciperoella* (*C. ciperoensis*), *Globoturborotalita* (*G. connecta*, *G. decoraperta*, *G. euapertura*, *G. ouachitaensis*, and *G. woodi*), *Dentoglobigerina* (*D. galavisi* and *D. tripartita*), and *Globigerinella* (*G. obesa*). *Globigerina pseudociperoensis*, still of uncertain generic affiliation, is tentatively placed in the genus *Ciperoella* (see the "Taxonomic notes" and Plate 2) and is still an ongoing topic for the upcoming Neogene atlas. *Globigerina* itself has now been reduced to a restricted set of species that share a pseudocancellate spinose wall texture forming ridges and a high-arched umbilical aperture bordered by an imperforate rim (Plate 5) (Spezzaferri et al., 2018; Brummer and Kucera, 2022; Fabbrini et al., 2023), while Miocene species referred by Poore to *Globoquadrina* (i.e. *G. altispira*, *G. baroemoenensis*, *G. larmeui*, and *G. venezuelana*) are now placed in *Dentoglobigerina* (Wade et al., 2018b) (Plates 3 and 4).

The genus *Globorotalia* has also undergone major changes. In the original study, *Globorotalia acrostoma, G. birnageae, G. continuosa, G. inflata, G. kugleri, G. mayeri, G. miotumida, G. minutissima, G. munda, G. nana, G. pseudokugleri, G. puncticulata*, and *G. siakensis* were classed as *Globorotalia* by Poore and are now placed in *Globoconella* (*G. inflata, G. miotumida,* and *G. puncticulata*), *Paragloborotalia* (*P. acrostoma, P. birnageae, P. continuosa, P. kugleri, P. mayeri, P. nana, P. pseudokugleri,* and *P. siakensis*), and *Tenuitella* (*G. minutissima* = *T. clemenciae*) (Table 5).

The genus *Globigerinoides* has also undergone considerable revision. After fossil and genetic evidence identified polyphyly in the group, species are now assigned to either *Globigerinoides* (*G. ruber*) or *Trilobatus (T. bisphericus*, *T. immaturus, T. quadrilobatus*, and *T. triloba*) (Spezzaferri et al., 2015).

Making a direct comparison between the Poore (1979) study and this study is not straightforward as both studies used a slightly different methodology, i.e. in the different size fractions observed (> 149 µm in the original and > 125 µm, in addition to 63–125 µm, in this study) and in determining species abundance (estimates vs. relative abundance counts, respectively), which means Poore's study recorded fewer small species such as *Tenuitellita fleisheri*. The differences between taxonomic assignment in the two studies are described in more detail below and illustrated in Table 4.

Species recognized in the Poore (1979) Site 407 range chart (Table 4) that were not found in this study are *Paragloborotalia opima*, *Globigerinoides primordius*, *Globoturborotalita druryi*, *Globorotalia margaritae*, *G. ventriosa*, *G. exserta*, *Globoconella miozea*, *Globigerina bulbosa*, *Beella praedigitata*, *Globigerina martini*, *Sphaeroidinellopsis seminulina*, and *Hastigerina pelagica*. We agree with the identification of *G. primordius*, *G. druryi*, *G. margaritae*, *G. exserta*, *G. miozea*, *S. seminulina*, and *H. pelagica* based on their holotype images and the images from Poore (1979) but disagree with the identification of *G. ventriosa* and *G. bulbosa*. The holotypes of both *G. ventriosa* and *G. bulbosa* are sketches, making it difficult evaluate the utility of these species. *Globorotalia ventriosa* seems to have more curved sutures (Ogniben, 1958) than the specimens from Poore (1979; Plate 4; Figs. 10–12), and the *Globigerina bulbosa* holotype's (LeRoy, 1944) final chamber is very bulbous and ovate, comprising the bulk (> 50 %) of the test, whereas the Poore (1979) *G. bulbosa* final chamber is more globular, making up roughly 50 % of the test. Furthermore, no images of *P. opima* and *B. praedigitata* are presented in Poore (1979), making it impossible to determine whether we agree or disagree with his identification.

Species recognized in this study but not found in material from Poore (1979) are *T. fleisheri* (Plate 21; Figs. 9–12), *C.* cf. *indianus* (Plate 1; Figs. 2, 3), *G. archeomenardii/G. praemenardii* plexus (Plate 7; Figs. 1–5), *G. truncatulinoides* (Plate 9; Figs. 4–6), *G. challengeri* (Plate 7; Figs. 6–10), *G. hexagonus* (Plate 10; Fig. 1), *P. semivera* (Plate 13; Fig. 6), *P. siakensis* (Plate 13; Fig. 7), *N. incompta* (Plate 15; Figs. 10–12), *G. neoparawoodi*, *G. ruber* (Plate 18; Fig. 1), *T. quadrilobatus*, *T. bisphericus* (Plate 18; Fig. 8), *T. immaturus* (Plate 18; Fig. 9), and *T. trilobus* (Plate 18; Fig. 10). An interesting observation is the absence of *T. primordius* in this study and the lack of *G. neoparawoodi* in the Poore (1979) work. We acknowledge that the two species can easily be confused due to their similar features and overlapping stratigraphic ranges, and we concur with the Poore (1979) identification of *T. primordius*. A more detailed comparison between the two species is provided in the "Taxonomic notes" section. Compared to the Poore (1979) work, this study employs a higher sampling resolution, and in addition to counting the > 125 µm size fraction, the 63–125 µm size fraction was scanned for rare species, where *T. fleisheri*, *G. truncatulinoides, G. hexagonus*, *Globigerinoides* spp., and *Trilobatus* spp. were found in low abundances, thus explaining the difference between both studies. The practice of making standardized assemblage counts also forced us to identify most specimens in the assemblage, which can also impact the species identification and diversity. One the most significant

Table 4. Compilation figure showing the taxonomy, samples, and stratigraphic ranges of species identified in this study (dark blue) and by Poore (1979) (grey) throughout the upper Oligocene to Pleistocene. Hiatuses are indicated with the wavy black line. Stratigraphic ranges of Catapsydrax–Globorotaloides.

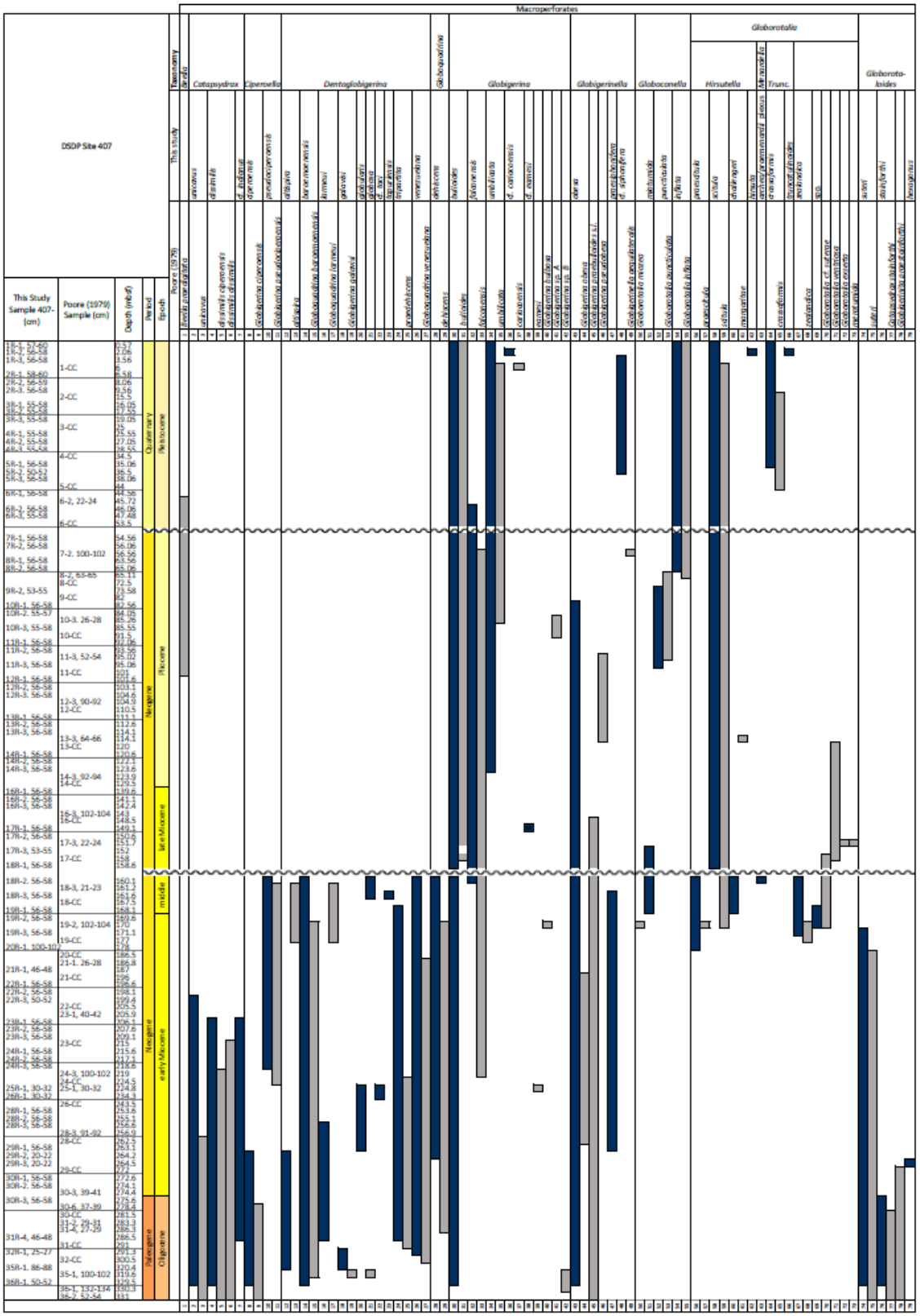

Table 5. Compilation figure showing the taxonomy, samples, and stratigraphic ranges of species identified in this study (dark blue) and by Poore (1979) (grey) throughout the upper Oligocene to Pleistocene. Hiatuses are indicated with the wavy black line. Stratigraphic ranges of *Globoturborotalita–Tenuitellita*. Neogloboquadrina du/pac is for dutertrei/pachyderma intergrade.

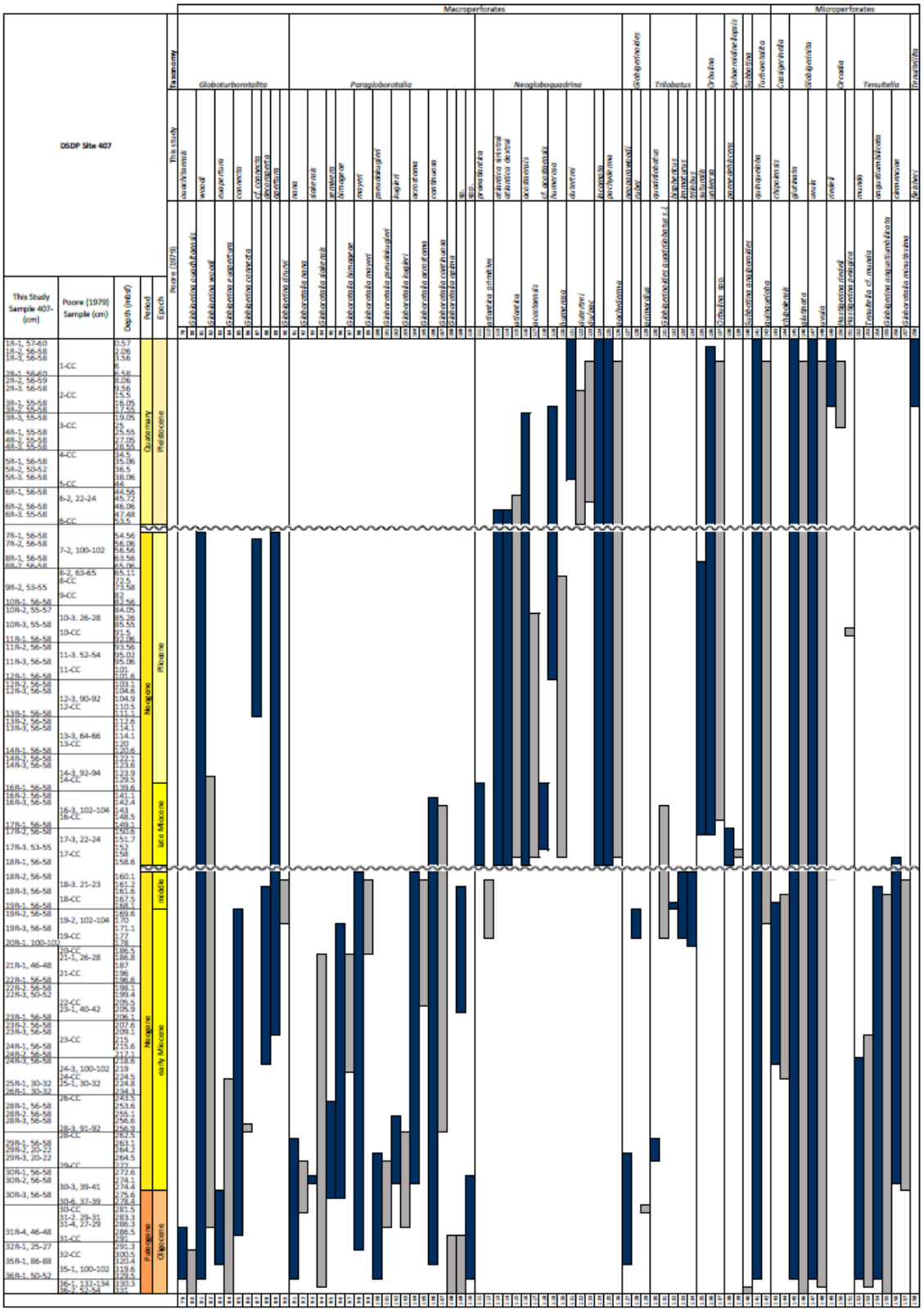

developments, relates to refined perspectives on species that have living counterparts for which genetic phylogenies exist (e.g. Morard et al., 2015). In the case of Site 407, this involves the species *Globigerina bulloides, Globigerinella* cf. *siphonifera, Globoconella inflata, Globorotalia scitula, G. hirsuta, G. crassaformis, G. truncatulinoides, Neogloboquadrina pachyderma*, *N. incompta*, *N. dutertrei*, *Orbulina universa*, and *Turborotalita quinqueloba*. Of particular importance is the case of genus *Neogloboquadrina*, which is explored in the following section.

4.4 North Atlantic *Neogloboquadrina*

Our results show that neogloboquadrinids have been a key component of high-latitude North Atlantic planktonic foraminifera assemblages since the late Miocene. Despite the 5 Myr long mid-Miocene hiatus at Site 407, in which the first appearance of the genus *Neogloboquadrina* is lost, the late Miocene to Pleistocene provides insights into the evolution of the genus, including the transition from assemblages dominated by *N. atlantica* in the Pliocene and Miocene to *N. pachyderma* domination in the Pleistocene. With abundances often exceeding 90 % of assemblages in many high-southern-latitude and high-northern-latitude regions, *N. pachyderma* is considered a polar extremist, and the only true polar species that can tolerate intensive sea ice conditions (Bé, 1977; Schiebel et al., 2017). To this day, *Neogloboquadrina* remains an enigmatic genus. Neogloboquadrinids have a strong preferential coiling direction, reaching 100 %, compared to other genera, where the coiling direction is 50 %, e.g. in *Turborotalita quinqueloba* (Darling et al., 2006). For decades, it was believed that the two distinct coiling forms of *N. pachyderma* were related to sea surface temperatures, and therefore they were used as a palaeoceanography proxy (e.g. Ericson, 1959; Kennett, 1968); i.e. an increase in *N. pachyderma* sinistral was indicative of cooler conditions, and vice versa, for *N. pachyderma* dextral. However, in the landmark study by Darling et al. (2006) it was shown that both coiling forms are in fact genetically distinct and should be considered distinct species. The right-coiling variant was recognized as *N. incompta*, and the left-coiling variant as *N. pachyderma*. Below, we identify five aspects of neogloboquadrinid classification that would benefit from future research in more complete sedimentary sequences.

– The origin of the of genus *Neogloboquadrina* remains uncertain. The current view is that *Paragloborotalia continuosa* (Blow 1959) (Plate 12; Figs. 8–11) is ancestral, with *Neogloboquadrina acostaensis* as the assumed first neogloboquadrinid (Kennett and Srinivasan, 1983). This is based on the (1) general similarity of wall textures (highly cancellate/rugose); (2) coiling pattern, i.e. slight terminal reduction in the chamber numbers per whorl; (3) similarity in test size, apertural size, orientation, and lip; and (4) overlap in stratigraphic ranges in the upper Miocene (Jenkins, 1967). An alternative phylogenetic model suggests that *N. praeatlantica* was the first species, having evolved from *Catapsydrax* (Foresi et al., 2002), a presumed non-spinose genus. Currently too few appropriate sections have been studied to test these alternatives, and *N. praeatlantica* has not been routinely recorded. From a genetic viewpoint, the modern genus *Neogloboquadrina* appears to constitute a monophyletic clade (Darling et al., 2006). Unfortunately, the interval potentially containing the *Neogloboquadrina* origin is missing from Site 407, falling within the major middle Miocene–late Miocene hiatus. Observations from Site 407 are consistent with the *P. continuosa* ancestry hypothesis in that all early neogloboquadrinids overlap in stratigraphic ranges with *P. continuosa*. We note that *N. praeatlantica* is closely comparable to *P. continuosa* in that it has 4 chambers, a similar test size, and the presence of a lip. In this study, *P. continuosa* was distinguished from *N. praeatlantica* in that it has a comma-shaped aperture, whereas *N. praeatlantica* has a higher arched aperture (e.g. Plate 17; Fig. 3). We note that *N. praeatlantica* had not yet been described at the time of Poore's study. Both *N. praeatlantica* and *P. continuosa* have a reticulate wall texture, often characterized by heavy gametogenic calcification. A possible argument against *Paragloborotalia* being the ancestor to all neogloboquadrinids is that *Paragloborotalia* is assumed to be sparsely to weakly spinose (Leckie et al., 2018), whereas *Neogloboquadrina* is non-spinose. *Paragloborotalia* spinosity, however, is controversial, as discussed by Leckie et al. (2018). Several species have been shown to have features interpreted as spine bases, including *P. pseudokugleri*, *P. kugleri*, *P. semivera*, and *P. siakensis* (Leckie et al., 2018), yet such evidence is rare and sometimes ambiguous. *Paragloborotalia continuosa* is thought to be sparsely spinose (Leckie et al., 2018), but due to heavy gametogenic calcification, it is difficult to see spine bases on SEM-imaged specimens. Also, no wall texture images of *P. continuosa* are included in the Oligocene atlas. In this case, the non-spinose *Catapsydrax* sp.–*N. praeatlantica* relationship might be worth further exploration.

– The species *N. atlantica* is currently poorly integrated into taxonomic and phylogenetic frameworks. The most recent taxonomic treatment of neogloboquadrinids (Kennett and Srinivasan, 1983) acknowledges the existence of *N. atlantica* but does not incorporate it into a phylogenetic model. As evidenced in this study, *N. atlantica* is one of the most common species in late Miocene and Pliocene mid- to high-latitude North Atlantic assemblages. It has value as an age marker in the late Miocene, based on a coiling shift from dominantly dextral to sinistral and calibrated to 6.97 Ma

(Berggren et al., 1995; Wade et al., 2011; Raffi et al., 2020), as well as a local change back to dominantly dextral coiling at 2.3 Ma (Spiegler and Jansen, 1989; Kaminski and Berggren, 2021). Like *N. pachyderma*, *N. atlantica* also shows great morphological plasticity (see "Taxonomic notes""; Plate 14 and Figs. 7–12; Plate 15 and Figs. 1–7). No attempts have yet been made to categorize morphotypes, and/or evaluate whether there is palaeoecological or stratigraphic value in doing so. It has been speculated that *N. atlantica* may be closely related to the *N. acostaensis–N. humerosa–N. dutertrei* lineage, based on morphological similarities within these species (Berggren, 1972). However, it is difficult to discern how *N. atlantica* would be ancestral to this lineage, since *N. acostaensis* shows more similarities with the purported neogloboquadrinid ancestor *P. continuosa* in being smaller and more compact than *N. atlantica*. Due to the middle–late Miocene hiatus, it is not possible to discern phylogenetic trends within this group, as the majority of neogloboquadrinids appear simultaneously just after the hiatus. *Neogloboquadrina atlantica* appears to be rather common and has been recognized in the northwest Pacific (Lam and Leckie, 2020b), although not apparently at high southern latitudes (see discussion above). Morphotypes originally described as *Globoquadrina asanoi* and *G. kagaensis* from the Pliocene of Japan (Maiya et al., 1976) may be conspecific with *N. atlantica* (Lam and Leckie, 2020b), as well as *Neogloboquadrina inglei* from the lower Pleistocene of the California margin (Kucera and Kennett, 2000), but this also needs further attention, and no direct comparisons with the Atlantic occurrences have yet been made.

– *N. praeatlantica*, which is the purported ancestor of *N. atlantica* and potentially the first neogloboquadrinid, is not included into the Neogene atlas (Kennett and Srinivasa, 1983) since it was only formally described in 2002 from the late middle Miocene Mediterranean of the Italian Tremiti Islands (Foresi et al., 2002). The first possible mention of *N. praeatlantica* in the literature is "*N. atlantica* primitive form" at Sites 407 and 408 (Poore, 1979). So far, *N. praeatlantica* has not been recorded outside of Site 407 and its Mediterranean-type locality (Hilgen et al., 2000a; Iaccarino et al., 2001; Foresi et al., 2002) and Sicily (DiStefano et al., 2002). We note that *N. praeatlantica* can be difficult to distinguish from *P. continuosa*, since both have a small-to-medium low-trochospiral test with 4 chambers in the final whorl, possibly explaining why it has not been recognized in other Neogene planktonic foraminifera studies. An alternative hypothesis argues that *N. praeatlantica* originated near Iceland (based on the work done by Poore, 1979) and migrated southwards to reach the Mediterranean and subtropical Atlantic (DSDP Site 397) but never got further south, as suggested by the absence of the species in the equatorial Atlantic (ODP Site 926) (Lirer and Iaccarino, 2005).

– The morphological plasticity of *N. pachyderma* (Plate 16; Figs. 1-12), currently acknowledged within a five-morphotype system used to describe modern and Pleistocene forms (Eynaud et al., 2009; Eynaud, 2011; El Bani Altuna et al., 2018), was not used in the past; therefore, it is unclear when this variability evolved and what the controls are. Multiple previous studies from the Pliocene to the modern have recognized plasticity in *N. pachyderma* test morphology, and there is a long history of discussing and naming of different morphotypes (e.g. Keller, 1978; Kennett, 1968; Kennett et al., 2000; Kennett and Srinivasan, 1980; Stehman, 1972; Vilks, 1975). Based on estimated genetic divergence times of the *N. pachyderma* genotypes, the genotype that is found in the central Arctic ocean and Nordic Seas (Type 1) diverged between 1.8–1.5 Ma from the Southern Hemisphere genotypes (Darling et al., 2004). This divergence coincided with strengthening of Northern Hemisphere cooling, suggesting that this genetic split marks the transformation of *N. pachyderma* into a true polar specialist; thus, its evolution and speciation was coupled to climate change (Darling et al., 2007). In the central Arctic Ocean, five morphotypes are recognized from studies of core-top samples in the Canadian Arctic archipelago (El Bani Altuna et al., 2018; Eynaud, 2011; Eynaud et al., 2009). However, how these fit in with the early evolution of *N. pachyderma,* including how it should be distinguished from ancestors that look rather similar to some of the modern *N. pachyderma* morphotypes, is less clear and something that needs attention. This study is the first to record the five "modern" morphotypes back to the early Pleistocene. Better age constraints are still needed to assess whether the split at 1.8–1.5 Ma gave rise to the five morphotypes in the North Atlantic and Arctic oceans.

Contrary to their Quaternary and Pliocene counterparts, Miocene *N. pachyderma* morphotypes have typically been lumped together in census studies. This shortcoming might be because characterizing the morphotypes is time-consuming, and the majority of Neogene planktonic foraminifera assemblages are published as DSDP/ODP/IODP data reports that mostly preceded the work by Eynaud et al. (2009). Furthermore, in the 1970s, the surface ultrastructural characteristics and porosity in Late Miocene to Recent specimen were considered to be phenetic changes as a consequence of environmental and palaeoceanographic changes, whereas modern DNA perspectives can also sometimes distinguish genetic differences (e.g. Darling et al., 2006; Huber et al., 1997).

- Where exactly *N. incompta* (Plate 15; Figs. 10–12) fits with the *Neogloboquadrina* phylogenetic history is uncertain. Few studies have recorded the FO of *N. incompta* since it was initially considered a dextral-coiling *N. pachyderma*, until genetics showed otherwise (Darling et al., 2006). According to some studies, *N. incompta* evolved before *N. pachyderma*, with a FO of 12 Ma (Kucera and Schönfeld, 2007), whereas the *N. pachyderma* FO is 9.37 Ma (Raffi et al., 2020).
- In Poore's work, Quaternary right-coiling neogloboquadrinids with 4–5 chambers in the final whorl are arbitrarily categorized as *Neogloboquadrina* du/pac (originally described as the P–D intergrade category by Kipp, 1976) and are considered to be intergrades between *N. incompta* and *N. dutertrei* (Plate 17; Figs. 9–11, 12; Poore, 1979). This study did not attempt to apply this category, as these specimens closely resemble *N. incompta*, i.e. compacted test and closed umbilicus, unlike *N. dutertrei*, which typically has a more globose test with an open aperture. Additionally, this term has been used to categorize Pliocene specimens that are transitional between *N. incompta* and *N. acostaensis* or *N. atlantica* (e.g. Dowsett et al., 1988; Dowsett and Poore, 1990). So, there is no common consensus on the usage of this term for four- to five-chambered right-coiling neogloboquadrinids, indicating a need for further evaluation.

In summary, the phylogeny of *Neogloboquadrina* needs revisiting. Currently, among age-calibrated planktonic foraminifera events, *N. acostaensis* is the first neogloboquadrinid to appear in the geological record, followed by *N. pachyderma*, *N. humerosa*, and *N. dutertrei* (Raffi et al., 2020). *Neogloboquadrina incompta*, *N. atlantica*, and *N. praeatlantica* still need to be incorporated into the phylogenetic tree of *Neogloboquadrina*. Dedicated work on well-dated and continuous northern North Atlantic records is needed to resolve these questions.

5 Conclusions

The present study documents high-latitude North Atlantic planktonic foraminifera biostratigraphy, taxonomy, and species composition in the Irminger Sea over roughly the past 25 million years, integrating these findings with calcareous nannofossil biostratigraphy as complementary tie points. The DSDP Site 407 record suggests quasi-continuous sedimentation with two hiatuses, namely a large hiatus spanning approximately 8 million years in the middle to late Miocene and a shorter hiatus separating the Pliocene and Pleistocene. Both hiatuses have been linked to the initiation of bottom-water currents in the Neogene, which eroded sediments at the site location.

DSDP Site 407 shows a steady decline in species richness and diversity from the late Oligocene to Pleistocene combined with a change in assemblages to a more (sub)polar assemblage as reflected in the high abundance of neogloboquadrinids in the late Miocene to Pleistocene. The highest species richness was recorded in the middle Miocene, most likely coinciding with the MCO, when low-latitude species such as *Globigerinoides ruber* and *Trilobatus* spp. appear in the assemblages.

The majority of standard biostratigraphic zonation schemes are based on low-latitude taxa, and since climate deterioration affected the species richness at Site 407, the application of low-latitude zonation schemes was only possible in the lower part of the sequence spanning the late Oligocene and early Miocene Zones O7 and M1. North Atlantic age-calibrated events such as the change in dominantly dextral to sinistral coiling in *Neogloboquadrina atlantica* in the late Miocene, the last occurrence of *Globoconella puncticulata* and the first occurrence of *Globoconella inflata* in the Pliocene, and the first common occurrence of *Neogloboquadrina pachyderma* in the Quaternary have improved the age constraint at Site 407. This study reports three proposed local biostratigraphic zones in order to improve the age constraint in the early Miocene, late Miocene, and Pliocene. These local zones are (1) the early–middle Miocene *"Ciperoella" pseudociperoensis* Zone, (2) the late Miocene *Neogloboquadrina praeatlantica* Zone, and (2) the Pliocene *Globoconella puncticulata* Zone. All zones cover the biostratigraphic interval between the first and last occurrence of their nominate taxa. However, whether these zones are applicable in other high-latitude North Atlantic studies needs to be investigated in the future. Unfortunately, the LO of "*C.*" *pseudociperoensis* and the FO and LO of *N. praeatlantica* fall within a hiatus limiting the possible extent of their true first and last occurrences.

Despite the large hiatus, Site 407 provides a useful record of pre-Pleistocene neogloboquadrinids, i.e. *N. praeatlantica, N. atlantica* (dex.), *N. atlantica* (sin.), *N. acostaensis, N. humerosa, N. dutertrei, N. incompta*, and *N. pachyderma*. This study has highlighted outstanding questions relating to neogloboquadrinids, such as how *N. praeatlantica*, *N. atlantica*, and *N. incompta* fit into the *Neogloboquadrina* phylogeny and the large morphological plasticity in *N. atlantica* and *N. pachyderma*. The origin and ancestry of *N. pachyderma* remains unsolved, and improved constraints on the timing of its first occurrence in the high-latitude North Atlantic are needed, as both events fall within the middle to late Miocene hiatus at Site 407.

Although uncertainties regarding high-latitude biostratigraphic zonation schemes and species ranges remain, this work provides new insights in North Atlantic planktonic foraminifera biostratigraphy, taxonomy, and assemblages. A novel aspect of this study is that it is the only study that has recorded planktonic foraminifera qualitative relative abundance over the past 25 million years in the high-latitude North Atlantic compared to the DSDP/ODP/IODP reports in which assemblage relative abundances are based

on estimates. Furthermore, this study recognizes the multiple central Arctic *N. pachyderma* morphotypes when *N. pachyderma* became abundant in the Pleistocene. This study provides a framework for the revision of the taxonomy and phylogeny of the Neogene and Quaternary planktonic foraminifera.

Taxonomic notes

One of the key goals of this study was to establish an updated catalogue of planktonic foraminifera from the high-latitude North Atlantic Ocean based on this revised study of DSDP Site 407. Stratigraphic ranges of all taxa are noted, as well as synonymy lists from previous DSDP/ODP/IODP studies in the North Atlantic. The taxonomic notes presented for each species are used to communicate our taxonomic philosophy and emphasize the most important and relevant morphological features for species identification, with an emphasis on genus the *Neogloboquadrina*, which dominates the Pliocene–Pleistocene sequence in the high-latitude North Atlantic. These notes should not be viewed as a complete description of any species. Plates are organized at different levels, namely macroperforates and microperforates, and within these, the groups' taxa are presented alphabetically by genus, then phylogenetically within a genus from earliest evolving to last evolving, if possible; otherwise, species are organized alphabetically. The evolutionary order is based on ranges given by Wade et al. (2018) and Kennett and Srinivasan (1983). The synonymy lists are not exhaustive, especially for the better-known species, but include a selection of published and SEM-imaged occurrences for each listed species from the Neogene relevant to the high-latitude North Atlantic focus of this study.

Genus *Catapsydrax* Bolli, Loeblich and Tappan 1957

Type species: Globigerina dissimilis Cushman and Bermúdez 1937

Catapsydrax dissimilis (Cushman and Bermúdez 1937)

Plate 1, Fig. 1

Globigerina dissimilis Cushman and Bermúdez, 1937:25, pl. 3, figs. 4–6 [Eocene, Havana Province, Cuba].

Globigerinita dissimilis (Cushman and Stainforth); Blow and Banner, 1962:106, pl. 14, fig. D [upper Eocene *Globigerapsis semiinvoluta* Zone, Lindi, Tanzania]; Berggren, 1972:981, pl. 3, figs. 15–16 [lower Oligocene, DSDP Site 116, Rockall Plateau, North Atlantic Ocean].

Catapsydrax dissimilis dissimilis (Cushman and Bermudez). Fleisher, 1974:1016, pl. 4, fig. 5 [Oligocene Zones O3–O5, DSDP Site 223, Arabian Sea]. Poore, 1979:507, pl. 15, fig. 4 [upper Oligocene, DSDP Site 407, Reykjanes Ridge, North Atlantic Ocean].

Globigerinita dissimilis ciperoensis Blow and Banner, 1962:107, pl. XIV, figs. a–c [lower Oligocene *Globigerina ampliapertura* Zone, Cipero Fm., Trinidad].

Catapsydrax dissimilis ciperoensis (Blow and Banner); Quilty, 1976:641, pl. 7, fig. 11 [upper Oligocene/lower Miocene Zone N4, DSDP Site 320, southeastern Pacific Ocean]; Poore, 1979:507, pl. 15, fig. 5 [upper Oligocene, DSDP Site 407, Reykjanes Ridge, North Atlantic Ocean].

Remarks. Rare in material from Site 407; often found outside the counting area (i.e. after the first ∼ 300 counted specimens). *Catapsydrax dissimilis* at Site 407 is a generally large species similar in size to *C. unicavus*. The test is trochospiral, with 4 subglobular chambers in the final whorl that are slightly appressed and embracing. The wall is heavily cancellate. It has 2–4 infralaminal openings around the umbilically positioned bulla compared to only one in *C. unicavus*.

Chronostratigraphic range. Zone O7 (407-36R-1, 50–52 cm; 329.5 m b.s.f.) to lower "*C.*" *pseudociperoensis* Zone (407-23R-1, 56–58 cm; 206.06 m b.s.f.).

Catapsydrax* cf. *indianus (Spezzaferri and Pearson 2009)

Plate 1, Figs. 2, 3

Catapsydrax indianus Spezzaferri and Pearson, 2009:114, pl. 1, figs. 1a–3c [lower Miocene Zone M1, ODP Hole 709B, Mascarene Plateau, Indian Ocean].

Remarks. Catapsydrax cf. *indianus* is very rare; it was only recorded in two samples when the whole sample was scanned. It is similar to *C. dissimilis* but has a higher trochospiral-coiling mode with more globular chambers compared to *C. dissimilis.* The bulla has 4–5 infralaminal openings (vs. 2–4 in *C. dissimilis*) but lacks the lobed bulla characteristic of *C. indianus* s.s.

Chronostratigraphic range. Zone O7 (407-31R-4; 46–48 cm; 286.46 m b.s.f.) and lower "*C.*" *pseudociperoensis* Zone (407-23R-1; 56–58 cm; 206.06 m b.s.f.).

Catapsydrax unicavus Bolli, Loeblich and Tappan 1957

Plate 1, Figs. 4–9

Catapsydrax unicavus Bolli, Loeblich and Tappan 1957:37, pl. 7, fig. 9a–c [upper Oligocene]

Catapsydrax unicavus Bolli, Loeblich, and Tappan 1957:37, pl. 7: fig. 9a–c [upper Oligocene *Globigerina ciperoensis ciperoensis* Zone, Cipero Fm., Trinidad], pl. 37, fig. 7a, b [middle 1165 Eocene *Truncorotaloides rohri* Zone, Navet Fm., Trinidad]; Aksu and Kaminski, 1989:302, pl. 2, figs. 9–11 [Oligocene, ODP Hole 647A, Labrador Sea]; Spezzaferri, 1998:189, pl. 2, fig. 6a–c [middle Eocene, ODP Hole 918D, East Greenland Margin].

Remarks. At Site 407, *C. unicavus* is identified as small to large species with 3–4 chambers in the final whorl; the

sutures are straight and depressed, and the wall texture is highly cancellate. *Catapsydrax unicavus* has a bulla that is attached on three sides and wraps around the umbilicus obscuring the aperture. This species is relatively abundant in the Oligocene–middle Miocene of Site 407. It can be distinguished from *Globorotaloides suteri* in that it has a higher spired test (vs. very low trochospiral *G. suteri*) (Coxall and Spezzaferri, 2018).

Chronostratigraphic range. Zone O7 (407-36R-1, 50–52 cm; 329.5 m b.s.f.) to lower "*C.*" *pseudociperoensis* Zone (407-22R-3, 50–52 cm;199.39 m b.s.f.).

Genus *Ciperoella* Olsson and Hemleben 2018

Type species: Globigerina ciperoensis Bolli, 1954

Ciperoella ciperoensis (Bolli, 1954)

Plate 2, Figs. 1–3

Globigerina ciperoensis Bolli, 1954:1, figs. 3-3a (holotype drawing of *Globigerina* cf. *concinna* Reuss from Cushman and Stainforth, 1945), figs. 4-4b [Oligocene, *Globigerina ciperoensis* Zone, Cipero Fm., Trinidad], figs. 5-5b (drawing of *Globigerina concinna* Reuss from Nuttall, 1932), fig. 6 (drawing of *Globigerina concinna* Reuss from Franklin, 1944).

Ciperoella ciperoensis (Bolli); Olsson et al., 2018:225, pl. 7.3, figs. 1–3 [Globigerina ciperoensis Zone, Cipero Fm. Trinidad], figs. 6–8 [Oligocene, Zone O6, Trinidad], figs. 4, 9 [Oligocene, Zone O7, western North Atlantic slope], figs. 5, 10–12 [Oligocene, Zone O6, western North Atlantic slope], fig. 13 [Oligocene, Zone O6, Cipero Fm. Trinidad], figs. 14–17 [Oligocene, Zone O6, Cipero Fm., Trinidad].

Remarks. At Site 407, *Ciperoella ciperoensis* is rare. The test is moderately low trochospiral with a slightly elevated initial whorl. The test outline is lobulate with 5 globular chambers in the final whorl, and the ultimate chamber is smaller than the penultimate chamber. The umbilicus is large, open, and surrounded by the chambers of the final whorl. The aperture is umbilical with a rounded arch and bordered by a thickened rim. This species has long been used in the tropical biozonation schemes as a zonal marker and nominate taxon for the Oligocene *Globigerina ciperoensis* Zone, defined in the Cipero Fm., Trinidad (Bolli, 1957), and also in the North Sea and Nordic Seas, where it is used as a marker for the earliest Miocene (Anthonissen, 2012). *Ciperoella ciperoensis* is also a prominent species in the Oligocene and Miocene of the central Paratethys (Rögl, 1994). This ubiquitous distribution is somewhat baffling, given the rather isolated nature of some of these enclosed seas during the Oligo-Miocene, and suggests either the rather broad ecological flexibility of the species or more marine connectivity than perhaps thought.

Chronostratigraphic range. Zone O7 (407-36R-1; 50–52 cm; 329.5 m b.s.f.) to Zone M1b (407-29R-2; 20–22 cm; 264.2 m b.s.f.).

"Ciperoella" pseudociperoensis (Blow 1969)

Plate 2, Figs. 4-12

Globigerina praebulloides pseudociperoensis Blow, 1969:381, pl. 17, figs. 8–9 [middle Miocene, Langhian, Zone N11 *Globorotalia praefohsi* consecutive range zone, lower Palembang Formation, central Sumatra].

Globigerina cf. *pseudociperoensis* Blow; Rögl, 1994:149 pl. 1, figs. 20–21 [late early Miocene, Carpathian, southern Slovakia, Čebovce, clay pit north of the village, central Paratethys], fig. 22 [middle Miocene, Badenian, Austria, Vienna, Grinzing, Tegel at Grinzing, central Paratethys].

Globigerina pseudociperoensis Blow; Poore, 1979:505 pl. 14, figs. 1, 2 [lower Miocene, DSDP Site 407, Reykjanes Ridge, North Atlantic Ocean].

Remarks. Following Poore (1979), in our Site 407 material, we recognize a form from the early Miocene that broadly fits the description of Blow's *pseudociperoensis*, which was described from the middle Miocene of central Sumatra. Originally named *Globigerina praebulloides pseudociperoensis*, Blow's (sub)species *pseudociperoensis* is said to differ from "*C.*" *ciperoensis* Bolli in having a wider umbilicus, in having a more rapidly opening and higher spire, and in having 4 chambers in the penultimate whorl ("globigeriniform coiling") compared to 4.5–5 in the penultimate whorl in *C. ciperoensis* (see the discussion in Rögl, 1994). However, the taxonomic status, and even the generic status, of this morphotype is unclear. The species was not dealt with by Spezzaferri (1994) or the Oligocene atlas (Wade et al., 2018), and there is no existing synonymy model as far as we are aware.

When comparing the wall textures of these taxa (from their holotype SEM images presented in Mikrotax; Young et al., 2019), both taxa have roughly comparable wall textures involving a (presumably spinose) *ruber-/sacculifer*-type wall with elongate-to-coalescing parallel ridges. Thus, *pseudociperoensis* might be attributable to the genus *Ciperoella* and may even be a junior synonym of *C. ciperoensis* (Bolli, 1954). In this case, the difference in early whorl coiling would be attributed to intraspecific variation, and the established range of the species would have to be extended into the early Miocene (currently listed as having its LO close to the Oligocene/Miocene boundary (Olsson et al., 2018).

Another possibility is that *pseudociperoensis* is allied to *Globigerinella* with which the "globigeriniform" subadult coiling morphology and the stratigraphic range (early Miocene) are consistent. Lightly reticulate wall textures, as seen in our *pseudociperoensis* specimens (Plate 2; figs. 4–12), are present to a degree in some early globigerinellids (e.g. *G. obesa* and *G. praesiphonifera*; see Olsson et al., 2018; Plate 6.8 and Plate 6.9) and also in our recognized Site 407 *G. praesophonifera* (Plate 6; figs. 8–12). Note that the one specimen of *G. praesophonifera* imaged in spiral view also shows "globigeriniform-style" coiling in the

early whorls comparable to *pseudociperoensis*. Moreover, in our Site 407 material, there is a tendency towards a more *bulloides*-type wall on the final chamber, typical of *Globigerinella* (Plate 2; fig. 7). Thus, arguments can be made for both *Ciperoella* and *Globigerinella*. Rögl (1994) recognized what he called "*Globigerina* cf. *pseudociperoensis*" in upper Miocene material from the central Paratethys (Carpathian, Deboyce, and Badenian). Rögl indicates that he believes the taxon belongs to the *ciperoensis* clade, but similar arguments to the ones above could be made regarding a *Globigerinella* connection. Schenk et al. (2018) also record *pseudociperoensis* in the Paratethys region; however, the figured specimens do not look similar to specimens from this study; i.e. the Schenk et al. (2018) plate shows a small and tightly coiled specimen with 4–5 chambers and a small umbilicus.

"Ciperoella" pseudociperoensis has been recorded in the early middle to middle Miocene in the Pacific Pohang Basin (Kim, 1999), Monterey Formation (DePaolo and Finger, 1990), southwest Japan's Takanabe Formation (Iwatani et al., 2012), southwest Japan's Josoji Formation (Nomura, 2021), and California (Poore et al., 1981). Of these records, only the Poore (1979) study has a SEM image that looks similar to the specimens from this study, i.e. 5 globular chambers with a large umbilicus and *Ciperoella*-type wall texture. In the Atlantic, besides Poore's 1979 study on Site 407, "*C*". *pseudociperoensis* has also been recorded in another southwest Iceland locality (DSDP Site 408; Poore, 1979) and in southeast Greenland (ODP Hole 918D; Spezzaferri, 1998), although images are missing for the latter. These observations point out that further research is needed to determine the generic affiliation of this species, which is beyond the scope of this paper. We here refer to the morphotype as *"Ciperoella" pseudociperoensis* and differentiate it from *Globigerinella praesiphonifera* by the more umbilically positioned aperture in "*C.*" *pseudociperoensis* vs. the umbilical–extraumbilical extending onto the peripheral edge in *G. praesiphonifera.*

Chronostratigraphic range. "*C.*" *pseudociperoensis* Zone (407-24R-3, 56–58 cm, to 407-18R-1, 56–58 cm; 218.6–158.56 m b.s.f.).

Genus *Dentoglobigerina* Blow 1979

Type species: Globigerina galavisi Bermúdez 1961

Dentoglobigerina altispira (Cushman and Jarvis 1936)

Globigerina altispira Cushman and Jarvis, 1936:4, pl.1, figs. 13, 14 [Miocene, Bowden Marl at milestone no. 71, east of Port Antonio, Jamaica].

Dentoglobigerina altispira Cushman and Jarvis; Weaver 1987: pl. 2, figs. 5, 6 [upper Pliocene, DSDP Site 607, upper western flank of the Mid-Atlantic Ridge, northwest of the Azores, North Atlantic Ocean].

Dentoglobigerina altispira Cushman and Jarvis; Weaver, 1987:726, pl. 2, figs. 5–6 [late Pliocene, Zone Pl4, DSDP Site 607, Azores, North Atlantic Ocean]; Spiegler 1996:167, pl. 2, fig. 9 [upper Pliocene, ODP Hole 910D, central Yermak Plateau, high-latitude North Atlantic].

Remarks. Distinguished from other dentoglobigerinids by its large and high trochospiral test.

Chronostratigraphic range. Zone O7 (407-35R-1; 86–88 cm; 320.36 m b.s.f.) to Zone M1b (407-29R-2; 20–22 cm; 264.2 m b.s.f.).

Dentoglobigerina baroemoenensis (LeRoy 1939)

Plate 3, Figs. 1–4

Globigerina baroemoenensis LeRoy, 1939:263, pl. 6, figs. 1, 2 [holotype, Miocene, Rokan, Tapanoeli area, Sumatra, Indonesia].

Globoquadrina baroemoenensis (LeRoy); Blow, 1969:340–341, pl. 28, fig. 8 [upper Oligocene Zone N3 = P22, Cipero Fm., Trinidad], pl. 28, fig. 4 [lower Miocene Zone N8, Cipero Fm., Trinidad]; Poore, 1979:470, pl. 18, figs. 8, 9 [lower Miocene Zone N7, DSDP Site 408, North Atlantic Ocean], figs. 10–12 [middle Miocene Zone N9-N11, DSDP Site 408, North Atlantic Ocean].

Dentoglobigerina baroemoenensis (LeRoy); Blow, 1979:763, 1300, pl. 28, fig. 8 (reproduced from Blow, 1969, pl. 28, fig. 8).

Remarks. Differs from *D. larmeui* in that is has more angular and reniform chambers and a broad and deep umbilicus.

Chronostratigraphic range. Zone O7 (407-36R-1; 50–52 cm; 329.5 m b.s.f.) to "*C.*" *pseudociperoensis* Zone (407-18R-2; 56–58 cm; 160.06 m b.s.f.).

Dentoglobigerina galavisi (Bermúdez 1961)

Plate 3, Figs. 5, 6

Globigerina galavisi Bermúdez, 1961:1183, pl. 4, fig. 3 [upper Eocene Jackson Fm., Mississippi]; Blow, 1969:319, pl. 5, figs. 1–3 (re-illustration of holotype), pl. 16, fig. 4 [upper Eocene Zone P16, upper Jackson Fm., Mississippi], pl. 16, fig. 5 [upper Eocene Zone P16, Lindi area, Tanzania].

Dentoglobigerina galavisi (Bermúdez); Blow, 1979:1301–1305 (partim), pl. 5, figs. 1–3 (holotype, reproduced from Blow, 1969), pl. 16, fig. 4 (reproduced from Blow, 1969, pl. 16, fig. 4), pl. 16, fig. 5 (reproduced from Blow, 1969, pl. 16, fig. 5) (not pl. 177, figs. 8, 9, and ? are for *Subbotina tecta*, pl. 186, figs. 8, 9, and ? are for *Subbotina projecta* n. sp., pl. 244, figs. 1 and 2 are for *Subbotina tecta*); Spezzaferri, 1998:189, pl. 2, figs. 8a–c [middle Eocene, Zone P10–P12, Hole 918D, East Greenland Margin, North Atlantic Ocean]; Wade et al., 2018:346, pl. 11.5, fig. 1–3 [Zone E15–16, upper Jackson Fm., Frost Bridge, Mississippi],

fig. 4 [Zone M1, ODP Site 904, western North Atlantic Ocean], fig. 5–7 [Zone E15/16, Tanzania, reproduced from Pearson and Wade, 2015], fig. 8 [Zone O1, IODP Hole U1367B, South Pacific Ocean], figs. 9–11 [Zone E15/16, Tanzania, reproduced from Pearson and Wade, 2015], fig. 12 [Zone E16/O1, Istra More-3 well, Adriatic Sea], figs. 13–14 [Zone O1, Tanzania, reproduced from Pearson and Wade, 2015], figs. 15–16 [Zone O2, Istra More-3 well, Adriatic Sea].

Remarks. Test trochospiral, globular, and oval to quadrate in the equatorial outline. The size of 3–3.5 ovoid chambers increase rapidly; the umbilicus is small and enclosed by surrounding chambers, and the aperture is centred over the umbilicus and bordered by an asymmetrical triangular-shaped tooth.

Chronostratigraphic range. Zone O7 (407-35R-1, 86–88 cm, to 407-32R-2, 25–27 cm; 320.36–291.25 m b.s.f.).

Dentoglobigerina globosa (Bolli 1957)

Globoquadrina altispira globosa Bolli, 1957:111, pl. 24, figs. 9a–10c [lower Miocene *Catapsydrax dissimilis dissimilis* Zone, Cipero Fm., Trinidad]; Stainforth and others, 1975:245, 248, fig. 101, no. 1–5 [lower Miocene Catapsydrax dissimilis Zone, Cipero Fm., Trinidad], fig. 101, no. 6a–c (reproduction of holotype of *Globoquadrina altispira globosa* Bolli from Bolli, 1957, pl. 24, fig. 9a–c.), fig. 101, no. 7a–c (reproduction from Blow, 1959, pl. 11, fig. 52a–c).

Dentoglobigerina altispira globosa (Bolli); Kennett and Srinivasan, 1983:89 (partim), pl. 44, fig. 4, pl. 46, figs. 7 and 9 [lower Miocene Zone N8, DSDP Site 289, western equatorial Pacific Ocean] (not pl. 46; fig. 8 is for *Dentoglobigerina altispira*); Spezzaferri and Premoli Silva, 1991:237, pl. 3, fig. 4a–c [upper Oligocene Zone P22, DSDP Hole 538A, Gulf of Mexico]; Spezzaferri, 1994:40, pl. 40, fig. 3 [upper Oligocene Subzone P21b, ODP Hole 709B, Mascarene Plateau, equatorial Indian Ocean].

Remarks. Differs from *D. globularis* in that it has 5–6 chambers and a wider umbilicus.

Chronostratigraphic range. "*C.*" *pseudociperoensis* Zone (407-18R-3, 56–58 cm, to 407-18R-2, 56–58 cm; 161.56–160.06 m b.s.f.).

Dentoglobigerina globularis

Plate 3, Figs. 7–9

Globoquadrina globularis Bermúdez, 1961:1311, pl. 13, figs. 4–6 ["middle" Oligocene, Tinguaro Fm., Matanzas province, Cuba].

Dentoglobigerina globularis (Bermúdez); Spezzaferri and Premoli Silva, 1991:237, pl. 2, figs. 5 and 7 [lower Oligocene Subzone P21a, DSDP Hole 538A, Gulf of Mexico], pl. 3, fig. 1 [upper Oligocene Zone P22, DSDP Hole 538A, Gulf of Mexico].

Remarks. Test large, globular, and medium trochospiral lobulate in the equatorial outline; chambers ovate and are slightly embracing, with 3.5–4 in final whorl; sutures are moderately depressed and straight, while the ultimate chamber may be reduced in size and directed over the umbilicus; the umbilicus is open and square with an aperture umbilical; the lip or tooth is highly variable; in the edge view, chambers globular to ovate, with the ultimate chamber directed over umbilicus.

Chronostratigraphic range. Lower "*C.*" *pseudociperoensis* Zone (407-29R-1, 56–58 cm, to 407-25R-1, 30–32 cm; 263.06–224.8 m b.s.f.).

Dentoglobigerina larmeui (Akers 1955)

Plate 3, Figs. 10–11

Globoquadrina larmeui Akers, 1955:661, pl. 65, figs. 4a–c [Miocene *Operculinoides* Zone, Shell Godchaux Sugars No. 1 well, Louisiana]; Poore, 1979:470, pl. 18, figs. 1–3 [middle Miocene Zone N12-N14, DSDP Site 407, North Atlantic Ocean].

Dentoglobigerina larmeui (Akers); Spezzaferri and Premoli Silva, 1991:243, pl. 2, figs. 6a–c [Oligocene Subzone P21a, DSDP Hole 538A, Gulf of Mexico].

Remarks. This species is rare at Site 407. The test is globular to subquadrate with 3.5–4 chambers in the final whorl. The final chamber is flattened and sloping towards the umbilicus. The aperture is bordered by a small triangular lip. *Dentoglobigerina larmeui* differs from *D. galavisi* in that it has a more open umbilicus and more chambers (3.5–4 vs. 3–3.5). The final chamber in *D. galavisi* is not flattened.

Chronostratigraphic range. Zone O7 (407-31R-4; 46–48 cm; 286.46 m b.s.f.) to Zone M1b (407-28R-3; 56–58 cm; 255.56 m b.s.f.).

***Dentoglobigerina* sp.**

Plate 3, Fig. 12

Remarks. Specimens belonging to *Dentoglobigerina* sp. have a large test, low trochospiral, and globular in outline, with 4 globular chambers in the final whorl. Sutures are depressed, straight, or slightly curved on the umbilical side. The umbilicus is moderately wide, rectangular, and deep, with an aperture umbilical that is centrally placed, usually with a lip of constant thickness.

Stratigraphic range. The samples 407-25R-1, 30–32 cm, to 407-26R-1, 30–32 cm (224.8–234.3 m b.s.f.)., fall between Zone M1b and the "*C.*" *pseudociperoensis* Zone.

Dentoglobigerina tapuriensis (Blow and Banner 1962)

Globigerina tripartita tapuriensis Blow and Banner, 1962:97–98, pl. 10, figs. H–K [lower Oligocene *G. oligocaenica* Zone, Lindi area, Tanzania].

"Globoquadrina" tapuriensis (Blow and Banner); Spezzaferri and Premoli Silva, 1991:248, pl. 9, figs. 3a–c [lower Oligocene Subzone P21a, DSDP Hole 538A, Gulf of Mexico].

Dentoglobigerina tapuriensis (Blow and Banner); Pearson and Wade, 2015:19, figs. 20.1a–d (SEMs of the holotype of *Globigerina tripartita tapuriensis* Blow and Banner), fig. 20.2 [lower Oligocene Zone O1, Tanzanian Drilling Project (TDP) Site 12, Stakishari, Tanzania], figs. 20.3, 20.5, 20.6, 20.8, 20.9 [lower Oligocene Zone O1, TDP Site 17, Stakishari, Tanzania], figs. 20.4a–b [upper Eocene Zone E15/16, TDP Site 12, Stakishari, Tanzania], fig. 20.7 [upper Eocene Zone E15/16, TDP Site 17, Stakishari, Tanzania].

Remarks. Dentoglobigerina tapuriensis is rare at Site 407. The test is large, moderately trochospiral with 3, occasionally up to 3.5, globular and appressed chambers in the final whorl that increase rapidly in size. The sutures are incised, straight, or slightly curved, while the umbilicus is wide, oval, and deep; the aperture umbilical, with a wide arch, is centrally placed, usually with a thin lip of constant thickness.

Chronostratigraphic range. "*C.*" *pseudociperoensis* Zone (407-18R-3; 56–58 cm; 161.56 m b.s.f.).

Dentoglobigerina tripartita (Koch 1926)

Plate 4, Figs. 1–4

Globigerina bulloides var. *tripartita* Koch, 1926:742, fig. 21a, b [middle Tertiary, lower *Globigerina* marl, Sadjau-Njak, southeast Bulongan, east Borneo].

Globoquadrina praedehiscens Blow and Banner; Berggren, 1972:981, pl. 3, figs. 13, 14 [early Miocene, DSDP Site 116, North Atlantic Ocean]; Poore, 1979:470, pl. 18, figs. 4–6 [lower Miocene Zone N5, DSDP Site 407, North Atlantic Ocean], fig. 7 [upper Oligocene Zone P22, DSDP Site 407, North Atlantic Ocean].

Dentoglobigerina tripartita (Koch); Fox and Wade, 2013:399, figs. 8.1–3 [middle Miocene Zone M7 (note that this specimen is from Sample U1338B-38H-2, 40–42 cm, and not Core 36H as it says in the caption), IODP Hole U1338B, equatorial Pacific Ocean].

Remarks. It is characterized by its small, triangular, and umbilical aperture bordered by an irregular triangular-shaped tooth.

Chronostratigraphic range. Zone O7 (407-31R-4; 46–48 cm; 286.46 m b.s.f.) to "*C.*" *pseudociperoensis* Zone (407-19R-1; 56–58 cm; 168.06 m b.s.f.).

Dentoglobigerina venezuelana (Hedberg 1937)

Plate 4, Figs. 5–7

Globigerina venezuelana Hedberg, 1937:681, pl. 92, fig. 7a, b [lower Miocene, Carapita Fm., northeastern Venezuela].

Globoquadrina venezuelana (Hedberg); Blow, 1959:186, pl. 11, figs. 58a–c [lower Miocene *Globigerinatella insueta* Zone, San Lorenzo Fm., Venezuela], pl. 11, fig. 59 [middle Miocene *Globorotalia mayeri* Zone, Pozon Fm., Venezuela]; Poore, 1979:505, pl. 14, figs. 4–7 [early–middle Miocene, DSDP Site 407, high-latitude North Atlantic].

Dentoglobigerina venezuelana (Hedberg); Wade and others, 2016:435, pl. 6, fig. 7 [upper Oligocene Zone O6, IODP Hole U1334A, equatorial Pacific Ocean].

Remarks. A large to very large spherical test. The final chamber is commonly reduced in size and partially closes the umbilicus. This differs from larger *C. unicavus* in that it has a higher spired initial whorl.

Chronostratigraphic range. Zone O7 (407-32R-1; 25–27 cm; 291.25 m b.s.f.) to "*C.*" *pseudociperoensis* Zone (407-18R-2; 56–58 cm; 160.06 m b.s.f.).

Genus *Globoquadrina* Finlay 1947

Type species: Globorotalia dehiscens Chapman, Parr, and Collins 1934

Globoquadrina dehiscens (Chapman, Parr, and Collins 1934)

Plate 4, Figs. 8, 9

Globorotalia dehiscens Chapman, Parr, and Collins, 1934:569, pl. 11, figs. 36a–c [Balcombian stage (= middle Miocene), Kackeraboite Creek, Victoria, Australia].

Globoquadrina dehiscens (Chapman, Parr, and Collins); Bolli, Loeblich, and Tappan, 1957:31, pl. 5, figs. 5a–c [hypotype, Balcombian stage (= middle Miocene), Victoria, Australia].

Remarks. Globoquadrina dehiscens is rare at Site 407 and often found outside the counting area. It is characterized by its subquadrate equatorial periphery and final chamber with a steep umbilical face.

Chronostratigraphic range. Zone M1b (407-29R-2; 20–22 cm; 264.5) to "*C.*" *pseudociperoensis* Zone (407-18R-2; 56–58 cm; 160.06 m b.s.f.).

Genus *Globigerina* d'Orbigny 1826

Type species: Globigerina bulloides d'Orbigny 1826

Globigerina bulloides (d'Orbigny 1826)

Plate 5, Figs. 1–3

Globigerina bulloides d'Orbigny, 1826 [Recent, Adriatic Sea, near Rimini, Italy]; Saito, Thompson, and Berger, 1981:40, pl. 7, figs. 1a–c [Recent, eastern North Atlantic Ocean]; Aksu and Kaminski, 1989:304, pl. 4, figs. 8, 10–12 [Late Pliocene, ODP Hole 647A, Labrador Sea,

North Atlantic Ocean]; Spiegler and Jansen, 1989:696, pl. 2, fig. 11 [late Miocene, ODP Hole 642B, Vøring Plateau, Nordic Seas]; Spiegler, 1996:166, pl. 1, fig. 3 [middle Miocene, ODP Hole 909C, Fram Strait, Nordic Seas].

Remarks. At Site 407, *G. bulloides* is present throughout the whole sequence and is a common species in the Pliocene and Pleistocene. The test is low trochospiral with 4 globular chambers. The aperture is umbilical with a broad arch bordered by a lip. Often specimens have a kummerform fifth final chamber tilted over the umbilicus (Plate 5; Figs. 6 and 7). *Globigerinella obesa* differs from *G. bulloides* in that it has a very low-trochospiral test and an umbilical–extraumbilical aperture reaching towards the periphery, whereas the aperture is clearly umbilical and very open in *G. bulloides*.

Chronostratigraphic range. Zone O7 (407-36R-1; 50–52 cm; 329.5 m b.s.f.) to *N. pachyderma* Zone (407-1R-1; 57–60 cm; 0.57 m b.s.f.).

Globigerina* cf. *cariacoensis (Rögl and Bolli 1973)

Plate 5, Fig. 4

Globigerina megastoma cariacoensis Rögl and Bolli, 1973:564, pl. 2, figs. 1–10 [Holocene, *Globorotalia fimbriata* Subzone, Site 147, Cariaco Basin, Caribbean Sea], pl. 12, figs. 5–6 [Holocene, *Globorotalia fimbriata* Subzone, Site 147, Cariaco Basin, Caribbean Sea].

Remarks. Rare at Site 407 and only present in one sample. It differs from *G. bulloides* in that it has a very high-trochospiral test with a wide aperture, a low arch without a lip, and a lower arched aperture. *Globigerina* cf. *cariacoensis* differs from *G. cariacoensis* s.s. in that it is more quadrate and has globular chambers (vs. more elongated chambers in *G. cariacoensis* s.s.). The chambers are also more globular in *G. cariacoensis* than in *G. bulloides*. *Globigerina cariacoensis* differs from *G. umbilicata* by being a higher and narrower trochospiral. *G. cariacoensis* is distinguished from *G. bulloides* and *G. umbilicata* in being a Late Pleistocene to Holocene marker (Rögl and Bolli, 1973).

Chronostratigraphic range. N. pachyderma Zone (407-1R-2; 56–58 cm; 2.06 m b.s.f.).

Globigerina* cf. *eamesi

Plate 5, Figs. 5, 6

Globigerina eamesi Blow, 1959:176, pl. 9, figs. 39a–c [Late Miocene, Pozon, eastern Falcón, Venezuela].

Remarks. This species is rare in Site 407 material, only one specimen found. The test is small, trochospiral, and compact with 4 chambers. The umbilicus is small and closed, and the aperture is an elongated slit with a thin lip; it is interiomarginal and umbilical. The test is covered in thick raised spine collars (Plate 5; Fig. 11).

Chronostratigraphic range. N. praeatlantica Zone (407-17R-1; 56–58 cm; 149.06 m b.s.f.).

Globigerina falconensis (Blow 1959)

Globigerina falconensis Blow, 1959:177, pl. 9, figs. 40a–c, 41 [Pozon, eastern Falcón, Venezuela]; Aksu and Kaminski, 1989:304, pl. 4, fig. 9 [Late Pleistocene, ODP Hole 646B, Labrador Sea, North Atlantic Ocean].

Remarks. Globigerina falconensis is rare at Site 407 and can be distinguished from *G. bulloides* in that it has a narrow arch (vs. high arch in *G. bulloides*) with a prominent lip.

Chronostratigraphic range. Upper "*C.*" *pseudociperoensis* Zone (407-18R-2; 56–58 cm; 160.06 m b.s.f.) to upper *G. inflata* PRZ (407-6R-2; 56–58; 46.06 m b.s.f.).

Globigerina umbilicata Orr and Zaitzeff, 1971

Plate 5, Figs. 7–9

Globigerina umbilicata Orr and Zaitzeff, 1971:18, pl. 1, figs. 1–4 [late Pliocene, Rio Del Formation, Centerville Beach, Humboldt County, California, USA]; Poore, 1979:505, pl. 14, fig. 12 [Late Pliocene, DSDP Hole 407, Irminger Sea, North Atlantic Ocean].

Remarks. Globigerina umbilicata is rare in Site 407 material, and it differs from *G. bulloides* in that it has one more chamber in the final whorl and in that it has a more open umbilicus. *Globigerina umbilicata* is a useful marker for the late Pliocene–Pleistocene (e.g. Kennett and Srinivasan, 1983).

Chronostratigraphic range. Lower *N. atlantica* (sin.) PRZ (407-14R-3; 56–58 cm; 123.6 m b.s.f.) to *N. pachyderma* Zone (407-1R-1; 57–60 cm; 0.57 m b.s.f.).

Genus *Globigerinella* Cushman 1927

Type species: Globigerina aequilateralis Brady 1879

Globigerinella obesa (Bolli 1957)

Plate 6, Figs. 1–7

Globorotalia obesa Bolli, 1957:119, pl. 29, figs. 2a–3 [middle Miocene *Globorotalia fohsi robusta* Zone, Cipero Fm., Trinidad].

Globigerinella obesa (Bolli); Kennett and Srinivasan, 1983:234, pl. 59, figs. 2–5 [early Pliocene *Globorotalia puncticulata* Zone, DSDP Site 281, South Tasman Rise, Tasman Sea]; Spiegler and Jansen, 1989:696, pl. 2, fig. 12 [late Miocene, ODP Hole 642B, Vøring Plateau, Nordic Seas]. Spezzaferri et al., 2018:198, pl. 6.1, figs. 14–17 [early Oligocene, Zone O1, *Pseudohastigerina naguewichiensis* Zone, Shubuta Formation, Alabama, USA], pl. 6.8, figs. 1–3 [middle Miocene, *Globorotalia fohsi robusta* Zone, Cipero Fm. Trinidad], figs. 4–6 [*Globigerinatella insueta/Globigerinoides bisphericus* Zone, Pozon Fm. Venezuela], figs. 7–9 [early Miocene, Subzone M1b, DSDP Hole 526A, South Atlantic Ocean], figs. 10–12 [late Oligocene, Zone O6, ODP Hole 709B, Indian Ocean], figs. 13–15 [early

Miocene, Subzone M1b, DSDP Hole 516F, South Atlantic Ocean], figs. 16–19 [late Oligocene, Zone O7, DSDP Hole 538A, Gulf of Mexico], figs. 20–23 [late Oligocene, Zone O7, DSDP Hole 538A, Gulf of Mexico].

Globigerina praebulloides Blow, 1959: pl. 8, figs. 47a–c, holotype [lower Miocene *Globigerinatella insueta/Globigerinoides bisphericus* Zone, Pozon Fm., Venezuela]; Berggren, 1972:981, pl. 3, fig. 5 [early/middle Miocene, DSDP Site 116, North Atlantic Ocean]; Aksu and Kaminski, 1989:304, pl. 4, figs. 5–7 [late Oligocene, ODP Hole 647A, Labrador Sea, North Atlantic Ocean]; Spiegler, 1996:166, pl. 1, fig. 16 [Miocene, ODP Hole 911A, central Yermak Plateau, high-latitude North Atlantic].

Remarks. Globigerinella obesa exhibits considerable variability in Oligocene to Pliocene sediments, often resembling *Globigerina bulloides*. The wall texture is *bulloides*-type. All specimen with a low arch and extraumbilical aperture were considered to be *G. obesa* (vs. the high arch and umbilical aperture in *G. bulloides*). No attempt was made to separate *Globigerinella obesa* from *Globigerinella pseudobesa*. *Globigerina praebulloides* Blow is considered a junior synonym of *Globigerinella obesa* Bolli (see Spezzaferri et al., 2018).

Chronostratigraphic range. Zone O7 (407-36R-1; 50–52 cm; 329.5 m b.s.f.) to *G. puncticulata* Zone (407-10R-1; 56–58 cm; 82.56 m b.s.f.).

Globigerinella praesiphonifera (Blow 1969)

Plate 6, Figs. 8–10

Hastigerina siphonifera praesiphonifera Blow, 1969:408, pl. 54, figs. 7–9 [middle Miocene, Zone N8, Aguide, Falcón, Venezuela].

Globigerinella praesiphonifera (Blow, 1969); Spezzaferri, 1994:50, pl. 17, figs. 2a–c; 4a–d [lower Miocene Subzone N4a, ODP Hole 709B, equatorial Indian Ocean].

Remarks. Globigerinella praesiphonifera is rare in Site 407 material. They test low trochospiral and are lobulate in outline, with 5 globular chambers. Wall texture is the *Globigerina*-type. It is umbilicus, small, open, and enclosed by surrounding chambers, the aperture has a low arch, with an umbilical–extraumbilical extending onto the peripheral edge and bordered by an imperforate rim. We differentiate *G. obesa* from *G. praesiphonifera* based on the latter having 5 chambers in the final whorl (vs. 4) and a more loosely coiled test. Differs from *"C." pseudociperoensis* in that it has an aperture extending onto the peripheral edge (vs. umbilical in *"C." pseudociperoensis*). As noted above, there is some similarity in wall textures, and future research may establish a taxonomic affinity between *praesiphonifera* and *pseudociperoensis*.

Chronostratigraphic range. Zone M1b (407-29R-1; 56–58 cm; 253.56 m b.s.f.) to "*C.*" *pseudociperoensis* Zone (407-18R-3; 56–58 cm; 161.56 m b.s.f.).

Globigerinella* cf. *siphonifera (d'Orbigny 1839)

Plate 6, Figs. 11, 12

Globigerina aequilateralis Brady, 1879:285, pl. 80, figs. 18-21 [Recent, North Pacific Ocean].

Globigerinella aequilateralis (Brady); Kennett and Srinivasan, 1984:238, pl. 60, figs. 4–5 [Late Pleistocene, *Globorotalia tosaensis* Zone, DSDP Site 206, southwest Pacific], fig. 6 [middle Miocene, Zone N12, DSDP Site 289, Ontong Java Plateau, equatorial western Pacific Ocean]; Poore, 1979:479, pl. 1, fig. 3 [Pleistocene, DSDP Site 412, North Atlantic Ocean]; Spiegler, 1996:167, pl. 2, fig. 6 [upper Pliocene, Zone N21, ODP Hole 910D, Fram Strait, Nordic Seas].

Globigerina siphonifera d'Orbigny, 1839: pl. 4, figs. 15–18 [Recent, Cuba, and Jamaica].

Globigerinella siphonifera (d'Orbigny); Todd, 1963:110; Spiegler, 1996:167, pl. 2, fig. 7 [upper Pliocene, Zone N21, ODP Hole 910D, Fram Strait, Nordic Seas].

Remarks. This species is rare at Site 407 and occurs only in two samples. *Globigerinella* cf. *siphonifera* differs from *G. siphonifera* s.s. by being smaller and less inflated. In the early stage, the test is low trochospiral, changing to nearly planispiral in the adult form. Juvenile *G. siphonifera* can resemble *G. praesiphonifera*, as both are low trochospiral; however, at Site 407, both species do not overlap stratigraphically. Therefore, low-trochospiral specimens found in Quaternary sediments are classified as *G.* cf. *siphonifera*.

Chronostratigraphic range. N. pachyderma Zone (407-5R-2, 50–52 cm, to 407-1R-1, 57–60 cm; 36.5–0.57 m b.s.f.).

Genus *Globorotalia* Cushman 1927

Type species: Pulvinulina menardii var. *tumida* Cushman 1927

***Globorotalia archeomenardii/G. praemenardii* plexus**

Plate 7, Figs. 1–5

Globorotalia archeomenardii Bolli, 1957:119, pl. 28, figs. 11a–c [*Globorotalia fohsi barisanensis* Zone, Trinidad].

Globorotalia praemenardii Cushman and Stainforth, 1945:70, pl. 13, figs. 14a–c [probably upper Oligocene, Cipero formation, Zone III (*Globorotalia fohsi* Zone), Trinidad].

Remarks. No attempt was made to separate *G. archeomenardii* from *G. praemenardii*.

Chronostratigraphic range. "*C.*" *pseudociperoensis* Zone (407-18R-2; 56–58 cm; 160.06 m b.s.f.).

Globorotalia challengeri Srinivasan and Kennett 1981

Plate 7, Figs. 6–10

Globorotalia challengeri Srinivasan and Kennett, 1981:449–533, pl.1 [middle Miocene, DSDP Site 281, South Tasman Rise, South Pacific].

Remarks. Globorotalia challengeri is similar to *G. praescitula* but is moderately low trochospiral (vs. low trochospiral in *G. praescitula*) with more inflated chambers. The peripheral margin is broadly rounded. This species has 5–5.5 chambers (vs. 4–4.5 in *G. praescitula*) in the final whorl.

Chronostratigraphic range. "*C.*" *pseudociperoensis* Zone (407-19R-1, 56–58 cm, to 407-18R-2, 56–58 cm; 169.56–160.06 m b.s.f.).

Globorotalia crassaformis (Galloway and Wissler 1927)

Plate 7, Fig. 11

Globigerina crassaformis Galloway and Wissler, 1927:41, pl. 7, fig. 12 [middle bed at the DMS Quarry; lower San Pedro Fm., Pleistocene, Lomita Quarry, Palos Verdes Hills, California, USA].

Globorotalia (Truncorotalia) crassaformis (Galloway and Wissler, 1927); Kennett and Srinivasan, 1983:145, pl. 34, figs. 6–8 [late early Pliocene, *Globorotalia crassaformis* Zone, DSDP Site 208, southwest Pacific]; Weaver, 1987:727, pl. 3, figs. 10, 11 [late Pliocene, PL3 Zone, DSDP 606, Azores, North Atlantic Ocean]; Aksu and Kaminski, 1989:301, pl. 1, figs. 9–12 [Pleistocene, ODP Hole 647A, Labrador Sea, North Atlantic Ocean].

Remarks. Globorotalia crassaformis differs from *Globoconella puncticulata* in that it has a more subangular peripheral margin (vs. rounded), more rectangular (vs. crescentic) chambers, and a low-arched aperture (vs. high arched).

Chronostratigraphic range. N. pachyderma Zone (407-5R-1, 56–58 cm, to 407-1R-1, 57–60 cm; 35.06–0.57 m b.s.f.).

Globorotalia hirsuta (d'Orbigny 1939)

Plate 8, 1–3

Rotalina hirsuta d'Orbigny, 1939:33, pl. 5, fig. 4 [Sables Marins, Recent, Tenerife, Canary Islands].

Globorotalia (Hirsutella) hirsuta, d'Orbigny; Kennett and Srinivasan, 1983:137, pl. 32, figs. 7–9 [*Globorotalia truncatulinoides* Zone, early Pleistocene, DSDP Site 284, Challenger Plateau, Aotearoa / New Zealand, South Pacific]. Weaver, 1987:726, pl. 2, fig. 2 [Pleistocene, DSDP Site 606, Azores, North Atlantic Ocean].

Remarks. This species is sparse at Site 407 and found in only one sample. It is characterized by its larger size compared to *G. scitula* and in that it has a thicker test.

Chronostratigraphic range. N. pachyderma Zone (407-1R-2; 56–58 cm; 2.06 m b.s.f.).

Globorotalia praescitula Blow 1959

Plate 7, Figs. 4–7

Globorotalia scitula praescitula, Blow 1959:221, pl. 19, figs. 128a-c [auger line near Pozon, eastern Falcón, Venezuela].

Remarks. Globorotalia praescitula is common to dominant in Site 407 material. It can be differentiated from *G. zealandica* by having more chambers in final whorl (4.5 vs. 4), having increased curvature of the sutures on the umbilical side, and having a peripheral compression. This species looks very similar to *G. scitula* but can be differentiated in that it has a more circular outline (vs. subcircular). *Globorotalia scitula* has a more lobulate equatorial periphery, whereas *G. praescitula* has a more subangular equatorial periphery.

Chronostratigraphic range. "*C.*" *pseudociperoensis* Zone (407-20R-1, 100–102 cm, to 407-18R-2, 56–58 cm; 178–160.06 m b.s.f.).

Globorotalia scitula (Brady 1882)

Plate 7, Figs. 8–12

Pulvinulina scitula Brady, 1882:716, pl. 103, figs. 7a–c [Recent, Faroe–Shetland Channel]; Banner and Blow, 1960:27, pl. 5, figs. 5a–c [Recent, Faroe Channel].

Globorotalia (Hirsutella) scitula Brady; Kennett and Srinivasan, 1983:135, pl. 31, figs. 1, 3–5 [*Globorotalia truncatulinoides* Zone, early Pleistocene, DSDP Site 284, Challenger Plateau, Aotearoa / New Zealand, South Pacific]; Aksu and Kaminski, 1989: 302, pl. 2, figs. 1–4 [Pliocene, ODP Hole 646B, Labrador Sea, North Atlantic Ocean].

Remarks. This species is rare in the late Miocene–Pleistocene section of Site 407. It differs from *G. praescitula* in that it has a smooth surface and subcircular outline. Under the light microscope, *G. scitula* has a more glassy appearance compared to *G. praescitula*. Specimens are generally small, but often larger specimens were found, and no attempt was made to differentiate these specimens into *G. gigantea*.

Chronostratigraphic range. N. praeatlantica Zone to *N. pachyderma* Zone (407-18R-1, 56–58 cm, to 407-1R-1, 56–60 cm; 158.56–0.57 m b.s.f.).

***Globorotalia* spp.**

Plate 9, Figs. 1–3

Remarks. The tests of *Globorotalia* spp. are large and moderately high trochospiral. The equatorial periphery is rounded, and the axial periphery subangular. It has 4.5 globular chambers in the final whorl. Sutures on the spiral side are curved and depressed; on the umbilical side, the sutures are slightly straight and depressed. The aperture is interiomarginal and umbilical–extraumbilical with a lip. No keel is present.

Chronostratigraphic range. "*C.*" *pseudociperoensis* Zone (407-19R-2, 56–58 cm, to 407-19R-1, 56–58 cm; 169.56–168.06 m b.s.f.).

Globorotalia truncatulinoides (d'Orbigny 1839)

Plate 9, Figs. 4–6

Rotalina truncatulinoides d'Orbigny, 1839:132, pl. 2, figs. 25–27 [Recent, Tenerife, Canary Islands].
Globorotalia (Truncorotalia) truncatulinoides (d'Orbigny); Kennett and Srinivasan 1983:149, pl. 34, fig. 2 [early Pleistocene, *Globorotalia truncatulinoides* Zone, DSDP Site 206, southwest Pacific]; Weaver, 1987:726, pl. 2, fig. 1 [Pleistocene, DSDP Site 606, Azores, North Atlantic Ocean].

Remarks. Globorotalia truncatulinoides is rare at Site 407 and is characterized by its almost circular equatorial periphery, an acute axial periphery with a pronounced keel, and an open umbilicus.

Chronostratigraphic range. N. pachyderma Zone (407-1R-2; 56–58 cm; 2.06 m b.s.f.).

Globorotalia zealandica Hornibrook 1958

Plate 9, Figs. 7, 8

Globorotalia zealandica Hornibrook, 1958:667, figs. 18, 19, 30 [Awamoan Stage, Pukeuri road cutting, Oamaru, Aotearoa / New Zealand]; Berggren, 1972:981, pl. 3, fig. 4 [middle Miocene, DSDP Site 116, North Atlantic Ocean]; Poore, 1979:491, pl. 7, figs. 10–12 [early Miocene Zone N8, DSDP Site 408, Irminger Sea, North Atlantic Ocean].

Remarks. We closely followed the Hornibrook holotype. Specimens are laterally inflated in side view.

Chronostratigraphic range. "*C.*" *pseudociperoensis* Zone (407-19R-3, 56–58 cm, to 407-18R-2, 56–58 cm; 171.06–160.06 m b.s.f.).

Genus *Globoconella* Bandy 1975

Type species: Globorotalia conomiozea Kennett 1966

Globoconella inflata (d'Orbigny 1839)

Plate 9, Fig. 10

Globigerina inflata d'Orbigny, 1839:134, pl. 12, figs. 7–9 [Holocene, Tenerife, Canary Islands].
Globorotalia (Globoconella) inflata (d'Orbigny); Kennett and Srinivasan, 1983:118, pl. 27, figs. 7–9 [Late Pliocene, *Globorotalia inflata* Zone, DSDP Site 284, southwestern Pacific Ocean]; Weaver, 1987:727, pl. 3, figs. 6–7 [Pleistocene, Zone N22, DSDP Site 606, Azores, North Atlantic Ocean].
Globoconella cf. *inflata* (d'Orbigny); Spiegler, 1996:166, pl. 1, fig. 9 [Quaternary, ODP Hole 911A, central Yermak Plateau, high-latitude North Atlantic].
1979 *Globorotalia inflata* Poore Plate 5, Figs. 1–3
1989 *Globorotalia (Globoconella) inflata* Aksu and Kaminski Plate 1, Figs. 1–3

Remarks. Globoconella inflata differs from *G. puncticulata* in that it has a rounded periphery, 3–3.5 chambers (vs. 4), a smooth cortex (vs. dense pustules on *G. puncticulata*), and a larger high-arched aperture.

Chronostratigraphic range. G. inflata PRZ to *N. pachyderma* Zone (407-8R-2, 56–58 cm, to 407-1R-1, 57–60 cm; 65.06–0.57 m b.s.f.).

Globoconella miotumida (Walters 1965)

Plate 9, Figs. 10, 11

Globorotalia miozea conoidea Walters, 1965:124, pl. 8, figs. A–S [Nine Fords Stream, Aotearoa / New Zealand].
Globorotalia (Globoconella) conoidea (Walters); Kennett and Srinivasan, 1983:112, pl. 26 figs. 4–6 [Late Miocene, *Globigerina nepenthes* Zone, DSDP Site 206, southwestern Pacific Ocean]; Weaver, 1987:727, pl. 3, figs. 1–2 [late Miocene, Zone N17, DSDP Site 608, King's Trough, North Atlantic Ocean].
Globorotalia menardii (d'Orbigny) subsp. *miotumida* Jenkins, 1960:362, pl. 4, figs. 9a–c [*Globorotalia menardii miotumida* Zone, Lakes Entrance Oil Shaft, Victoria, Australia].

Remarks. Globoconella miotumida is rare at Site 407. It differs from *Glocobonella conomiozea* in that it has a $> 90°$ angle (see Lam and Leckie, 2018).

Chronostratigraphic range. "*C.*" *pseudociperoensis* Zone to *N. praeatlantica* Zone (407-19R-1, 56–58 cm to 407-17R-3, 53–55 cm; 168.1–152.0 m b.s.f.).

Globoconella puncticulata (Deshayes 1932)

Plate 9, Fig. 12

Globigerina puncticulata Deshayes 1832:170, pl. 5, figs. 7a–c [Recent, Rimini, Italy].
Globorotalia (Globoconella) puncticulata (Deshayes); Kennett and Srinivasan 1984:116, pl. 27, figs. 4–6 [early Pliocene, *Globorotalia puncticulata* Zone, DSDP Site 284, southwestern Pacific Ocean]; Weaver, 1987:727, pl. 3, figs. 8–9 [late Pliocene, PL3 Zone, DSDP Site 606, Azores, North Atlantic Ocean].
1979 *Globorotalia puncticulata* Poore Plate 5, Figs. 4–6
1989 *Globorotalia (Globoconella) puncticulata* Aksu and Kaminski Plate 1, Figs. 4–8

Remarks. See *Globoconella inflata*.

Chronostratigraphic range. G. puncticulata Zone (407-11R-3, 56–58 cm, to 407-9R-2, 53–55 cm; 95.06–73.58 m b.s.f.).

Genus *Globorotaloides* Bolli 1957

Type species: Globorotaloides variabilis Bolli 1957

Globorotaloides hexagonus (Natland, 1938)

Plate 10, Fig. 1

Globigerina hexagona Natland, 1938:149, pl. 36, figs. 3a–c, holotype [seafloor sample collected off Long Beach, California; 33°27.20′ N, 118°19.00′ W; 884 m water depth].

Globorotaloides hexagona (Natland); Lipps, 1964:128 (placed in *Globorotaloides* for first the time; no illustration).

Globorotaloides hexagonus (Natland); Hemleben and others, 1989:27, pl. 2.6, figs. n–p [Recent].

Remarks. Only one specimen of this species was found at Site 407. However, it was easily identified by its almost flat spiral side and coarsely cancellate texture with large hexagonal-shaped pores. There are 5 chambers in the final whorl with a low umbilical–extraumbilical aperture. In the modern oceans, *G. hexagonus* is described as an Indo-Pacific species, most likely becoming extinct in the Atlantic in the Pleistocene (see Coxall and Spezzaferri, 2018). However, in the eastern tropical Atlantic, *G. hexagonus* reaches into the lower Miocene Zone M2 (Spezzaferri, 1994).

Chronostratigraphic range. Zone M1b (407-29R-3; 20–22 cm; 264.5 m b.s.f.).

Globorotaloides stainforthi (Bolli, Loeblich, and Tappan 1957)

Plate 10, Figs. 2, 3

Catapsydrax stainforthi Bolli, Loeblich, and Tappan, 1957:37, pl. 7, fig. 11, [Miocene *Catapsydrax stainforthi stainforthi* Zone, Cipero Fm., Trinidad]; Poore, 1979:507, pl. 15, figs. 1–3 [late Oligocene, DSDP Site 407, Irminger Sea, North Atlantic Ocean].

Globorotaloides stainforthi (Bolli, Loeblich, and Tappan); Coxall and Spezzaferri, 2018:105, pl. 4.8, figs. 1–3 [*Catapsydrax stainforthi* Zone, Zone N6, Cipero Fm., Trinidad], figs. 4-6, 9–11 [Zone O7, ODP Sample 667, Sierra Leone Rise, equatorial Atlantic Ocean], figs. 7, 8, 12, 13 [*type Catapsydrax dissimilis* Zone, Zone N5, Cipero Fm., Trinidad], figs. 14–16 [Zone N5, DSDP Site 151, Beata Ridge, Caribbean Sea].

Remarks. Globorotaloides stainforthi is rare at Site 407 and was only found in two samples. It differs from *G. suteri* in that it has a bulla with three–five infralaminal apertures.

Chronostratigraphic range. Zone O7 (407-36R-1, 50–52 cm, and 407-30R-3, 56–58 cm; 329.5 and 275.56 m b.s.f.).

Globorotaloides suteri Bolli 1957

Plate 10, Figs. 4, 5

Globorotaloides suteri Bolli 1957:117 (partim), pl. 27, fig. 13a–b, holotype, and pl. 27, figs. 9a–c, 11a–b, paratypes [lower Oligocene *Globigerina ampliapertura* Zone, Cipero Fm. Trinidad].

Remarks. The test is low trochospiral and lobulate, with a rounded axial periphery. *Globorotaloides suteri* has 4–5 chambers in the final whorl, and the aperture is a low arch. At Site 407, specimens are rare and often have a small bulla covering the aperture that covers the umbilicus. Specimens without a bulla-like final chamber have a well-developed lip. *G. suteri* differs from *C. unicavus* in that it is lower trochospiral, has a flattened spiral side, and has more chambers (three–four in *C. unicavus*).

Chronostratigraphic range. Zone O7 to "*C.*" *pseudociperoensis* Zone (407-36R-1, 50–52 cm, to 407-19R-3, 56–58 cm; 329.5–171.06 m b.s.f.).

Genus *Globoturborotalita* Hofker 1976

Type species: Globigerina rubescens Hofker 1956

Globoturborotalita apertura (Cushman 1918)

Plate 10, Figs. 6, 7

Globigerina apertura Cushman, 1918:57, pl. 12, figs. 8a–c [Miocene, Yorktown Fm., Virginia, USA]; Berggren, 1972:981, pl. 3, fig. 3 [Late Miocene, DSDP Site 116, North Atlantic Ocean].

Globigerina (Zeaglobigerina) apertura (Cushman); Kennett and Srinivasan, 1983:44, pl. 8, figs. 4–6 [early Pliocene, Zone N19, DSDP Site 289, Ontong Java Plateau, equatorial western Pacific Ocean].

Remarks. This species differs from *G. woodi* in that it has a very large semi-circular umbilical aperture with a distinct rim.

Chronostratigraphic range. "*C.*" *pseudociperoensis* Zone to *G. inflata* PRZ (407-23R-3, 56–58 cm, to 407-7R-1, 56–58 cm; 209.1-54.56 m b.s.f.).

Globoturborotalita connecta (Jenkins 1964)

Plate 10, Figs. 8–10

Globigerina woodi connecta Jenkins, 1964:72, figs. 1a–c [lower Miocene, North Island, Aotearoa / New Zealand].

Globigerina connecta (Jenkins); Poore, 1979:501, pl. 12, figs. 6, 9 [early Miocene, DSDP Site 408, Irminger Sea, North Atlantic Ocean].

Globoturborotalita connecta (Jenkins); Li and McGowran, 2000:44, fig. 20H [lower Miocene, Zone SN2, southeastern Australia].

Remarks. Globoturborotalita connecta is rare at Site 407, the test is very low trochospiral and compact, with 3 subglobular embracing chambers. It has a distinct *sacculifer*-type wall texture. The umbilicus is small, and the aperture is slit-like and umbilical to extraumbilical with a very low arch. These morphospecies are common in the Southern Ocean at high latitudes but rare in the high-latitude North Atlantic.

Chronostratigraphic range. Zone O7 to "*C.*" *pseudociperoensis* Zone (407-31R-4, 46–48 cm, to 407-19R-2, 56–58 cm; 286.5–169.6 m b.s.f.).

Globoturborotalita* cf. *connecta

Plate 10, Figs. 11, 12

Remarks. Globoturborotalita cf. *connecta* is similar to *G. connecta*, but the aperture is more open, with a low arch. Tests are heavily calcified, but the *sacculifer*-type wall texture is not well visible. Relatively abundant in the late Pliocene, reaching values up to 13 %.

Chronostratigraphic range. N. atlantica (sin.) PRZ to *G. inflata* PRZ (407-13R-1, 56–58 cm to 407-7R-2; 56–58 cm; 111.06–56.06 m b.s.f.).

Globoturborotalita decoraperta (Takayanagi and Saito 1962)

Plate 11, Figs. 1, 2

Globigerina druryi (Akers) subsp. *decoraperta* Takayanagi and Saito, 1962:85, pl. 28, figs. 10a–c [Miocene, Tortonian, Nobori Fm., Japan].

Globigerina decoraperta (Takayanagi and Saito); Poore, 1979:501, pl. 12, figs. 7, 8 [late Miocene, DSDP Site 410, North Atlantic Ocean].

Globigerina (Zeaglobigerina) decoraperta (Takayanagi and Saito); Kennett and Srninivasan, 1983:48, pl. 9, figs. 4–6 [Late Miocene, Neogloboquadrina continuosa Zone, DSDP Site 207A, Tasman Sea].

Remarks. This species differs from *G. woodi* in that it has a high-trochospiral test and is rare at Site 407.

Chronostratigraphic range. "*C.*" *pseudociperoensis* Zone (407-24R-3, 56–58 cm, and 407-18R-3, 56–58 cm; 218.56 and 161.56 m b.s.f.).

Globoturborotalita euapertura (Jenkins 1960)

Globigerina euapertura Jenkins, 1960:351, pl. 1, figs. 8a–c [lower Miocene pre-*Globoquadrina dehiscens* Zone, Lakes Entrance Oil Shaft, Victoria, southeastern Australia].

Globoturborotalita euapertura (Jenkins); Spezzaferri et al., 2018:224, pl. 8.6, figs. 1–3 [Miocene, Victoria, southeastern Australia], figs. 4–6 [Whaingaroa, Raglan Harbour section, Aotearoa / New Zealand], figs. 7–9 [Zone P22, ODP Hole 588C, Tasman Sea], figs. 10–12 [?], figs. 13–16 [early Miocene, Subzone M1b, ODP Hole 588C, Tasman Sea].

Remarks. Globoturborotalita euapertura differs from *G. woodi* in that it has 4 wedge-like chambers, and the final chamber is reniform extending over the umbilicus in edge view. This species is rare at Site 407.

Chronostratigraphic range. Zone O7 (407-35R-1, 86–88 cm, and 407-30R-3, 56–58 cm; 320.36 and 275.56 m b.s.f.).

Globoturborotalita ouachitaensis (Howe and Wallace 1932)

Plate 10, Figs. 3–6

Globigerina ouachitaensis Howe and Wallace, 1932:74 (partim), pl. 10, fig. 5a–b [upper Eocene, Jackson Fm., Danville Landing, Louisiana]; Leckie and others, 1993:124, pl. 9, figs. 11, 12 [upper Eocene, ODP Hole 628A, Little Bahama Bank, western Atlantic Ocean]; Cicha and others, 1998:100, pl. 31, figs. 14–17 [central Paratethys, lower Oligocene (locality unspecified)], fig. 21 [lower Oligocene, Pouzdřany unit, Pouzdřany, Moravia]; Poore, 1979:517, pl. 20, fig. 7 [late Oligocene, DSDP Site 407, Irminger Sea, North Atlantic Ocean].

Globoturborotalita ouachitaensis (Howe and Wallace); Olsson and others, 2006:122, 125, pl. 6.5, fig. 7 [middle Eocene Zone E15/16, Shubuta Clay, Wayne County, Mississippi], figs. 15, 16, [middle Eocene Zone E10/11, Guayabal Fm., type locality, Tampico, Mexico].

Remarks. Small and low trochospiral test with 4 globular chambers. The profile is diamond-shaped. This species is relatively rare at Site 407.

Chronostratigraphic range. Zone O7 (407-36R-1, 50–52 cm, to 407-30R-3, 56–58 cm; 329.5–286.5 m b.s.f.).

Globoturborotalita woodi (Jenkins 1960)

Plate 11, Figs. 7–11

Globigerina woodi Jenkins, 1960:352, pl. 2, fig. 2a–c [lower Miocene, southeastern Australia]; Jenkins, 1978:726, pl. 1, figs. 6, 7 [lower Miocene, *Globigerinoides trilobus* Zone, DSDP Site 362, Walvis Ridge, southeastern Atlantic Ocean]; Poore, 1979:503, pl. 13, figs. 1–2 [late Miocene, DSDP Site 410, North Atlantic Ocean], figs. 3–4 [late Miocene, DSDP Hole 408, Irminger Sea, North Atlantic Ocean], figs. 5–10 [early Miocene, DSDP Site 408, Irminger Sea, North Atlantic Ocean].

Globigerina (*Zeaglobigerina*) *woodi* Jenkins; Kennett and Srinivasan, 1983:43, pl. 7, figs. 4–6 [upper Miocene *Globigerina nepenthes* Zone, DSDP Site 207A, Lord Howe Rise, southwestern Pacific Ocean]; Aksu and Kaminski, 1989:302, pl. 2, figs. 13–16 [late Miocene, ODP Hole 646B, Labrador Sea, North Atlantic Ocean].

Globoturborotalita woodi (Jenkins); Li and McGowran, 2000:45, fig. 20G [lower Miocene, Zone SN2, southeastern Australia].

Remarks. Globoturborotalita woodi is rare to present at Site 407 throughout the record but was common during the middle Miocene. *G. woodi* is common to abundant in the mid-latitude North Atlantic Ocean, but rare in the high-latitude North Atlantic. These morphospecies are common in the Southern Ocean at high latitudes.

Chronostratigraphic range. Zone O7 to *G. inflata* PRZ (407-36R-1, 50–52 cm, to 407-7R-1, 56–58 cm; 329.5–54.56 m b.s.f.).

Genus *Paragloborotalia* Cifelli, 1982

Type species: Globorotalia opima subsp. *opima* Bolli 1957

Paragloborotalia acrostoma (Wezel 1966)

Plate 12, Figs. 1–5

"Globorotalia" acrostoma Wezel, 1966:1298–1301, pl. 101, figs. 1–8 [lower Miocene *Globigerinoides trilobus trilobus* Zone, Zona a scaglie tettoniche, Tempio River, Mirabella, Sicily, Italy].

Globorotalia acrostoma (Wezel); Poore, 1979:495, pl. 9, figs. 6, 8 [early Miocene, DSDP Site 408, Irminger Sea, North Atlantic Ocean], figs. 7, 9 [middle Miocene, DSDP Site 407, Irminger Sea, North Atlantic Ocean].

Paragloborotalia acrostoma (Wezel); Spezzaferri, 1994:56, pl. 21, figs. 5a–d [lower Miocene, Zone N7/N8, DSDP Hole 548A, Goban Spur, eastern North Atlantic Ocean], pl. 22, figs. 3a–c [lower Miocene Zone N7/N8, DSDP Hole 548A, Goban Spur, eastern North Atlantic Ocean]; Leckie et al., 2018:130, pl. 5.1, figs. 1–3.

Remarks. See *Paragloborotalia mayeri*.

Chronostratigraphic range. Zone O7 to "*C.*" *pseudociperoensis* Zone (407-30R-2, 56–58 cm, to 407-18R-2, 56–58 cm; 274.06–160.06 m b.s.f.).

Paragloborotalia birnageae (Blow 1959)

Plate 12, Figs. 6, 7

Globorotalia birnageae Blow, 1959:210–211, pl. 17, figs. 108a-c [lower Miocene *Globigerinatella insueta* Zone, Pozon Fm., eastern Falcón, Venezuela]; Berggren, 1972:981, pl. 3, figs. 11, 12 [early Miocene, DSDP Site 116, North Atlantic Ocean]; Poore, 1979:470, pl. 10, figs. 4, 5, 7, 8 [lower Miocene Zone N7, DSDP Site 407, North Atlantic Ocean].

Paragloborotalia birnageae (Blow); Leckie et al., 2018:132, pl. 5.2, figs. 1–3 [lower Miocene, *Globigerinatella insueta* Zone, Pozon Fm., Venezuela], figs. 4–6 [upper Oligocene, Zone N3, JOIDES drill hole 3, western North Atlantic], figs. 7–9 [upper Oligocene, Zone N3, DSDP Hole 64.1, Ontong Java Plateau, western equatorial Pacific Ocean], pl. 5.3, figs. 1–3 [upper Oligocene, Zone O7, ODP Hole 628A, Little Bahama Bank, western North Atlantic Ocean], fig. 4 [lower Miocene, Zone M1, ODP Hole 806B, Ontong Java Plateau, western equatorial Pacific Ocean], figs. 5–7 [Zone N8, DSDP Site 289, Ontong Java Plateau, western equatorial Pacific Ocean], figs. 8, 12 [Subzone N4b, ODP Hole 806B, Ontong Java Plateau, western equatorial Pacific Ocean], figs. 9–11 [Subzone N4a, ODP Hole 709B, Madingley Rise, Indian Ocean], figs. 13–15 [upper Oligocene, Zone O7, ODP Hole 709B, Madingley Rise, Indian Ocean], fig. 16 [upper Oligocene, Zone O7,DSDP Hole 64A, Ontong Java Plateau, western equatorial Pacific Ocean].

Remarks. Paragloborotalia birnageae is rare at Site 407 with 4.5 chambers in the final whorl. The final chamber is often kummerform bordered by a prominent lip.

Chronostratigraphic range. Zone O7 to "*C.*" *pseudociperoensis* Zone (407-30R-3, 56–58 cm, to 407-19R-3, 56–58 cm; 275.56–171.06 m b.s.f.).

Paragloborotalia continuosa (Blow 1959)

Plate 12, Fig. 8–11

Globorotalia opima subsp. *continuosa* Blow, 1959:218–219, pl. 19, figs. 125a–c [middle Miocene *Globorotalia mayeri* Zone, Pozon Fm., eastern Falcón, Venezuela].

Globorotalia continuosa Blow; Berggren, 1972:979, pl. 2, figs. 15, 16 [Middle-Late Miocene, DSDP Site 116, North Atlantic Ocean]; Poore, 1979:471, pl. 9, figs. 10–12 [upper Miocene Zone N16, DSDP Site 408, North Atlantic Ocean].

Neogloboquadrina continuosa (Blow); Kennett and Srinivasan, 1983:192, pl. 47, figs. 3–5 [lower Miocene Zone N6, DSDP Site 289, Ontong Java Plateau, western equatorial Pacific Ocean]; Weaver, 1987:725, pl. 1, figs. 7–9 [late Miocene, DSDP Site 610, Feni Drift, North Atlantic Ocean]; Aksu and Kaminski, 1989: pl. 4, figs. 1–4 [late Miocene, ODP Hole 646B, Labrador Sea, North Atlantic Ocean]; Spiegler and Jansen, 1989: pl. 1, fig. 7 [early Pliocene, ODP Hole 642B, Vøring Plateau, Nordic Seas].

Paragloborotalia continuosa (Blow); Spezzaferri, 1994:54, pl. 20, figs. 7a–c [lower Miocene Zone N5, DSDP Site 151, Gulf of Mexico]; Spiegler, 1996:166, pl. 1, figs. 12–13 [Miocene, ODP Hole 911A, central Yermak Plateau, high-latitude North Atlantic]; Leckie et al., 2018:137, pl. 5.4, figs. 1–3 [middle Miocene *Globorotalia mayeri* Zone, Pozon Fm., Venezuela], fig. 4 [Zone N8/N9, ODP Hole 806B, Ontong Java Plateau, western equatorial Pacific Ocean], fig. 8 [Zone N5, ODP Hole 806B, Ontong Java Plateau, western equatorial Pacific Ocean].

Remarks. Paragloborotalia continuosa is rare at Site 407 and is regarded as being important for the ancestry of the neogloboquadrinids. The sutures on the umbilical side form a cross. *Paragloborotalia continuosa* differs from *P. nana* in that is less compact and a more lobulate periphery. The aperture is higher arched and comma-shaped, with a more distinctive lip than in *P. nana*. No attempt was made to separate *P. continuosa* from *P. pseudocontinuosa*.

Chronostratigraphic range. Zone O7 to *N. praeatlantica* Zone (407-30R-2, 56–58 cm, to 407-16R-3, 56–58 cm; 274.06-142.4 m b.s.f.).

Paragloborotalia kugleri (Bolli 1957)

Plate 12, Fig. 12

Globorotalia kugleri Bolli, 1957:118, pl. 28, figs. 5a–6 [lower Miocene *Globorotalia kugleri* Zone, Cipero Fm., Trinidad]; Poore, 1979:497, pl. 10, figs. 1–3 [early Miocene, DSDP Site 407, Irminger Sea, North Atlantic Ocean].

Paragloborotalia kugleri (Bolli); Spezzaferri, 1991:317, pl. 1, fig. 5a–c [reproduced from Premoli Silva and Spezzaferri, 1990, pl. 3, figs. 5a–c], pl. 2, figs. 1a-d [lower Miocene Subzone N4a, ODP Hole 709C, Madingley Rise, western equatorial Indian Ocean]; Leckie et al., 2018:141, pl. 5.5, figs. 1–3 [lower Miocene, *Globorotalia kugleri* Zone, Cipero Fm., Trinidad], figs. 4, 8, 12, 16 [Subzone N4a, ODP Hole 803D, Ontong Java Plateau, western equatorial Pacific Ocean], figs. 5–7 [Subzone N4b, ODP Hole 709B, Madingley Rise, Indian Ocean], figs. 9–11 [*Globorotalia kugleri* Zone, Mosquito Creek, Trinidad], fig. 13 [Zone M1, ODP Site 904, New Jersey slope, North Atlantic Ocean], fig. 15 [*kugleri* type locality, Trinidad].

Remarks. Very rare at Site 407 but still a useful age marker for the base of the Miocene. This species is similar to *P. pseudokugleri*, but the final chamber shows a distinct pinching; the chambers are less inflated and more appressed; the outline is more ovate and less lobulate; spiral side sutures are more strongly curved and less depressed.

Chronostratigraphic range. Zone M1 (407-30R-2, 56–58 cm, to 407-28R-3, 56–58 cm; 274.06–256.56 m b.s.f.).

Paragloborotalia mayeri (Cushman and Ellisor, 1939)

Plate 13, Figs. 1, 2

Globorotalia mayeri Cushman and Ellisor, 1939:11, pl. 2, figs. 4a–c [Miocene, Humble Oil and Refining Company, Ellender, Louisiana]; Poore, 1979:471, pl. 9, figs. 1, 2 [middle Miocene Zone N14, DSDP Site 408, North Atlantic Ocean], figs. 3–5 [middle Miocene Zone N8-N11, DSDP Site 407, North Atlantic Ocean].

Neogloboquadrina mayeri (Cushman and Ellisor); Spiegler and Jansen 1989:695, pl. 1, figs. 13–14 [middle Miocene, ODP Hole 642C, Vøring Plateau, Nordic Seas], fig. 15 [late Miocene, ODP Hole 642B, Vøring Plateau, Nordic Seas].

Remarks. It is difficult to separate from *P. acrostoma*, which often has 4–5 (vs. 5) chambers. Both species occur in the same material from the early to mid-Miocene. All specimens with a closed umbilicus are considered to be *P. acrostoma*, and specimens with an open umbilicus are *P. mayeri*. Both species are rare at Site 407.

Chronostratigraphic range. Zone O7 to "*C.*" *pseudociperoensis* Zone (407-32R-1, 25–27 cm, to 407-18R-3, 56–58 cm; 291.25–161.56 m b.s.f.).

Paragloborotalia nana (Bolli 1957)

Plate 13, Fig. 3

Globorotalia opima nana Bolli, 1957:118, pl. 28, fig. 3a–c [Oligocene *Globorotalia opima* Zone, Cipero Fm., Trinidad].

Paragloborotalia opima nana (Bolli); Spezzaferri and Premoli Silva, 1991:248, pl. XI, figs. 4a–c [lower Oligocene Subzone P21a, DSDP Hole 538A, Gulf of Mexico].

Paragloborotalia nana (Bolli); Leckie and others, 1993:124, pl. 7, fig. 1 [upper Oligocene Zone P22, ODP Hole 628A, Little Bahama Bank, western North Atlantic Ocean], pl. 7, fig. 2 [lower Oligocene Zone P19, ODP Hole 628A, Little Bahama Bank, western North Atlantic Ocean]; Spiegler, 1996:166, pl. 1, fig. 17 [Miocene, ODP Hole 911A, central Yermak Plateau, high-latitude North Atlantic].

Remarks. Paragloborotalia nana is common in the lowermost sample, but the abundance decreases upwards when it becomes rare in the early Miocene. The test is small, compact, and quadrangular. Usually there are 4 chambers in the final whorl. Sutures on the umbilical side form a cross. The umbilicus is very narrow, and sutures are radial. There is an aperture with a prominent lip. This species is important for being the purported ancestor of *Paragloborotalia continuosa* and, in turn, the neogloboquadrinids.

Chronostratigraphic range. Zone O7 to Zone M1b (407-36R-1, 50–52 cm, to 407-29R-1, 56–58 cm; 329.5–263.06 m b.s.f.).

Paragloborotalia pseudokugleri (Blow 1969)

Plate 13, Figs. 4, 5

Globorotalia (*Turborotalia*) *pseudokugleri* Blow, 1969:391, pl. 10, figs. 4–6 [reproduced from Bolli, 1957, pl. 28, figs. 7a–c], pl. 39, figs. 5, 6 [*Globorotalia kugleri* Zone, Mosquito Creek, Cipero Fm., Trinidad].

Globorotalia pseudokugleri Blow; Poore, 1979:497, pl. 10, fig. 6 [late Oligocene, DSDP Site 407, Irminger Sea, North Atlantic Ocean].

Paragloborotalia pseudokugleri (Blow); Spezzaferri and Premoli Silva, 1991:248–253, pl. XI, fig. 7a–c [upper Oligocene Zone P22, DSDP Hole 538A, Gulf of Mexico]; Leckie et al., 2018:160, pl. 5.9, figs. 1–3 [*Globorotalia kugleri* Zone, Cipero Fm., Trinidad], figs. 4, 8 [Zone O7, ASP 5B, western North Atlantic Slope], figs. 5–7 [Zone M1, ODP Site 904, New Jersey slope, North Atlantic Ocean], figs. 9–11 [Zone P22, ODP Hole 709B, Madingley Rise, equatorial Indian

Ocean], figs. 12, 16 [ODP Hole 803D], figs. 13–15 [Zone M1, ODP Site 904, New Jersey slope, North Atlantic Ocean].

Remarks. this species is rare at Site 407. See remarks for *Paragloborotalia kugleri*.

Chronostratigraphic range. Zone O7 to M1a (407-36R-1, 50–52 cm, to 407-29R-3, 20–22 cm; 329.5–264.5 m b.s.f.).

Paragloborotalia semivera (Hornibrook, 1961)

Plate 13, Fig. 6

Globigerina semivera Hornibrook, 1961:149–150, pl. 23, figs. 455–457 [lower Miocene *G. trilobus* Zone, Rifle Butts Fm., Awamoan Stage, Campbells Bay Beach, South Island, Aotearoa / New Zealand].

Paragloborotalia semivera (Hornibrook); Premoli Silva and Spezzaferri, 1990:304, pl. 3, figs. 8a–c [lower Miocene Zone N4, ODP Hole 709B, Madingley Rise, western equatorial Indian Ocean].

Remarks. See *Paragloborotalia siakensis*.

Chronostratigraphic range. Zone O7 to early Miocene (407-30R-3, 56–58 cm, to 407-28R-1, 56–58 cm; 275.56–253.06 m b.s.f.).

Paragloborotalia siakensis (LeRoy 1939)

Plate 13, Fig. 7

Globorotalia siakensis LeRoy, 1939:262, pl. 4, figs. 20–22 [Miocene?, Rokan–Tapanoeli region, central Sumatra].

Paragloborotalia siakensis (LeRoy); Spezzaferri and Premoli Silva, 1991:253, pl. XI, figs. 2a–c [upper Oligocene Zone P22, DSDP Hole 538A, Catoche Knoll, Gulf of Mexico].

Remarks. The test is large in size and low trochospiral. It is strongly lobulate in the equatorial outline, and there are 5–6 globular chambers. *Paragloborotalia siakensis* differs from *Paragloborotalia semivera* in that it has a strongly lobulate equatorial outline (vs. moderately lobulate).

Chronostratigraphic range. Zone M1a (407-30R-2; 56–58 cm; 274.06 m b.s.f.).

***Paragloborotalia* sp.**

Plate 13, Figs. 8–12

Remarks. Paragloborotalia sp. refers to a morphotype with a low trochospiral that is globular, compact, and subquadrate to quadrate in outline, with (sub)globular chambers. Sutures are depressed and straight. In the umbilical view, it has 4 globular chambers. The wall texture is coarsely cancellate, with possible evidence of spine holes (likely spinose) (Plate 13, Figs. 9, 11). The aperture is an umbilical–extraumbilical and has high arch bordered with a narrow lip. *Paragloborotalia* sp. differs from *P. acrostoma* and *P. mayeri* in that it has fewer chambers (4 vs. 5 or more). *Paragloborotalia* sp. differs from *N. praeatlantica* in that it lacks the heavy secondary encrustation seen in *N. praeatlantica*.

Chronostratigraphic range. "*C.*" *pseudociperoensis* Zone (407-23R-1, 56–58 cm, to 407-18R-3, 56–58 cm; 206.06–161.56 m b.s.f.). There is a questionable occurrence in Sample 407-29R-3, 20–22 cm, at 264.5 m b.s.f. (Zone M1a).

***Paragloborotalia* spp.**

Remarks. Paragloborotalia spp. refers to specimens found in the lowermost part of the sequence that are assumed to be paragloborotalids but that cannot be narrowed down to any particular species or morphotype because of glauconite infills that obscure the aperture and other parts of the test. Specimens mostly have 5 chambers and look similar to *P. siakensis*, *P. mayeri*, and *P. semivera*. These specimens are rare.

Chronostratigraphic range. Zone O7 to "*C.*" *pseudociperoensis* Zone (407-36R-1, 50–52 cm, to 407-20R-1, 100–102 cm; 329.5–178 m b.s.f.).

Genus *Neogloboquadrina* Bandy, Frerichs and Vincent 1967

Type species: Globigerina dutertrei d'Orbigny 1839

Neogloboquadrina acostaensis (Blow 1959)

Plate 14, Figs. 1–3

Globorotalia acostaensis Blow, 1959:208, pl. 17, figs. 106a-c [Pozon, eastern Falcón, Venezuela]; Berggren, 1972:979, pl. 2, figs. 13, 14 [late Miocene, DSDP Site 116, North Atlantic Ocean].

Neogloboquadrina acostaensis (Blow); Srinivasan and Kennett, 1976: [Late Miocene]; Poore, 1979:511, pl. 17, figs. 1–3 [late Miocene, DSDP Site 408, Irminger Sea, North Atlantic Ocean]; Weaver, 1987:725, pl. 1, figs. 5, 6 [late Miocene, *G. conomiozea Zone*, DSDP Site 608, Azores, North Atlantic Ocean]; Aksu and Kaminski, 1989:303, pl. 3, figs. 13–16 [late Pliocene, ODP Hole 646B, Labrador Sea, North Atlantic Ocean]; Spiegler and Jansen, 1989:695, pl. 1, figs. 9–12 [late Miocene, ODP Hole 642C, Vøring Plateau, Nordic Seas].

Neogloboquadrina acostaensis (Blow); Srinivasan and Kennett, 1983:196, pl. 47, fig. 1 [Late Miocene, Zone N18, DSDP Site 289, Ontong Java Plateau, equatorial western Pacific Ocean], pl. 48, figs. 1–3 [Late Miocene, Zone N18, DSDP Site 289, Ontong Java Plateau, equatorial western Pacific Ocean].

Remarks. Neogloboquadrina acostaensis has 4–5 chambers in the final whorl, but the majority have 4.5 chambers.

Chronostratigraphic range. N. praeatlantica Zone to *N. pachyderma* Zone (407-18R-1, 56–58 cm, to 407-3R-3, 55–58 cm; 158.56–19.05 m b.s.f.).

Neogloboquadrina* cf. *acostaensis

Plate 14, Figs. 4–6

Remarks. Specimens belonging to *N.* cf. *acostaensis* are small and tightly coiled, with 3–4 chambers in the final whorl. The final chamber has a well-developed lip covering the aperture. This differs from *N. acostaensis* s.s. by having fewer chambers and being very compact. It looks similar to *G. suteri* or *C. unicavus* but is non-spinose when seen on SEM images. The only way of distinguishing *N.* cf. *acostaensis* from *G. suteri* and *C. unicavus* is that *N.* cf. *acostaensis* has no stratigraphic overlap with *G. suteri* and *C. unicavus*.

Chronostratigraphic range. N. praeatlantica Zone (407-17R-3, 53–55 cm, to 407-16R-1, 56–58 cm; 152-139.56 m b.s.f.).

Neogloboquadrina atlantica (Berggren 1972)

Neogloboquadrina atlantica dextral Plate 14, Figs. 7–12
Neogloboquadrina atlantica sinistral Plate 15, Figs. 1–7
Globigerina atlantica Berggren, 1972:972, pl. 1, figs. 1–4 [Late Pliocene, DSDP Site 111, North Atlantic Ocean], figs. 5–7 [early Pliocene, DSDP Site 111, North Atlantic], pl. 2, figs. 5–8 [Late Pliocene, DSDP Hole 116A, North Atlantic Ocean].
Neogloboquadrina atlantica (Berggren); Poore and Berggren, 1975:77, pl. 1, figs. 1–13 [Late Pliocene, DSDP Hole 116A, North Atlantic Ocean], pl. 2, figs. 1–12 [Late Pliocene, DSDP Hole 116A, North Atlantic], pl. 3, figs. 1–12 [Late Pliocene, DSDP Hole 116A, North Atlantic Ocean]; Poore, 1979:509, pl. 16, figs. 1–4 [early Pliocene, DSDP Site 407, Irminger Sea, North Atlantic Ocean], figs. 5–9 [late Miocene, DSDP Site 407, Irminger Sea, North Atlantic Ocean]; Weaver, 1987:725, pl. 1., figs. 13–15; Aksu and Kaminski, 1989:303, pl. 3, figs. 6–9 [late Miocene, ODP Hole 646B, Labrador Sea, North Atlantic Ocean].
Globoquadrina asanoi Maya, Saito, and Sato, 1976, pl. 3, figs. 1–3 [Pliocene, Nomura Mudstone Member, Funakawa Fm., Japan], pl. 5, figs. 1–2 [Pliocene, Nomura Mudstone Member, Funakawa Fm., Japan].
Neogloboquadrina humerosa (Takayanagi and Saito); Aksu and Kaminski, 1989:303, pl. 3, figs. 1–5 [early Pliocene, ODP Hole 646B, Labrador Sea, North Atlantic Ocean].
Neogloboquadrina atlantica (Berggren) sinistral; Spiegler and Jansen, 1989:695, pl. 1, fig. 6 [late Pliocene, ODP Hole 642C, Vøring Plateau, Nordic Seas]. Spiegler, 1996:166, pl. 1, figs. 7–8 [upper Pliocene, ODP Hole 909C, Fram Strait, Nordic Seas].
Neogloboquadrina dutertrei (d'Orbigny) dextral; Spiegler and Jansen, 1989:695, pl. 1, fig. 1 [late Miocene, *N. atlantica* (sin.) Zone, ODP Hole 642B, Vøring Plateau, Norwegian Sea].
Neogloboquadrina dutertrei (d'Orbigy) sinistral; Spiegler and Jansen, 1989:695, pl. 1, figs. 2, 3 [late Miocene, *N. atlantica* (dex.) Zone, ODP Hole 642B, Vøring Plateau, Norwegian Sea].
Neogloboquadrina asanoi (Maya, Saito, and Sato); Spiegler, 1996:166, pl. 1, figs. 5–6 [upper Pliocene, ODP Hole 910C, Fram Strait, Nordic Seas].
Neogloboquadrina atlantica (Berggren); Kaminski and Berggren, 2021:106, pl. 1, figs. 1–3 [(1a–c = neotype), DSDP Hole 116A, North Atlantic Ocean].

Remarks. Neogloboquadrina atlantica is the main contributor to late Miocene and Pliocene assemblages at Site 407 and a distinct shift from dextral to sinistral is recorded in the late Miocene. *Neogloboquadrina atlantica* shows a large morphological variability; it can be low to high trochospiral and has 4–5 globular chambers. The final chamber can be kummerform. The aperture can be umbilical to extra-umbilical, often with a lip. *Neogloboquadrina atlantica* differs from the other neogloboquadrinids in its large size and its a cancellate wall with a heavy granular wall texture resembling sugar, and it is comparable to the encrusted test of other neogloboquadrinds. It differs from *N. dutertrei* in generally being bigger and its heavy granular wall texture, and it also has fewer chambers. So far, this species is only recorded in the North Atlantic and North Pacific oceans, whereas late Miocene and Pliocene assemblages in the high southern latitudes are dominated by *N. pachyderma*.

Chronostratigraphic range. N. praeatlantica Zone to *G. inflata* PRZ (407-18R-1, 56–58 cm, to 407-6R-3, 55–58 cm; 158.56–47.48 m b.s.f.).

Neogloboquadrina dutertrei (d'Orbigny 1839)

Plate 15, Fig. 8

Globigerina dutertrei d'Orbigny, 1839:84, pl. 4, figs. 19–21 [Recent, Cuba, Martinique, and Guadalupe]; Banner and Blow, 1960:11, pl. 2, fig. 1 [(lectotype) Recent, Cuba, Martinique, and Guadalupe Island].
Neogloboquadrina dutertrei (d'Orbigny); Kennett and Srinivasan, 1983:198, pl. 48, figs. 7–8 [Pleistocene, Zone N22, DSDP Site 208], fig. 9 [Pleistocene, Zone N22, DSDP Site 209].

Remarks. Neogloboquadrina dutertrei has 5 inflated chambers in the final whorl with an open, broad, and deep umbilicus with a lip. No umbilical plate is present in specimens from Site 407. It is rare in Site 407 material. It is differentiated from *N. atlantica* by having the classic "*Neogloboquadrina*" wall texture vs. the more granular *N. atlantica* wall texture.

Chronostratigraphic range. N. pachyderma Zone (407-5R-3, 56–58 cm, to 407-1R-1, 57–60 cm; 38.06–0.57 m b.s.f.).

Neogloboquadrina humerosa (Takayanagi and Saito, 1962)

Plate 15, Fig. 9

Globorotalia humerosa Takayanagi and Saito, 1962:78, pl. 28, figs. 1–2 [Miocene, Nobori Fm., Shikoku, Japan]; Berggren, 1972:978, pl. 2, figs. 9–12 [Middle-Late Miocene, DSDP Site 116, North Atlantic Ocean].

Neogloboquadrina dutertrei humerosa (Takayanagi and Saito); Srinivasan and Kennett, 1976: [Pliocene].

Neogloboquadrina humerosa (Takayanagi and Saito); Poore, 1979:511, pl. 17, figs. 4–6 [late Miocene, DSDP Site 408, Irminger Sea, North Atlantic Ocean].

Remarks. This species is rare at site 407. It differs from *N. acostaensis* in that it has ≥ 6 chambers in the final whorl, a wider umbilicus, and a reduced apertural lip.

Chronostratigraphic range. N. atlantica (sin.) PRZ to *N. pachyderma* Zone (407-12R-1, 56–58 cm, to 407-3R-2, 55–58 cm; 101.56–17.55 m b.s.f.).

Neogloboquadrina incompta (Cifelli 1961)

Plate 15, Figs. 10–12

Globigerina incompta Cifelli, 1961:84, pl. 4, figs. 1–7 [Recent, North Atlantic Slope, Gulf Stream, and Sargasso Sea].

Globigerina pachyderma (Ehrenberg); Parker, 1962:224, pl. 1, figs. 32, 35 [Downwind BG 62:47°37′ S, 121°02′ W, 3800 M], pl. 2, fig. 1 [Downwind BG 61:46°44′ S, 123°01′ W, 4250 M], figs. 3–6 [Scruton E 180:52°13′ N, 173°35' E, 137 M]; Berggren, 1972:979, pl. 2, fig. 4 [early Pleistocene, DSDP Site 113, North Atlantic].

Globorotalia (Turborotalia) pachyderma (Ehrenberg) dextral; Bandy, 1972:301, pl. 1, figs. 1–3 [upper Miocene, Neogene zone 14, Mohole, Guadalupe site, Equatorial Pacific Ocean], pl. 2, figs. 1–4 [upper Miocene, Neogene zones 14–15, Mohole, Guadalupe site, Equatorial Pacific Ocean], pl. 5, figs. 1–5 [Holocene, off California, Pacific Ocean], figs. 6–8 [Holocene, Bay of Biscay, Atlantic Ocean], pl. 7, fig. 8 [Modern, Drake Passage, 57°45′ S, 67°33′ W, subantarctic region], figs. 9–11, 14 [Modern, Eltanin Station 39–82, 32°39′ S, 171°50′ E, subantarctic region], fig. 12 [Modern, Eltanin Station 39–76, 36°30′ S, 161°14′ E, subantarctic region], fig. 13 [Modern, Eltanin Station 39–67, 43°38′ S, 151°58.9′ E, subantarctic region].

Neogloboquadrina pachyderma (Ehrenberg); Collen and Vella, 1973:19, pl. 1, fig. 11 [lower Pliocene, upper Gilbert Geomagnetic Epoch, upper Opoitian Stage, Aotearoa / New Zealand], pl. 2, figs. 1–3 [lower Pliocene, upper Gilbert Geomagnetic Epoch, upper Opoitian Stage, Aotearoa / New Zealand]; Poore, 1979:511, pl. 17, fig. 10 [Late Miocene DSDP Site 408, North Atlantic Ocean].

Neogloboquadrina pachyderma (Ehrenberg) dextral; Weaver, 1986:725, pl. 1, figs. 1–2 [Pleistocene, DSDP Hole 611D, Gardar Drift, North Atlantic Ocean]; Spiegler and Jansen, 1989:696, pl. 2, fig. 5 [Pleistocene, ODP Hole 644A, Nordic Seas], fig. 6 [Pleistocene, ODP Hole 642B, Nordic Seas]; Spiegler, 1996:166, pl. 1, fig. 18 [Miocene, ODP Hole 911A, central Yermak Plateau, high-latitude North Atlantic].

Neogloboquadrina pachyderma (Ehrenberg) s.l.; Poore, 1979:511, pl. 17, fig. 10 [upper Miocene, DSDP Site 408, Irminger Sea, North Atlantic Ocean].

Neogloboquadrina humerosa (Takayanagi and Saito); Poore, 1979:511, pl. 17, fig. 8 [upper Miocene, DSDP Site 408, North Atlantic Ocean].

Neogloboquadrina du/pac; Poore, 1979:511, pl. 17, figs. 8, 9, 11, 12 [Late Pleistocene, DSDP Site 407, North Atlantic Ocean].

Neogloboquadrina incompta (Cifelli); Darling et al., 2006.

Remarks. The dextral-coiling species *Neogloboquadrina incompta* has a stable morphology throughout the Site 407 sequence. It has 4 chambers in the final whorl with a distinct lip. The sutures on the umbilical side form a distinct cross. *Neogloboquadrina incompta* differs from *P. continuosa* in that it has a more open umbilicus, whereas *P. continuosa* has a closed umbilicus. It differs from right-coiling *N. pachyderma* in that it has a more open aperture, although this distinction can be tricky. To test whether *N. incompta* is present in the population, it is necessary to do coiling direction counts on the *N. incompta/N. pachyderma* components. If there are > 3 % right-coiling forms, then there is a mixture of *N. incompta/N. pachyderma*. If there are < 3 % right-coiling forms, then the population could be composed of all *N. pachyderma* (Darling et al., 2006).

Chronostratigraphic range. N. praeatlantica Zone to *N. pachyderma* Zone (407-18R-1, 56–58 cm, to 407-1R-1, 57–60 cm; 158.56–0.57 m b.s.f.).

Neogloboquadrina pachyderma (Ehrenberg, 1861)

Plate 16, Figs. 1–12

Neogloboquadrina pachyderma Plate 16, Figs. 1, 2

Neogloboquadrina pachyderma morphotype Nps-1 Plate 16, Figs. 3–5

Neogloboquadrina pachyderma morphotype Nps-2 Plate 16, Figs. 6, 7

Neogloboquadrina pachyderma morphotype Nps-3 Plate 16, Figs. 8

Neogloboquadrina pachyderma morphotype Nps-4 Plate 16, Figs. 9, 10

Neogloboquadrina pachyderma morphotype Nps-5 Plate 16, Figs. 11, 12

Aristospira pachyderma Ehrenberg, 1861:4, pl. 3, figs. 4a–c [Recent, Davis Strait].

Globigerina bulloides var. *borealis* Brady, 1881:412 [Franz Josef Land and the Novaya Zemlya sea].

Globigerina pachyderma (Ehrenberg); Parker, 1962:224, pl. 1, figs. 26–30 394:63°13′ S,147°45′ E, Antarctica],

figs. 31, 33, 34 [Downwind BG 62:47°37′ S, 121°02′ W, 3800 M].pl. 2, fig. 2 [Downwind BG 61:46°44′ S, 123°01′ W, 4250 M], figs. 3–6 [Scruton E 180:52°13′ N, 173°35′ E, 137 m]; Berggren, 1972:978, pl. 2, figs. 1–3 [early Pleistocene, DSDP Site 113, North Atlantic].

Globorotalia (Turborotalia) pachyderma (Ehrenberg) sinistral; Bandy, 1972:307, pl. 3, figs. 1–3 [upper Miocene, Neogene zone 18, Mohole section, Guadalupe site, Equatorial Pacific Ocean], pl. 4, figs. 1–5 [upper Pleistocene, Continental Borderland, California], pl. 6, figs. 1, 9 [Modern, Station 47A (plankton tow, 0–100 m), Fletcher's Ice Island T-3, 84°13′ N, 114°42′ W, Arctic Ocean], figs. 2, 7 [Modern, Station 2 (2760 m), Fletcher's Ice Island T-3, 86°54′ N, 80°00′ W, Arctic Ocean], figs. 3, 8, 10 [Modern, Station 1A (plankton tow, 0–100 m), Fletcher's Ice Island T-3, 84°22′ N, 112°32′ W, Arctic Ocean], figs. 4–6, 11 [Modern, Station 5 (2386 m), Fletcher's Ice Island T-3, 86°06′ N, 95°20′ W, Arctic Ocean], pl. 7, figs. 1, 3, 6, 7 [Modern, Eltanin Station 308, 59°00′ S, 71°00′ W, subantarctic region], fig. 2, 4 [Modern, Eltanin Station 39–40, 52°03′ S, 133°57′ E, subantarctic region], fig. 5 [Modern, Eltanin Station 39–67, 43°38′ S, 151°58.9′ E, subantarctic region].

Neogloboquadrina pachyderma (Ehrenberg); Collen and Vella, 1973:19, pl. 1, fig. 12 [lower Pliocene, upper Gilbert Geomagnetic Epoch, upper Opoitian Stage, Aotearoa / New Zealand; Aksu and Kaminski, 1989:303, pl. 3, figs. 10–12 [Pleistocene, ODP Hole 645B, Labrador Sea, North Atlantic Ocean].

Globquadrina dutertrei (d'Orbigny); Herman, 1974: pl 4, fig. 21) [Pleistocene, Core D.st.A. 6, 51.7, Mendeleev Rise, central Arctic Ocean].

Globigerina occlusa Herman, 1974:300, pl. 10, figs. 3 and 4 [Pleistocene, Core T66, Mendeleev Rise, central Arctic Ocean].

Globigerina cryophila Herman, 1980, pl. 10, figs. 3 and 4 [Pleistocene, Core T66, Mendeleev Rise, central Arctic Ocean].

Neogloboquadrina pachyderma (Ehrenberg) sinistral; Weaver, 1987:725, pl. 1, figs. 3, 4 [Pleistocene, Zone N22, DSDP Site 610, Feni Drift, North Atlantic Ocean]; Spiegler and Jansen, 1989:, pl. 2, figs. 1–4, 7 [Pleistocene, ODP Hole 642B, Vøring Plateau, Nordic Seas]; Spiegler, 1996:166, pl. 1, figs. 1–2 [Pleistocene, Zone N22, ODP Hole 910C, Fram Strait, Nordic Seas].

Not *Neogloboquadrina humerosa* (Takayanagi and Saito); Poore, 1979:511, pl. 17, fig. 7 [upper Miocene, DSDP Site 408, Irminger Sea, North Atlantic Ocean].

Not *Neogloboquadrina* du/pac; Poore, 1979:511, pl. 17, figs. 11, 12 [Pleistocene, DSDP Site 407, Irminger Sea, North Atlantic Ocean].

Remarks. Familiar-looking *N. pachyderma* species appear in the early Pleistocene (44.56 m b.s.f.). at Site 407 and dominate the assemblage thereafter. During this Pleistocene part of their range, it is possible to recognize forms consistent with the five morphotypes recognized elsewhere and first described in the Arctic Ocean (Eynaud, 2009) (Plate 16; Fig. 3–12). These have variously been assigned species level names, including *Globigerina occlusa* (Herman, 1974), which Herman later renamed *Globigerina cryophila* 1980, and *Neogloboquadrina pachyderma*, which is considered to have first appeared ca. 9 Ma (Berggren et al., 1995a) and is not as abundant in the Pliocene and late Miocene as in the Pleistocene. These older forms are either quadrate (Plate 16; Fig. 1) or lozenge-shaped (Plate 16, Fig. 2) and often possess a kummerform final chamber. Like *P. continuosa* and *N. incompta,* the sutures on the umbilical side of *N. pachyderma* form a cross. In the late Miocene, *P. continuosa* can be distinguished from *N. pachyderma* by its distinct comma-shaped aperture.

Chronostratigraphic range. N. praeatlantica Zone to *N. pachyderma* Zone (407-18R-1, 56–58 cm, to 407-1R-1, 57–60 cm; 158.56–0.57 m b.s.f.).

Neogloboquadrina praeatlantica Foresi, Iaccarino and Salvatorini 2002

Plate 17, Figs. 1–12

Neogloboquadrina atlantica (Berggren) primitive; Poore, 1979:509, pl. 16, figs. 10–12 [middle Miocene, DSDP Site 407, Irminger Sea, North Atlantic Ocean].

Neogloboquadrina atlantica praeatlantica Foresi, Iaccrino, and Salvatorini, 2002:327, pl. 1, figs. 1a–c [Serravallian, *N. atlantica praeatlantica* Zone, Cretaccio Fm, San Nicola Island, Adriatic Sea (holotype)], figs. 2–13, pl. 2, figs. 1–14.

Remarks. Neogloboquadrina praeatlantica is low trochospiral with a non-spinose with a cancellate *Neogloboquadrina*-type wall texture. Specimens referable to *Neogloboquadrina praeatlantica* have 4 (sub)globular chambers with an umbilical–extraumbilical aperture. The aperture is a high arch and often comma-shaped with a lip. It appears at Site 407 after the large hiatus, together with the other neogloboquadrinids and disappears in the latest Miocene. This species may be as important as the neogloboquadrinid phylogeny because it is the first neogloboquadrinid to appear.

Chronostratigraphic range. N. praeatlantica Zone (407-18R-1, 56–58 cm, to 407-16R-1, 56–58 cm; 158.56–139.56 m b.s.f.).

Genus *Globigerinoides* Cushman 1927, emend Spezzaferri et al., 2015

Type species: Globigerina rubra d'Orbigny 1839

Globigerinoides neoparawoodi Spezzaferri 2018

Globigerinoides parawoodi Keller 1981 (partim, not holotype), pl. 4, figs. 1–3, 9–11 [lower Miocene Zone N4, DSDP Site 292, northwestern Pacific Ocean]; Spezzaferri, 1994:187, pl. 13, figs. 6a–c [lower Miocene Subzone M1b, DSDP Hole 516F, South Atlantic Ocean].

Globigerinoides neoparawoodi Spezzaferri, 2018:282, pl. 9.5, figs. 1–3 [Subzone M1b, DSDP Site 292, Pacific Ocean], figs. 4–6 [Subzone M1b, Cipero Fm., Trinidad], figs. 7–9 [Zone M2, DSDP Site 151, Gulf of Mexico], figs. 10–13 [Subzone M1b, Cipero Fm., Trinidad], figs. 14–17 [Subzone M1b, Cipero Fm., Trinidad].

Remarks. *Globigerinoides neoparawoodi* is rare at Site 407 and differs from *G. woodi* in that it has a supplementary aperture on the spiral side. *Globigerinoides neoparawoodi* closely resembles *Trilobatus primordius*, as described by Poore (1979; Plate 11; Figs. 7, 8). However, *G. neoparawoodi* differs by having 4 subglobular chambers in the final whorl compared to the 3 chambers of *T. primordius* Poore.

Chronostratigraphic range. Zone O7 to M1a (407-35R-1, 86–88 cm, to 407-29R-3, 20–22 cm; 320.36–264.5 m b.s.f.).

Globigerinoides ruber (d'Orbigny 1839)

Plate 18, Fig. 1

Globigerina rubra d'Orbigny, 1839:82, pl. 4, figs. 12–14 [Recent, Cuba, Jamaica, Guadalupe, and Martinique].

Globigerinoides ruber (d'Orbigny); Kennett and Srinivasan, 1983:78, pl. 10, fig. 6; pl. 17, figs. 1–3 [latest Miocene, Zone N19, DSDP Site 289, southwest Pacific Ocean]; Spiegler, 1996:167, pl. 2, figs. 3–4 [upper Pliocene, Zone N21, ODP Hole 910D, Fram Strait, Nordic Seas].

Remarks. The primary aperture is a small arch in specimens found at Site 407.

Chronostratigraphic range. "*C.*" *pseudociperoensis* Zone (407-19R-3, 56–58 cm, to 407-19R-2, 56–58 cm; 171.06–169.56 m b.s.f.).

Genus *Orbulina* d'Orbigny 1839

Type species: Orbulina universa d'Orbigny 1839

Orbulina suturalis Brönnimann 1951

Plate 18, Fig. 2

Orbulina suturalis Brönnimann, 1951:135, pl. 2, figs. 1–15 [upper Oligocene, Naparima area, Trinidad], pl. 3, figs. 3–8, 11, 13–16, 18, 20–22, [upper Oligocene, Naparima area, Trinidad], pl. 4, figs. 2–4, 7–12, 15–16, 19–22 [lower Miocene, *Globorotalia menardii* Zone, Naparima area, Trinidad].

Remarks. Earlier chambers protrude through the final chamber. Areal apertures are aligned along the sutures of the protruding earlier chambers.

Chronostratigraphic range. *N. praeatlantica* Zone to *G. inflata* PRZ (407-17R-2, 56–58 cm, to 407-8R-2, 56–58 cm; 150.56–65.06 m b.s.f.).

Orbulina universa d'Orbigny 1839

Plate 18, Figs. 3–7

Orbulina universa d'Orbigny, 1839:3, pl. 1. fig. 1 [Recent, Rimini, Italy; coast of Algeria; Tenerife, Canary Islands; Cuba, Jamaica, Saint Thomas, Guadalupe, and Martinique, Indian Ocean]; Spiegler, 1996:166, pl. 1, fig. 4 [Quaternary, ODP Hole 911A, central Yermak Plateau, high-latitude North Atlantic].

Remarks. *Orbulina universa* shows large morphological variability at Site 407. Poore (1979) combined *O. suturalis* and *O. universa* in *Orbulina* spp., while here we separate the two in that the final chamber in *O. suturalis* does not fully envelope the earlier chambers, resulting in earlier chambers protruding, whereas the *O. universa* final chamber entirely envelopes the earlier chambers.

Chronostratigraphic range. *N. praeatlantica* Zone to *N. pachyderma* Zone (407-17R-2, 56–58 cm, to 407-1R-2, 56–58 cm; 150.56–2.06 m b.s.f.).

Genus *Trilobatus* Spezzaferri et al., 2015

Type species: Trilobatus trilobus Reuss 1850

Trilobatus bisphericus (Todd 1954)

Plate 18, Fig. 8

Globigerinoides bispherica Todd et al., 1954:680, pl. 1, fig. 1 [upper Oligocene, Saipan, Mariana Islands, Pacific Ocean], fig. 4 [Saint Croix Quarry, Prince Town, Trinidad].

Trilobatus bisphericus (Todd, 1954); Spezzaferri et al., 2015

Remarks. This species is rare in Site 407 material, with only a single specimen found in the middle Miocene. *Trilobatus bisphericus* is bilobate outline with three chambers, of which the final chamber almost completely hides the umbilicus.

Chronostratigraphic range. "*C.*" *pseudociperoensis* Zone (407-19R-1; 56–58 cm; 168.06 m b.s.f.).

Trilobatus immaturus (LeRoy 1939)

Plate 18, Fig. 9

Globigerinoides sacculiferus (Brady) var. *immaturus* LeRoy, 1939:236, pl. 3, figs. 19-21 [Miocene, Rokan–Tapanoeli area, central Sumatra, Indonesia].

Globigerinoides immaturus LeRoy; Kennett and Srinivasan, 1983:64, pl. 10, fig. 3; pl. 13, figs. 7–9 [upper Miocene Zone N16, DSDP Site 289, Ontong Java Plateau, western equatorial Pacific Ocean].

Trilobatus immaturus (LeRoy); Spezzaferri et al., 2018:289, pl. 9.9, figs. 1–4 [Miocene, Rokan–Tapanoeli area, central Sumatra, Indonesia], figs. 5–8 [Subzone M1b, Cipero Fm., Trinidad], figs. 9–12 [Zone M2, DSDP Site 151, Gulf of Mexico], figs. 13–15 [Subzone M1b, Cipero Fm., Trinidad], figs. 16–18 [Subzone M1b, Cipero Fm., Trinidad].

Remarks. Trilobatus immaturus can be distinguished from *T. trilobus* by having the primary aperture with a low arch across the antepenultimate chamber (vs. an umbilical–extraumbilical elongated slit in *T. trilobus*). This species is rare at Site 407 and only recorded in the middle Miocene.

Chronostratigraphic range. "*C.*" *pseudociperoensis* Zone (407-19R-3, 56–58 cm, to 407-18R-2, 56–58 cm; 171.06–160.06 m b.s.f.).

Trilobatus quadrilobatus (d'Orbigny 1846)

Globigerina quadrilobata d'Orbigny, 1846:164, pl. 9, figs. 7–10 [middle Miocene upper Lagenid Zone (*fide* Papp and Schmid, 1985), vicinity of Nußdorf, north of Vienna, Vienna Basin, Austria].

Globigerinoides quadrilobatus (d'Orbigny); Papp and Schmid, 1985:63, pl. 54, fig. 7 [holotype of d'Orbigny (1846) re-illustrated], fig. 8 [lectotype], figs. 9–12 [middle Miocene upper Lagenid Zone].

Trilobatus quadrilobatus (d'Orbigny); Spezzaferri et al., 2015:14

Remarks. Trilobatus quadrilobatus has a primary aperture with a high umbilical arch and 1 to 2 small- and low-arched supplementary apertures. This species is rare and only found in the lower Miocene samples at Site 407.

Chronostratigraphic range. Zone M1 (407-29R-3, 20–22 cm, and 407-29R-1, 56–58 cm; 264.5 and 263.06 m b.s.f.).

Trilobatus trilobus (Reuss 1850)

Plate 18, Fig. 10

Globigerina triloba Reuss, 1850:374, pl. 47, figs. 11a–e [middle Miocene, Bega Basin, Transylvania, Romania].

Globigerinoides trilobus Spezzaferri, 1994:37, pl. 13, figs. 1a–c; [lower Miocene Subzone N4b, DSDP Hole 516F, eastern South Atlantic Ocean], pl. 15, figs. 6a–c [lower Miocene, Subzone N4b, DSDP Site 98, North Atlantic Ocean]; Spiegler, 1996:167, pl. 2, fig. 5 [upper Pliocene, Zone N21, ODP Hole 910D, Fram Strait, Nordic Seas].

Trilobatus trilobus (Reuss); Spezzaferri et al., 2018:300, pl. 9.14, figs. 1–3 [middle Miocene, Wieliczka, Poland], figs. 4–6 [Subzone M1b, Lemme section at 10 m, northern Italy], figs. 7–9 [Zone M3, Cipero Fm., Trinidad], figs. 10–13 [Subzone M1b, DSDP Hole 588C, Tasman Sea], figs. 14–17 [Zone M2, DSDP Site 151, Gulf of Mexico].

Remarks. Trilobatus trilobus is rare in the middle Miocene samples of Site 407.

Chronostratigraphic range. "*C.*" *pseudociperoensis* Zone (407-20R-1, 100–102 cm, to 407-18R-2, 56–58 cm; 178–160.06 m b.s.f.).

Genus *Sphaeroidinellopsis* Banner and Blow 1959

Type species: Globigerina seminulina Schwager 1866

Sphaeroidinellopsis paenedehiscens Blow 1969

Plate 18, Fig. 11

Sphaeroidinellopsis subdehiscens paenedehiscens Blow, 1969:386, pl. 30, figs. 4, 5, 9 [Pliocene, Zone N19, *Sphaeroidinella dehiscens dehiscens, Globoquadrina altispira* Partial Range Zone, San Clay member, Bowden Fm., Drivers River, Jamaica].

Sphaeroidinellopsis sp. juv., aff. *S. paenedehiscens* (Blow); Spiegler, 1996:167, pl. 2, fig. 1 [upper Pliocene, Zone N21, ODP Hole 910D, Fram Strait, Nordic Seas].

Remarks. This is a rare species. It is easily recognized by its coarsely perforate surface that is covered by a cortex resulting in a smooth, polished, and glossy appearance to the test. It has 3 subglobular chambers in the final whorl. The umbilicus is open and bordered by a thickened crenulate margin. *Sphaeroidinellopsis paenedehiscens* differs from *S. seminulina* in that it has a more rounded periphery and tighter coiling. No other *Sphaeroidinellopsis* species were found at Site 407.

Chronostratigraphic range. N. praeatlantica Zone (407-18R-1, 56–58 cm, to 407-17R-2, 56–58 cm; 158.56–150.56 m b.s.f.).

Genus *Turborotalita* Blow and Banner 1962

Type species: Turborotalita humilis Brady 1884

Turborotalita quinqueloba (Natland 1938)

Plate 19, Figs. 1–9

Globigerina quinqueloba Natland, 1938:149, pl. 6, figs. 7a–c [Recent, off Long Beach, California, USA].

Turborotalita quinqueloba (Natland); Pearson and Wade, 2009:209, pl. 7, figs. 1–6 [Zone O6 (= O7 in this work), Cipero Fm., Trinidad]; Poore, 1979: 507, pl. 15, figs. 9, 10 [upper Pliocene, DSDP Site 409, Reykjanes Ridge, North Atlantic Ocean]; Spiegler, 1996:166, pl. 1, figs. 14, 15 [Miocene, ODP Hole 909C, Fram Strait, Nordic Seas].

Remarks. Turborotalita quinqueloba is common at Site 407 in the Pliocene and Pleistocene but sparse to rare in the Oligocene and lower and middle Miocene. It is recognized by the petaloid peripheral margin and characteristics of the final chamber, which is commonly reduced in size and teardrop-shaped, with a flap developing into a broad extension towards

the umbilicus (usually with a prominent lip). This can turn into a rather elaborate bulla-like covering in some specimens (e.g. Plate 19; Fig. 7). Immature specimens lack the teardrop-shaped final chamber (Plate 19; Fig. 5). When heavily calcified, the outline is more compact, and the sutures can be obscured (Plate 19; Figs. 3, 4). Evidence of spine holes and bases can sometimes be seen in the less calcified specimens (e.g. Plate 19; Fig. 5).

Chronostratigraphic range. Zone O7 to *N. pachyderma* Zone (407-36R-1, 50–52 cm, to 407-1R-1, 57–60 cm; 329.5–0.57 m b.s.f.).

Genus *Cassigerinella* Pokorny 1955, emended Li 1986

Type species: Cassigerinella boudecensis Pokory 1955

Cassigerinella chipolensis (Cushman and Ponton 1932)

Plate 20, Figs. 1, 2

Cassidulina chipolensis Cushman and Ponton, 1932:98, pl. 15, figs. 2a–c [late Oligocene–early Miocene, Chipola Formation, Calhoun County, Florida, USA].

Cassigerinella chipolensis (Cushman and Ponton); Bolli, 1957:108, pl. 22, figs. 3a–c [lower Oligocene *Globorotalia opima opima* Zone, Cipero Fm., Trinidad]; Poore, 1979:517, pl. 20, figs. 3, 4 [lower Miocene, DSDP Site 407, Irminger Sea, North Atlantic Ocean].

Remarks. Cassigerinella chipolensis is rare in Site 407 material and was only found in two samples. It is recognized by its globular and irregular outline and asymmetrical appearance. The highly arched to virguline-shaped aperture surrounded by an irregular lip with lateral flanges.

Chronostratigraphic range. "*C.*" *pseudociperoensis* Zone (407-24R-3, 56–58 cm, and 407-19R-1, 56–8 cm; 218.56 and 168.06 m b.s.f.).

Genus *Globigerinita* Brönnimann 1951

Type species: Globigerinita naparimaensis Brönnimann 1951

Globigerinita glutinata (Egger 1893)

Plate 20, Figs. 3–6

Globigerina glutinata Egger, 1893:371, pl. 13 (on p. 356), figs. 19–21 (three views of same specimen: locality of figured specimen not given; probably Holocene sediment from the cruise of the *Gazelle*).

Globigerinita glutinata (Egger); Parker, 1962:246, pl. 9, figs. 1–9 [Holocene, "Downwind" Expedition Station BG 134, equatorial eastern Pacific Ocean], pl. 9, figs. 10–16 [Holocene, Downwind Expedition Station BG 70, mid-latitude South Pacific Ocean]; Kennett and Srinivasan, 1983:224, pl. 56, figs. 1, 3–5 [lower Miocene Subzone N4b, DSDP Site 289, Ontong Java Plateau, equatorial western Pacific Ocean]; Spiegler, 1996:166, pl. 1, figs. 10–11 [upper Pliocene, ODP Hole 909C, Fram Strait, Nordic Seas].

Globigerinita glutinata (Egger), forma *ambitacrena* (Loeblich and Tappan); Spiegler, 1996:166, pl. 1, fig. 11 [Miocene, ODP Hole 909C, Fram Strait, Nordic Seas].

Remarks. This species is abundant in the > 125 µm size fraction during the Oligocene and early to middle Miocene part of the section, becoming sparse in the Pliocene and Pleistocene part of the section. *Globigerinita glutinata* co-occurs with *G. uvula* and is distinguished from *G. uvula* by being low to medium trochospire (vs. high trochospire) and often by having a bulla.

Chronostratigraphic range. Zone O7 to *N. pachyderma* Zone (407-36R-1, 50–52 cm, to 407-1R-1, 57–60 cm; 329.5–0.57 m b.s.f.).

Globigerinita uvula (Ehrenberg 1862)

Plate 20, Figs. 7–9

Pylodexia uvula Ehrenberg, 1861:308 [modern ocean, Gulf Stream off Florida].

Globigerinita uvula (Ehrenberg); Parker, 1962:252, pl. 8, figs. 14–20 [Holocene, Discovery Station 385, southeast Pacific Ocean west of Drake Passage], pl. 8, figs. 21–23 [Holocene, Downwind Expedition Station BG 68, Pacific Antarctic Ridge, south Pacific Ocean], figs. 24–26 [Scripps Station V-1, offshore California, Pacific Ocean]. Ocean]; Kennett and Srinivasan, 1983:224, pl. 56, figs. 6–8 [lower Miocene Subzone N4b, DSDP Site 289, Ontong Java Plateau, equatorial western Pacific Ocean].

Remarks. This species is rare in both the 63–125 and the > 125 µm size fractions throughout the section.

Chronostratigraphic range. Zone O7 to *N. pachyderma* Zone (407-36R-1, 50–52 cm, to 407-1R-1, 57–60 cm; 329.5–0.57 m b.s.f.).

Genus *Orcadia* Boltovskoy and Watanabe 1982

Type species: Hastigerinella riedeli Rögl and Bolli 1973

Orcadia riedeli (Rögl and Bolli 1973)

Plate 20, Figs. 10–12

Hastigerinella riedeli Rögl and Bolli, 1973 [Late Pleistocene, *Globorotalia truncatulinoides truncatulinoides* Zone, *Globigerina calida calida* Subzone, DSDP Site 147, Cariaco Basin, Caribbean Sea].

Hastigerinopsis riedeli (Rögl and Bolli); Poore, 1979:515, pl. 19, figs. 1–4 [Pleistocene, DSDP Site 407, Irminger Sea, North Atlantic Ocean].

Orcadia riedeli (Rögl and Bolli); Boltovskoy and Watanabe, 1982:5, pl. 1, figs. 1–20 [Recent, South Atlantic].

Remarks. This is a very small species appearing in the 63–125 µm size fraction. In SEM images, *O. riedeli* has a distinct row of spine bases on top of the final chamber (e.g. Plate 20; figs. 10, 11).

Chronostratigraphic range. N. pachyderma Zone (407-3R-1, 55–58 cm, to 407-1R-1, 57–60 cm; 16.05–0.57 m b.s.f.).

Genus *Tenuitella* Fleisher 1974, emended Li 1987

Type species: Globorotalia gemma Jenkins 1966

Tenuitella angustiumbilicata (Bolli 1957)

Plate 21, Figs. 1, 2

Globigerina ciperoensis subsp. *angustiumbilicata* Bolli, 1957:109, pl. 22, fig. 12 [Oligocene, *Globigerina ciperoensis ciperoensis* Zone, Trinidad].

Tenuitella angustiumbilicata (Bolli); Pearson and Wade, 2009:213, pl. 8, figs. 4a–d [upper Oligocene Zone, O6, Cipero formation, Trinidad].

Remarks. Tenuitella angustiumbilicata is rare at Site 407 and found in the 63–125 and > 125 µm size fractions. This species is distinguished from *T. munda* in that it has 4–5 chambers in the final whorl (vs. 4–4.5 in *T. munda*), and a more circular outline than *T. munda*, which is subquadrate. Additionally, *T. angustiumbilicata* often features a bulla, which is absent in *T. munda*.

Chronostratigraphic range. Zone O7 to "*C.*" *pseudociperoensis* Zone (407-36R-1, 50–52 cm, to 407-18R-3, 56–58 cm; 329.5–161.56 m b.s.f.).

Tenuitella clemenciae (Bermúdez 1967)

Plate 21, Figs. 3, 4

Turborotalia clemenciae Bermúdez, 1961:1321, pl. 17, figs. 10a–b [Miocene, Texistepec, Isthmus of Tehuantepec, Mexico].

Globorotalia minutissima Bolli, 1957: [*Globorotalia fohsi fohsi* Zone, Trindad]; Poore, 1979:485, pl. 4, figs. 7–9 [lower Miocene, DSDP Site 407, Irminger Sea, North Atlantic Ocean].

Globorotalia (Tenuitella) clemenciae (Bermúdez); Kennett and Srinivasan, 1984:163, pl. 39, figs. 1, 3, pl. 40, figs. 1–6 [figs. 4–6, middle Miocene, DSDP Site 289, Ontong Java Plateau, Pacific, figs. 1, 3, middle Miocene, DSDP Site 407, North Atlantic].

Remarks. Tenuitella clemenciae is rare at Site 407 and found in the 63–125 and > 125 µm size fractions. It differs from *T. munda* in that it has a larger test with more chambers (5 vs. 4–4.5) and having a flattened lip almost covering the umbilicus. If differs from *T. angustiumbilicata* in that it has a lower arched aperture and is low trochospiral (vs. very low).

Chronostratigraphic range. Zone O7 to "*C.*" *pseudociperoensis* Zone (407-30R-2, 56–58 cm, to 407-18R-1, 56–58 cm; 274.06–158.56 m b.s.f.).

Tenuitella munda (Jenkins 1966)

Plate 21, Figs. 5–8

Globorotalia munda Jenkins, 1966:1121, fig. 14, nos. 126–133; pl. 13, nos. 152–156 [Oligocene, Whaingaroan/Duntroonian Stage, Aotearoa / New Zealand].

Globorotalia (Tenuitella) munda Jenkins; Kennett and Srnivasan, 1984:163, pl. 39, figs. 5–7 [early Miocene, *Globoquadrina dehiscens* Zone, DSDP Site 206, southwestern Pacific]; Poore, 1979:517, pl. 20, figs. 8–10 [lower Oligocene, DSDP Site 407, Irminger Sea, North Atlantic Ocean].

Globorotalia cf. *G. munda* Poore, 1979:517, pl. 20, figs. 11–13 [lower Miocene, DSDP Site 407, Irminger Sea, North Atlantic Ocean].

Remarks. Tenuitella munda has a small and low trochospiral test with 4–4.5 globular chambers in the final whorl. The surface is smooth with fine pustules, and the umbilicus is narrow, with an aperture bordered by a low arch with a thin lip. Some specimens can have a bulla covering the umbilicus (Plate 21; Fig. 12). This species is found in the 63–125 and > 125 µm size fractions. No attempt was made to separate *Globorotalia* cf. *G. munda* Poore from *T. munda*. Compared to Southern Ocean high-latitude assemblages of equivalent age, *T. munda* is rare to common in the late Oligocene–early Miocene section of Site 407.

Chronostratigraphic range. Zone O7 to "*C.*" *pseudociperoensis* Zone (407-36R-1, 50–52 cm, to 407-24R-3, 56–58 cm; 329.5–218.56 m b.s.f.).

Genus *Tenuitellita* Li 1987

Type species: Globigerinita iota Parker 1962

Tenuitellita fleisheri (Li 1987)

Plate 21, Figs. 9–12

Tenuitella fleisheri Li, 1987:305, pl. 4, figs. 1–7 [Late Quaternary, Zakynthos Channel, Greece].

Tenuitellita fleisheri (Li); Brummer and Kucera, 2022:65

Remarks. Tenuitellita fleisheri is rare at Site 407 and only found in the 63–125 µm size fraction. It is peripheral margin spherical to subspherical. It has 6 ovoid to subspherical chambers and curved to straight sutures on the umbilical side. The umbilicus is small to closed, and the aperture is umbilical–extraumbilical and low arch, with a prominent lip.

Chronostratigraphic range. N. pachyderma Zone (407-3R-1, 55–58 cm, to 407-1R-1, 57–60 cm; 16.05–0.57 m b.s.f.).

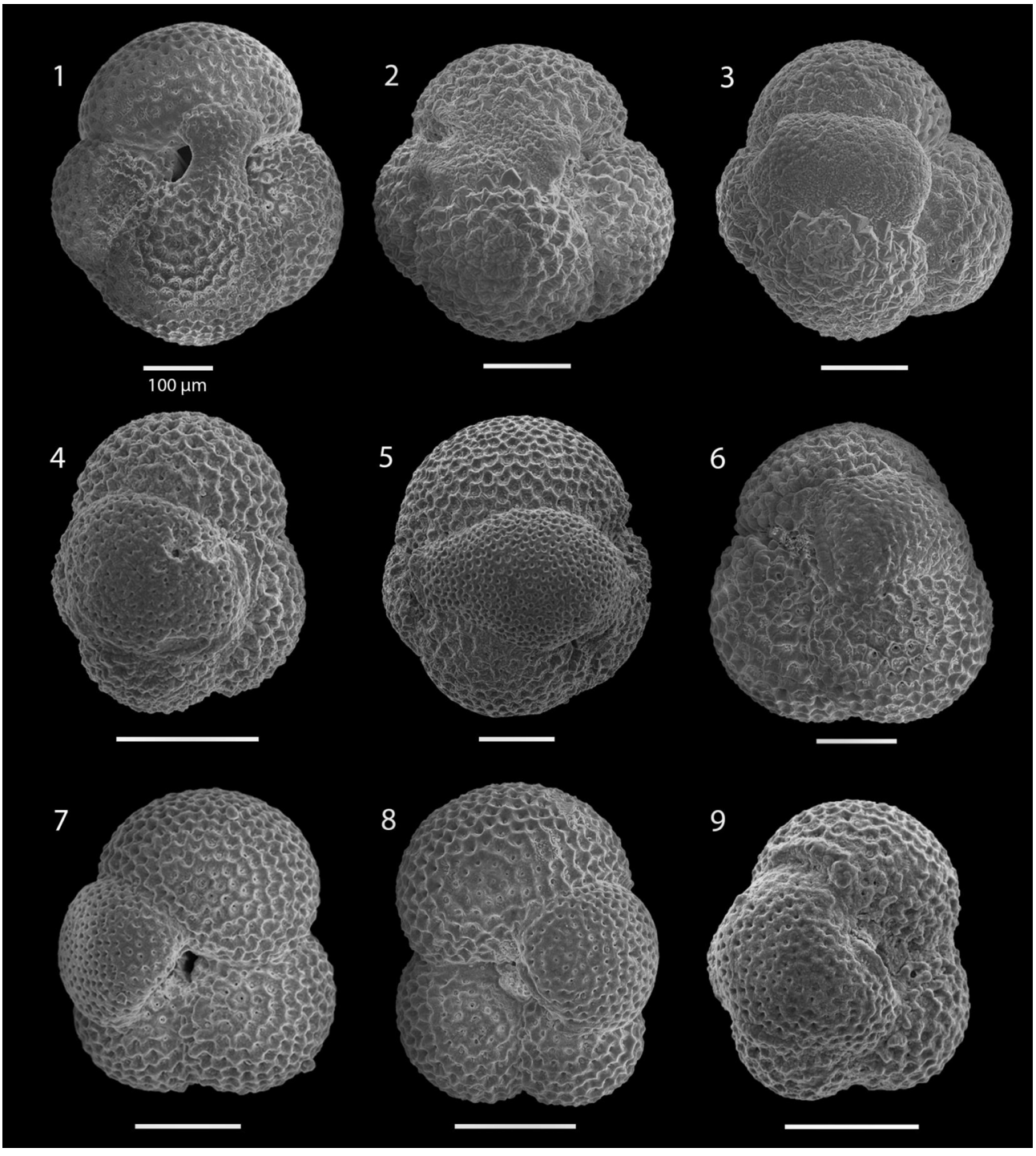

Plate 1. *Catapsydrax*. Species are organized alphabetically, along with their corresponding age and biozone, when available. Scale bars are 100 µm, unless otherwise noted. All figures are in umbilical view, unless otherwise noted. **(1)** *Catapsydrax dissimilis*, Sample 407-23R-1, 56–58 cm (early Miocene; "*C.*" *pseudociperoensis* Zone). **(2, 3)** *Catapsydrax* cf. *indianus*. **(7)** Sample 407-31R-4, 46–48 cm (late Oligocene; Zone O7). **(8)** Sample 407-23R-1, 56–58 cm (early Miocene; "*C.*" *pseudociperoensis* Zone). (4–9) *Catapsydrax unicavus*. **(4)** Sample 407-35R-1, 86–88 cm (late Oligocene; Zone O7).**(5)** Sample 407-31R-4, 46–48 cm (late Oligocene; Zone O7).**(6)** Sample 407-30R-3, 56–58 cm (late Oligocene; Zone O7). **(7, 8)** Sample 407-23R-1, 56–58 cm (early Miocene; "*C.*" *pseudociperoensis* Zone). **(9)** Sample 407-36R-1, 50–52 cm (late Oligocene; Zone O7).

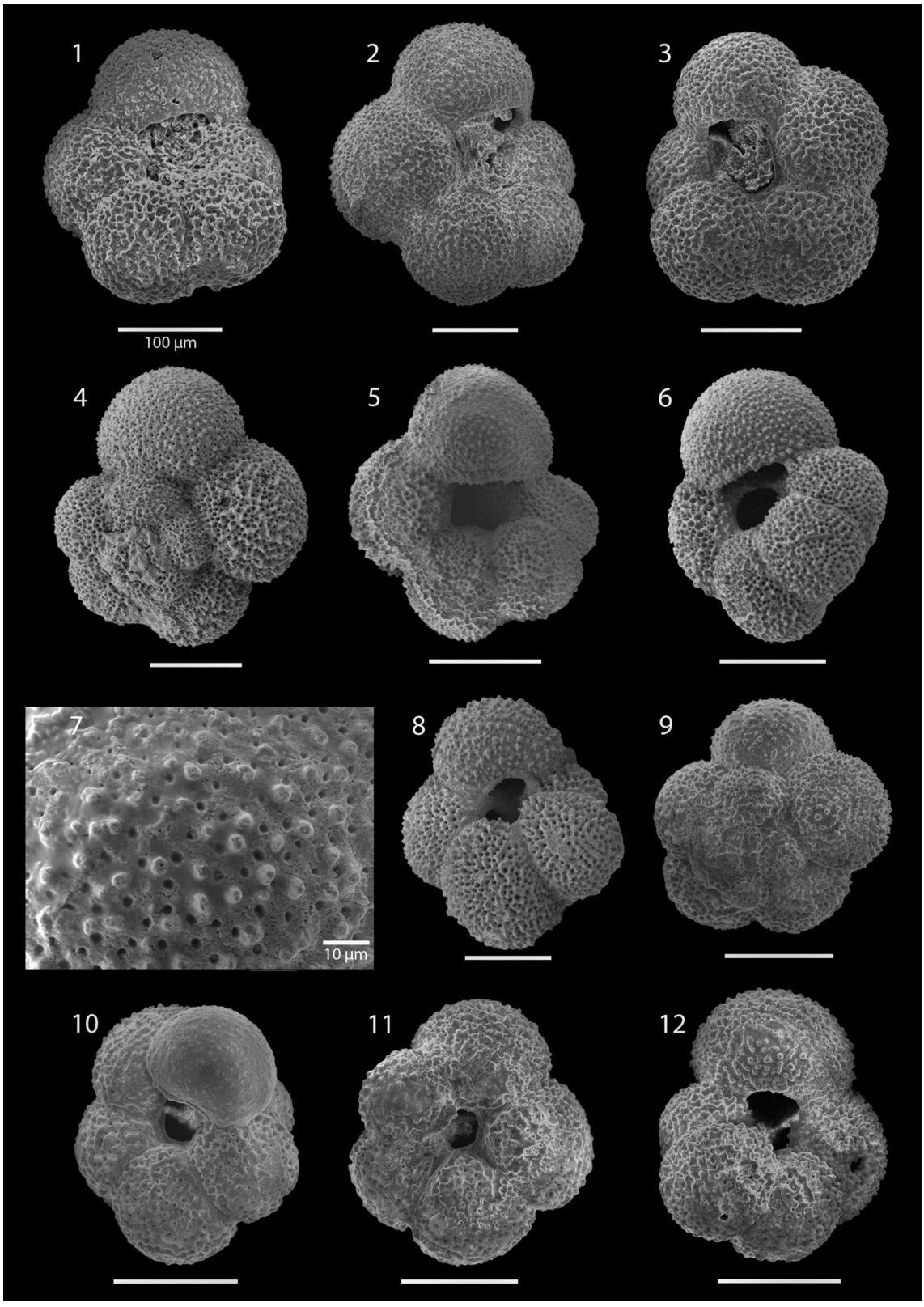

Plate 2. *Ciperoella*. Species are organized alphabetically, along with their corresponding age and biozone, when available. Scale bars are 100 µm, unless otherwise noted. All figures are in umbilical view, unless otherwise noted. **(1–3)** *Ciperoella ciperoensis*. **(1)** Sample 407-32R-1, 25–27 cm (late Oligocene; Zone O7). **(2, 3)** Sample 407-35R-1, 86–88 cm (late Oligocene; Zone O7). **(4–12)** "*Ciperoella*" *pseudociperoensis*. **(4, 5, 9–12)** Sample 407-18R-3, 56–58 cm (middle Miocene; "*C.*" *pseudociperoensis* Zone). **(6)** Sample 407-18R-3, 56–58 cm, spiral view (middle Miocene; "*C.*" *pseudociperoensis* Zone). **(7)** Sample 407-18R-3, 56–58 cm, wall texture of Fig. 6.

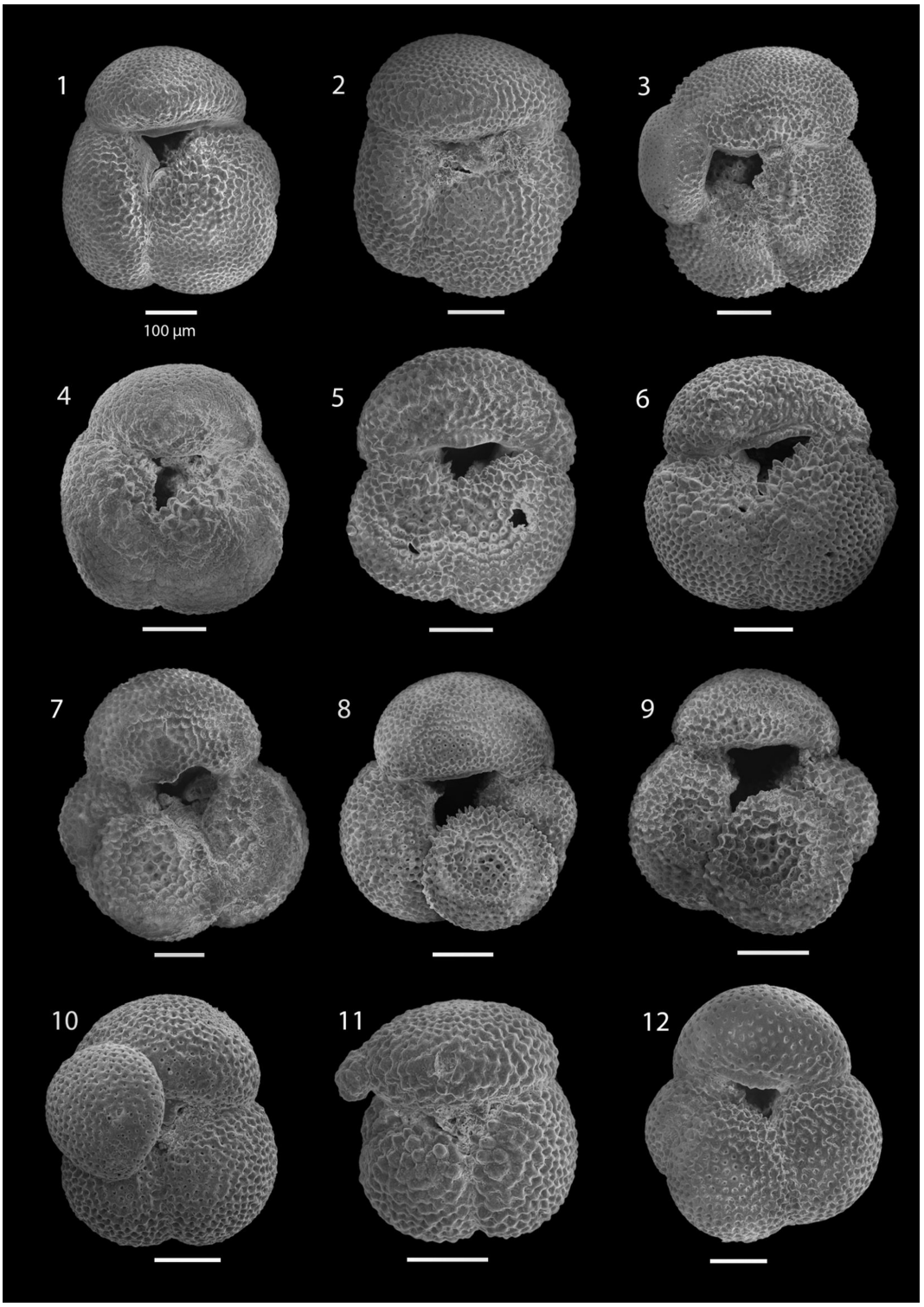

Plate 3. *Dentoglobigerina*. Species are organized alphabetically, along with their corresponding age and biozone, when available. Scale bars are 100 µm, unless otherwise noted. All figures are in umbilical view, unless otherwise noted. **(1–4)** *Dentoglobigerina baroemoenensis*. **(1–3)** Sample 407-31R-4, 46–48 cm (late Oligocene; Zone O7). **(4)** Sample 407-20R-1, 100–102 cm (early Miocene; "*C.*" *pseudociperoensis* Zone). **(5, 6)** *Dentoglobigerina galavisi*. **(5)** Sample 407-28R-1, 56–58 cm (early Miocene). **(6)** Sample 407-28R-3, 56–58 cm (early Miocene; Zone M1b). **(7–9)** *Dentoglobigerina globularis*. **(7)** Sample 407-29R-2, 20–22 cm (early Miocene; Zone M1a). **(8, 9)** Sample 407-22R-2, 56–58 cm (early Miocene; "*C.*" *pseudociperoensis* Zone). **(10, 11)** *Dentoglobigerina larmeui*. **(10)** Sample 407-28R-3, 56–58 cm (early Miocene; Zone M1b). **(11)** Sample 407-31R-4, 46–48 cm (late Oligocene; Zone O7). **(12)** *Dentoglobigerina* sp., Sample 407-25R-1, 30–32 cm (early Miocene).

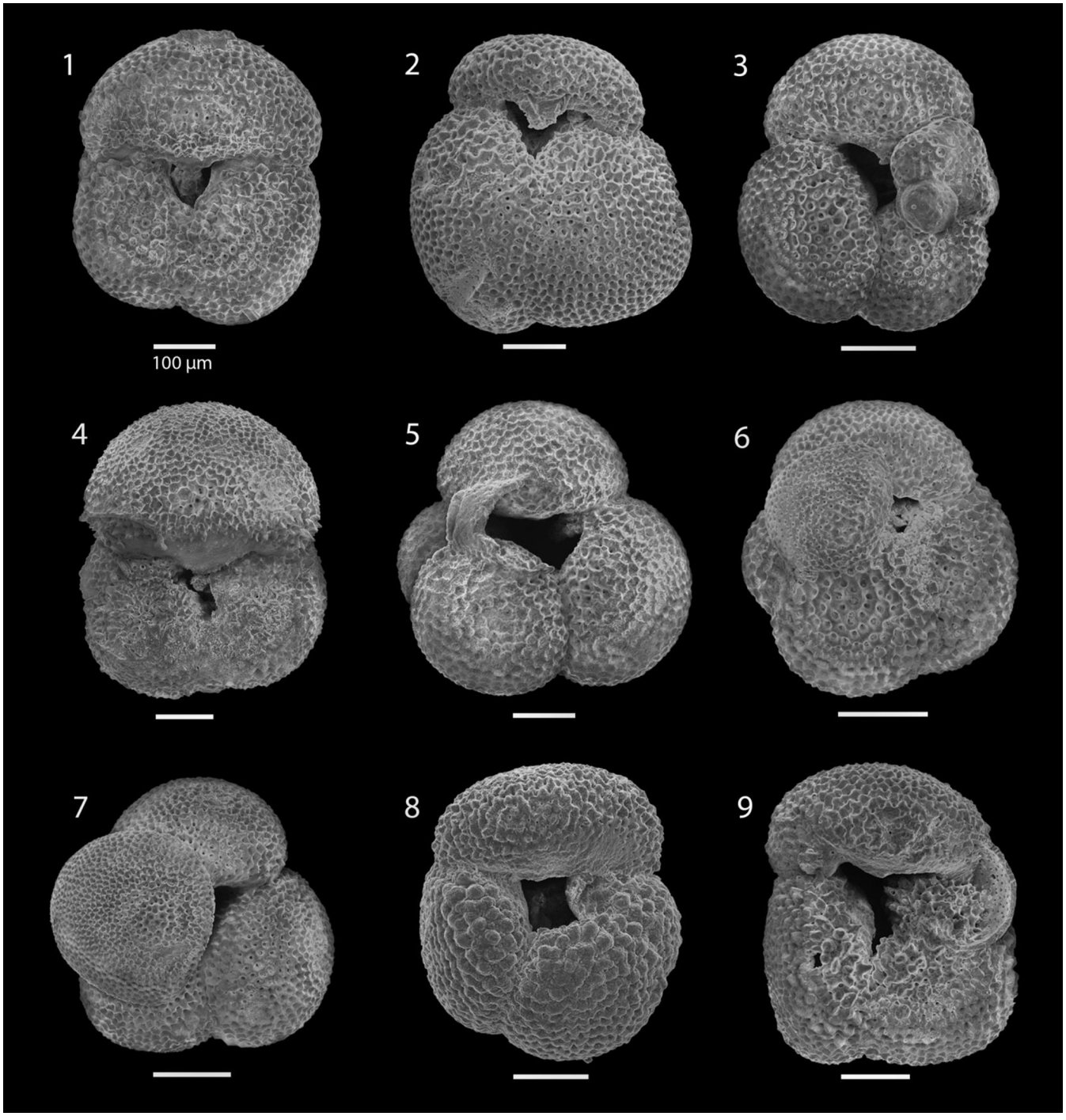

Plate 4. *Dentoglobigerina* and *Globoquadrina*. Genera and species are organized alphabetically, along with their corresponding age and biozone, when available. Scale bars are 100 µm, unless otherwise noted. All figures are in umbilical view, unless otherwise noted. **(1–4)** *Dentoglobigerina tripartita*. **(1)** Sample 407-28R-1, 56–58 cm (early Miocene). **(2)** Sample 407-28R-3, 56–58 cm (early Miocene; Zone M1b). **(3)** Sample 407-29R-3, 20–22 cm (early Miocene; Zone M1a). **(4)** Sample 407-18R-3, 56–58 cm (late Miocene; ‘‘*C.*” *pseudociperoensis* Zone). **(5–7)** *Dentoglobigerina venezuelana*. **(5)** Sample 407-29R-3, 20–22 cm (early Miocene; Zone M1a). **(6,7)** Sample 407-22R-2, 56–58 cm (early Miocene; “*C.*” *pseudociperoensis* Zone). **(8, 9)** *Globoquadrina dehiscens*. **(8)** Sample 407-20R-1, 100–102 cm (early Miocene; “*C.*” *pseudociperoensis* Zone). **(9)** Sample 407-28R-3, 56–58 cm (early Miocene; Zone M1b).

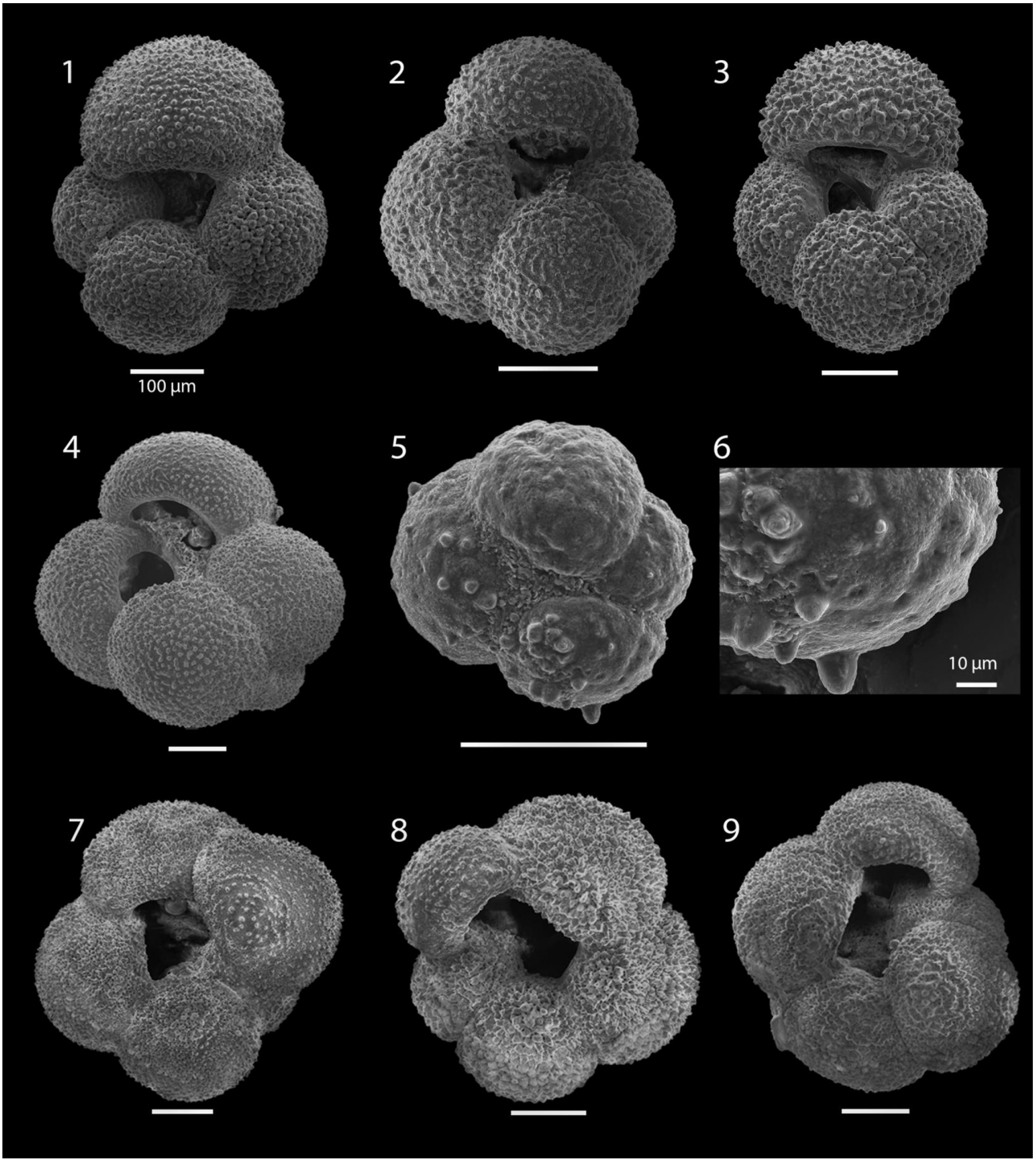

Plate 5. *Globigerina*. Species are organized alphabetically, along with their corresponding age and biozone, when available. Scale bars are 100 µm, unless otherwise noted. All figures are in umbilical view, unless otherwise noted. **(1–3)** *Globigerina bulloides*. **(1)** Sample 407-31R-4, 46–48 cm (late Oligocene; Zone O7). **(2)** Sample 407-12R-1, 56–58 cm (early Pliocene; *N. atlantica* (sin.) PRZ). **(3)** Sample 407-1R-1, 57–60 cm (Pleistocene; *N. pachyderma* Zone). **(4)** *Globigerina* cf. *cariacoensis*, Sample 407-1R-2, 56–58 cm (Pleistocene; *N. pachyderma* Zone). **(5, 6)** *Globigerina* cf. *eamesi,* Sample 407-17R-1, 56–58 cm (Pleistocene; *N. praeatlantica* Zone). **(6)** Wall texture and thick spines from Fig. 10. **(7–9)** *Globigerina umbilicata*. **(7)** Sample 407-1R-2, 56–58 cm (Pleistocene; *N. pachyderma* Zone). **(8)** Sample 407-7R-2, 56–58 cm (late Pliocene; *G. inflata* PRZ). **(9)** Sample 407-8R-1, 56–58 cm (late Pliocene; *G. inflata* PRZ).

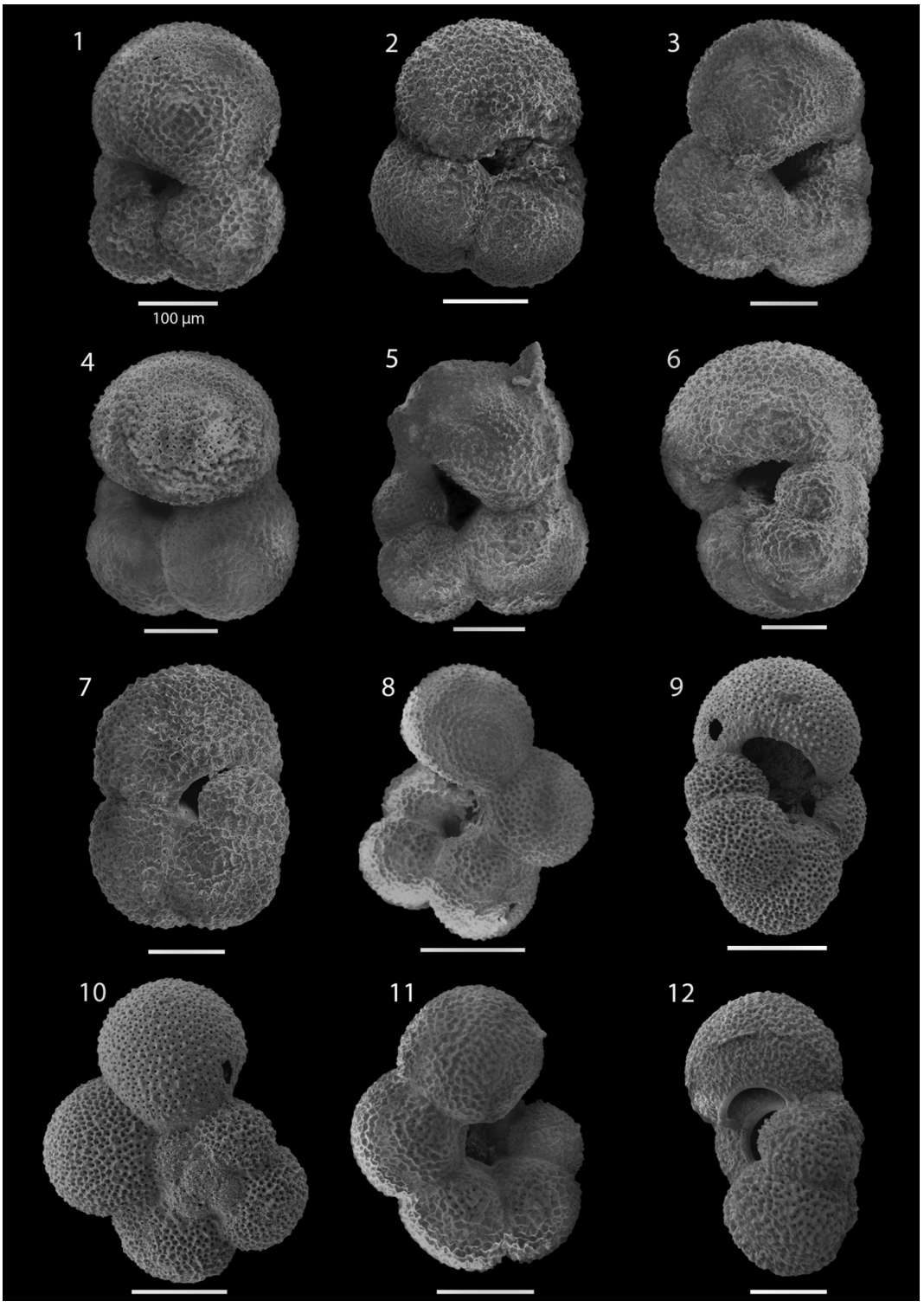

Plate 6. *Globigerinella*. Species are organized alphabetically, along with their corresponding age and biozone, when available. Scale bars are 100 µm, unless otherwise noted. All figures are in umbilical view, unless otherwise noted. **(1–7)** *Globigerinella obesa*. **(1)** Sample 407-30R-1, 56–58 cm (early Miocene; Zone M1a). **(2, 4)** Sample 407-17R-3, 53–55 cm (late Miocene; *N. praeatlantica* Zone). **(5)** Sample 407-30R-3, 56–58 cm (late Oligocene; Zone O7). **(6)** Sample 407-17R-3, 53–55 cm (late Miocene; *N. praeatlantica* Zone), edge view of a *G. obesa* representative. **(7)** Sample 407-23R-1, 56–58 cm (early Miocene; "*C.*" *pseudociperoensis* Zone), edge view of a *G. obesa* representative. **(8–10)** *Globigerinella praesiphonifera*, Sample 407-18R-3, 56–58 cm (middle Miocene; "*C.*" *pseudociperoensis* Zone). **(9)** Edge view of Fig. 8. **(10)** Spiral view of Fig. 8. **(11, 12)** *Globigerinella* cf. *siphonifera*, Sample 407-1R-1, 57–60 cm (Pleistocene; *N. pachyderma* Zone). **(12)** Edge view of Fig. 11.

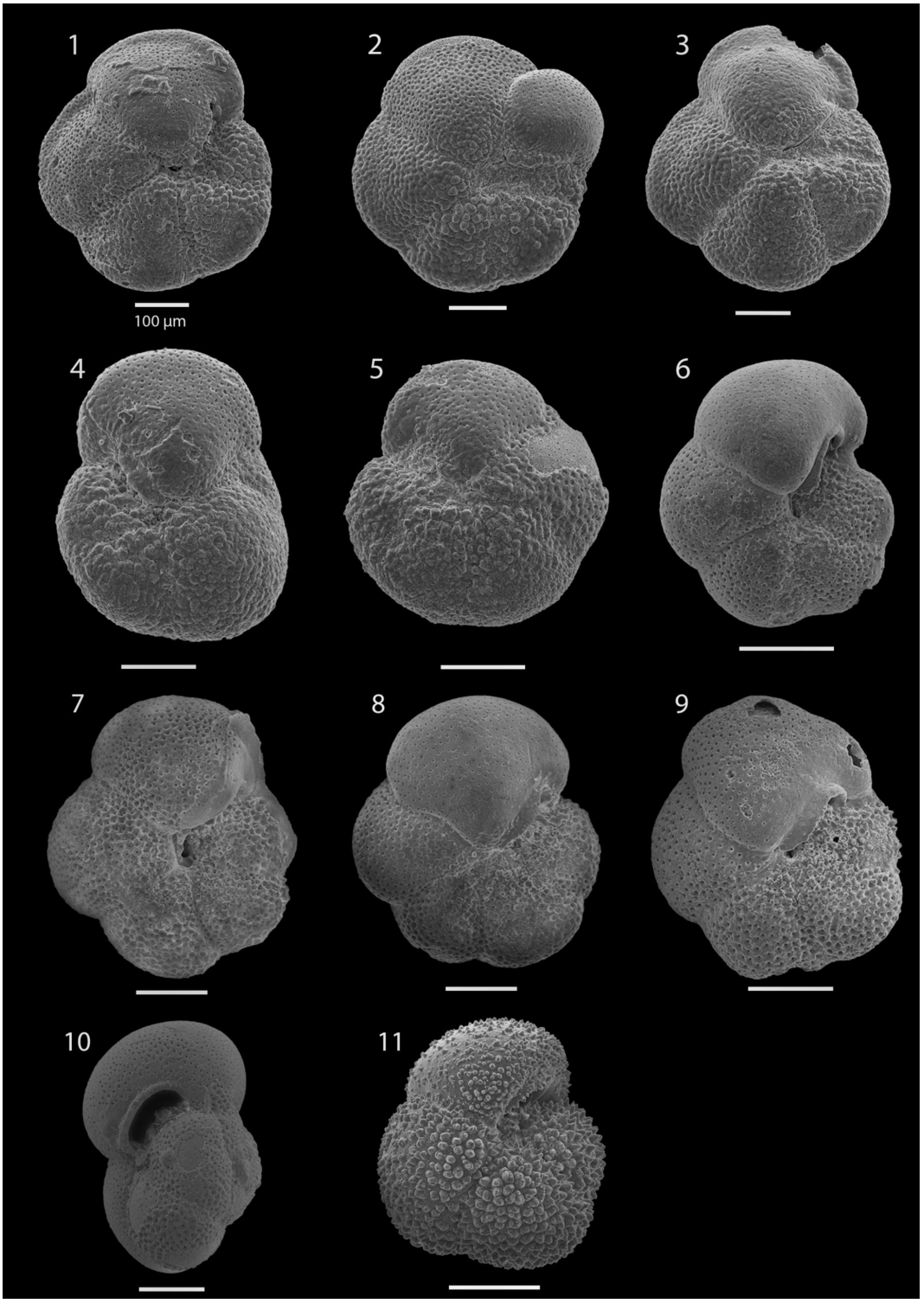

Plate 7. *Globorotalia*. Species are organized alphabetically, along with their corresponding age and biozone, when available. Scale bars are 100 µm, unless otherwise noted. All figures are in umbilical view, unless otherwise noted. **(1–5)** *Globorotalia archeomenardii/praemenardii* plexus, Sample 407-18R-2, 56–58 cm (middle Miocene; "*C.*" *pseudociperoensis Zone*). **(6–10)** *Globorotalia challengeri*. **(6, 8)** Sample 407-19R-1, 56–58 cm (middle Miocene; "*C.*" *pseudociperoensis* Zone). **(7)** Sample 407-18R-2, 56–58 cm (middle Miocene; "*C.*" *pseudociperoensis* Zone). **(9)** Sample 407-18R-3, 56–58 cm (middle Miocene; "*C.*" *pseudociperoensis* Zone). **(10)** Sample 407-19R-1, 56–58 cm (middle Miocene; "*C.*" *pseudociperoensis* Zone), edge view. **(11)** *Globorotalia crassaformis*, Sample 407-3R-1, 55–58 cm (Pleistocene; *N. pachyderma* Zone).

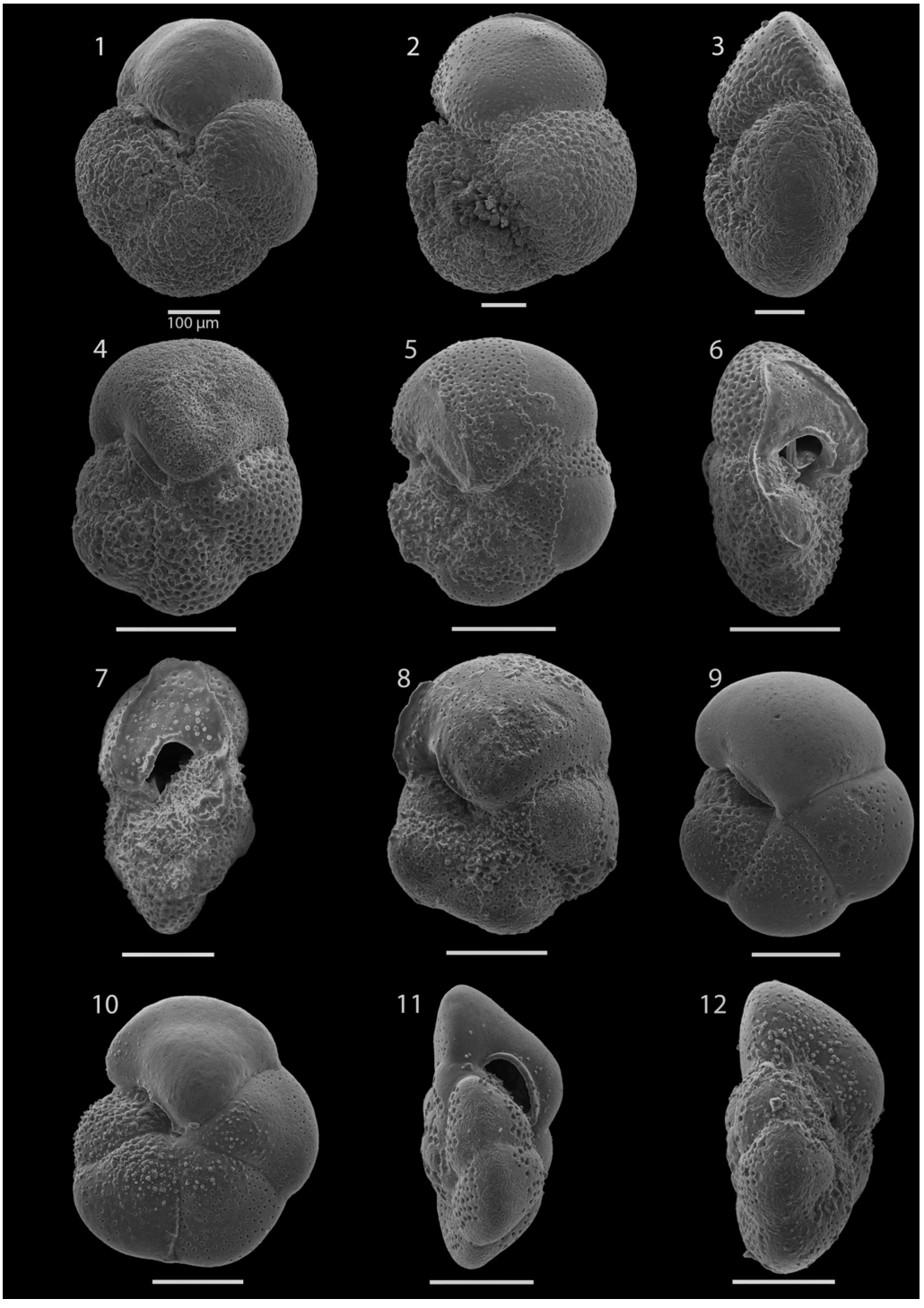

Plate 8. *Globorotalia*. Species are organized alphabetically, along with their corresponding age and biozone, when available. Scale bars are 100 µm, unless otherwise noted. All figures are in umbilical view, unless otherwise noted. **(1–3)** *Globorotalia hirsuta*, Sample 407-1R-2, 56–58 cm (Pleistocene; *N. pachyderma* Zone). **(3)** Sample 407-1R-2, 56–58 cm (Pleistocene; *N. pachyderma* Zone), edge view. **(4–7)** *Globorotalia praescitula*. **(4, 5)** Sample 407-18R-2, 56–58 cm (middle Miocene; "*C.*" *pseudociperoensis* Zone). **(6)** Sample 407-18R-2, 56–58 cm (middle Miocene; "*C.*" *pseudociperoensis* Zone), edge view. **(7)** Sample 407-19R-1, 56–58 cm (middle Miocene; "*C.*" *pseudociperoensis* Zone), edge view. **(8–12)** *Globorotalia scitula*. **(8)** Sample 407-16R-1, 56–58 cm (Pleistocene; *N. praeatlantica* Zone). **(9)** Sample 407-10R-1, 56–58 cm (early Pliocene; *G. puncticulata* Zone). **(10)** Sample 407-3R-1, 55–58 cm (Pleistocene; *N. pachyderma* Zone). **(11)** Sample 407-10R-1, 56–58 cm (early Pliocene; *G. puncticulata* Zone), edge view. **(12)** Sample 407-5R-2, 50–52 cm (Pleistocene; *N. pachyderma* Zone), edge view.

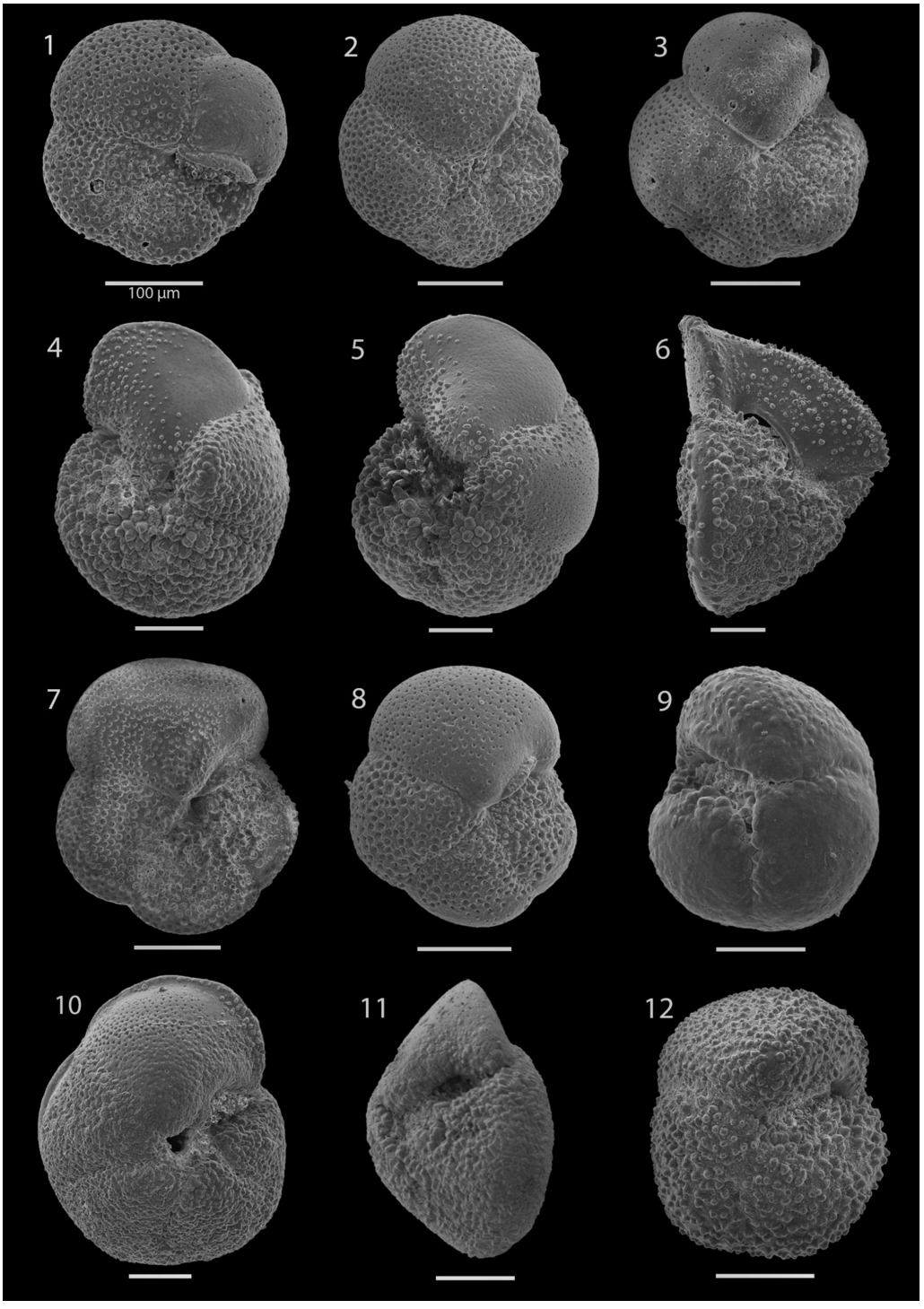

Plate 9. *Globorotalia* and *Globoconella*. Species are organized alphabetically, along with their corresponding age and biozone, when available. Scale bars are 100 µm, unless otherwise noted. All figures are in umbilical view, unless otherwise noted. **(1–3)** *Globorotalia* spp. **(1, 2)** Sample 407-19R-1, 56–58 cm (middle Miocene; "*C.*" *pseudociperoensis* Zone). **(3)** Sample 407-18R-3, 56–58 cm (middle Miocene; "*C.*" *pseudociperoensis* Zone). **(4–6)** *Globorotalia truncatulinoides*, Sample 407-1R-2, 56–58 cm (Pleistocene; *N. pachyderma* Zone). **(6)** Sample 407-1R-2, 56–58 cm (Pleistocene; *N. pachyderma* Zone), edge view. **(7, 8)** *Globorotalia zealandica*. **(7)** Sample 407-18R-3, 56–58 cm (middle Miocene; "*C.*" *pseudociperoensis* Zone). **(8)** Sample 407-19R-1, 56–58 cm (middle Miocene;"*C.*" *pseudociperoensis* Zone). **(9)** *Globoconella inflata*, Sample 407-1R-2, 56–58 cm (Pleistocene; *N. pachyderma* Zone). **(10, 11)** *Globoconella miotumida*, Sample 407-17R-3, 53–55 cm (late Miocene; *N. praeatlantica* Zone). **(11)** Edge view. **(12)** *Globoconella puncticulata*, Sample 407-10R-1, 56–58 cm (early Pliocene; *G. puncticulata* Zone).

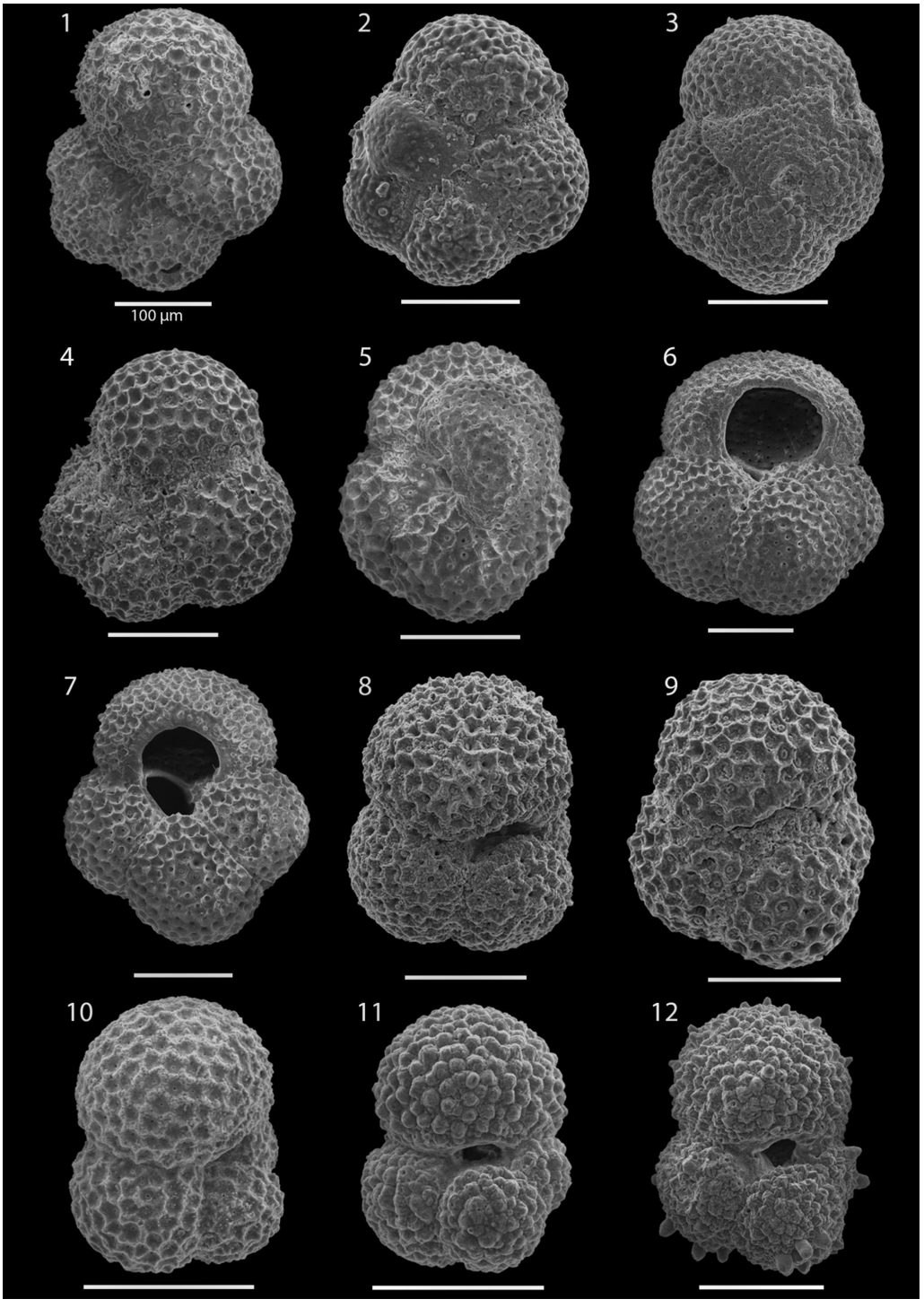

Plate 10. *Globorotaloides* and *Globoturborotalita*. Genera and species are organized alphabetically, along with their corresponding age and biozone, when available. Scale bars are 100 µm, unless otherwise noted. All figures are in umbilical view, unless otherwise noted. **(1)** *Globorotaloides hexagonus*, Sample 407-29R-3, 20–22 cm (early Miocene; Zone M1a). **(2, 3)** *Globorotaloides stainforthi*. **(2)** Sample 407-36R-1, 50–52 cm (late Oligocene; Zone O7). **(3)** Sample 407-35R-1, 86–88 cm (late Oligocene; Zone O7), edge view. **(4, 5)** *Globorotaloides suteri*. **(4)** Sample 407-28R-3, 56–58 cm (early Miocene; Zone M1b). **(5)** Sample 407-20R-1, 100–102 cm (early Miocene; "*C.*" *pseudociperoensis* Zone). **(6, 7)** *Globoturborotalita apertura*. **(6)** Sample 407-21R-1, 46–48 cm (early Miocene; "*C.*" *pseudociperoensis* Zone). **(7)** Sample 407-22R-2, 56–58 cm (early Miocene; "*C.*" *pseudociperoensis* Zone). **(8–10)** *Globoturborotalita connecta*. **(8, 9)** Sample 407-20R-1, 100–102 cm (early Miocene; "*C.*" *pseudociperoensis* Zone). **(10)** Sample 407-13R-1, 56–58 cm (early Pliocene; *N. atlantica* (sin.) PRZ). **(11, 12)** *Globoturborotalita* cf. *connecta*, Sample 407-7R-2, 56–58 cm (late Pliocene; *G. inflata* PRZ).

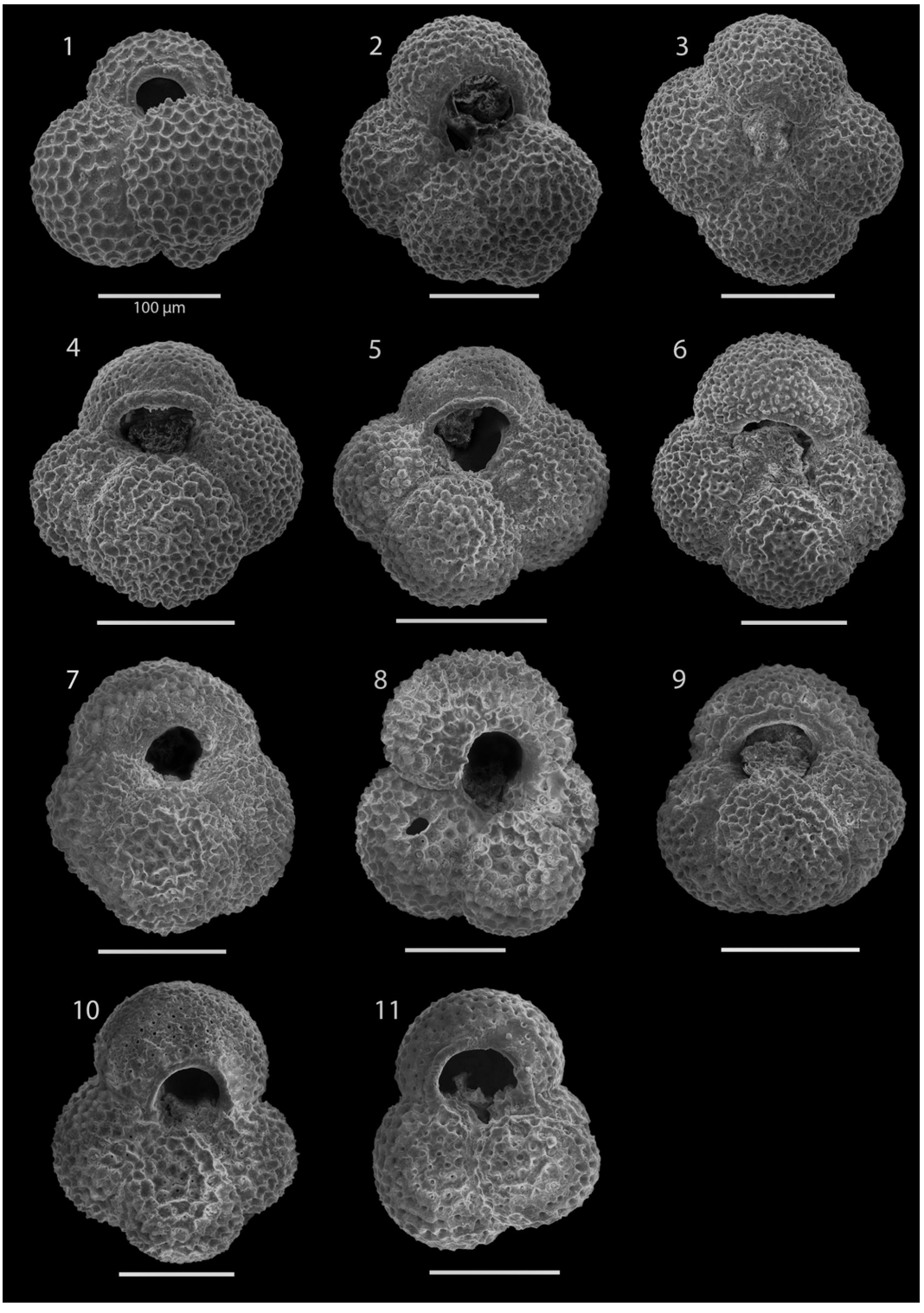

Plate 11. *Globoturborotalita*. Species are organized alphabetically, along with their corresponding age and biozone, when available. Scale bars are 100 µm, unless otherwise noted. All figures are in umbilical view, unless otherwise noted. **(1, 2)** *Globoturborotalita decoraperta*. **(1)** Sample 407-13R-1, 56–58 cm (early Pliocene; *N. atlantica* (sin.) PRZ). **(2)** Sample 407-18R-3, 56–58 cm (middle Miocene; "*C.*" *pseudociperoensis* Zone). **(3–6)** *Globoturborotalita ouachitaensis*, Sample 407-35R-1, 86–88 cm (late Oligocene; Zone O7). **(7–11)** *Globoturborotalita woodi*. **(7)** Sample 407-29R-2, 20–22 cm (early Miocene; Zone M1a). **(8)** Sample 407-21R-1, 46–48 cm (early Miocene; "*C.*" *pseudociperoensis* Zone). **(9)** Sample 407-35R-1, 86–88 cm (late Oligocene; Zone O7). **(10, 11)** Sample 407-22R-2, 56–58 cm (early Miocene; "*C.*" *pseudociperoensis* Zone).

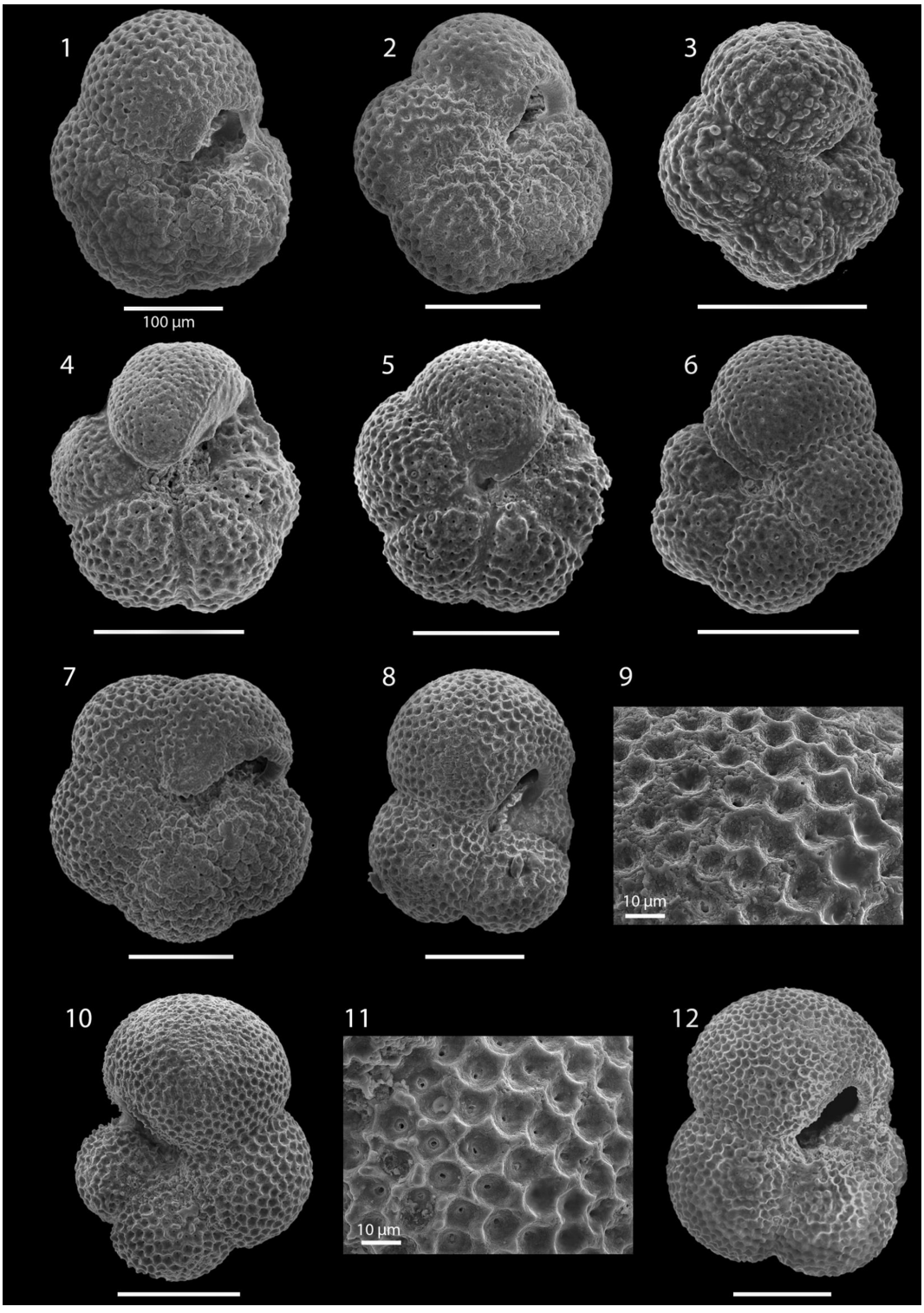

Plate 12. *Paragloborotalia*. Species are organized alphabetically, along with their corresponding age and biozone, when available. Scale bars are 100 µm, unless otherwise noted. All figures are in umbilical view, unless otherwise noted. **(1–5)** *Paragloborotalia acrostoma*. **(1)** Sample 407-21R-1, 46–48 cm (early Miocene; "*C.*" *pseudociperoensis* Zone). **(2, 4, 5)** Sample 407-20R-1, 100–102 cm (early Miocene; "*C.*" *pseudociperoensis* Zone). **(3)** Sample 407-19R-3, 56–58 cm (middle Miocene; "*C.*" *pseudociperoensis* Zone). **(6, 7)** *Paragloborotalia birnageae*. **(6)** Sample 407-30R-3, 56–58 cm (late Oligocene; Zone O7). **(7)** Sample 407-30R-2, 56–58 cm (early Miocene; Zone M1a). **(8–11)** *Paragloborotalia continuosa*. **(8)** Sample 407-25R-1, 30–32 cm (early Miocene). **(9)** Sample 407-20R-1, 100–102 cm (early Miocene; "*C.*" *pseudociperoensis* Zone). **(10)** Sample 407-18R-2, 56–58 cm (middle Miocene; "*C.*" *pseudociperoensis* Zone). **(11)** Sample 407-17R-2, 56–58 cm (late Miocene; *N. praeatlantica* Zone). **(12)** *Paragloborotalia kugleri* Sample 407-29R-2, 20–22 cm (early Miocene; Zone M1a).

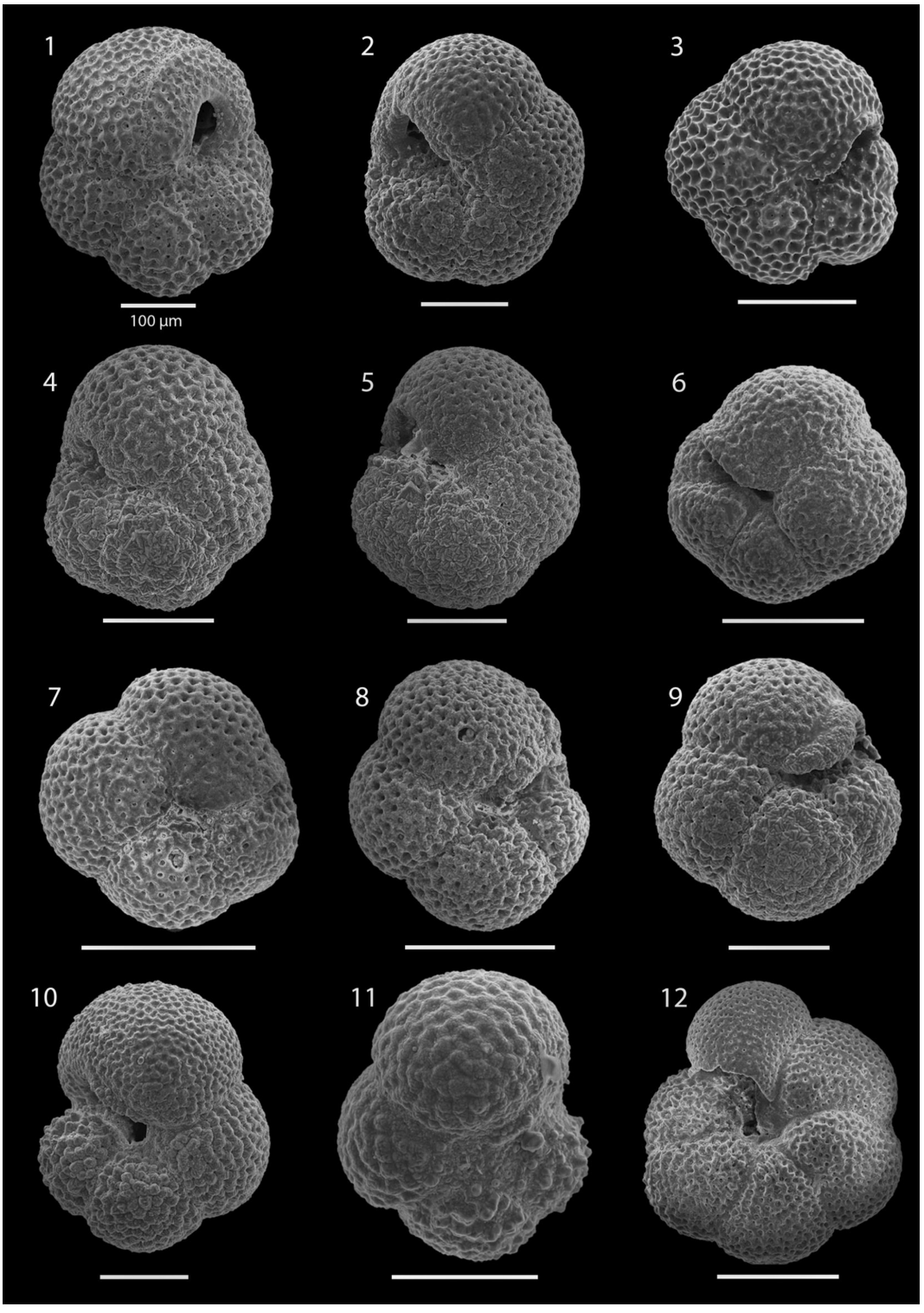

Plate 13. *Paragloborotalia*. Species are organized alphabetically, along with their corresponding age and biozone, when available. Scale bars are 100 µm, unless otherwise noted. All figures are in umbilical view, unless otherwise noted. **(1, 2)** *Paragloborotalia mayeri*, Sample 407-20R-1, 100–102 cm (early Miocene; "*C.*" *pseudociperoensis* Zone). **(3)** *Paragloborotalia nana*, Sample 407-28R-3, 56–58 cm (early Miocene; Zone M1b). **(4, 5)** *Paragloborotalia pseudokugleri*. **(10)** Sample 407-29R-2, 20–22 cm (early Miocene; Zone M1a). **(11)** Sample 407-31R-4, 46–48 cm (late Oligocene; Zone O7). **(6)** *Paragloborotalia semivera*, Sample 407-30R-3, 56–58 cm (late Oligocene; Zone O7). **(7)** *Paragloborotalia siakensis*, Sample 407-21R-1, 46–48 cm (early Miocene; "*C.*" *pseudociperoensis* Zone). **(8–12)** *Paragloborotalia* sp. **(8, 10, 12)** Sample 407-18R-3, 56–58 cm (middle Miocene; "*C.*" *pseudociperoensis* Zone). **(9)** Wall texture of Fig. 8. **(11)** Wall texture of Fig. 10.

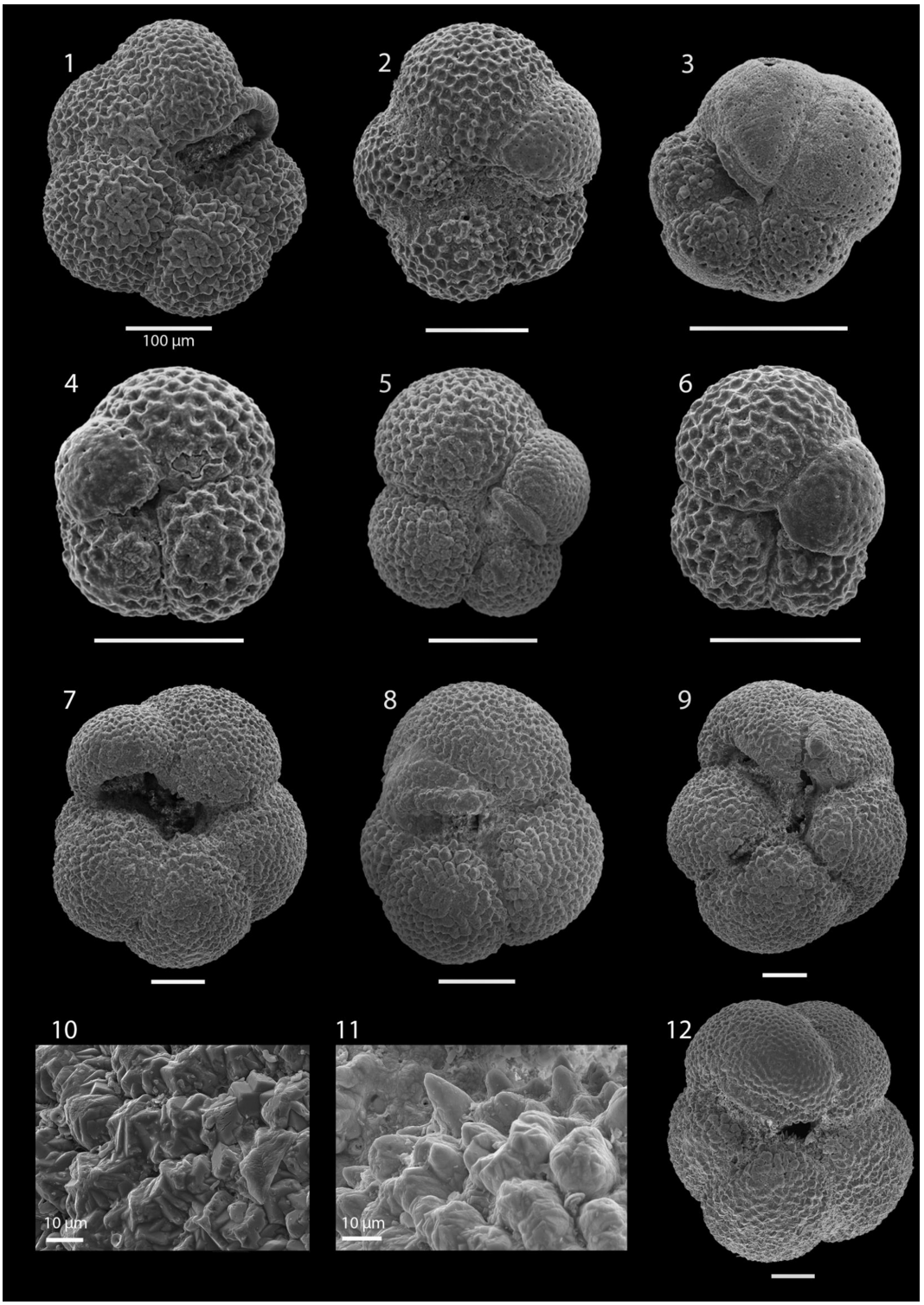

Plate 14. *Neogloboquadrina*. Species are organized alphabetically, along with their corresponding age and biozone, when available. Scale bars are 100 µm, unless otherwise noted. All figures are in umbilical view, unless otherwise noted. **(1–3)** *Neogloboquadrina acostaensis*. **(1)** Sample 407-5R-3, 56–58 cm (Pleistocene; *N. pachyderma* Zone). **(2)** Sample 407-16R-1, 56–58 cm (late Miocene; *N. praeatlantica* Zone). **(3)** Sample 407-14R-1, 56–58 cm (early Pliocene; *N. atlantica* (sin.) PRZ). **(4–6)** *Neogloboquadrina* cf. *acostaensis*. **(4, 6)** Sample 407-16R-1, 56–58 cm (late Miocene; *N. praeatlantica* Zone). **(5)** Sample 407-14R-1, 56–58 cm (early Pliocene; *N. atlantica* (sin.) PRZ). **(7–12)** *Neogloboquadrina atlantica* dextral. **(7, 10)** Sample 407-18R-1, 56–58 cm (late Miocene; *N. praeatlantica* Zone). **(8)** Sample 407-17R-3, 53–55 cm (late Miocene; *N. praeatlantica* Zone). **(9, 12)** Sample 407-17R-1, 56–58 cm (late Miocene; *N. praeatlantica* Zone). **(10)** Wall texture of Fig. 7. **(11)** Wall texture of Fig. 8.

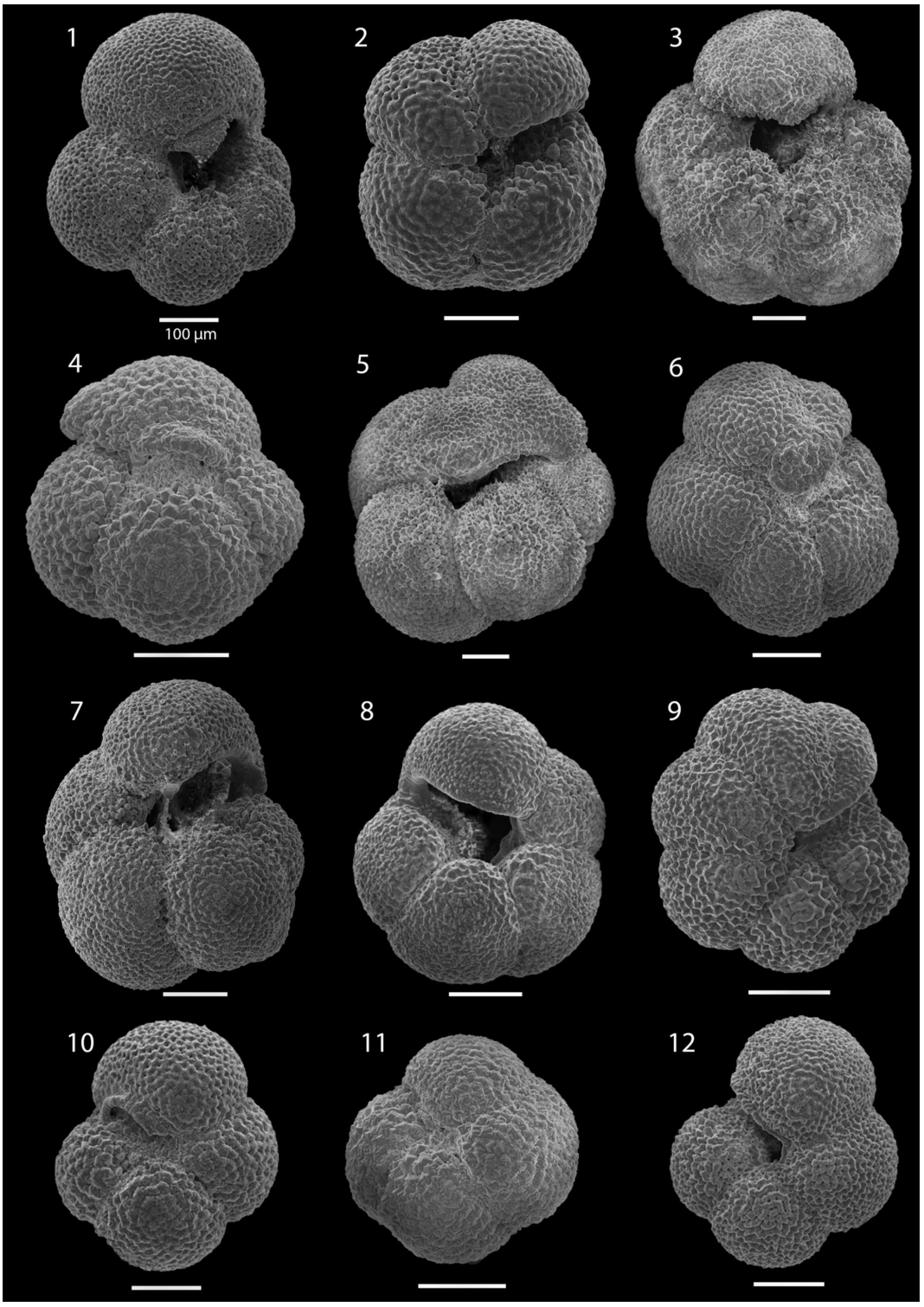

Plate 15. *Neogloboquadrina*. Species are organized alphabetically, along with their corresponding age and biozone, when available. Scale bars are 100 µm, unless otherwise noted. All figures are in umbilical view, unless otherwise noted. **(1–7)** *Neogloboquadrina atlantica* sinistral. **(1)** Sample 407-18R-1, 56–58 cm (late Miocene; *N. praeatlantica* Zone). **(2)** Sample 407-17R-1, 56–58 cm (late Miocene; *N. praeatlantica* Zone). **(3–5)** Sample 407-14R-3, 56–58 cm (early Pliocene; *N. atlantica* (sin.) PRZ). **(6)** Sample 407-13R-1, 56–58 cm (early Pliocene; *N. atlantica* (sin.) PRZ). **(7)** Sample 407-12R-1, 56–58 cm (early Pliocene; *N. atlantica* (sin.) PRZ). **(8)** *Neogloboquadrina dutertrei*, Sample 407-1R-1, 57–60 cm (Pleistocene; *N. pachyderma* Zone). **(9)** *Neogloboquadrina humerosa*, Sample 407-3R-2 (Pleistocene; *N. pachyderma* Zone). **(10–12)** *Neogloboquadrina incompta*. **(10)** Sample 407-18R-1, 56–58 cm (late Miocene; *N. praeatlantica* Zone). **(11)** Sample 407-17R-3, 53–55 cm (late Miocene; *N. praeatlantica* Zone). **(12)** Sample 407-2R-3, 56–58 cm (Pleistocene; *N. pachyderma* Zone).

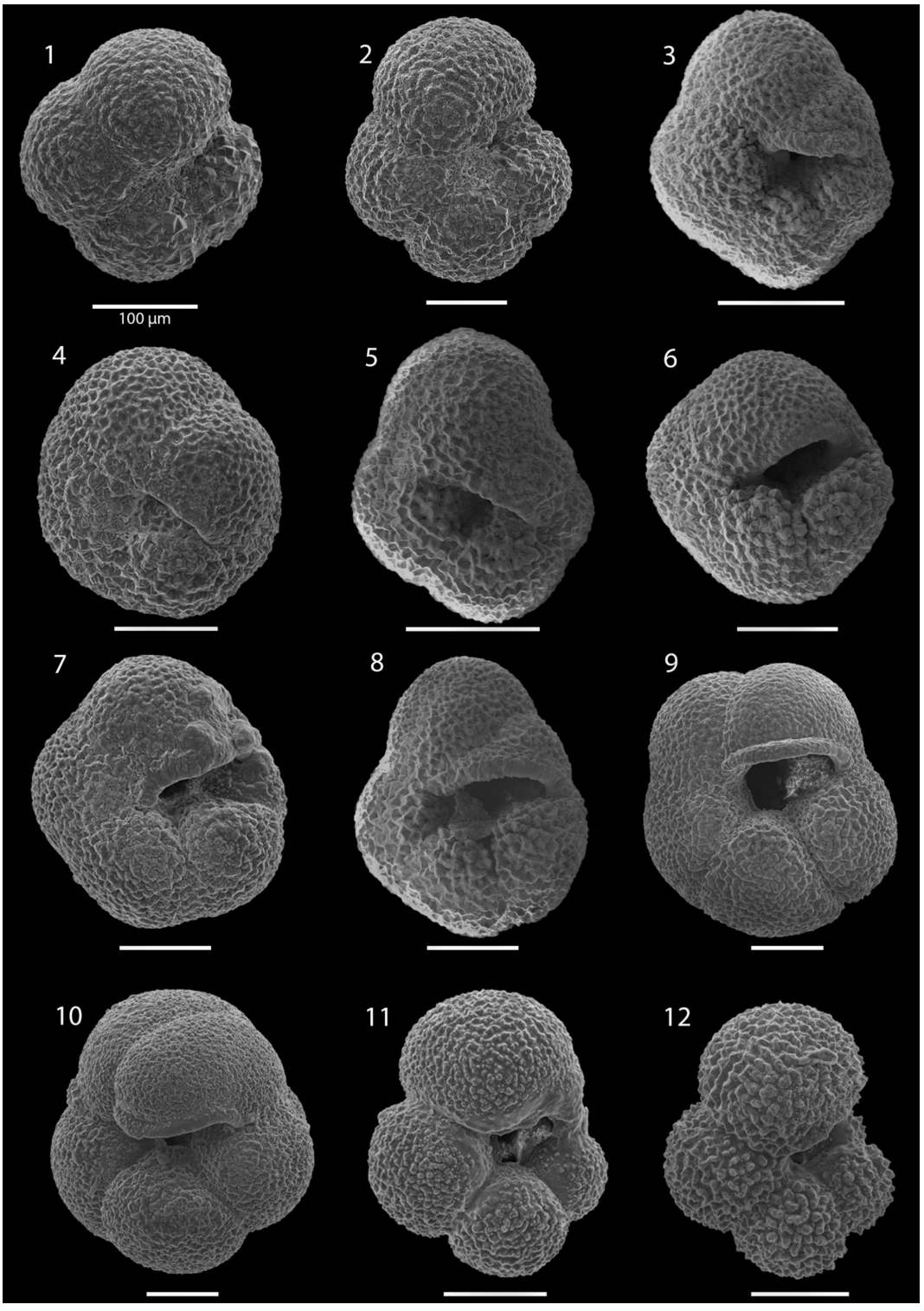

Plate 16. *Neogloboquadrina pachyderma*. Plate is organized stratigraphically from older to younger, along with their corresponding age and biozone, when available. Scale bars are 100 µm, unless otherwise noted. **(1, 2)** *Neogloboquadrina pachyderma*. **(1)** Sample 407-17R-1, 56–58 cm (late Miocene; *N. praeatlantica* Zone). **(2)** Sample 407-17R-2, 56–58 cm (late Miocene; *N. praeatlantica* Zone). **(3–5)** *Neogloboquadrina pachyderma* morphotype Nps-1, Sample 407-5R-2, 50–52 cm (Pleistocene; *N. pachyderma* Zone). **(6, 7)** *Neogloboquadrina pachyderma* morphotype Nps-2. **(6)** Sample 407-1R-1, 57–60 cm (Pleistocene; *N. pachyderma* Zone). **(7)** Sample 407-5R-2, 50–52 cm (Pleistocene; *N. pachyderma* Zone). **(8)** *Neogloboquadrina pachyderma* morphotype Nps-3, Sample 407-1R-1, 57–60 cm (Pleistocene; *N. pachyderma* Zone). **(9, 10)** *Neogloboquadrina pachyderma* morphotype Nps-4, Sample 407-1R-1, 57–60 cm (Pleistocene; *N. pachyderma* Zone). **(11, 12)** *Neogloboquadrina pachyderma* morphotype Nps-5, Sample 407-1R-1, 57–60 cm (Pleistocene; *N. pachyderma* Zone).

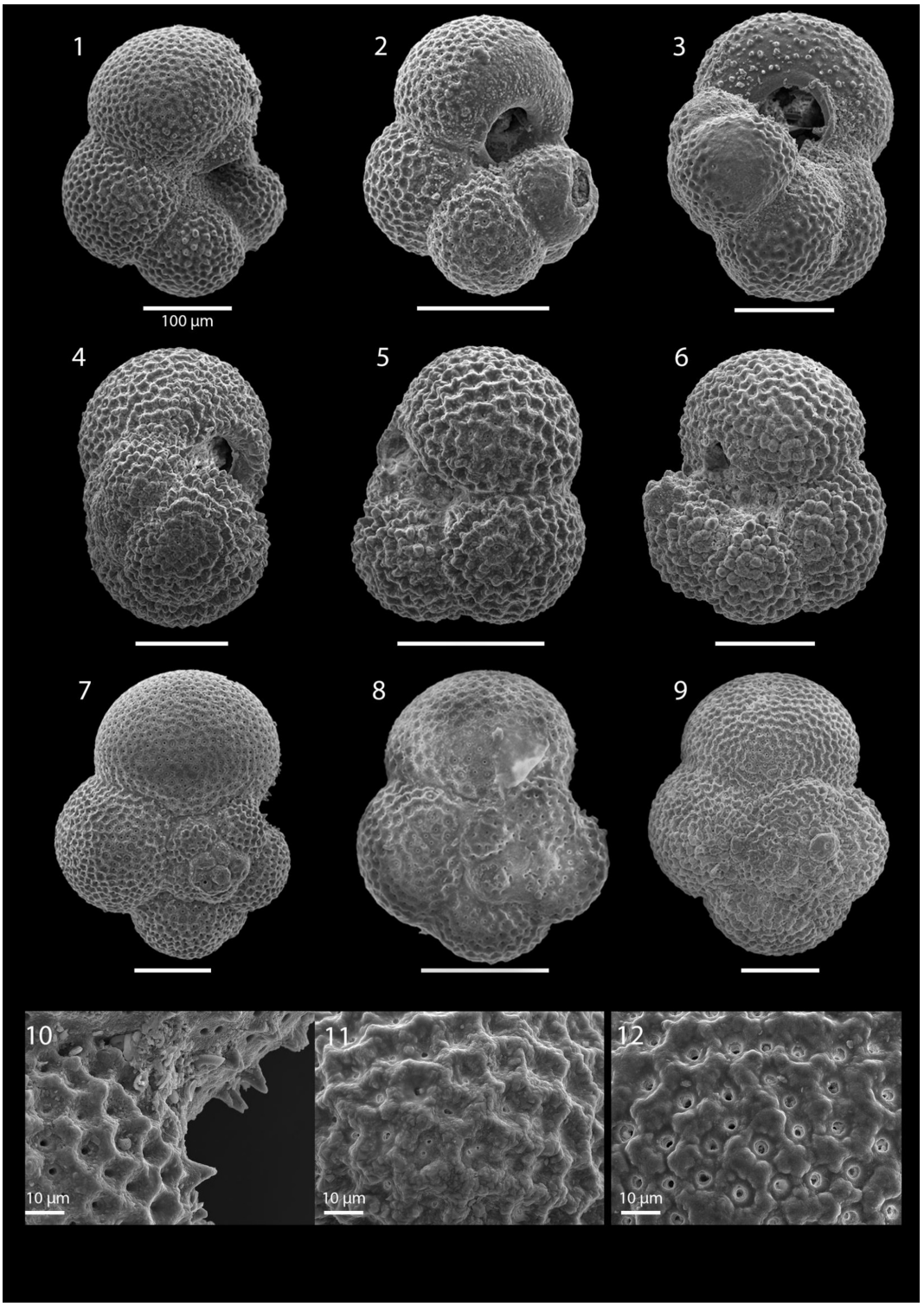

Plate 17. *Neogloboquadrina praeatlantica*. Corresponding age and biozone are indicated, when available. Scale bars are 100 µm, unless otherwise noted. All figures are in umbilical view, unless otherwise noted. **(1–12)** *Neogloboquadrina praeatlantica*. **(1, 2)** Sample 407-18R-1, 56–58 cm (late Miocene; *N. praeatlantica* Zone). **(3)** Edge view, Sample 407-18R-1, 56–58 cm (late Miocene; *N. praeatlantica* Zone). **(4)** Edge view, Sample 407-17R-3, 53–55 cm (late Miocene; *N. praeatlantica* Zone). **(5)** Sample 407-16R-1, 56–58 cm (late Miocene; *N. praeatlantica* Zone). **(6)** Sample 407-17R-1, 56–58 cm (late Miocene; *N. praeatlantica* Zone). **(7, 8)** Spiral view, Sample 407-18R-1, 56–58 cm (late Miocene; *N. praeatlantica* Zone). **(9)** Spiral view, Sample 407-17R-3, 53–55 cm (late Miocene; *N. praeatlantica* Zone). **(10)** Wall texture of Fig. 7. **(11)** Wall texture of Fig. 8. **(12)** wall texture of Fig. 9.

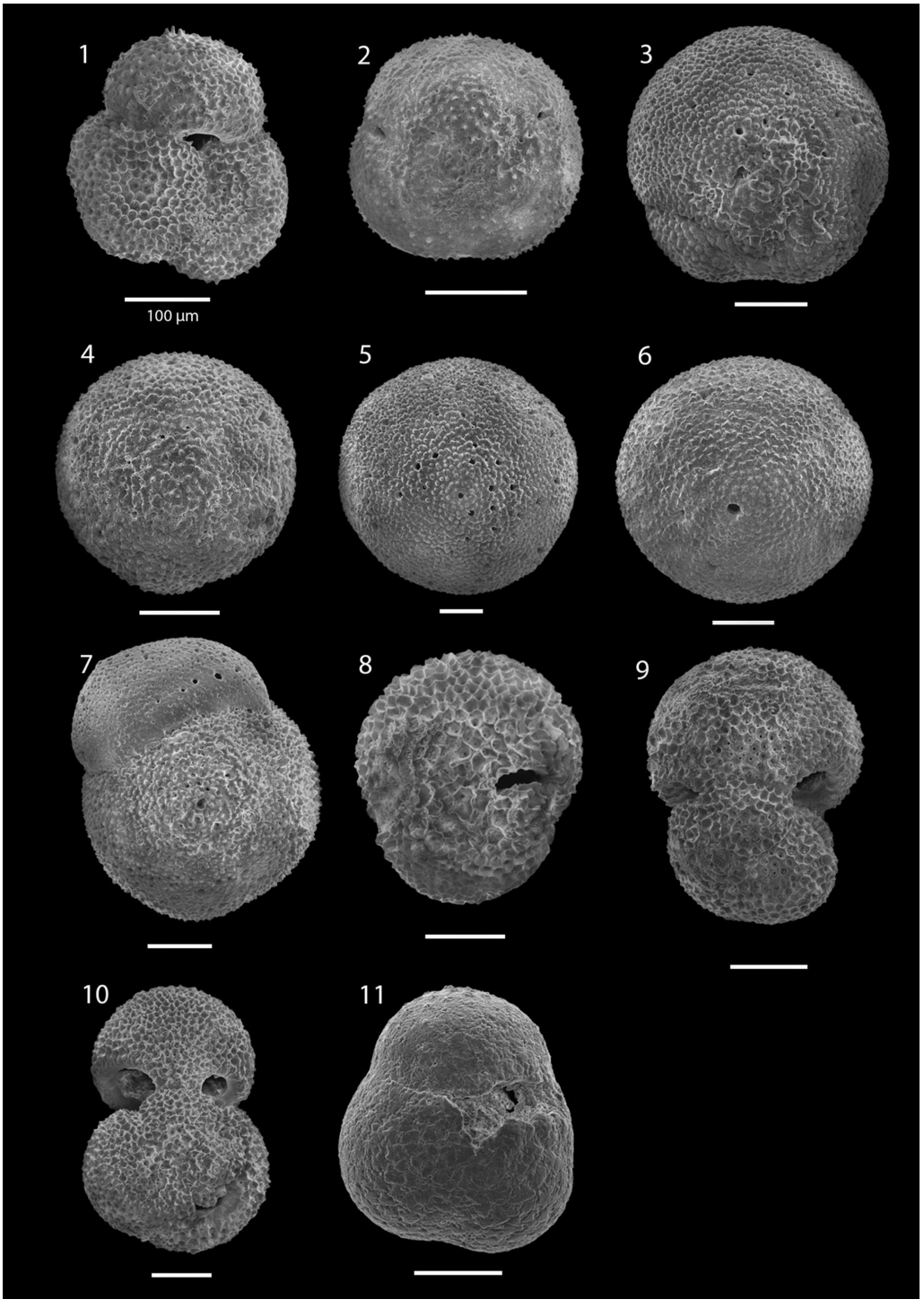

Plate 18. *Globigerinoides*, *Orbulina, Trilobatus*, and *Sphaeroidinellopsis*. Genera and species are organized alphabetically, along with their corresponding age and biozone, when available. Scale bars are 100 µm, unless otherwise noted. All figures are in umbilical view, unless otherwise noted. **(1)** *Globigerinoides ruber*, Sample 407-23R-1, 56–58 cm (early Miocene; "*C.*" *pseudociperoensis* Zone). **(2)** *Orbulina suturalis*, Sample 407-17R-2, 56–58 cm (late Miocene; *N. praeatlantica* Zone). **(3–7)** *Orbulina universa*. **(3, 4, 7)** Sample 407-1R-2, 56–58 cm (Pleistocene; *N. pachyderma* Zone). **(5)** Sample 407-8R-1, 56–58 cm (late Pliocene; *G. inflata* PRZ). **(6)** Sample 407-17R-2, 56–58 cm (late Miocene; *N. praeatlantica* Zone). **(8)** *Trilobatus bisphericus*, Sample 407-19R-2, 56–58 cm (middle Miocene; "*C.*" *pseudociperoensis* Zone). **(9)** *Trilobatus immaturus*, Sample 407-18R-2, 56–58 cm (middle Miocene; "*C.*" *pseudociperoensis* Zone). **(10)** *Trilobatus trilobus*, Sample 407-18R-2, 56–58 cm (middle Miocene; "*C.*" *pseudociperoensis* Zone). **(11)** *Sphaeroidinellopsis paenedehiscens*, Sample 407-17R-2, 56–58 cm (late Miocene; *N. praeatlantica* Zone).

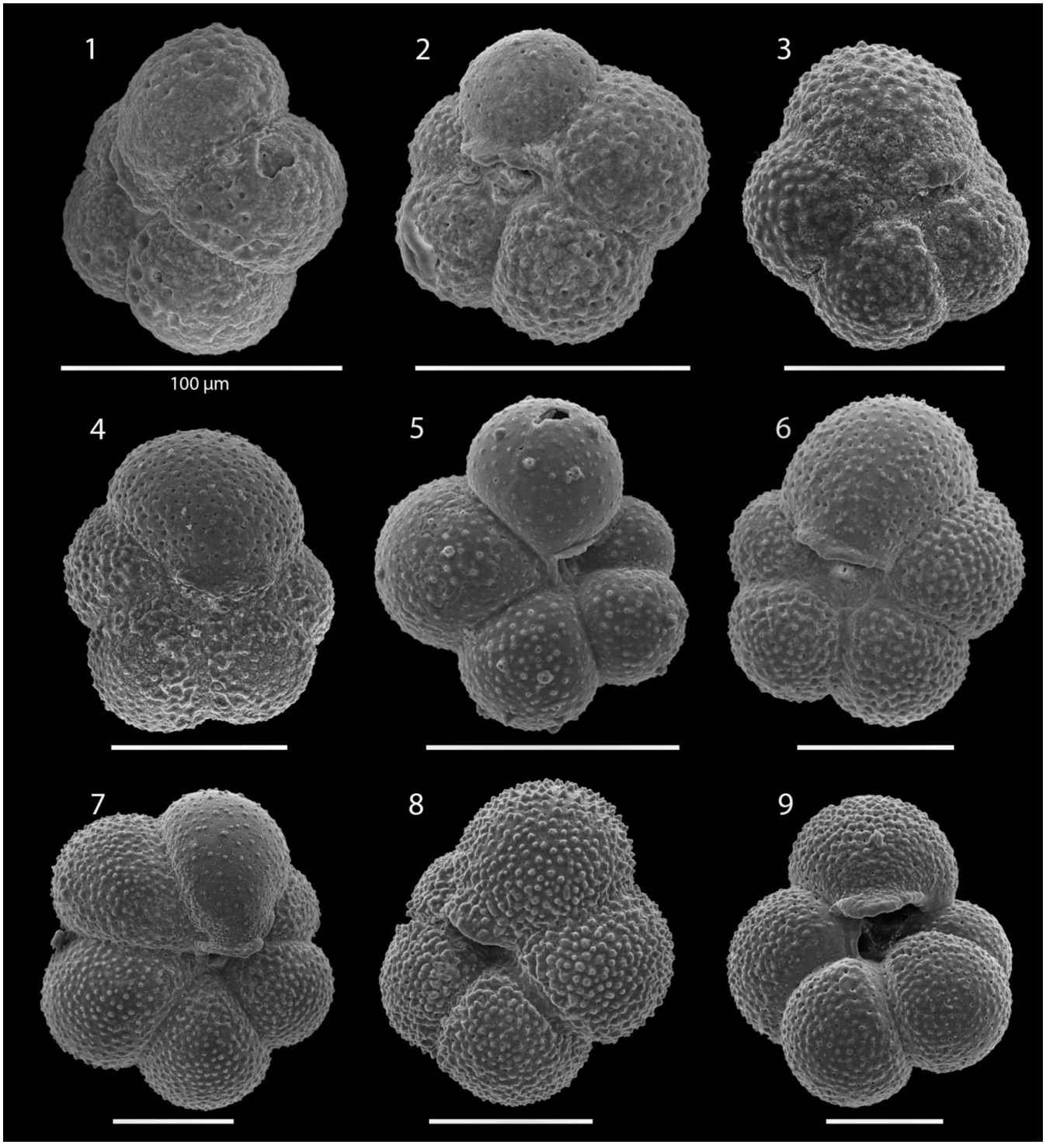

Plate 19. *Turborotalita quinqueloba*. Corresponding age and biozone are indicated, when available. Scale bars are 100 µm, unless otherwise noted. **(1–9)** *Turborotalita quinqueloba*. **(1)** Sample 407-28R-1, 56–58 cm (early Miocene). **(2)** Sample 407-20R-1, 100–102 cm (early Miocene; "*C.*" *pseudociperoensis* Zone). **(3)** Sample 407-17R-1, 56–58 cm (late Miocene; *N. praeatlantica* Zone). **(4)** Sample 407-12R-1, 56–58 cm (early Pliocene; *N. atlantica* (sin.) PRZ). **(5)** Sample 407-3R-1, 55–58 cm (Pleistocene; *N. pachyderma* Zone). **(6, 7)** Sample 407-1R-2, 56–58 cm (Pleistocene; *N. pachyderma* Zone). **(8, 9)** Sample 407-1R-1, 57–60 cm (Pleistocene; *N. pachyderma* Zone).

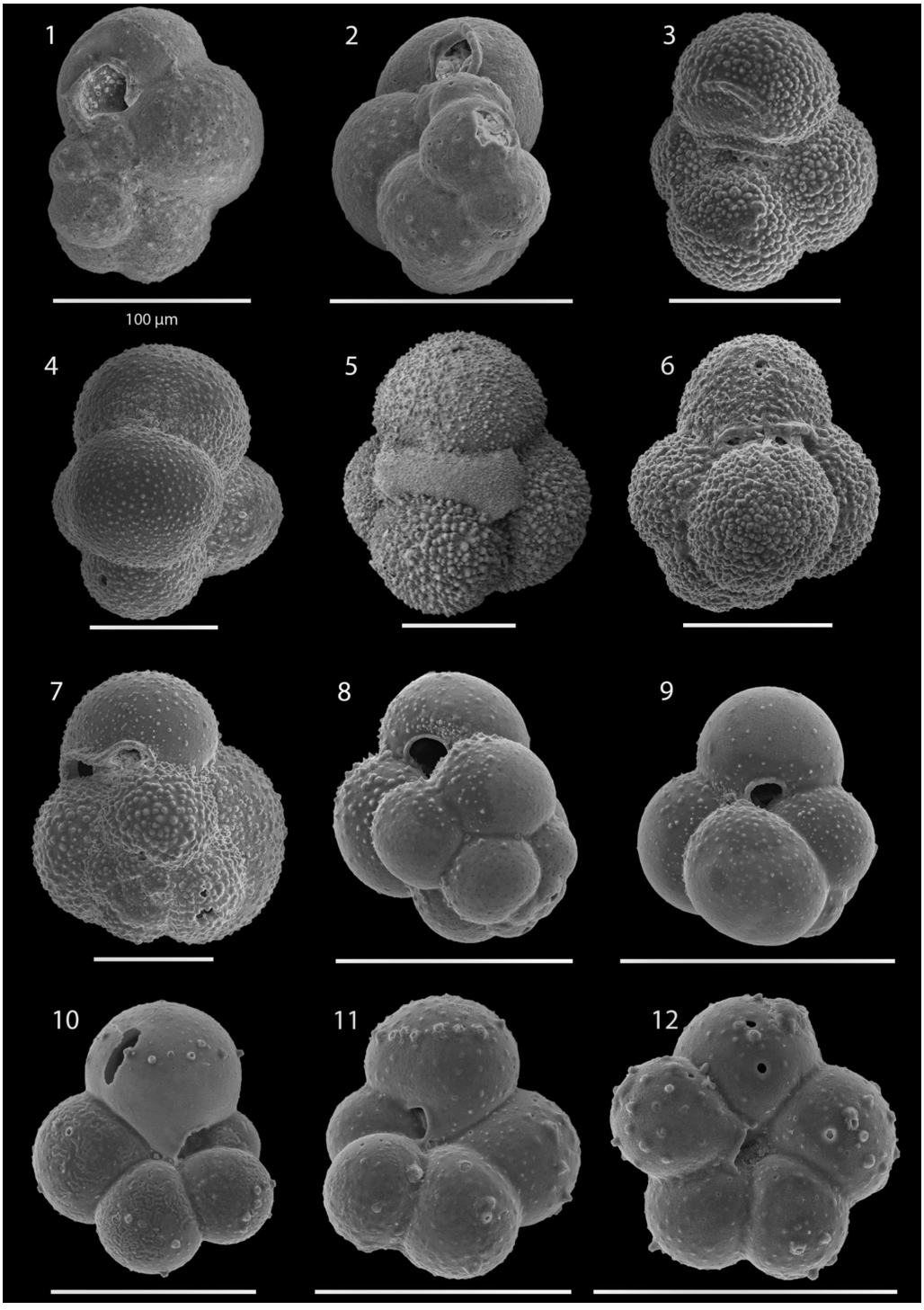

Plate 20. Microperforates, namely *Cassigerinella*, *Globigerinita*, and *Orcadia*. Genera and species are organized alphabetically, along with their corresponding age and biozone, when available. Scale bars are 100 µm, unless otherwise noted. All figures are in umbilical view, unless otherwise noted. **(1, 2)** *Cassigerinella chipolensis*. **(1)** Sample 407-28R-3, 56–58 cm (early Miocene; Zone M1b). **(2)** Sample 407-24R-3, 56–58 cm (early Miocene; "*C.*" *pseudociperoensis* Zone). **(3–6)** *Globigerinita glutinata*. **(3)** Sample 407-36R-1, 50–52 cm (late Oligocene; Zone O7). **(4)** Sample 407-26R-1, 30–32 cm (early Miocene). **(5)** Sample 407-19R-3, 56–58 cm (middle Miocene; "*C.*" *pseudociperoensis* Zone). **(6)** Sample 407-16R-1, 56–58 cm (late Miocene; *N. praeatlantica* Zone). **(7–9)** *Globigerinita uvula*. **(7)** Sample 407-26R-1, 30–32 cm (early Miocene). **(8, 9)** Sample 407-1R-1, 57–60 cm (Pleistocene; *N. pachyderma* Zone). **(10–12)** *Orcadia riedeli*. **(10)** Sample 407-2R-2, 56–59 cm (Pleistocene; *N. pachyderma* Zone). **(11, 12)** Sample 407-1R-1, 57–60 cm (Pleistocene; *N. pachyderma* Zone).

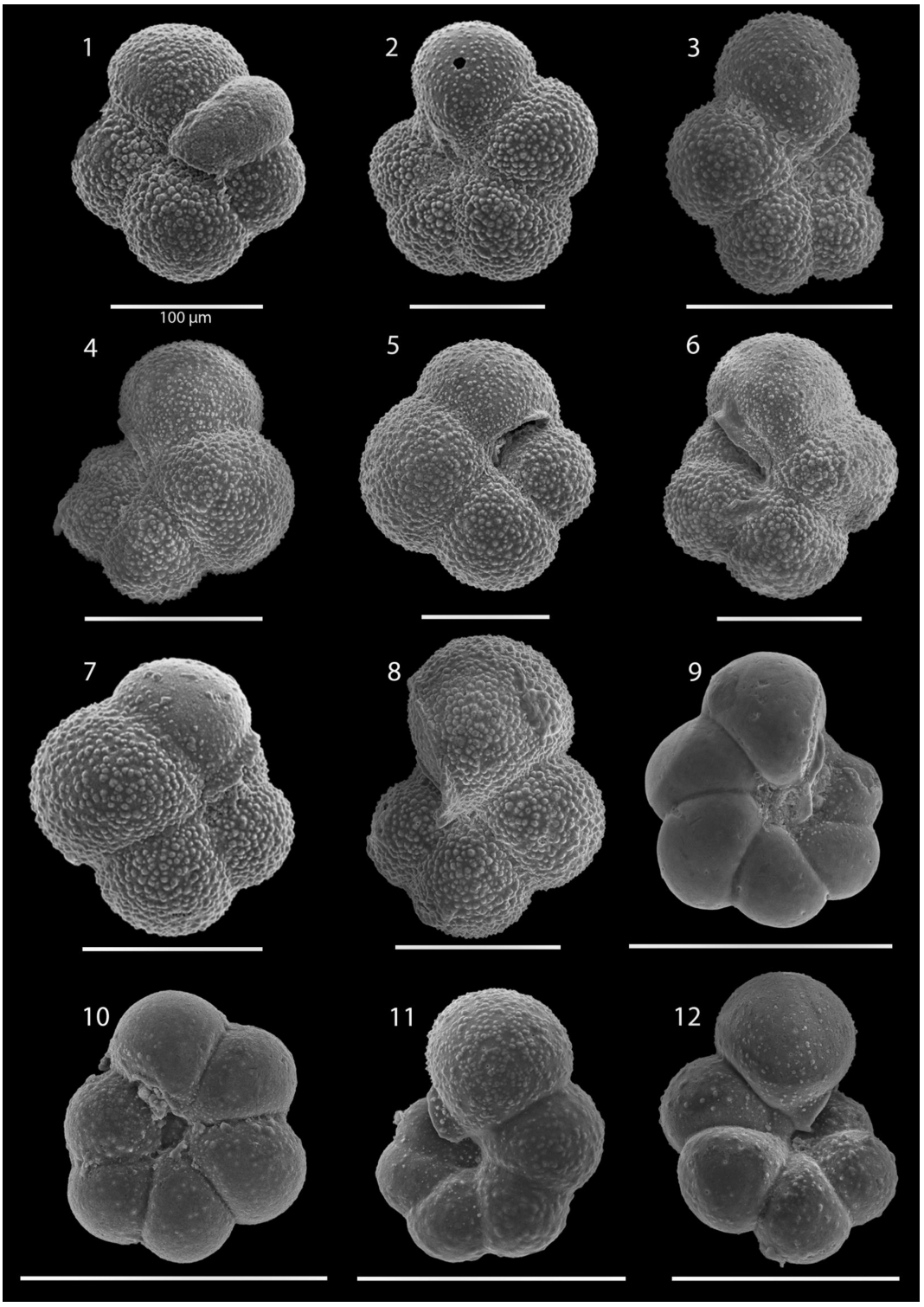

Plate 21. Microperforates, namely *Tenuitella* and *Tenuitellita*. Genera and species are organized alphabetically, along with their corresponding age and biozone, when available. Scale bars are 100 µm, unless otherwise noted. All figures are in umbilical view, unless otherwise noted. **(1, 2)** *Tenuitella angustiumbilicata*. **(1)** Sample 407-36R-1, 50–52 cm (late Oligocene; Zone O7). **(2)** Sample 407-19R-3, 56–58 cm (middle Miocene; "*C.*" *pseudociperoensis* Zone). **(3, 4)** *Tenuitella clemenciae*, Sample 407-28R-1, 56–58 cm (early Miocene). **(5–8)** *Tenuitella munda*. **(1)** Sample 407-30R-3, 56–58 cm (late Oligocene; Zone O7). **(2, 3)** Sample 407-29R-2, 20–22 cm (early Miocene; Zone M1a). **(4)** Sample 407-28R-1, 56–58 cm (early Miocene). **(9–12)** *Tenuitellita fleisheri*. **(9)** Sample 407-2R-1, 58–60 cm (Pleistocene; *N. pachyderma* Zone). **(10, 12)** Sample 407-2R-2, 56–59 cm (Pleistocene; *N. pachyderma* Zone). **(11)** Sample 407-3R-1, 55–58 cm (Pleistocene; *N. pachyderma* Zone).

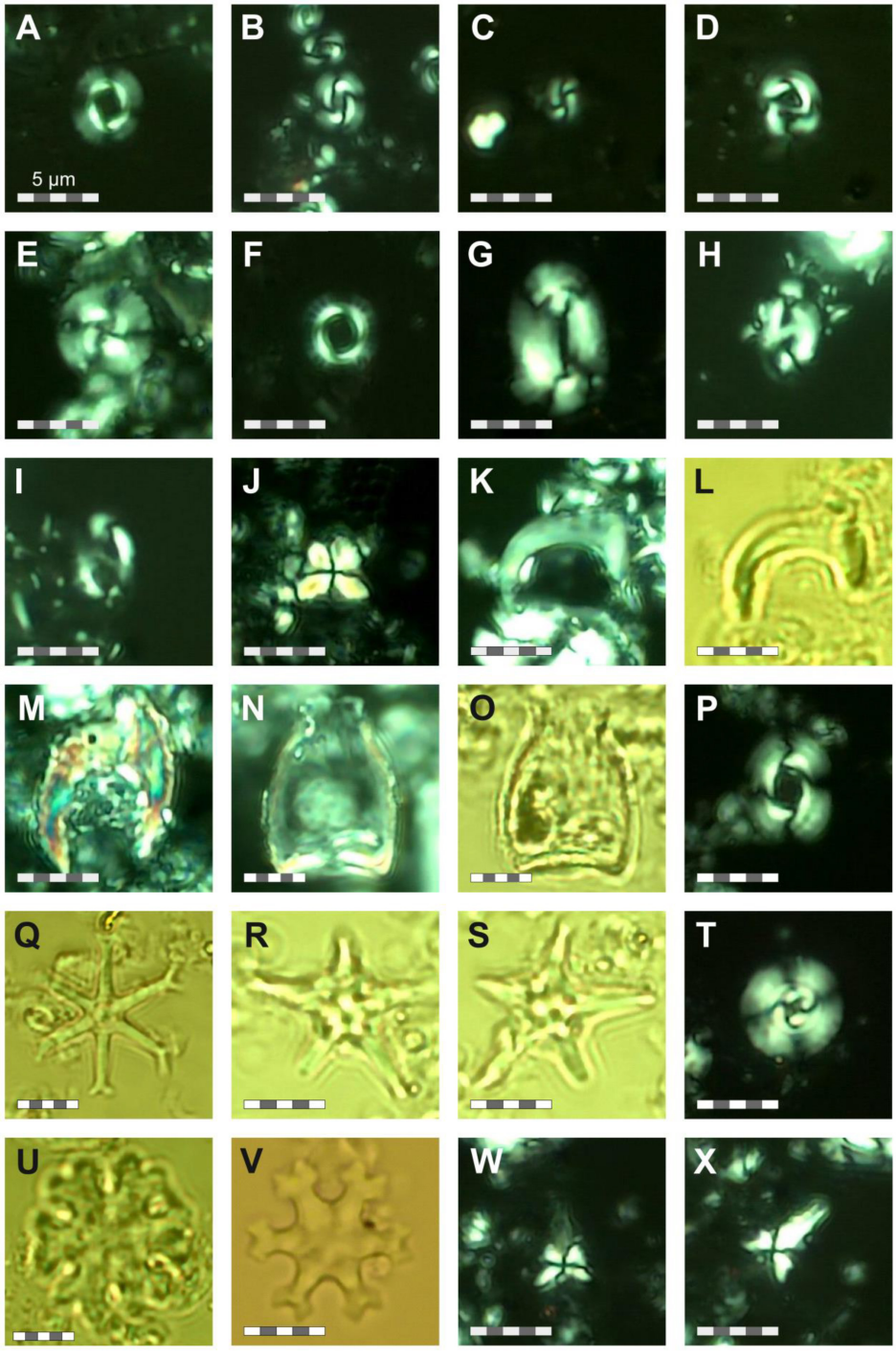

Plate 22. Scale bars are 5 µm unless otherwise noted. **(A)** *Gephyrocapsa huxleyi*; light cross-polarised light (XPL), 407-1R-1, 57–60 cm. **(B)** *Gephyrocapsa caribbeanica*; light XPL, 407-2R-2, 56–59 cm. **(C)** *Gephyrocapsa* small form; light XPL, 407-4R-2, 55–58 cm. **(D)** *Gephyrocapsa oceanica*; light XPL, 407-4R-2, 55–58 cm. **(E)** *Calcidiscus leptoporus*; light XPL, 407-8R-2, 56–58 cm. **(F)** *Pseudoemiliania lacunosa*; light XPL, 407-4R-1, 55–58 cm. **(G)** *Helicosphaera carteri*; light XPL, 407-4R-1, 55–58 cm. **(H, I)** *Helicosphaera sellii*; light XPL, 407-8R-2, 56–58 cm. **(J)** *Sphenolithus moriformis*; light XPL, 407-8R-2, 56–58 cm. **(K, L)** *Amaurolithus tricorniculatus*; **(K)** XPL, **(L)** plane-polarised light (PPL), 407-12R-1, 56–58 cm. **(M)** *Amaurolithus tricorniculatus*; light XPL, 407-12R-3, 56–58 cm. **(N, O)** *Scyphosphaera lagena*; **(N)** XPL, **(O)** PPL, 407-12R-3, 56–58 cm. **(P)** *Reticulofenestra pseudoumbilicus*; light XPL, 407-17R-1, 56–58 cm. **(Q)** *Discoaster variabilis*; light XPL, 407-17R-1, 56–58 cm. **(R, S)** *Discoaster quinqueramus* group; light PPL, 407-17R-2, 56–58 cm. **(T)** *Cyclocargolithus floridanus*; light XPL, 407-18R-2, 56–58 cm. **(U)** *Discoaster deflanderi*; light PPL, 407-18R-2, 56–58 cm. **(V)** *Discoaster deflanderi*; light PPL, 407-31R-4, 46–48 cm. **(W, X)** *Sphenolithus heteromorphus*; light PPL, **(X)** rotated, 407-18R-2, 56–58 cm.

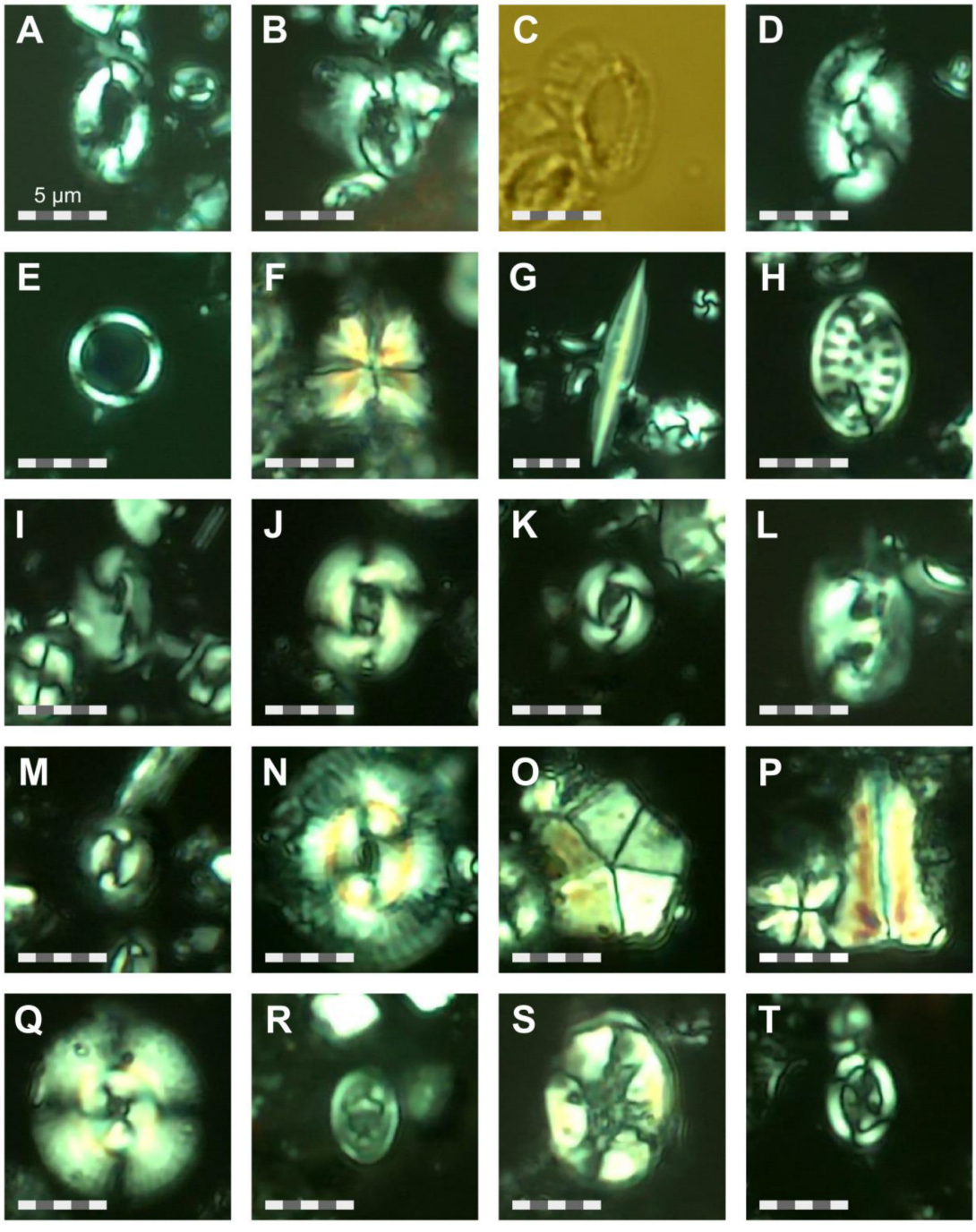

Plate 23. Scale bars are 5 µm unless otherwise noted. **(A)** *Helicosphaera ampliaperta* group; light XPL, 407-19R-3, 56–58 cm. **(B)** *Helicosphaera magnifica*; light XPL, rotated, 407-19R-3, 56–58 cm. **(C)** *Helicosphaera magnifica*; light PPL, 407-18R-3, 56–58 cm. **(D)** *Helicosphaera euphratis*; light XPL, 407-29R-1 56–58 cm. **(E)** *Coronocyclus nitescens*; light XPL, 407-19R-3, 56–58 cm. **(F)** *Sphenolithus puniceus*; light XPL, 407-19R-3, 56–58 cm. **(G)** *Triquetrorhabdulus carinatus*; light XPL, rotated, 407-28R-3 56–58 cm. **(H)** *Pontosphaera multipora*; light XPL, 407-28R-3 56–58 cm. **(I)** *Helicosphaera perch-nielseniae*; light XPL, 407-29R-1 56–58 cm. **(J)** *Reticulofenestra daviesii*; light XPL, 407-31R-4, 46–48 cm. **(K)** *Reticulofenestra daviesii*; light XPL, 407-18R-2, 56–58 cm. **(L)** *Helicosphaera recta*; light XPL, 407-28R-3, 56–58 cm. **(M, N)** *Coccolithus pelagicus* (M – small; N – large); light XPL, 407-19R-3, 56–58 cm. **(O)** *Braarudosphaera bigelowii*; light XPL, 407-36R-1 50–52 cm. **(P)** *Zygrhablithus bijugatus* (right) and *Sphenolithus moriformis* (left down); light XPL, 407-28R-3 56–58 cm. **(Q)** *Reticulofenestra* sp.; light XPL, 407-35R-1 86–88 cm. **(R)** *Tranolithus orionatus*; light XPL, 407-4R-1, 55–58 cm. **(S)** *Eiffellithus eximius*; light XPL, 407-4R-2, 55–58 cm. **(T)** *Arkhangelskiella* sp.; light XPL, 407-2R-2, 56–59 cm.

Appendix A: Planktonic foraminifera raw counts and relative abundance at DSDP Site 407

Table A1. Planktonic foraminifera assemblage species raw counts from Site 407. The raw counts are made on the > 125 µm size fraction. Species identified outside the counting area are made on the > 63 µm size fraction and are indicated with "R" (rare).

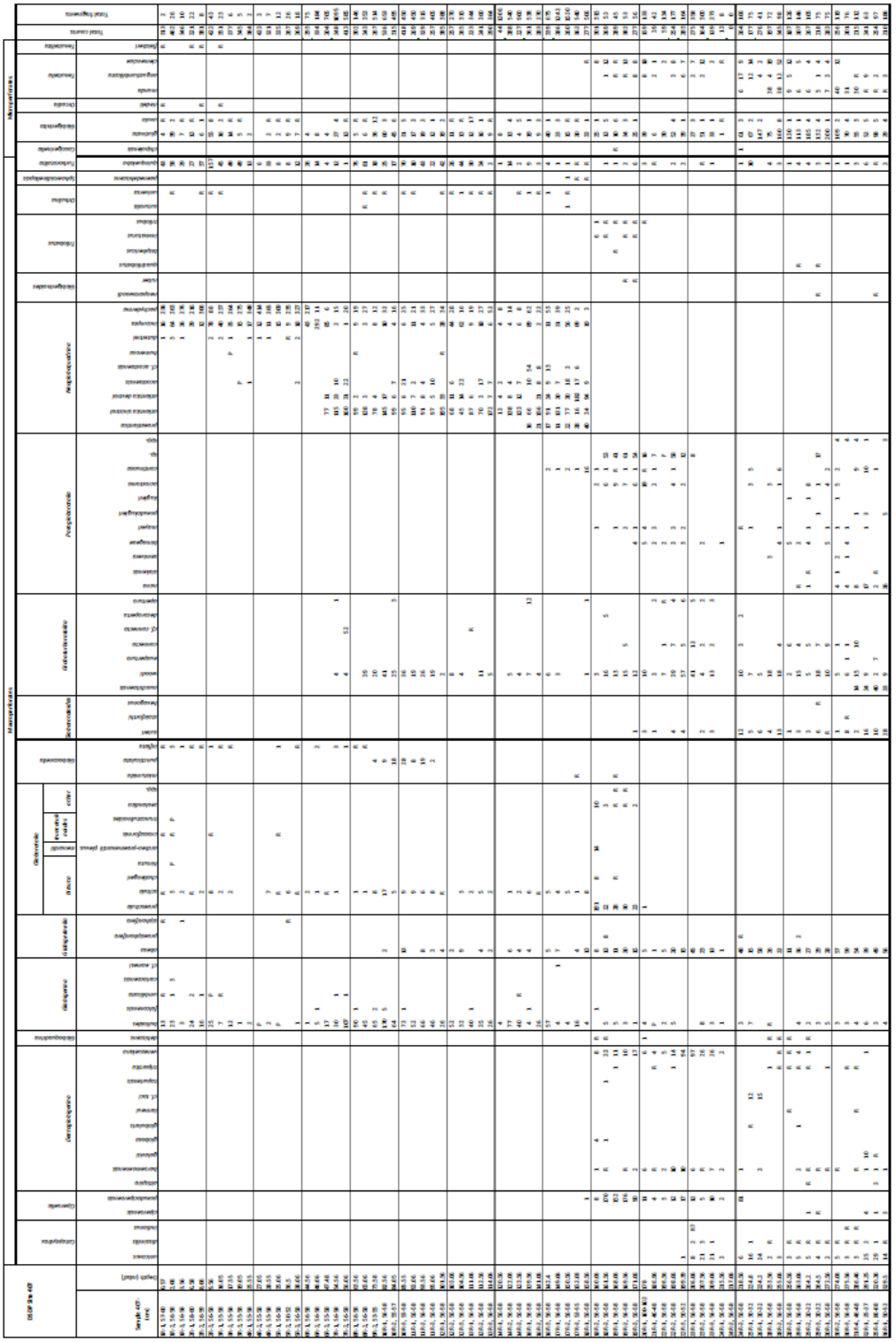

Table A2. Planktonic foraminifera assemblage species relative abundance (%) from Site 407. The raw counts are made on the > 125 µm size fraction. Species identified outside the counting area are made on the > 63 µm size fraction and are indicated with R (rare).

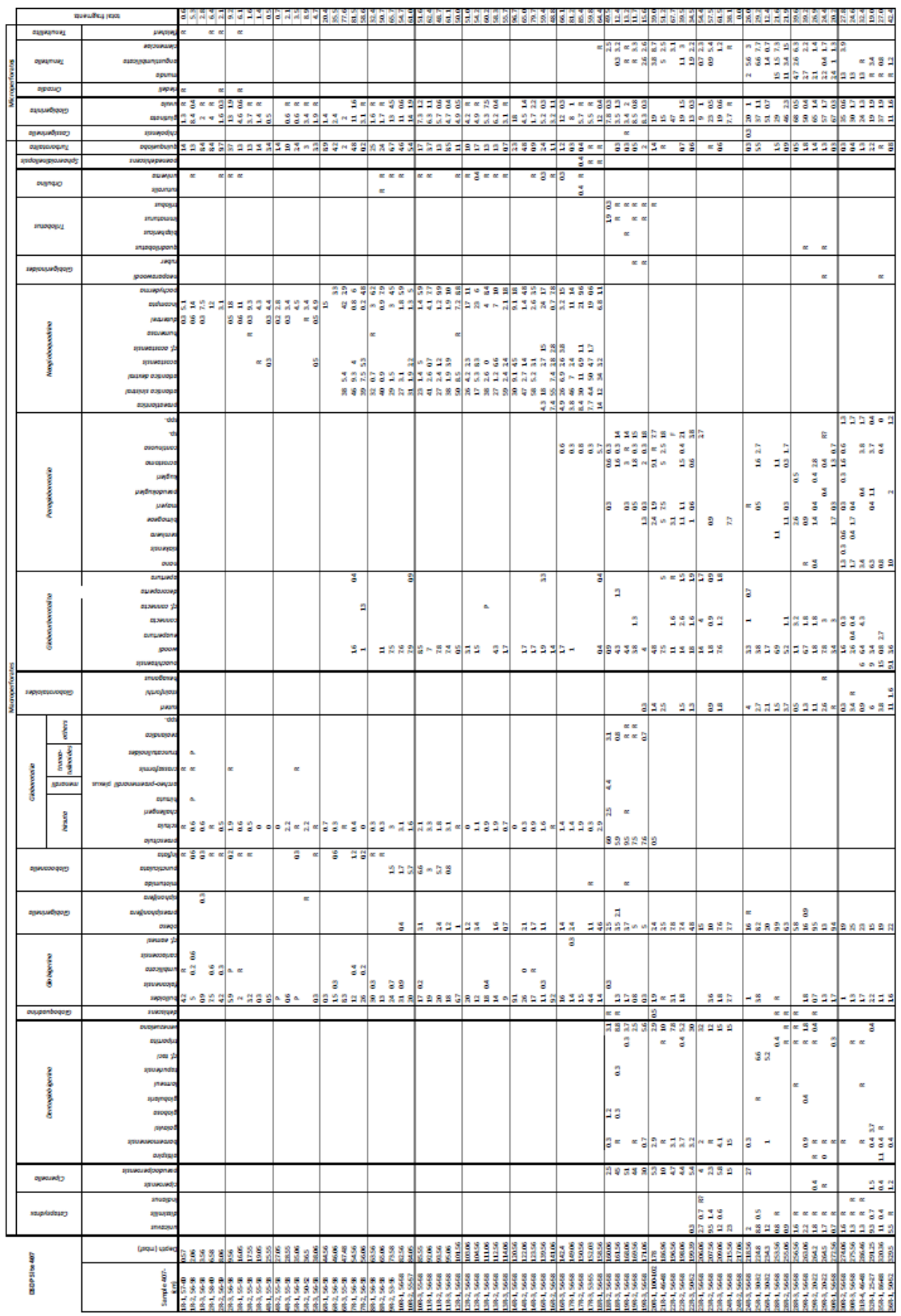

Appendix B: Calcareous nannofossil occurrence at Site DSDP 407

Table B1. Quantitative assessment of calcareous nannofossil occurrences and other constituents (biosilica) at Site 407. D is for dominant, P is for present, RW is for reworked, and R is for rare.

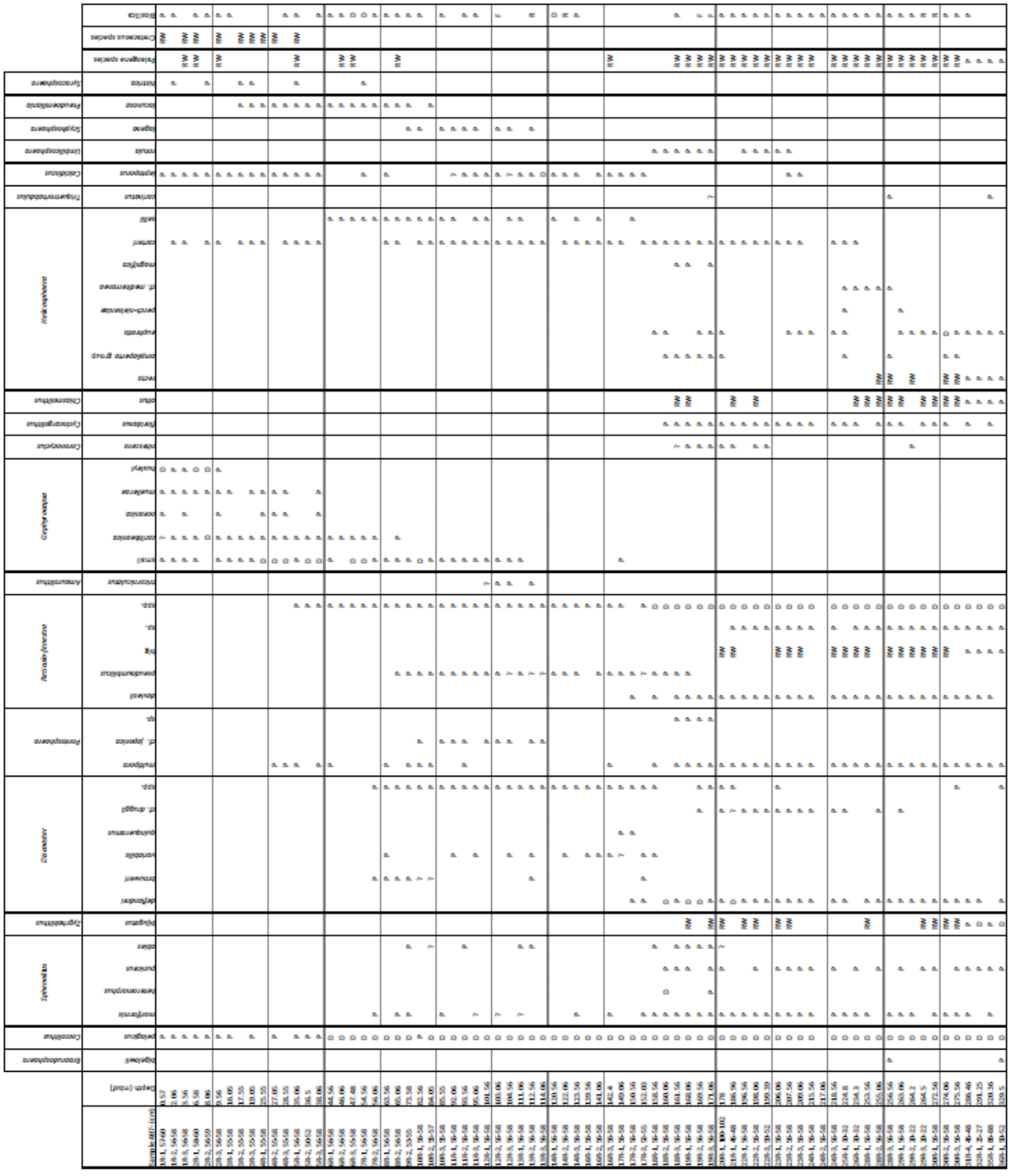

Appendix C: Chronologic ages of planktonic foraminifera and calcareous nannofossil events at DSDP Site 407

Table C1. Chronologic ages of planktonic foraminifera events in Site 407, based on calibrated ages from Raffi et al. (2020) (R20), Wade et al. (2011) (W11), and Weaver and Clement (1986) (WC86). The zonation is based on Raffi et al. (2020) and Wade et al. (2011). Primary zonal markers are indicated in bold. All species used in the age–depth model (Fig. 3) are indicated with a number. X indicates dominating coil change.

		Core, section, interval (cm)		Age (Ma)	Zone	Depth (m b.s.f.)				Ref.
Marker species	No. in Fig. 3	Top	Bottom			Top	Bottom	Mid-point	±	
Planktonic foraminifera										
LO *N. acostaensis*	3	3R-2, 55–58	3R-3, 55–58	1.58	PT1a	17.55	19.05	18.3	0.75	R20
FO "modern" *N. pachyderma*	**4**	6R-1, 56–58	6R-2, 56–58	1.77		44.56	46.06	45.31	0.75	WC86: DSDP Site 611
LO *N. atlantica*		6R-2, 56–58	6R-3, 55–58	2.26–2.3		46.06	47.48	46.77	0.71	WC86: DSDP Site 611
LO *G. woodi*	7	6R-3, 55–58	7R-1, 56–58	2.3	PL6	47.48	54.56	51.02	3.54	R20; W11
FO *G. inflata*	**6**	8R-2, 56–58	9R-2, 53–55	3.24	PL3	65.06	73.58	69.32	4.26	R20
FO *G. puncticulata*	11	11R-3, 56–58	12R-1, 56–58	4.12–4.18		158.56	160.06	98.31	3.25	WC86: DSDP Site 611
LO G. *dehiscens*	12	18R-1, 56–58	18R-2, 56–58	5.91	PL1	158.56	160.06	159.31	0.75	R20
X (dex–sin) *N. atlantica*	***13***	17R-2, 56–58	17R-3, 53–55	6.97	M13	150.56	152	151.295	0.71	R20
FO *N. pachyderma*	16	18R-1, 56–58	18R-2, 56–58	9.37	M13	158.56	160.06	159.31	0.75	R20
FO *N. acostaensis*	17	18R-1, 56–58	18R-2, 56–58	9.89	M13	158.56	160.06	159.31	0.75	R20
LO *P. mayeri*	18	18R-1, 56–58	18R-2, 56–58	10.57	M11	158.56	160.06	159.31	0.75	R20
LO *T. clemenciae*	20	17R-3, 53–55	18R-1, 56–58	12.37	M9	152	158.56	155.295	0.75	R20
LO *G. praescitula*	24	18R-1, 56–58	18R-2, 56–58	13.78	M7	158.56	160.06	159.31	0.75	R20
LO *G. archeomenardii*	25	17R-3, 53–55	18R-1, 56–58	13.86	M7	152	158.56	155.295	0.75	R20
FO *G. archeomenardii*	25	17R-3, 53–55	18R-1, 56–58	13.86	M7	152	158.56	155.295	0.75	R20
FO *G. zealandica*	28	19R-3, 56–58	20R-1, 100, 102	17.18	M4a	171.06	178	174.53	3.47	R20
LO *C. dissimilis*	29	22R-3, 50–52	23R-1, 56–58	17.54	M4a	199.39	206.06	202.725	3.34	R20
FO *G. praescitula*	31	20R-1, 100–102	21R-1, 46–48	18.22	M3	178	186.96	182.48	4.48	R20
LO *T. munda*	33	24R-2, 56–58	24R-3, 56–58	20.83	M2	217.06	218.56	217.81	0.75	R20
LO *P. kugleri*	**34**	28R-2, 56–58	28R-3, 56–58	**21.12**	**M2**	255.06	256.56	255.81	0.75	R20
FO *G. dehiscens*	**35**	29R-2, 20–22	29R-3, 20–22	**22.5**	**M1b**	264.2	264.5	264.35	0.15	R20
LO *C. ciperoensis*	36	29R-1, 56–58	29R-2, 20–22	22.9	M1a	263.06	264.2	263.36	0.57	R20
FO *P. kugleri*	**37**	30R-2, 56–58	30R-3, 56–58	**22.96**	**M1a**	274.06	275.56	274.81	0.75	R20
FO *P. pseudokugleri*	**38**	36R-1, 50–52	36R-1, 50–52	**25.9**	**O7**	329.5	329.5	329.5	0	R20

Table C2. Chronologic ages of calcareous nannofossil events in Site 407, based on calibrated ages from Raffi et al. (2020) (R20), Wade et al. (2011) (W11), and Weaver and Clement (1986 (WC86). The zonation is based on Raffi et al. (2020) and Wade et al. (2011). Primary zonal markers are indicated in bold. All species used in the age–depth model (Fig. 3) are indicated with a number.

		Core, section, interval (cm)		Age (Ma)	Zone	Depth (m b.s.f.)				Ref.
Marker species	No. in Fig. 3	Top	Bottom			Top	Bottom	Mid-point	±	
Calcareous nannofossils										
FO *G. huxleyi*	**1**	2R-3, 56–58	3R-1, 55–58	**0.29**	**NN20/21**	9.56	16.05	12.805	3.25	R20
LO *P. lacunosa*	2	3R-1, 55–58	3R-2, 55–58	0.43	NN19/20	16.05	17.55	16.8	0.75	R20
LO *H. sellii*		5R-3, 56–58	6R-1, 56–58	1.24	NN19	38.06	44.56	41.31	3.25	R20
LO *D. brouweri*	5	7R-1, 56–58	7R-2, 56–58	1.93	NN18	54.56	56.06	55.31	0.75	R20
LO *Sphenolithus* spp.	8	7R-1, 56–58	7R-2, 56–58	3.61	NN16	54.56	56.06	55.31	0.75	R20
LO *R. pseudoumbilicus*	9	8R-1, 56–58	8R-2, 56–58	3.82	NN15	63.56	65.06	64.31	0.75	R20
LO *A. tricorniculatus*	10	11R-3, 56–58	12R-1, 56–58	3.93	NN15 + 14	95.06	101.56	98.31	3.25	R20
LO *D. quinqueramus*	**11**	16R-3, 56–58	17R-1, 56–58	**5.53**	**NN11**	**142.4**	**149.06**	145.73	3.33	R20
FO *D. quinqueramus*	**15**	17R-2, 56–58	17R-3, 53–55	**8.1**	**NN11**	**150.56**	**152.03**	151.295	0.74	R20
FO *D. brouweri*	19	17R-3, 53–55	18R-1, 56–58	10.78	NN8	152.02	158.56	155.295	3.26	R20
LO *C. nitescens*	21	18R-3, 56–58	19R-1, 56–58	12.45	NN6	161.56	168.06	164.81	3.25	R20
LO *C. floridanus*	22	18R-1, 56–58	18R-2, 56–58	13.33	NN6	158.56	160.06	159.31	0.75	R20
LO *S. heteromorphus*	23	18R-1, 56–58	18R-2, 56–58	13.6	NN5	158.56	160.06	159.31	0.75	R20
LO *H. ampliaperta*		18R-1, 56–58	18R-2, 56–58	14.86	NN4/ NN5	158.56	160.06	159.31	0.75	R20
FO *S. heteromorphus*	30	19R-3, 56–58	20R-1, 100–102	17.65	NN4	171.06	178	174.53	3.47	R20
LO *T. carinatus*		28R-2, 56–58	28R-3, 56–58	19.18	NN2	255.06	256.56	255.81	0.75	R20
FO *H. ampliaperta*	32	30R-3, 56–58	31R-4, 46–48	20.43	NN2	275.56	286.46	281.01	5.45	R20

Data availability. The data that support the findings of this study are openly available in the Bolin Centre Database at https://doi.org/10.17043/weitkamp-2024-foraminifera-nannofossils-1 (Weitkamp, 2024).

Author contributions. TMW and HKC conceptualized and designed the experiments. TMW conducted the planktonic foraminifera analysis, and MJR performed the calcareous nannofossil analysis. TMW wrote the original draft, with all authors contributing to the review and editing. PNP provided focused contributions on the taxonomic analysis.

Competing interests. The contact author has declared that none of the authors has any competing interests.

Disclaimer. Publisher's note: Copernicus Publications remains neutral with regard to jurisdictional claims made in the text, published maps, institutional affiliations, or any other geographical representation in this paper. While Copernicus Publications makes every effort to include appropriate place names, the final responsibility lies with the authors.

Acknowledgements. This research has been supported by Swedish Research (VR) (grant no. 31001728) awarded to Helen K. Coxall. This contribution was greatly improved by the thoughtful comments and suggestions provided by Brian Huber, Tracy Aze, and Alessio Fabbrini.

Financial support. This research has been supported by the Vetenskapsrådet (grant no. 31001728).

The publication of this article was funded by the
Swedish Research Council, Forte, Formas, and Vinnova.

Review statement. This paper was edited by Sev Kender and reviewed by Brian Huber, Tracy Aze, and Alessio Fabbrini.

References

Aksu, A. E. and Kaminski, M. A: Neogene planktonic foraminiferal biostratigraphy and biochronology in Baffin Bay and the Labrador Sea, College Station, TX, Ocean, in: Proceedings of the Ocean Drilling Program, edited by: Srivastava, S. P., Arthur, M. A., Clement, B., et al., Sci. Res., 105, 287–304, 1989.

Anthonissen, E. D.: A new Pliocene biostratigraphy for the northeastern North Atlantic, Newsl. Stratigr., 43, 91–126, https://doi.org/10.1127/0078-0421/2009/0043-009, 2009.

Anthonissen, E. D.: A new Miocene biostratigraphy for the northeastern North Atlantic: An integrated foraminiferal, bolboformid, dinoflagellate and diatom zonation, Newsl. Stratigr., 45, 281–307, https://doi.org/10.1127/0078-0421/2012/0025, 2012.

Aze, T., Ezard, T. H. G., Purvis, A., Coxall, H. K., Stewart, D. R. M., Wade, B. S., and Pearson, P. N.: A phylogeny of Cenozoic macroperforate planktonic foraminifera from fossil data, Biol. Rev., 86, 900–927, https://doi.org/10.1111/j.1469-185X.2011.00178.x, 2011.

Bandy, O. L.: Neogene planktonic foraminiferal zones, California, and some geologic implications, Palaeogeogr., Palaeocl., 12, 131–150, https://doi.org/10.1016/0031-0182(72)90010-7, 1972.

Banner, F. T. and Blow, W. H.: Some primary types of species belonging to the Superfamily Globigerinacea, Contributions from the Cushman Laboratory for Foraminiferal Research, 11, 1–41, 1960.

Bé, A. W.: An ecological, zoogeographic and taxonomic review of recent planktonic foraminifera, Oceanic Micropaleontology, edited by: Ramsey, A. T. S., Academic Press, London, 1–100, 1977.

Berggren, W. A.: Rates of evolution in some Cenozoic planktonic foraminifera, Micropaleontology, 15, 351–365, 1969.

Berggren, W. A.: Cenozoic biostratigraphy and paleobiogeography of the North Atlantic, Initial Rep. Deep Sea, 12, 965–1001, 1972.

Berggren, W. A.: Recent advances in Cenozoic planktonic foraminiferal biostratigraphy, biochronology, and biogeography: Atlantic Ocean, Micropaleontology, 24, 337–370, https://doi.org/10.2307/1485368, 1978.

Berggren, W. A.: Neogene Planktonic foraminifera magnetobiostratigraphy of the Southern Kerguelen Plateau (Sites 747, 748 and 751), in: Proc. ODP, Sci. Results., edited by: Wise, S. W., Schlich, R., et al., College Station, TX, 631–647, 1992.

Berggren, W. A. and Schnitker, D.: Cenozoic Marine Environments in the North Atlantic and Norwegian-Greenland Sea, in: Structure and Development of the Greenland-Scotland Ridge: New Methods and Concepts, edited by: Bott, M. H. P., Saxov, S., Talwani, M., and Thiede, J., Springer US, 495–548, https://doi.org/10.1007/978-1-4613-3485-9_26, 1983.

Berggren, W. A., Kent, D. V., Swisher III, C. C., and Aubry, M.-P.: A revised Cenozoic geochronology and chronostratigraphy, in: Geochronology, Time Scales and Global Stratigraphic Correlation, edited by: Berggren, W. A., Kent, D. V., Aubry, M.-P., and Hardenbol, J., SEPM Special Publication, 54, 129–212, 1995.

Blow, W. H.: Age, correlation and biostratigraphy of the upper Tocuyo (San Lorenzo) and Pozon Formations, eastern Falcon, Venezuela, Bull. Am. Paleontol., 39, 67–251, 1959.

Blow, W. H.: Late middle Eocene to Recent planktonic foraminiferal biostratigraphy, 1st International Conference on PlanktonicMicrofossils Geneva, 1967, 199–421, 1969.

Boesiger, T. M., De Kaenel, E., Bergen, J. A., Browning, E., and Blair, S. A.: Oligocene to Pleistocene taxonomy and stratigraphy of the genus Helicosphaera and other placolith taxa in the circum North Atlantic Basin, J. Nannoplankt. Res., 37, 145–175, 2017.

Bolli, H. M.: Planktonic foraminifera from the Oligocene- Miocene Cipero and Lengua formations of Trinidad, B. W. I., in: Studies in Foraminifera, edited by: Loeblich Jr., A. R.,, Tappan, H., Beckmann, J. P., Bolli, H. M., Gallitelli, E. M., and Troelsen, J. C., United States National Museum Bulletin 215, Washington DC: U.S. Government Printing Office, 97–124, 1957.

Bolli, H. M., Loeblich, A. R., and Tappan, H.: Planktonic foraminiferal families Hantkeninidae, Orbulinidae, Globorotaliidae and Globotruncanidae, United States National Museum Bulletin, 215, 3–50, 1957.

Bolli, H. M. and Bermúdez, P.: Zonation based on planktonic foraminifera of middle Miocene to Pliocene warm-water sediments, Boletin Informativo Associacion Venezolana de Geologia, Mineria y Petroleo, 8, 119–149, 1965.

Bolli, J. B. and Saunders, H.: Oligocene to Holocene low latitude planktonic foraminifera, Plankton stratigraphy, Cambridge University Press, 1985.

Bolli, H. M., Saunders, J. B., and Perch-Nielsen, K.: Plankton Stratigraphy: Volume 1, Planktic Foraminifera, Calcareous Nannofossils and Calpionellids, CUP Archive, 1989.

Boscolo-Galazzo, F., Jones, A., Dunkley Jones, T., Crichton, K. A., Wade, B. S., and Pearson, P. N.: Late Neogene evolution of modern deep-dwelling plankton, Biogeosciences, 19, 743–762, https://doi.org/10.5194/bg-19-743-2022, 2022.

Bott, M. H. P.: Deep Structure and Geodynamics of the Greenland-Scotland Ridge: An Introductory Review, in: Structure and Development of the Greenland-Scotland Ridge, edited by: Bott, M. H. P., Saxov, S., Talwani, M., and Thiede, J., Springer US, 3–9, https://doi.org/10.1007/978-1-4613-3485-9_1, 1983.

Bown, P. R. and Young, J. R.: Techniques, in: Calcareous Nannofossil Biostratigraphy (British Micropalaeontological Society Publications Series), edited by: Bown, P. R., Chapman and Kluwer Academic, London, 16–28, 1998.

Brummer, G.-J. A. and Kučera, M.: Taxonomic review of living planktonic foraminifera, J. Micropalaeontol., 41, 29–74, https://doi.org/10.5194/jm-41-29-2022, 2022.

Chaabane, S., De Garidel-Thoron, T., Giraud, X., Schiebel, R., Beaugrand, G., Brummer, G.-J., Casajus, N., Greco, M., Grigoratou, M., Howa, H., Jonkers, L., Kucera, M., Kuroyanagi, A., Meilland, J., Monteiro, F., Mortyn, G., Almogi-Labin, A., Asahi, H., Avnaim-Katav, S., Bassinot, F., Davis, C. V., Field, D. B., Hernández-Almeida, I., Herut, B., Hosie, G., Howard, W., Jentzen, A., Johns, D. G., Keigwin, L., Kitchener, J., Kohfeld, K. E., Lessa, D. V. O., Manno, C., Marchant, M., Ofstad, S., Ortiz, J. D., Post, A., Rigual-Hernandez, A., Rillo, M. C., Robinson, K., Sagawa, T., Sierro, F., Takahashi, K. T., Torfstein, A., Venancio, I., Yamasaki, M., and Ziveri, P.: The FORCIS database: A global census of planktonic Foraminifera from ocean waters, Sci. Data, 10, 354, https://doi.org/10.1038/s41597-023-02264-2, 2023.

Cifelli, R.: Radiation of Cenozoic Planktonic Foraminifera, Syst. Zool., 18, 154, https://doi.org/10.2307/2412601, 1969.

Crundwell, M. P. and Nelson, C. S.: A magnetostratigraphically-constrained chronology for late Miocene bolboformids and planktic foraminifers in the temperate Southwest Pacific, Stratigraphy, 4, 1–34, https://doi.org/10.29041/strat.04.1.01, 2007.

Cushman, J. A. and Bermudez, P. J.: Further new species of foraminifera from the Eocene of Cuba, Contributions from the Cushman Laboratory for Foraminiferal Research, 13, 1–29, 1937.

Daniault, N., Mercier, H., Lherminier, P., Sarafanov, A., Falina, A., Zunino, P., Pérez, F. F., Ríos, A. F., Ferron, B., Huck, T., Thierry, V., and Gladyshev, S.: The northern North Atlantic Ocean mean circulation in the early 21st century, Prog. Oceanogr., 146, 142–158, https://doi.org/10.1016/j.pocean.2016.06.007, 2016.

Darling, K. F., Kucera, M., Kroon, D., and Wade, C. M.: A resolution for the coiling direction paradox in Neogloboquadrina pachyderma: coiling direction in N. pachyderma, Paleoceanography, 21, 1–14, https://doi.org/10.1029/2005PA001189, 2006.

Darling, K. F., Kucera, M., Pudsey, C. J., and Wade, C. M.: Molecular evidence links cryptic diversification in polar planktonic protists to Quaternary climate dynamics, P. Natl. Acad. Sci., 101, 7657–7662, https://doi.org/10.1073/pnas.0402401101, 2004.

De Vleeschouwer, D., Vahlenkamp, M., Crucifix, M., and Pälike, H.: Alternating Southern and Northern Hemisphere climate response to astronomical forcing during the past 35 m.y., Geology, 45, 375–378, 2017.

Dirzo, R. and Mendoza, E.: Biodiversity, in: Encyclopedia of Ecology, edited by: Jørgensen, S. E. and Fath, B. D., Academic Press, 368–377, https://doi.org/10.1016/B978-008045405-4.00460-2D, 2008.

Dowsett, H. J., Gosnell, L. B., and Poore, R. Z.: Pliocene planktic foraminifer census data from Deep Sea Drilling Project, U.S. Geological Survey, Open-File Report 88-654, 1–14, 1988.

Dowsett, H. J. and Poore, R. Z.: A new planktic foraminifer transfer function for estimating pliocene – Holocene paleoceanographic conditions in the North Atlantic, Mar. Micropaleontol., 16, 1–23, https://doi.org/10.1016/0377-8398(90)90026-I, 1990.

Dowsett, H. J. and Poore, R. Z.: Data report: Pliocene planktonic foraminifers from the California margin: Site 1021, Proceedings of the Ocean Drilling Program: Scientific Results, 167, 115–117, 2000.

El Bani Altuna, N., Pieńkowski, A. J., Eynaud, F., and Thiessen, R.: The morphotypes of Neogloboquadrina pachyderma: Isotopic signature and distribution patterns in the Canadian Arctic Archipelago and adjacent regions, Mar. Micropaleontol., 142, 13–24, https://doi.org/10.1016/j.marmicro.2018.05.004, 2018.

Eynaud, F.: Planktonic foraminifera in the Arctic: Potentials and issues regarding modern and quaternary populations, IOP Conference Series: Earth and Environmental Science, IOP, 27 June–12 July 2010, Rimouski, Quebec, Montreal, Canada, 14, 012005, https://doi.org/10.1088/1755-1315/14/1/012005, 2011.

Eynaud, F., Cronin, T. M., Smith, S. A., Zaragosi, S., Mavel, J., Mary, Y., Mas, V,. and Pujol, C.: Morphological variability of the planktonic foraminifer Neogloboquadrina pachyderma from ACEX cores: Implications for Late Pleistocene circulation in the Arctic Ocean, Micropaleontology, 55, 101–116, https://doi.org/10.47894/MPAL.55.2.02, 2009.

Ericson, D. B.: Coiling Direction of Globigerina pachyderma as a Climatic Index, Science, 130, 219–220, https://doi.org/10.1126/science.130.3369.219, 1959.

Ezard, T. H. G., Aze, T., Pearson, P. N., and Purvis, A.: Interplay Between Changing Climate and Species' Ecology Drives Macroevolutionary Dynamics, Science, 332, 349–351, https://doi.org/10.1126/science.1203060, 2011.

Fabbrini, A., Baldassini, N., Caricchi, Ch., Di Stefano, A., Dinarès-Turell, J., Foresi, L. M., Lirer, F., Patricolo, S., Sagnotti, L., and Winkler, A.: Integrated Quantitative Calcareous Plankton Bio-Magnetostratigraphy of the Early Miocene from IODP Leg 342, Hole U1406A, Newfoundland Ridge, NW Atlantic Ocean, Stratigr. Geol. Correl., 27, 259–276, 2019.

Fabbrini, A., Greco, M., Iacoviello, F., Kucera, M., Ezard, T. H. G., and Wade, B. S.: Bridging the extant and fossil record of planktonic foraminifera: implications for the Globigerina lineage, Palaeontology, 66, e12676, https://doi.org/10.1111/pala.12676, 2023.

Fenton, I. S., Aze, T., Farnsworth, A., Valdes, P., and Saupe, E. E.: Origination of the modern-style diversity gradient 15 million

years ago, Nature, 614, 7949, https://doi.org/10.1038/s41586-023-05712-6, 2023.

Fenton, I. S., Woodhouse, A., Aze, T., Lazarus, D., Renaudie, J., Dunhill, A. M., Young, J. R., and Saupe, E. E.: Triton, a new species-level database of Cenozoic planktonic foraminiferal occurrences, Sci. Data, 8, 160, https://doi.org/10.1038/s41597-021-00942-7, 2021.

Flower, B. P.: Data report: Planktonic foraminifers from the subpolar North Atlantic and Nordic Seas, sites 980–987 and 907, Proceedings of the Ocean Drilling Program, Scientific Results, 162, 19–34, 1999.

Fraass, A. J., Kelly, D. C., and Peters, S. E.: Macroevolutionary History of the Planktic Foraminifera, Annu. Rev. Earth Pl. Sc., 43, 139–166, https://doi.org/10.1146/annurev-earth-060614-105059, 2015.

Foresi, L. M., Iaccarino, S. M., and Salvatorini, G.: Neogloboquadrina atlantica praeatlantica, new subspecies from late Middle Miocene, Riv. Ital. Paleontol. S., 108, 325–336, 2000.

Hammer, Ø., Harper, D. A. T., and Ryan, P. D.: Past: Paleontological Statistics Software Package for Education and Data Analysis, Palaeontol. Electron., 4, 1–9, http://palaeo-electronica.org/2001_1/past/issue1_01.htm, 2001.

Hansen, B. and Østerhus, S.: North Atlantic–Nordic seas exchanges, Prog. Oceanogr., 45, 109–208, 2000.

Hátún, H., Lohmann, K., Matei, D., Jungclaus, J. H., Pacariz, S., Bersch, M., Gislason, A., Ólafsson, J., and Reid, P. C.: An inflated subpolar gyre blows life toward the northeastern Atlantic, Prog. Oceanogr., 147, 49–66, 2016.

Hemleben, C., Spindler, M., and Anderson, O. R.: Modern planktonic Foraminifera. Springer, Berlin, 1989.

Hilgen, F. J., Iaccarino, S., Krijgsman, W., Villa, G., Langereis, C. G., and Zachariasse, W. J.: The global boundary stratotype section and point (GSSP) of the Messinian Stage (uppermost Miocene), Episodes, 23, 172–178, 2000.

Huber, B. T., Bijma, J., and Darling, K.: Cryptic speciation in the living planktonic foraminifer Globigerinella siphonifera (d'Orbigny), Paleobiology, 23, 33–62, https://doi.org/10.1017/S0094837300016638, 1997.

Huddlestun, P. F.: Planktonic foraminiferal biostratigraphy, Deep-Sea Drill. Project. Leg. 81, In DSDP, 81, 429–438, 1984.

Hutchinson, D. K., Coxall, H. K., O'Regan, M., Nilsson, J., Caballero, R., and De Boer, A. M.: Arctic closure as a trigger for Atlantic overturning at the Eocene-Oligocene Transition, Nat. Commun., 10, 3797, https://doi.org/10.1038/s41467-019-11828-z, 2019.

Iaccarino, S., Foresi, L., Mazzei, R., and Salvatorini, G.: Calcareous plankton biostratigraphy of the Miocene sediments of the Tremiti Islands (Southern Italy), Rev. Esp. Micropal., 33, 237–248, 2001.

Iwatani, H., Irizuki, T., and Hayashi, H.: Global cooling in marine climates and local tectonic events in Southwest Japan at the Plio–Pleistocene boundary, Palaeogeogr. Palaeocl., 350, 1–18, 2012.

Jenkins, G. D.: Planktonic foraminiferal zones and new taxa from the Lower Miocene to the pleistocene of New Zealand, New Zeal. J. Geol. Geop., 10, 1064–1078, https://doi.org/10.1080/00288306.1967.10423209, 1967.

Jenkins, D. G.: Southern mid-latitude Paleocene to Holocene planktic foraminifera, in: Plankton Stratigraphy, edited by: Bolli, H. M., Saunders, J. B., and Perch-Nielsen, K., 263–282, Cambridge University Press, New York, 1985.

Kaminski, M. A. and Berggren, W. A.: A Neotype for Neogloboquadrina atlantica (Berggren 1972), Micropaleontology, 67, 106–107, https://doi.org/10.47894/mpal.67.1.08, 2021.

Kaneps, A.: 13. Cenozoic Planktonic Foraminifera from Antarctic Deep-Sea Sediments, Leg 28, DSDP, in: Init. Repts, DSDP, 28, edited by: Hayes, D. E., Frakes, L. A., Barrett, P. J., Burns, D. A., et al., 573–583 https://doi.org/10.2973/dsdp.proc.28.113.1975, 1975.

Keller, G.: Morphologic variation of Neogloboquadrina pachyderma (Ehrenberg) in sediment of the marginal and central Northeast Pacific and paleoclimatic interpretation, J. Foramin. Res., 8, 208–224, 1978.

Kennett, J. P.: The Globorotalia crassaformis bioseries in north Westland and Marlborough, New Zealand, Micropaleontology, 12, 235–245, 1966.

Kennett, J. P.: Latitudinal variation in Globigerina pachyderma (Ehrenberg) in surface sediments of the southwest Pacific Ocean, Micropaleontology, 14, 305–318, 1968.

Kennett, J. P., Rozo-Vera, G. A., and Machain Castillo, M. L.: Latest Neogene planktonic foraminiferal biostratigraphy of the California margin, Proceedings of the Ocean Drilling Program, 167, 41–62, 2000.

Kennett, J. P. and Srinivasan, M. S.: Surface ultrastructural variation in Neogloboquadrina pachyderma (Ehrenberg): Phenotypic variation and phylogeny in the Late Cenozoic, Cushman Foundation Special Publication, 19, 134–162, 1980.

Kennett, J. P. and Srinivasan, M. S.: Neogene planktonic foraminifera, Hutchinon Ross Publishing Co., Stroudsburg, Pennsylvania, 1–265, 1983.

Kim, J.-M.: Early Neogene biochemostratigraphy of Pohang Basin: A paleoceanographic response to the early opening of the Sea of Japan (East Sea), Mar. Micropaleontol., 36, 269–290, 1999.

King, D. J., Wade, B. S., Liska, R. D., and Miller, C. G.: A review of the importance of the Caribbean region in Oligo-Miocene low latitude planktonic foraminiferal biostratigraphy and the implications for modern biogeochronological schemes, Earth-Sci. Rev., 202, 102968, https://doi.org/10.1016/j.earscirev.2019.102968, 2020.

Kipp, N. G.: New transfer function for estimating past sea-surface conditions from sea-bed distribution of planktonic foraminiferal assemblages in the North Atlantic, in: Investigations of Late Quaternary Paleoceanography and Paleoclimatology, edited by: Cline, R. M. and Hays, J. D., Mere. Geol. Soc. Am., 145, 3–42, 1976.

Krasheninnikov, V. A. and Basov, I. A.: 30. Cenozoic Planktonic Foraminifers of the Falkland Plateau and Argentine Basin, Deep Sea Drilling Project Leg 71, in: Init. Repts, DSDP, 71, edited by: Ludwig, W. J., Krasheninnikov, V. A., and Wise Jr., S. W., 821–858, https://doi.org/10.2973/dsdp.proc.71.130.1983, 1983.

Kucera, M.: Chapter six planktonic foraminifera as tracers of past oceanic environments, Dev. Mar. Geol., 1, 213–262, 2007.

Kucera, M. and Kennett, J. P.: Biochronology and evolutionary implications of Late Neogene California margin planktonic foraminiferal events, Mar. Micropaleontol., 40, 67–81, https://doi.org/10.1016/S0377-8398(00)00029-3, 2000.

Kucera, M. and Schonfeld, J.: The origin of modern oceanic foraminiferal faunas and Neogene climate change, in: Deep-Time Perspectives on Climate Change: Marrying the Signal from Computer Models and Biological Proxies, edited by:

Williams, M., Haywood, A. M., Gregory, F. J., and Schmidt, D. N., The Geological Society of London on behalf of The Micropalaeontological Society, Geological Society of London, 409–425, https://doi.org/10.1144/TMS002.18, 2007.

Kucera, M., Rosell-Melé, A., Schneider, R., Waelbroeck, C., and Weinelt, M.: Multiproxy approach for the reconstruction of the glacial ocean surface (MARGO), Quaternary Sci. Rev., 24, 813–819, https://doi.org/10.1016/j.quascirev.2004.07.017, 2005.

Labrecque, J. L., Kent, D. V., and Cande, S. C.: Revised magnetic polarity time scale for Late Cretaceous and Cenozoic time, Geology, 5, 330–335, 1977.

Lam, A. R. and Leckie, R. M.: Subtropical to temperate late Neogene to Quaternary planktic foraminiferal biostratigraphy across the Kuroshio Current Extension, Shatsky Rise, northwest Pacific Ocean, PLOS ONE, 15, e0234351, https://doi.org/10.1371/journal.pone.0234351, 2020a.

Lam, A. R. and Leckie, R. M.: Late Neogene and Quaternary diversity and taxonomy of subtropical to temperate planktic foraminifera across the Kuroshio Current Extension, northwest Pacific Ocean, Micropaleontology, 66, 177–268, https://doi.org/10.47894/mpal.66.3.01, 2020b.

Lamb, J. L. and Beard, J. H.: Late Neogene planktonic foraminifers in the Caribbean, Gulf of Mexico, and Italian stratotypes, Kansas Univ. Paleont. Contr., no. 57 (Protozoa, art. 8), 1–67, 1972.

Laughton, A. S. and the Exp. 12 Scientific Party: Initial Reports of the Deep Sea Drilling Project, 12, 1243, U.S. Government Printing Office, Washington, D.C., 1972.

Larsen, H. C., Saunders, A. D., Clift, P. D., and the Leg 152 Shipboard Scientific Party: Proc. ODP, Initial Reports, Vol. 152, Ocean Drilling Program, College Station, TX, 977, 1994a.

Le Breton, E., Cobbold, P. R., Dauteuil, O., and Lewis, G.: Variations in amount and direction of seafloor spreading along the northeast Atlantic Ocean and resulting deformation of the continental margin of northwest Europe, Tectonics, 31, 2011TC003087, https://doi.org/10.1029/2011TC003087, 2012.

Leckie, R. M.: Seeking a better life in the plankton, P. Natl. Acad. Sci. USA, 106, 14183–14184, https://doi.org/10.1073/pnas.0907091106, 2009.

Leckie, R. M., Wade, B. S., Pearson, P. N., Fraass, A. J., King, D. J., Olsson, R. K., Premoli Silva, I., Spezzaferri, S., and Berggren, W. A.: Taxonomy, biostratigraphy, and phylogeny of Oligocene and Early Miocene Paragloborotalia and Parasubbotina, Cushman Foundation for Foraminiferal Research, https://discovery.ucl.ac.uk/id/eprint/10049515/ (last access: 18 December 2024), 2018.

LeRoy, L. W.: Some small foraminifera ostracoda and otoliths from the Neogene (Miocene) of the Rokan-Tapanoeli area, central Sumatra, Natuurkunde Tijdschrift voor Nederlandsch-Indië, 99, 215–296, 1939.

LeRoy, L. W.: Miocene foraminifera from Sumatra and Java, Netherlands East Indies, part 1. Miocene foraminifera of central Sumatra, Netherlands East Indies, Colo. School Mines Q., 39, 1–69, 1944.

Lirer, F. and Iaccarino, S.: Integrated stratigraphy (cyclostratigraphy and biochronology) of late Middle Miocene deposits in the Mediterranean area and comparison with the North and Equatorial Atlantic Oceans: Synthesis of the major results, Terra Nova, 17, 338–349, https://doi.org/10.1111/j.1365-3121.2005.00619.x, 2005.

Lowery, C. M., Bown, P. R., Fraass, A. J., and Hull, P. M.: Ecological Response of Plankton to Environmental Change: Thresholds for Extinction. Annu. Rev. Earth Pl. Sc., 48, 403–429, https://doi.org/10.1146/annurev-earth-081619-052818, 2020.

Luyendyk, B. P. and Cann, J. R.: 37. General Implications Of The Leg 49 Drilling Program For North Atlantic Ocean Geology, http://deepseadrilling.org/49/volume/dsdp49_37.pdf (last access: 18 December 2024), 1979.

Martini, E.: Standard Tertiary and Quaternary Calcareous Nannoplankton Zonation, Proceedings of the II Planktonic Conference, Roma, 1970, Edizioni Tecnoscienza, 2, 739–785, 1971.

Maiya, S., Saito, T., and Sato, T.: Late Cenozoic planktonic foraminiferal biostratigraphy of northwest Pacific sedimentary sequences, in: Progress in Micropaleontology, edited by: Takayanagi, Y. and Saito, T., Micropaleontology Press, New York, 395–422, 1976.

Miller, K. G. and Tucholke, B. E.: Development of Cenozoic Abyssal Circulation South of the Greenland-Scotland Ridge, in: Structure and Development of the Greenland-Scotland Ridge, edited by: Bott, M. H. P., Saxov, S., Talwani, M., and Thiede, J., Springer US, 549–589, https://doi.org/10.1007/978-1-4613-3485-9_27, 1983.

Morard, R., Darling, K. F., Mahé, F., Audic, S., Ujiié, Y., Weiner, A. K. M., André, A., Seears, H. A., Wade, C. M., Quillévéré, F., Douady, C. J., Escarguel, G., De Garidel-Thoron, T., Siccha, M., Kucera, M., and De Vargas, C.: PFR2: A curated database of planktonic foraminifera 18S ribosomal DNA as a resource for studies of plankton ecology, biogeography and evolution, Mol. Ecol. Resour., 15, 1472–1485, https://doi.org/10.1111/1755-0998.12410, 2015.

Morard, R., Hassenrück, C., Greco, M., Fernandez-Guerra, A., Rigaud, S., Douady, C. J., and Kucera, M.: Renewal Of Planktonic Foraminifera Diversity After The Cretaceous Paleogene Mass Extinction By Benthic Colonizers, Nat. Commun., 13, 7135, https://doi.org/10.1038/S41467-022-34794-5, 2022.

Murray, J. W.: Cenozoic biostratigraphy and paleoecology of Sites 403 to 406 based on the foraminifers, Montadert, L., Roberts, Dg, Initial Reports of the Deep Sea Drilling Project, 48, 415–430, 1979.

Nilsen, T. H.: Influence of the Greenland-Scotland Ridge on the Geological History of the North Atlantic and Norwegian-Greenland Sea Areas, in: Structure and Development of the Greenland-Scotland Ridge: New Methods and Concepts, edited by: Bott, M. H. P., Saxov, S., Talwani, M., and Thiede, J., Springer US, 457–478, https://doi.org/10.1007/978-1-4613-3485-9_24, 1983.

Nomura, R.: Geologic age of the lower Josoji Formation, Shimane Peninsula, Southwest Honshu, Japan: Implications for an abrupt change to deep-water during the earlier opening stage of the Japan Sea, Island Arc., 30, e12421, https://doi.org/10.1111/iar.12421, 2021.

Ogniben, L.: Stratigrafie e microfaune del Terzierio della zona di Caiazzo (Caserta), 6; descrizione paleontologiche, Riv. Ital. Paleontol. S., 65, 199–286, 1958.

Olsson, R. K., Berggren, W. A., Hemleben, C., And Huber, B. T.: Atlas of Paleocene Planktonic Foraminifera. Smithsonian Contributions to Paleobiology, nr. 85, Washington, DC, Smithsonian Institution Press, 1–259, 1999

Parker, F. L.: Living planktonic foraminifera from the Gulf of California, J. Foramin. Res., 3, 70–77, 1973.

Parnell-Turner, R., Briais, A., Levay, L., and the Expedition 395 Scientists: Expedition 395 Preliminary Report: Reykjanes Mantle Convection and Climate, International Ocean Discovery Program, College Station TX, https://doi.org/10.14379/iodp.pr.395.2024, 2024.

Pearson, P. N., Olsson, R. K., Huber, B. T., Hemleben, C., and Berggren, W. A.: Atlas of Eocene Planktonic Foraminifera, Cushman Foundation for Foraminiferal Research, 2006.

Pearson, P. N.: Wall textures and higher taxonomy of Oligocene micro- and medioperforate planktonic foraminifera, in: Atlas of Oligocene Planktonic Foraminifera, edited by: Wade, B. S., Olsson, R. K., Pearson, P. N., Huber, B. T., and Berggren, W. A., Cushman Foundation for Foraminiferal Research, 46, 415–428, 2018.

Perch-Nielsen, K.: Cenozoic calcareous nannofossils, Plankton Stratigraphy, 427–455, 1985.

Poore, R. Z.: Oligocene through Quaternary planktonic foraminiferal biostratigraphy of the North Atlantic: DSDP Leg 49, in: Init. Repts, DSDP, 49, edited by: Luyendyk, B. P., Cann, J. R., et al., 447–517, 1979.

Poore, R. Z. and Berggren, W. A.: Late Cenozoic planktonic foraminiferal biostratigraphy and paleoclimatology of the northeastern Atlantic, DSDP Site 116, J. Foraminiferal Res, 5, 270–293, 1975.

Poore, R. Z., Mcdougall, K., Barron, J. A., Brabb, E. E., and Kling, S. A.: Microfossil biostratigraphy and biochronology of the type Relizian and Luisian Stages of California, https://archives.datapages.com/data/pac_sepm/030/030001/pdfs/15.pdf (last access: 18 December 2024), 1981.

Premoli Silva, I. and Spezzaferri, S.: Paleogene planktonic foraminifer biostratigraphy and paleoenvironmental remarks on Paleogene sediments from Indian Ocean sites, Leg 115, in: Proceedings of the Ocean Drilling Program, Scientific Results: Ocean Drilling Program, edited by: Duncan, R. A., Backman, J., Peterson, L. C., et al., College Station, TX, Vol. 115, 277–314, 1990

Pujol, C. and Bourrouilh, R.: 11. Late Miocene to Holocene Planktonic Foraminifers from the Subantarctic South Atlantic, in: Proceedings of the Ocean Drilling Program, Scientific Results, Vol. 114, edited by: Ciesielki, P. F., Kristoffersen, Y., et al., 217-232, https://doi.org/10.2973/odp.proc.sr.114.129.1991, 1991.

Raffi, I., Wade, B. S., Pälike, H., Beu, A. G., Cooper, R., Crundwell, M. P., Krijgsman, W., Moore, T., Raine, I., Sardella, R., and Vernyhorova, Y. V.: Chapter 29 – The Neogene Period, in: Geologic Time Scale 2020, edited by: Gradstein, F. M., Ogg, J. G., Schmitz, M. D., and Ogg, G. M., Elsevier, 1141–1215, https://doi.org/10.1016/B978-0-12-824360-2.00029-2, 2020.

Rögl, F.: 33. Late Cretaceous to Pleistocene Foraminifera from the Southeast Pacific Basin, DSDP Leg 35, in: Init. Repts. DSDP, 35, edited by: Hollister, C. D. and Craddock, C., 539–555, https://doi.org/10.2973/dsdp.proc.35.133.1976, 1976.

Rögl, F.: Globigerina ciperoensis (Foraminiferida) in the Oligocene and Miocene of the Central Paratethys, Annalen Des Naturhistorischen Museums in Wien, Serie A Für Mineralogie Und Petrographie, Geologie Und Paläontologie, Anthropologie Und Prähistorie, 133–159, 1994.

Sahoo, N., Saalim, S. M., Matul, A., Mohan, R., Tikhonova, A., and Kozina, N.: Planktic Foraminiferal Assemblages in Surface Sediments From the Subpolar North Atlantic Ocean, Front. Mar. Sci., 8, 781675, https://doi.org/10.3389/fmars.2021.781675, 2022.

Schenk, B., Gebhardt, H., Wolfgring, E., and Zorn, I.: Cyclic paleo-salinity changes inferred from benthic foraminiferal assemblages in the Upper Burdigalian (Lower Miocene) Korneuburg Basin, Austria, Palaeogeogr. Palaeocl., 490, 473–487, https://doi.org/10.1016/j.palaeo.2017.11.027, 2018.

Schiebel, R., Spielhagen, R. F., Garnier, J., Hagemann, J., Howa, H., Jentzen, A., Martínez-Garcia, A., Meilland, J., Michel, E., Repschläger, J., Salter, I., Yamasaki, M., and Haug, G.: Modern planktic foraminifers in the high-latitude ocean, Mar. Micropaleontol., 136, 1–13, https://doi.org/10.1016/j.marmicro.2017.08.004, 2017.

Shannon, C. E. and Weaver, W.: The mathematical theory of communication, University of Illinois Press, Urbana, 117, 1–132, 1949.

Shipboard Scientific Part: Site 407, in: Initial Reports of the Deep Sea Drilling Project, edited by: Luyendyk, B. P., Cann, J. R., Roberts, W. P., Shor, A. N., et al., Vol. 49, 21–100, Texas A & M University, Ocean Drilling Program, College Station, https://doi.org/10.2973/dsdp.proc.49.1979, 1979.

Shor, A. N. and Poore, R. Z.: Bottom Currents and Ice Rafting in the North Atlantic: Interpretation of Neogene Depositional Environments of Leg 49 Cores: DSDP Leg 49, in: Init. Repts. DSDP, 49, edited by: Luyendyk, B. P., Cann, J. R., et al., 447–517, 1979.

Siccha, M. and Kucera, M.: ForCenS, a curated database of planktonic foraminifera census counts in marine surface sediment samples, Sci. Data, 4, 170109, https://doi.org/10.1038/sdata.2017.109, 2017.

Sierro, F. J., Hernandez-Almeida, I., Alonso-Garcia, M., and Flores, J. A.: Data report: Pliocene–Pleistocene planktonic foraminifer bioevents at IODP Site U13131, Proc. IODP, Vol. 303, 2008.

Spezzaferri, S.: Planktonic foraminiferal biostratigraphy and taxonomy of the Oligocene and lower Miocene in the oceanic record: An overview, Paleontogr. Ital., 81, 1994.

Spezzaferri, S.: Planktonic foraminifer biostratigraphy and paleoenvironmental implications of Leg 152 Sites (East Greenland Margin), Proceedings-Ocean Drilling Program Scientific Results, 161–190, 1998.

Spezzaferri, S. and Pearson, P. N.: Distribution and ecology of Catapsydrax indianus, a new planktonic foraminifer index species for the Late Oligocene–Early Miocene, J. Foramin. Res., 39, 112–119, https://doi.org/10.2113/gsjfr.39.2.112, 2009.

Spezzaferri, S., Kucera, M., Pearson, P. N., Wade, B. S., Rappo, S., Poole, C. R., Morard, R., and Stalder, C.: Fossil and Genetic Evidence for the Polyphyletic Nature of the Planktonic Foraminifera "Globigerinoides", and Description of the New Genus Trilobatus, PLOS ONE, 10, 1–20, https://doi.org/10.1371/journal.pone.0128108, 2015.

Spezzaferri, S., Coxall, H. K., Olsson, R. K., and Hemleben, C.: Taxonomy, biostratigraphy, and phylogeny of Oligocene Globigerina, Globigerinella, and Quiltyella n. gen., in: Atlas of Oligocene Planktonic Foraminifera, edited by: Wade, B. S., Olsson, R. K., Pearson, P. N., Huber, B. T., and Berggren, W. A. Cushman Foundation for Foraminiferal Research, Special Publication, 46, 179–214, 2018.

Spiegler, D.: Planktonic foraminifer Cenozoic biostratigraphy of the Arctic Ocean, Fram Strait (Sites 908–909), Yermak Plateau (Sites 910–912), and East Greenland Margin (Site 913),

Proceedings-Ocean Drilling Program Scientific Results, 153–168, http://www-odp.tamu.edu/PUBLICATIONS/srv/abstr151/151-8.htm (last access: 18 December 2024), 1996.

Spiegler, D. and Jansen, E.: Planktonic foraminifer biostratigraphy of Norwegian Sea sediments: ODP Leg 104, Proceedings of the Ocean Drilling Program: Scientific Results, 104, 681–696, https://oceanrep.geomar.de/id/eprint/46666, 1989.

Stärz, M., Jokat, W., Knorr, G., and Lohmann, G.: Threshold in North Atlantic-Arctic Ocean circulation controlled by the subsidence of the Greenland-Scotland Ridge, Nat. Commun., 8, 15681, https://doi.org/10.1038/ncomms15681, 2017.

Stehman, C. F.: Planktonic Foraminifera in Baffin Bay, Davis Strait and the Labrador Sea, Atl. Geol., 8, 13–19, https://doi.org/10.4138/1398, 1972.

Steinthorsdottir, M., Coxall, H. K., De Boer, A. M., Huber, M., Barbolini, N., Bradshaw, C. D., Burls, N. J., Feakins, S. J., Gasson, E., Henderiks, J., Holbourn, A., Kiel, S., Kohn, M. J., Knorr, G., Kürschner, W. M., Lear, C. H., Liebrand, D., Lunt, D. J., Mörs, T., Pearson, P. N., Pound, M. J., Stoll, H., and Strömberg, C. A. E.: The Miocene: the Future of the Past, Paleoceanogr. Paleocl., 36, e2020PA004037, https://doi.org/10.1029/2020PA004037, 2021.

St. John, K. E. K. and Krissek, L. A.: The late Miocene to Pleistocene ice-rafting history of southeast Greenland, Boreas, 31, 28–35, https://doi.org/10.1111/j.1502-3885.2002.tb01053.x, 2002.

Strack, T., Jonkers, L., Rillo, M. C., Hillebrand, H., and Kucera, M.: Plankton response to global warming is characterized by non-uniform shifts in assemblage composition since the last ice age, Nat. Ecol. Evol., 6, 1871–1880, https://doi.org/10.1038/s41559-022-01888-8, 2022.

Swift, J. H., Aagaard, K., and Malmberg, S.-A.: The contribution of the Denmark Strait overflow to the deep North Atlantic, Deep-Sea Res. Pt. A, 27, 29–42, 1980.

Rasmussen, S., Lykke-Andersen, H., Kuijpers, A., and Troelstra, S. R.: Post-Miocene sedimentation at the continental rise of Southeast Greenland: The interplay between turbidity and contour currents, Mar. Geol., 196, 37–52, https://doi.org/10.1016/S0025-3227(03)00043-4, 2003.

Talwani, M. and Udintsev, G.: Site 336 and 352, Init. Rep. Deep Sea Drill, Proj., 38, 23–116, 1976.

Talwani, M. and Eldholm, O.: Evolution of the Norwegian-Greenland Sea, Geol. Soc. Am. Bull., 88, 969, https://doi.org/10.1130/0016-7606(1977)88<969:EOTNS>2.0.CO;2, 1977

Tappan, H. and Loeblich, A. R.: Foraminiferal Evolution, Diversification, and Extinction, J. Paleontol., 62, 695–714, 1988.

Tolderlund, D. S. and Bé, A. W. H.: Seasonal Distribution of Planktonic Foraminifera in the Western North Atlantic, Micropaleontology, 17, 297–329, https://doi.org/10.2307/1485143, 1971.

Uenzelmann-Neben, G. and Gruetzner, J.: Chronology of Greenland Scotland Ridge overflow: What do we really know?, Mar. Geol., 406, 109–118, https://doi.org/10.1016/j.margeo.2018.09.008, 2018.

Valentine, J. W. and Jablonski, D.: A twofold role for global energy gradients in marine biodiversity trends, J. Biogeogr., 42, 997–1005, https://doi.org/10.1111/jbi.12515, 2015.

Vilks, G.: Comparison of Globorotalia pachyderma (Ehrenberg) in the water column and sediments of the Canadian Arctic, J. Foramin. Res., 5, 313–325, https://doi.org/10.2113/gsjfr.5.4.313, 1975.

Wade, B. S., Olsson, R. K., Pearson, P. N., Huber, B. T., and Berggren, W. A.: Atlas of Oligocene Planktonic Foraminifera, Cushman Foundation for Foraminiferal Research, 2018.

Wade, B. S., Pearson, P. N., Berggren, W. A., and Pälike, H.: Review and revision of Cenozoic tropical planktonic foraminiferal biostratigraphy and calibration to the geomagnetic polarity and astronomical time scale, Earth-Sci. Rev., 104, 111–142, https://doi.org/10.1016/j.earscirev.2010.09.003, 2011.

Weaver, P. P. E.: Late Miocene to Recent planktonic foraminifers from the North Atlantic: Deep Sea Drilling Project Leg 94, Initial Reports of the Deep Sea Drilling Project, https://cir.nii.ac.jp/crid/1361699995093110912 (last access: 18 December 2024), 1987.

Weaver, P. P. E. and Clement, B. M.: Synchroneity of Pliocene planktonic foraminiferal datums in the North Atlantic, Mar. Micropaleontol., 10, 295–307, https://doi.org/10.1016/0377-8398(86)90033-2, 1986.

Wei, K.-Y. and Kennett, J. P.: Taxonomic evolution of Neogene planktonic foraminifera and paleoceanographic relations, Paleoceanography, 1, 67–84, https://doi.org/10.1029/PA001i001p00067, 1986.

Weitkamp, T. M.: North Atlantic Oligocene-Pleistocene planktonic foraminifera and calcareous nannofossil abundances. Dataset version 1, Bolin Centre Database [data set], https://doi.org/10.17043/weitkamp-2024-foraminifera-nannofossils-1, 2024.

Wold, C. N.: Cenozoic sediment accumulation on drifts in the northern North Atlantic, Paleoceanography, 9, 917–941, https://doi.org/10.1029/94PA01438, 1994.

Woodhouse, A., Swain, A., Fagan, W. F., Fraass, A. J., and Lowery, C. M.: Late Cenozoic cooling restructured global marine plankton communities, Nature, 614, 713–718, 2023.

Wright, J. D. and Miller, K. G.: Control of North Atlantic Deep Water Circulation by the Greenland-Scotland Ridge, Paleoceanography, 11, 157–170, https://doi.org/10.1029/95PA03696, 1996.

Young, J. R.: Neogene, in: Calcareous Nannofossil Biostratigraphy, edited by: Bown, P., Br. Micropaleontol. Soc. Publ., London, 225–265, https://doi.org/10.1007/978-94-011-4902-0_8, 1998

Young, J. R., Wade, B. S., and Huber B. T.: pforams@mikrotax website, http://www.mikrotax.org/pforams (last access: 18 December 2024), 2017.

Young, J. R., Bown ,P. R., and Lees, J. A.: Nannotax3 website, International Nannoplankton Association, https://www.mikrotax.org/Nannotax3 (last access: 15 September 2023), 2023.

Zachos, J., Pagani, M., Sloan, L., Thomas, E., and Billups, K.: Trends, Rhythms, and Aberrations in Global Climate 65 Ma to Present, Science, 292, 686–693, https://doi.org/10.1126/science.105941, 2001.